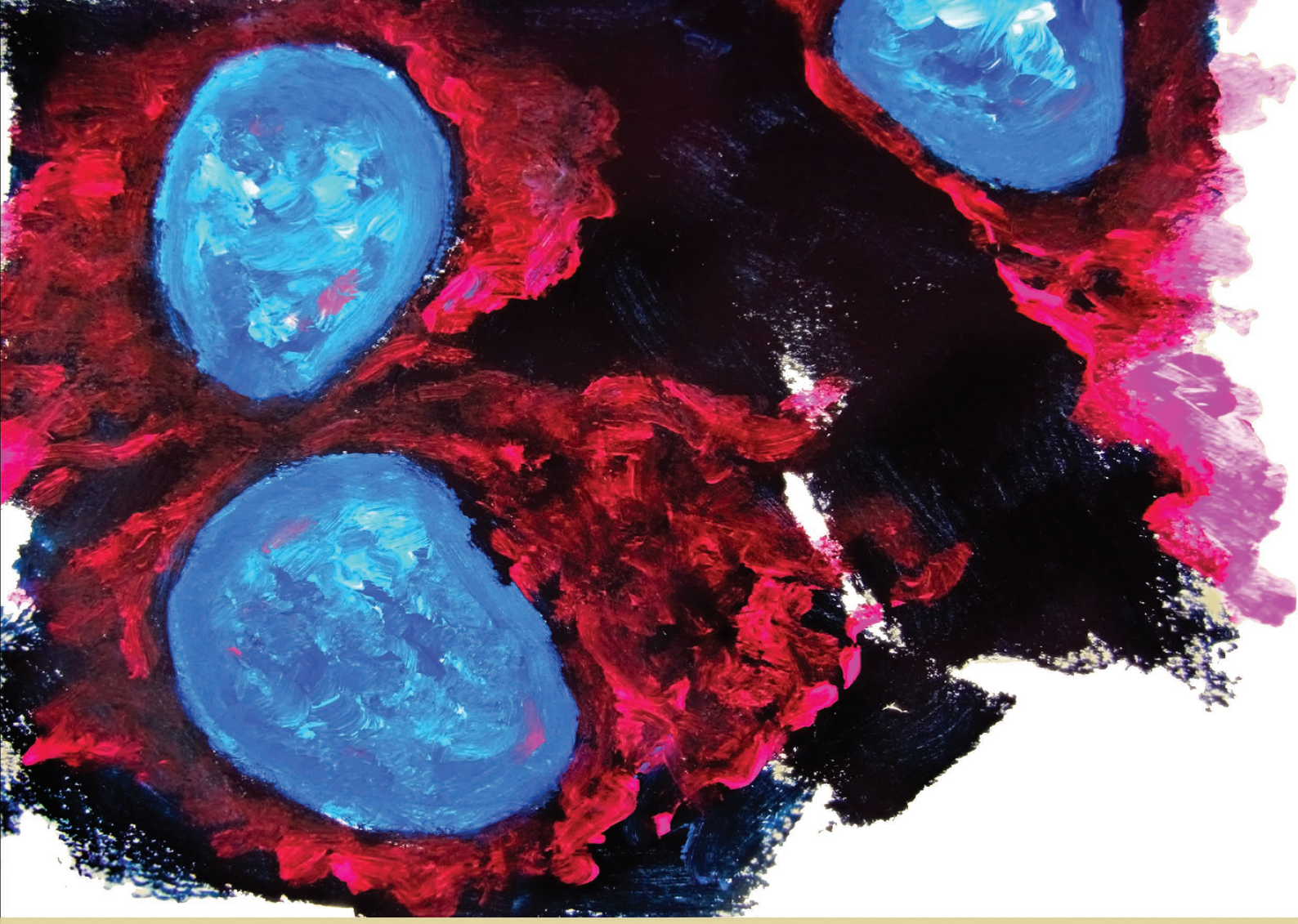

Inês Biscaia de Andrade Barbosa

TRAP1 regulation of mitochondrial homeostasis and cellular quality control

Doctoral Dissertation in the scientific field of Biology with specialization in Cell Biology, under the supervision of Maria S. Santos, PhD and Paulo J. Oliveira, PhD presented to the Department of Life Sciences from the Faculty of Sciences and Technology of University of Coimbra

September 2013

· U C ·

Universidade de Coimbra

TRAP1 regulation of mitochondrial homeostasis and cellular quality control

UNIVERSIDADE DE COIMBRA

Inês A. Barbosa, BSc
Faculty of Sciences and Technology
Department of Life Sciences
University of Coimbra

Dissertation submitted as requirement for candidature for degree of

PhD in Biology
Specialization in Cell Biology

Supervisors: Paulo J. Oliveira, PhD
Maria S. Santos, PhD

Coimbra, September 2013

Cover Illustration Credit: Élia Sofia
eliaramalho@gmail.com

This work was conducted under the supervision of Maria Sancha Santos, PhD, Department of Life Sciences, University of Coimbra; and Paulo J. Oliveira, PhD in the Center for Neurosciences and Cell Biology, Coimbra, Portugal.

The work presented in this dissertation was supported by a PhD fellowship from the Portuguese Foundation for Science and Technology (FCT) addressed to the author (SFRH/BD/48157/2008), the research grant from FCT addressed to Ignacio Vega Naredo (PTDC/SAU-TOX/117912/2010), and by the institutional grant to CNC (PEst-C/SAU/LA0001/2013-2014).

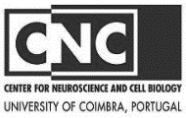

This work also resulted from a collaboration with Patricia Scott, PhD, in the Department of Biomedical Sciences, University of Minnesota - Medical School, Duluth, MN, USA.

À minha mãe e irmã, sempre presentes, pelo apoio incondicional e pelo alento e dedicação ao longo de todos estes anos. Ao meu pai, pela orientação mas sobretudo paciência.

Ao Gonçalo, pela amizade e amor. A teu lado todos os sonhos são possíveis, todas as barreiras ultrapassáveis, todas as horas partilhadas.

A vós que sempre acreditastes que seria possível, dedico este trabalho, tornando-o nosso.

"Nothing in life is to be feared,
it is only to be understood.
Now is the time to understand more
so that we may fear less."

Marie Curie

Statement of originality

This thesis includes material from an original paper that has been previously published in a peer reviewed journal and is referred below:

> Barbosa IA *et al*. **Mitochondrial remodeling in cancer metabolism and survival: potential for new therapies.** *Biochim. Biophys. Acta*, vol 1826 (1), p. 238-254, 2012.

Part of this thesis work has been presented among national and international scientific community in the form of oral and poster communication in several scientific meetings. Data obtained in the course of this work will be also published as full-length peer-reviewed scientific papers.

I certify that the intellectual content of this thesis is the product of my own work, i.e. key ideas, primary contributions, experimental designs, data analysis and interpretation, were performed by the author during her registration as graduate student at the University of Coimbra. Nevertheless, all assistance received in preparing this thesis and sources have been acknowledged.

I declare that, to the best of my knowledge, my thesis does not infringe upon anyone's copyright nor violate any proprietary rights and that any ideas, techniques, quotations, or any other material from the work of other people included in my thesis, published or otherwise, are fully acknowledged in accordance with the standard referencing practices. Moreover, a detailed section regarding copyright license agreements and permission for the usage of published pictures in the present theisis is provided in Appendix A.

I declare that this is a true copy of my thesis, including any final revisions, as approved by my supervisors, and that this thesis has not been submitted for a higher degree to any other University or Institution.

Inês A. Barbosa, BSc

September 2013

Abstract

Through years of evolution and in order to maintain viable protein homeostasis, cells have developed defense mechanisms against the accumulation of misfolded proteins and aggregates. This mechanism comprises a complex network of specialized proteins designated as heat shock proteins (HSPs). Tumor necrosis factor receptor (TNFR)-associated protein 1 (TRAP1) is a 90 KDa HSP family member that has received large attention over the past years. The interest in TRAP1 originated from its identification as a mitochondrial chaperone whose expression is augmented in several human neoplasias. Since its identification, TRAP1 was described to play important anti-oxidant and anti-apoptotic roles, conferring tumor cells growth advantage. Despite the increasing knowledge, the mechanisms of TRAP1 cytoprotective actions are not yet fully understood. In fact, reports in literature are sometimes contradictory or describe alterations without providing a detailed mechanism of action.

The present dissertation aims to contribute with new insights on the role of TRAP1 in conferring mitochondrial protection and regulating cellular quality control systems. We hypothesize that TRAP1 contributes to tumor homeostasis allowing cell growth and survival under stressful environments by preserving mitochondrial functionality and viability as well as through the regulation of cellular quality control systems, including autophagy and apoptosis. To test the hypothesis, the A549 lung carcinoma cell line was used due to its high expression of TRAP1. TRAP1 depletion in this system was achieved through small interference RNA. In addition, a parallel study was performed using MRC-5 cells, a normal lung fibroblast cell line, with low TRAP1 content. The use of the MRC-5 cell line would allow exploring the effects of TRAP1 silencing in a non-tumor cell line, with a low basal expression of that protein.

We initially verified that TRAP1 localization in A549 cells was predominantly mitochondrial, whereas TRAP1 was localized in non-mitochondrial areas in MRC-5 cells. Overall, the results presented in this thesis regarding mitochondrial function are in agreement with previous observations showing that TRAP1 contributes to the maintenance of mitochondrial membrane potential and to decrease ROS production in tumor cells, while the same was not observed in normal MRC5 cells. Although TRAP1 function in mPTP modulation has been previously described, we show for the first time the direct effect of TRAP1 silencing on basal mPTP state. Surprisingly, and contrarily to what was expected, mPTP existed in a more closed conformation in A549 TRAP1-depleted cells. Another breakthrough of the present work regards ROS modulation in the tumor cell line, which according to our results may involve p66SHC phosphorylation in Ser36 residue. Additionally, TRAP1 silencing in A549 cells resulted in mitochondrial fragmentation, possibly involving DRP-1 fission protein.

Although increased lysosome content (in A549 cells) and decreased p62 levels (in both cell lines) suggest an increased autophagic flux, our data showed a decrease in the expression of several macroautophagy markers in TRAP1-depleted cells. However, these apparently contradictory results are explained by a lower ubiquitin content and increased LAMP2A levels suggesting the activation of an alternative autophagy pathway, involving chaperone-mediated autophagy (CMA). Nonetheless, this activation of CMA was only observed in A549 cells. Moreover, incubation of TRAP1-silenced cells with the autophagy inducer rapamycin resulted in increased cellular growth, mainly in A549 cells, suggesting that autophagy signaling in these cells are pro-tumorigenic. Regarding TRAP1 silencing effects on apoptotic signaling, results for both cell lines showed an increase in caspase 3/7-like activity with no alterations in the apparent activity of initiator caspases (8, 9 and 12). Additionally, TRAP1 silencing shifts the BAX/BCL-xL balance in favor of

apoptosis in A549 cells suggesting that these cells have an active apoptotic signaling, whereas MRC-5 cells are not affected.

In conclusion, besides TRAP1 differential expression in normal *versus* cancer cells, its subcellular localization may contribute to the distinct effects observed after TRAP1 silencing (or chemical inhibition). The present work also suggests that p66SHC is a good candidate to mediate TRAP1 ROS modulation in cancer. Moreover, our data suggests that TRAP1 controls mitochondrial morphology through DRP1 content and, additionally, plays an important role in the maintenance of cellular quality control systems. Our results are relevant to clarify not only the role of TRAP1 as an anti-cancer target but also as to understand off-target effects of TRAP1 silencing/inhibition in non-tumor cells.

Keywords: TRAP1, mitochondria, apoptosis, autophagy,oxidative stress.

Resumo

De modo a manter a qualidade e homeostase das proteínas, as células desenvolveram mecanismos de defesa para evitar a acumulação de agregados proteicos e proteínas defeituosas, que envolve uma rede complexa de proteínas especializadas designadas de proteínas de choque térmico (HSPs). A TRAP1 (do Inglês *Tumor necrosis factor receptor-associated protein 1*) é membro da família da proteína de choque térmico de 90KDa (HSP90). O crescente interesse na proteína TRAP1 advém do facto de ser uma chaperona mitochondrial cuja expressão se encontra aumentada nas células tumorais. Desde a sua descoberta, várias funções foram atribuídas à TRAP1 incluindo actividade antioxidante e antiapoptotica, conferindo vantagem seletiva às células tumorais. Contudo, ainda muito falta saber sobre o papel cito-protetor da TRAP1, considerando que muitas das informações obtidas na literatura são fragmentadas, sem providenciar um mecanismo detalhado de ação para a TRAP1.

Esta dissertação tem como principal objetivo contribuir com novas informações acerca do papel da TRAP1 na manutenção da função mitocondrial bem como na regulação de sistemas de controlo de qualidade. A nossa hipótese é a de que a TRAP1 contribui para manutenção da homeostase tumoral, permitindo o crescimento e sobrevivência celulares em ambientes de elevado stresse, através da preservação da função e viabilidade mitocondrial e pela regulação de sistemas de controlo de qualidade como a autofagia e apoptose. Deste modo, usou-se uma linha celular de cancro de pulmão, A549, que expressa elevados níveis de TRAP1. Para trabalho, silenciamos a TRAP1 utilizando ARN pequeno de interferência. Para além dos estudos conduzidos em A549, um estudo complementar foi efetuado usando uma linha celular de fibroblastos pulmonares normais, MRC-5, que expressa níveis reduzidos de TRAP1. Esta última linha celular foi escolhida de modo a explorar os efeitos do

silenciamento da TRAP1 numa linha celular não tumoral com baixa expressão daquela proteína.

De acordo com os dados publicados, a TRAP1 revelou uma localização predominantemente mitocondrial nas células tumorais. Contudo, os nossos resultados sugerem uma distribuição extra-mitocondrial da TRAP1 nas células MRC-5. Esta localização diferencial ajuda à melhor compreensão dos distintos efeitos do silenciamento da TRAP1 nas duas linhas celulares. Deste modo, ao contrário do observado nas MRC-5, os resultados demonstram que a TRAP1 contribui nas células tumorais para a manutenção do potencial de membrana mitocondrial e para a regulação de espécies reativas de oxigénio (ERO). O silenciamento da TRAP1 resultou num aumento da disfunção mitocondrial com repercussões ao nível da sua morfologia. Verificou-se que, especialmente em células A549, a TRAP1 modula o poro de permeabilidade transitória (PTP) mitocondrial, cujo estado nunca tinha sido directamente avaliado. Outra novidade do nosso trabalho resultou do estudo do papel da TRAP1 na regulação das ERO, que poderá envolver a fosforilação da p66SHC no seu resíduo de Ser36.

Tendo em conta que a acumulação de mitocôndrias danificadas resulta na ativação de sistemas de controlo de qualidade, tais como autofagia e apoptose, o silenciamento da TRAP1 resultou num aumento do conteúdo lisossomal (nas A549) e redução da expressão da proteína p62 (nas duas linhas celulares). Apesar dos resultados sugerirem um aumento do fluxo autofágico, existiu uma redução na expressão de diferentes proteínas envolvidas em autofagia, principalmente em A549. Apesar de aparentemente contraditórias, estas observações são explicadas tendo em conta a redução dos níveis de ubiquitina bem como do aumento da expressão da LAMP2A resultantes do silenciamento da TRAP1 em células A549. Além destas alterações, o silenciamento da TRAP1 resultou ainda num aumento da atividade aparente da caspase 3/7 e em alterações no equilíbrio da razão BAX/BCL-xL em prol da via apoptótica

sugerindo a ativação da via de morte celular nas A549, não afetando contudo as MRC-5.

Em resumo, diferente expressão da TRAP1, bem como diferenças na localização intracelular entre células tumorais e normais poderão estar na base dos distintos efeitos do silenciamento desta chaperona nas linhas celulares estudadas. Nas células tumorais, o silenciamento da TRAP1 parece ter efeitos mais devastadores, que incluem a acumulação de mitocôndrias danificadas e, eventualmente, de proteínas deformadas resultando de reduzido fluxo autofagico. Deste modo e numa tentativa de recuperação, as células respondem aumentando os níveis de vias alternativas para remoção de lixo intracelular que contudo são mais limitados. Esta crescente acumulação de lixo culmina então com a ativação da via de morte celular por apoptose. Assim, estes resultados são uma mais-valia para a compreensão da função cito-protetora da TRAP1 e ajudam a clarificar não só o papel da TRAP1 como alvo de terapia anti-cancro mas também na compreensão dos efeitos do seu silenciamento e/ou inibição em células não tumorais.

Palavras chave: TRAP1, mitocondria, apoptose, autofagia, stresse oxidativo.

Acknowledgements

I would like to start by thanking the Portuguese Foundation for Science and Technology for the PhD fellowship and research grants that financially supported the work in our laboratory and which gave me the opportunity to pursue my dreams.

This scientific journey, which I hope will mark the beginning of my professional life, would not be possible without the support, scientific orientation and encouragement of my advisors to whom I will first address my acknowledgements.

I would like to express my deepest gratitude to Doctor Paulo Oliveira, whom I hold in high esteem. I am thankful for the opportunity that has been given to me. I am indebted for the unflagging encouragement and guidance along these years of hard work. Doctor Oliveira largely contributed to my development as a scientist with his support but, and perhaps more importantly, by giving me the freedom to pursue independent work.

Along these years I had the great opportunity of working with Doctor Patricia Scott, to whom I am eternally grateful. Doctor Scott kindly welcomed me in her laboratory and provided unreserved support during my PhD. Under her guidance I successfully overcame difficulties and learned a lot. I am thankful for her valuable advice, constructive criticism and extensive discussions about my work.

I take this opportunity to sincerely acknowledge Doctor Sancha and Professor Moreno the two main pillars of the laboratory. I thank their availability in all occasions and numerous efforts to successfully help getting the required resources for work.

I would also like to thank all the personnel from the Department of Biomedical Sciences at UMD, especially Julie for her help when I first arrived and for her constant availability.

My time in Duluth was made enjoyable in large part due to the friends that soon became a part of my life. I am grateful for all the new friendships I made and the old ones that revived. My thanks go in particular to my “sister” Elaine, my dear friend in and outside the laboratory, I thank her for the unconditional support and companionship. I would also

like to acknowledge Carolina, whom I got to know well during my (our) stay in Duluth and with whom I shared great and memorable times.

I acknowledge the staff of the Department of Life Sciences in special “dona” Paula for her dedication and support in the laboratory.

This journey would not have been possible without the support of my friends, Ana, Catarina, Katy, Lara, and Rui. A special thank to my dear friend Carlos with whom I directly shared this long road. I thank him for the friendship, support and more importantly for making the writing of this thesis a lot more enjoyable. We definitely made a good team. Also, I thank Ines for the help and for always being there for me when I needed. No words can describe how lucky I feel for having such good friends by my side and with whom I am proud to share this important moment of my life.

I thank Nacho, Rita, Ana Branco and Rute, for their valuable contribution to this work. Nacho, I am grateful for your friendship and for all the long discussions, valuable suggestions and inspirations that guided me along this path. To Rute for always bringing joy to the laboratory, and for helping me with mitochondria-related questions.

Finally, I would like to thank my family in special to my grandmothers, for their encouragement, for always beliving in me, and specially for understanding that I could not be around as often as I wished I could, you are always I my heart.

Gostaria de agradecer à minha família, em especial às minhas avós, pela força, motivação e por sempre acreditarem em mim e nas minhas capacidades, mas especialmente por compreenderem que nem sempre pude estar tão presente como gostaria porém estão sempre no meu coração. A vós o meu muito obrigada.

Contents

Abstract i
Resumo v
Acknowledgements ix
Contents xi
List of Figures xvii
List of Tables xix
List of Abbreviations xxi

PART I GENERAL INTRODUCTION

Chapter 1 Cancer: from basics to complexity 3
1.1 Historical notes 4
1.1.1 Theories on cancer development 6
1.2 Modern knowledge on cancer 8
1.2.1 Cancer therapies: overview 12
1.3 Cancer Incidence and Statistics 14
1.3.1 Lung Cancer 15

Chapter 2 Mitochondria in tumor cells: what is so different about them? 19
2.1 The Warburg Effect and mitochondrial metabolism in tumor cells 20
2.1.1 The Warburg effect 20
2.1.2 Metabolic reprogramming provides a selective advantage for cancer cells 21
Glycolytic remodeling 21
Glutamine metabolism 23
Regulation of metabolic reprogramming 23

Mitochondrial succinate dehydrogenase and fumarate hydratase as tumor suppressors 26
2.1.3 Targeting aerobic glycolysis 27
2.2 Altered mitochondrial oxidant production in cancer cells 30
2.2.1 Targeting mitochondrial oxidative stress in tumor cells 32
2.3 Mitochondrial DNA mutations and cancer 38
2.3.1 Mitochondrial DNA as a predictive marker in the diagnosis and staging of cancer 40
2.4 Altered mitochondrial transmembrane electric potential in cancer cells 41
2.4.1 Targeting mitochondrial hyperpolarization in tumor cells 42

Chapter 3 Cell quality control systems and tumorigenesis 45
3.1 Apoptosis 46
3.1.1 Abnormal mitochondrial apoptotic signaling in cancer cells 48
3.1.2 Targeting the aberrant mitochondrial apoptotic machinery 50
3.2 Autophagy 51
3.2.1 Macroautophagy 52
A particular case: Mitophagy 54
3.2.2 Chaperone-Mediated Autophagy 58
3.2.3 The "Janus-faced" role of autophagy in cancer 59
3.2.4 Targeting altered autophagy pathways in tumor cells 61

Chapter 4 Heat Shock Proteins in cancer 63
4.1 HSP90 family 64
4.1.1 TRAP1: the mitochondrial HSP90 66
TRAP1 structure 67
TRAP1 subcellular localization 67
TRAP1 functions and regulators 68
4.1.2 Targeting the mitochondrial complex of HSP90, TRAP1 and CypD in cancer cells 70

Chapter 5 Hypothesis and Aims 73

Part II Experimental Procedures & Results

Chapter 6 Material and Methods **77**

6.1 Materials 77

6.1.1 Standard solutions and buffers 77

6.1.2 Reagents and kits 78

6.2 Cell Culture 80

6.2.1 Cell lines 80

6.2.2 siRNA Transfection 81

6.3 Experimental design 82

6.4 Sulforhodamine B assay 84

6.4.1 Cell proliferation assay 85

Drug toxicity assay 86

6.5 Material harvesting 86

6.5.1 Total RNA 86

6.5.2 Total protein 87

6.6 Protein Quantification 88

6.6.1 Bicinchonic acid assay (BCA) 88

6.7 Protein quantification and cellular localization 89

6.7.1 Immunoblotting 89

6.7.2 Immunocytochemistry 92

6.8 Quantitative RT-PCR 93

6.8.1 Primer design 93

Primers for the HSP90 family 95

6.8.2 Step one: reverse transcription 95

6.8.3 Step two: real-time PCR 96

6.8.4 DNA standards preparation 97

6.8.5 mRNA expression analysis 98

6.9 Evaluation of oxygen consumption 99

6.10 Evaluation of mitochondrial membrane potential 100

6.10.1 Microplate assay 100

6.10.2 Flow cytometer 101

6.10.3 Confocal microscopy 101

6.11 Evaluation of oxidative stress 102
6.11.1 Flow cytometry 102
6.11.2 Confocal microscopy 103
6.12 Evaluation of mitochondrial permeability transition pore opening 103
6.13 Caspases-like activity 104
6.13.1 Caspase 3/7 and Caspase 9-like activities 104
6.13.2 Caspase 8-like activity 105
6.13.3 Caspase 12-like activity 105
6.14 Fluorescence detection of lysosomal bodies 106
6.15 Statistics 106

Chapter 7 TRAP1 regulates of mitochondrial function and dynamics, as well as cellular quality control systems in A549 lung cancer cells 107

7.1 Introduction 108
7.2 Results 109
7.2.1 TRAP1 silencing efficiency 109
7.2.2 TRAP1 silencing effect on cell growth and susceptibility to DOX-induced toxicity 110
7.2.3 TRAP1 modulation of mitochondrial function 112
TRAP1 preferentially localizes to mitochondria 112
TRAP1 silencing results in $\Delta\Psi_m$ depolarization 114
TRAP1 silencing results in a higher closed-conformation of the mPTP 115
TRAP1 silencing decreases oxygen consumption 119
TRAP1 silencing results in increased ROS production 119
7.2.4 TRAP1 silencing affects mitochondrial morphology and dynamics 123
TRAP1 silencing results in mitochondrial fragmentation 124
Effects of TRAP1 silencing on mitochondrial dynamics 124
7.2.5 TRAP1 silencing affects autophagy pathways 126
TRAP1 silencing decreases macroautophagy levels 126
TRAP1 silencing decreases ubiquitin content and increases CMA 133
7.2.6 TRAP1 silencing affects apoptosis regulators 134

TRAP1 silencing results in increased caspase 3-like activity while not affecting initiator caspases-like activities 135
TRAP1 silencing shifts the balance BAX/BCL-xL in favor of apoptosis 135
7.3 Discussion 135
7.4 Conclusions 145

Chapter 8 TRAP1 regulates autophagy in MRC-5 lung cells but has reduced effects on mitochondrial function 147
8.1 Introduction 148
8.2 Results 149
8.2.1 TRAP1 expression and silencing efficiency 149
8.2.2 TRAP1 silencing effect on cell proliferation and susceptibility to DOX-induced toxicity 151
8.2.3 TRAP1 modulation of mitochondrial function 154
TRAP1 is highly localized in extramitochondrial sites 154
TRAP1 silencing does not affect $\Delta\Psi_m$ 155
TRAP1 silencing effect on mPTP modulation 156
TRAP1 silencing does not alter cellular oxidative stress 157
8.2.4 TRAP1 silencing effect on mitochondrial morphology and dynamics 159
TRAP1 silencing does not alter mitochondrial morphology 159
TRAP1 silencing does not affect the expression levels of proteins involved in mitochondrial dynamics 160
8.2.5 TRAP1 silencing effect on autophagy pathways 162
TRAP1 silencing decreases macroautophagy levels 162
TRAP1 silencing does not affect ubiquitin content and CMA levels 165
8.2.6 TRAP1 silencing affects apoptosis regulators 165
TRAP1 silencing results in increased caspase 3-like activity and decreased caspase 12-like activity 165
TRAP1 silencing did not affect pro-apoptotic and pro-survival BCL-2 family proteins 166
8.3 Discussion 166
8.4 Conclusions 172

Part III Final Remarks

Chapter 9 Final Conclusions 175

Chapter 10 Future Perspectives 181

Bibliography 185

Appendix Copy Right License Agreements 219

List of Figures

Figure 1.1 – Major events on the history of cancer 5
Figure 1.2 - The hallmarks of cancer. 11
Figure 1.3 - Lung cancer incidence. 16

Figure 2.1 - Metabolic remodeling in cancer cells 24
Figure 2.2 - Chemotherapeutic agents targeting mitochondrial alterations 37

Figure 3.1 - Apoptotic pathways: extrinsic vs intrinsic 47
Figure 3.2 - Different types of autophagy and autophagosome formation during macroautophagy. 57

Figure 4.1 - TRAP1 cytoprotective functions in tumor cells. 71

Figure 6.1 - siRNA pathway. 82
Figure 6.2 - Cell transfection scheme 83
Figure 6.3 - Experimental design 84

Figure 7.1 - TRAP1 silencing efficiency in A549 cells 111
Figure 7.2 - TRAP1 silencing effect on cell growth and susceptibility to DOX treatment. 113
Figure 7.3 - TRAP1 subcellular localization 115
Figure 7.4 - Mitochondrial membrane potential alterations upon TRAP1 silencing 116
Figure 7.5 - TRAP1 expression and mitochondrial permeability transition pore (mPTP) modulation 118
Figure 7.6 - Mitochondrial HSP90 and HSP60 chaperone content 120
Figure 7.7 - TRAP1 silencing effect on intracellular and mitochondrial reactive oxygen species (ROS) 121
Figure 7.8 - TRAP1 silencing effects on SHC1 gene and p66Shc and SOD2 protein content. SHC1 mRNA content alterations were analyzed by qRT-PCR 122
Figure 7.9 - Mitochondria morphology alterations upon TRAP1 silencing 125

Figure 7.10 - Measurement of mitochondrial dynamics-related proteins. evaluated by western blot. 127
Figure 7.11 - Alterations in macroautophagy-related proteins during TRAP1 silencing. 129
Figure 7.12 - p62 and lysosome content after TRAP1 silencing..... 130
Figure 7.13 - Effect of macroautophagy modulators in the proliferation of TRAP1 silenced cells. 131
Figure 7.14 - Effect of TRAP1 silencing in both ubiquitin and LAMP2A content..... 134
Figure 7.15 - TRAP1 silencing effect on caspase-like activities and BCL-2 family protein levels 136
Figure 8.1 - TRAP1 differential expression 150
Figure 8.2 - TRAP1 silencing efficiency in MRC-5 cells 151
Figure 8.3 - TRAP1 silencing effect on cell growth and susceptibility to DOX treatment 152
Figure 8.4 - TRAP1 subcellular localization 153
Figure 8.5 - Mitochondrial HSP90 and HSP60 chaperones content..... 155
Figure 8.6 - Mitochondrial membrane potential alterations upon TRAP1 silencing. 157
Figure 8.7 - TRAP1 expression and mitochondrial permeability transition pore (mPTP) modulation 158
Figure 8.8 - TRAP1 silencing and oxidative stress 160
Figure 8.9 - Mitochondria morphology and dynamics in TRAP1-depleted cells 161
Figure 8.10 - Alterations in macroautophagy-related proteins during TRAP1 silencing 164
Figure 8.11 - p62 and lysosome content after TRAP1 silencing 166
Figure 8.12 - Effect of macroautophagy modulators in the proliferation of TRAP1 silenced cells 168
Figure 8.13 - Effects of TRAP1 silencing in both ubiquitin an LAMP2A content..... 170
Figure 8.14 - TRAP1 silencing effect on caspase-like activities and BCL-2 family protein levels 171
Figure 9.1 - Effects of TRAP1 disruption in A549 cells 177

List of Tables

Table 2.1 - Summary of the anti-cancer agents and phase of their clinical development 28

Table 6.1 - Drug concentrations and combinations used in SRB proliferation assays 86

Table 6.2 - List of primary antibodies used in Western Blot protein analysis 91

Table 6.3 - List of primers used in the present work 94

Table 7.1 - Mitochondrial membrane potential and basal O2 consumption in A549 cell groups 119

List of Abbreviations

α-KG	α-ketoglutarate
α-TOS	α-tocopherol succinate
2-DG	2-Deoxyglucose
2-ME	2-Methoxyestradiol
3-MA	3-methyladenine
Acetyl Co-A	acetyl coenzyme A
ACL	acute promyelocytic leukemia
ADP	adenosine diphosphate
AIF	apoptosis-inducing factor
AKT	serine/threonine protein kinase
AMBRA1	autophagy/beclin-1 regulator 1
AMPK	AMP-activated protein kinase
ANT	adenine nucleotide translocase
APAF-1	apoptotic peptidase activating factor 1
ATG	autophagy related genes
ATP	adenosine triphosphate
BAD	BCL-2 associated agonist of cell death
BAG1	BCL-2 associated athanogene 1
BAK	BCL-2 antagonist/killer
BAX	BCL-2 associated X protein
BCL-2	B-cell CLL/lymphoma
BCL-w	BCL-2-like protein 2
BCL-XL	B-cell lymphoma extra large
BH	BCL-2-homology domains
BID	BH3 interacting domain death agonist
BIM	BCL2-like 11
BNIP3	BCL-2 /E1B 19KDa-interacting protein 3-like protein
BRCA1	breast cancer 1
C/EBP	cytidine-cytidine-adenosine-adenosine-thymidine (CCAT)-enhancer-binding protein
Cav-1	caveolin-1

CHOP	C/EBP-homologous protein
CMA	chaperone mediated autophagy
COX	cytochrome c oxidase
CQ	chloroquine
CsA	cyclosporin A
CT	computed Tomography
CypD	cyclophilin D
DCA	dichloroacetate
DNA	deoxyribonucleic acid
DOX	doxorubicin
DRP1	dynein-related protein 1
EGCG	epigallocatechin-3-gallate
EGFR	epidermal growth factor receptor
ER	endoplasmic reticulum
ERK	extracellular signal-regulated kinase
ETC	electron transport chain
FADD	Fas-Associated protein with death domain
FCCP	trifluorocarbonylcyanide phenylhydrazone
FH	fumarate hydratase
FIS1	mitochondrial fission 1 protein
GA	geldanamycin
GLS	glutaminase
GLUT	glucose transporter
GPx	glutathione peroxidase
GRed	glutathione reductase
GS	glycogen synthase
GS3-K	glycogen synthase kinase 3
GSH	reduced glutathione
HCQ	hydroxychloroquine
HIF	hypoxic transcription factor
HIP	huntingtin-interacting protein
HKII	hexokinase II
HOP	homeodomain-only protein
HSC	heat shock cognate protein
HSF	heat shock factor
HSP	heat shock protein
IMM	inner mitochondrial membrane
IMRT	intensity-modulated radiation therapy

Io	ionomycin
JNK1	c-Jun N-terminal kinase 1
LAMP2A	lysosome-associated membrane protein type 2A
LC3	light chain 3
LDH	lactate dehydrogenase
LKB1	serine/threonine kinase 11
LMP	lysosomal membrane permeabilization
MAPK	mitogen-activated protein kinase
MFN	mitofusins
miRNA	microRNA
MOMP	mitochondrial outer membrane permeabilization
MPT	mitochondrial permeability transition
mPTP	mitochondrial permeability transition pore
mtDNA	mitochondrial DNA
MTG	mitotracker green
mTOR	mechanistic target of rapamycin (serine/threonine kinase)
MTR	mitotracker red
MYC	v-myc myelocytomatosis viral oncogene homolog
NADH	nicotinamide adenine dinucleotide, reduced form
NADPH	nicotinamide adenine dinucleotide phosphate, reduced form
NBR1	neighbor of BRCA1
NIX	BCL2/adenovirus E1B interacting protein 3-like
Noxa	phorbol-12-myristate-13-acetate-induced protein 1
NQO1	NAD(P)H quinone oxidoreductase 1
OMM	outer mitochondrial membrane
OPA1	optic atrophy 1
OXPHOS	oxidative phosphorylation
PBR	peripheral benzodiazepine receptor
PDH	pyruvate dehydrogenase enzyme
PDK	pyruvate dehydrogenase kinase
PDT	photodynamic therapy
PE	phosphatidylethanolamine
PEITCs	Phenyl ethyl isothiocyanates
PI3K	Phosphatidylinositol 3-kinase
PI3P	phosphatidylinositol-3-phosphate
PiC	phosphate carrier
PINK1	PTEN-induced putative kinase 1
PIP	phosphatidylinositol phosphate

PK	pyruvate kinase
PKCβ	protein kinase c beta
PKM2	pyruvate kinase isoform M2
$PPAR_{\gamma}$	peroxisome proliferator activated receptor gamma
PPIF	peptidyl-prolyl cis-trans isomerase F
PPP	pentose phosphate pathway
PTEN	phosphatase and tensin homolog
PUMA	p53-upregulated modulator of apoptosis
RB	retinoblastoma 1
RNA	ribonucleic acid
ROS	reactive oxygen species
rRNA	ribossomal RNA
SDH	succinate dehydrogenase
siRNA	small interfering RNA
SLC5A1	solute carrier family 5 member 1
SLC7A1	solute carrier family 7 member 1
SMAC/Diablo	Second mitochondrial-derived activator of caspases/direct
SOD	superoxide dismutase
SRB	sulforhodamine B assay
SRC	v-src avian sarcoma (Schmidt-Ruppin A-2) viral oncogene homolog
SRS	Stereotactic RadioSurgery
STAT3	Signal transducer and activator of transcription 3
tBHP	tert-butyl hydroperoxide
TBP7	Tat-binding protein 7
TCA	tricarboxylic acid
TMRM	Tetramethylrhodamine, methyl ester
TNF	tumor necrosis factor
TNFR1	tumor necrosis factor receptor 1
TOM20	translocase of outer mitochondrial membrane 20 homolog
TP53	tumor protein p53
TRAP1	tumor necrosis factor receptor-associated protein 1
tRNA	Transfer RNA
TSPO	18 kDa translocator protein
ULK1	UNC-51–like kinase 1
UPR	unfolded protein response
VDAC	Voltage-dependent anion channel
VHL	von Hippel-Lindau tumor suppressor

In this dissertation the guidelines for gene and protein nomenclatures were applied, i.e. whenever italized the abbreviations refer to gene whereas non-italized refers to protein.

Part I

General Introduction

Chapter 1

Cancer: from basics to complexity

1.1 Historical notes
    1.1.1 Theories on cancer development
1.2 Modern knowledge on cancer
    1.2.1 Cancer therapies: overview
1.3 Cancer Incidence and Statistics
    1.3.1 Lung Cancer

Although cancer was recognized thousands of years ago as a medical condition, paleopathologic findings indicate this disease is actually older than mankind. The knowledge on cancer advanced greatly along human history until our current understanding of cancer as a highly complex disease that results from a multistep process. This progress on cancer knowledge contributed not only to the understanding of the process of neoplastic transformation, but also to the development of new therapies. This chapter is an overview of the major cancer developments and advances along history for a better understanding of how the overall knowledge of cancer accompanied the greatest scientific discoveries. The chapter will also focus on the importance of the global burden of this disease and the progress made regarding therapeutic approaches. It will start from a historical perspective (Section 1.1) and move to modern knowledge of cancer (Section 1.2.), followed by information on global cancer incidence and mortality (Section 1.3).

1.1 Historical notes

Contrarily to what some might think, cancer is not a modern disease. Evidence from fossils, bones and mummified bodies support the fact that cancer was recognized several thousand years ago. The origin of the word cancer is attributed to the Greek physician Hippocrates to whom the cancerous growth reminded of a moving crab, adhering to surrounding structures with his claws. These observations led to the Greek term *karkinos*, and later to the Latin word cancer, to describe masses of cancerous cells. However, despite naming "cancer" Hippocrates did not discover the disease. In fact, historically, the world oldest documented case of cancer dates back to about 3000 B.C. in Egypt. The Edwin Smith Papyrus recorded eight cases of breast tumors. In the document, the writer concluded that it was a serious disease for which there was no treatment available [1].

Since then, the knowledge on neoplastic transformation has progressively increased. In the seventeenth century, Hooke applied the word "cell" and with it created the understanding that it represents the biological unit of living organisms. Another important advance was the implementation of autopsy as a tool for the study of human pathologies provided bases to the better understanding of disease development. Several physicians, such as Giovanni Morgagni in 1761, performed routine postmortem examinations establishing a correlation between patient illness and pathologic findings [2]. Latter, the Scottish surgeon John Hunter suggested that some cancers could be surgically removed proposing guidelines to how a surgeon could decide which cancer to operate on [3]. However, it was not until one century later that surgery as a method for cancer treatment became widely used. In 1846, the development of general anesthesia allowed the elimination of excruciating pain experienced by surgical patients as well as the progress of classic cancer operations such as the radical mastectomy [4].

With the evolution of scientific tools, such as the development of the modern microscope, the correlation between microscopic alterations and illness was established. In the nineteenth century, Rudolf Virchow's work supported emerging ideas on cell division stating that all living cells originate from other living cells. These observations reinforced his theory that diseases involve changes in normal cells, and that pathology is ultimately a disease of the cell [5]. This assumption had a high impact on cancer surgery improvement as it allowed pathologists to identify abnormal tissue from selected samples for more precise diagnostics.

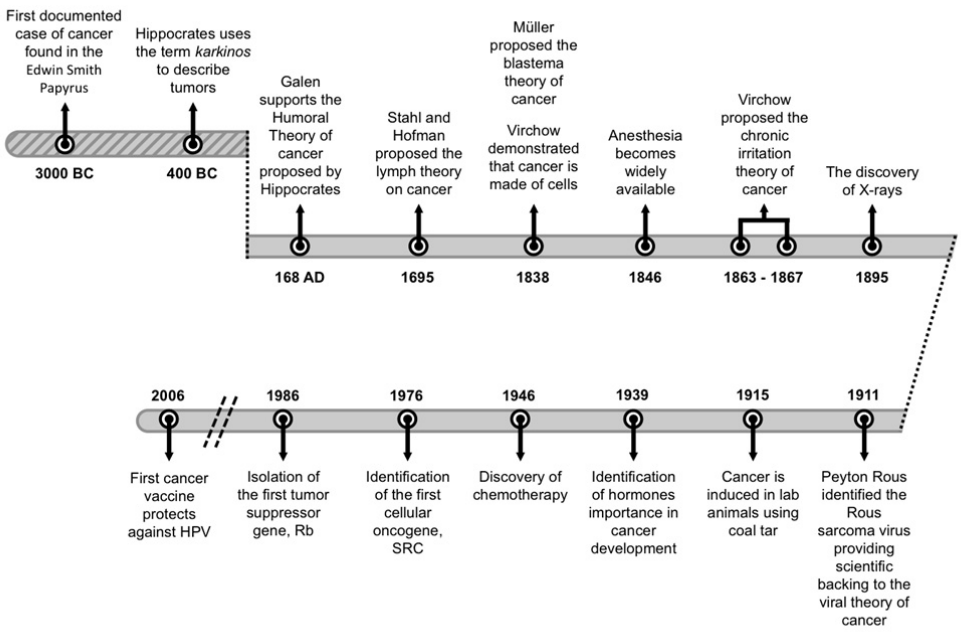

Figure 1.1 – Major events on the history of cancer. A timeline of cancer discoveries and theories.

The twentieth century saw extraordinary advances in cancer therapy. In 1903, five years after Marie Curie discovery of radium, the first use of a radioactive element to cure cancer was made [6]. Today, radiation is delivered with precision to destroy tumor cells limiting the damage caused to nearby normal tissues. During World War II the study of the effects of a number of chemicals developed as war agents, provided new insights to cancer treatment. In the course of this work, a nitrogen compound, showed its effectiveness in the cure of lymphomas [7]. These works potentiated rapid advances in chemotherapy. In 1958, scientists demonstrated that the combined use of chemotherapeutic agents caused remission of acute leukemia [8].

Moreover, the knowledge of the origin of cancer also suffered a fast evolution along this period of time with contributions from both epidemiology and molecular biology. Advances in epidemiology contributed to the identification of many specific events that cause cancer, such as exposure to coal tars or ionizing radiation whereas molecular biology focused on the interactions between genes and external factors [9-11]. At this point, scientists knew that chemicals, radiation, and viruses could cause cancer, and that

it could also be hereditary. However, the discovery of deoxyribonucleic acid (DNA) chemical structure by James Watson and Francis Crick, as well as the understanding of how genes worked allowed the perception that DNA damage by multiple factors could lead to cancer development [12]. The next breakthrough came with the discovery of two particularly important cancer-related gene families, oncogenes and tumor suppressor genes. The discovery of oncogenes and proto-oncogenes, i.e. normal genes that after mutations or deletions acquire the ability to function as an oncogene, provided information about how cells proliferate, since these specific genes cause cell to grow out of control. Conversely, tumor suppressor genes operate to constrain or suppress cell division [13]. The importance of specific genetic changes in cancer was soon used to develop targeted therapies to overcome the downstream impact of genetic alterations.

The last decades led to a remarkable understanding of cancer (Fig.1.1). The development of techniques of molecular biology, as well as the improvement in specialized tools, were highly responsible for this success.

1.1.1 Theories on cancer development

As previously mentioned, the increased knowledge of human body, epidemiology, and molecular biology contributed to advances on the understanding of cancer and its development.

Centuries of research led to several theories explaining the causes of cancer (Fig.1.1). While ancient Egyptians blamed cancers on gods, Hippocrates believed that cancer was caused by an unbalance in *humor* content, the *humoral* theory of cancer. Hippocrates (460-370 BC) theorized that the human body was composed by four humors (body fluids) – blood, phlegm, yellow bile, and black bile. According to the *humoral* theory, cancer would then be caused by an excess in black bile [14]. With the decline and fall of ancient Greece, the *humoral* theory of cancer was adopted by the Romans and remained unchanged for 1,300 years.

The *humoral* theory was later replaced by the lymph theory. In 1695, Stahl and Hoffman proposed that life consisted of continuous and appropriate movement of body fluids, namely blood and lymph, through solid parts. According to this theory, malignant cancers

resulted from fermentation and degeneration of the lymph [15]. The lymph theory prevailed for almost 150 years and was abandoned due to lack of evidences.

In the 1830s, the German pathologist Johannes Müller and his student Rudolf Virchow revolutionized the view on cancer with the demonstration that cancer is a disease of cells and not lymph. Müller proposed that cancer cells originate from building blocks called blastema [2]. However, Virchow disapproved the blastema theory by demonstrating that cancer cells are derived from other cells.

During the nineteenth century, several theories proposed explanations for the origin of cancer, some of which are still accepted as valid, although with minor modifications, nowadays. Virchow postulated that chronic irritation was the cause of cancer, despite incorrectly believing that metastatic cancers were spread by a liquid [16]. Later, Karl Thiersch demonstrated that cancer metastasizes from the spread of malignant cells and not through fluid. The discovery of X-rays in 1895 and the observations that exposure to this form of radiation could induce tissue damage supported the idea that cancer arises from chronic irritation. While Virchow proposed the chronic irritation theory, Hugo Ribbert named trauma as the cause of cancer [17].

Cancer was soon thought to be a contagious disease. In 1649, the contagious theory was publicized and all cancer patients were isolated in hospitals outside the cities [18]. This theory was later rejected due to failure in experimentally verification [2]. Although cancer itself is not contagious, discoveries in the early twentieth century regarding certain virus and bacteria yielded clues about the molecular mechanisms that trigger the development of human cancer. In 1911, Peyton Rous described a sarcoma in chicken caused by what was later known as the Rous sarcoma virus [19]. Since then several virus have been linked to cancer [20, 21].

Although the hereditary causes of cancer have been debated for centuries, a report published in 1913 on several examined cases showed the influence of hereditary on carcinogenesis [22]. In 1915, Yamagiwa and Ichikawa were able to induce cancer in laboratory animals by applying coal tar to their skin [9]. This and other similar experiments brought clues about the existence of specific substances that cause cancer, the so-called carcinogens.

The fragmented findings regarding cancer origin and development created confusion about the disease. Moreover, the discovery of compounds that potentiate carcinogenesis,

as well as the identification of certain bacteria and virus as cancer promoters seemed to be in conflict with findings showing that cancer is hereditary. The identification of DNA as the carrier of the cellular genetic code, as well as the understanding on how this code is translated, allowed great advances on the conception of a unified view on cancer origin and development.

1.2 Modern knowledge on cancer

Cancer is a disease characterized by an uncontrolled growth and division of abnormal cells, which culminates with acquisition of the ability of the cell to invade and colonize other tissues in the organism. In normal cells, processes of cell division and death are highly regulated ensuring the homeostasis of cell number and maintenance of tissue architecture. On the other hand, cancer cells are resistant to signals that control cell growth and even evade programmed cell death following their own agenda regarding proliferation.

Carcinogenesis constitutes a multistep process through which cells acquire a series of genetic alterations that drive the progressive transformation of normal into malignant cells [23]. These alterations may be either inherited and/or result from a sequence of genetic events that leads to the acquisition of somatic mutations, these being acquired genetic alterations induced by spontaneous stochastic events, carcinogens and/or viral or bacterial infection. In addition to the mentioned alterations, epigenetic changes have also been associated with tumor development [24]. Epigenetics refers to alterations in the pattern of gene expression that are mediated by mechanisms independent from DNA sequence alterations, namely DNA methylation and histone modifications including methylation, acetylation, and phosphorylation [25]. These mechanisms usually result in inappropriate gene silencing or activation in tumor cells.

Classically, two classes of cancer-related genes, oncogenes and tumor suppressor genes are described. Alterations in these genes are shown to induce clonal expansion leading to neoplastic initiation [26]. As previously introduced in Section 1.1, oncogenes refer to the mutated version of normal cell genes termed proto-oncogenes. These genes encode proteins involved in cell cycle progression as well as inhibition of cell differentiation and cell death pathways. The normal form of those proteins is of great importance for normal

cell development and tissue and organ maintenance. The malignant phenotype is acquired upon dominant gain-of-function mutations in these genes leading to increased cell division, and decreased cell differentiation and cell death [27]. Advances in the knowledge and identification of oncogenes were made through the study of retrovirus [28, 29]. The first oncogene discovered was *SRC*, identified by Peyton Rous following studies with Rous Sarcoma Virus (Fig.1.1) [19]. This gene is involved in a series of signal transduction cascades that influence cellular proliferation, differentiation, motility, and survival [30]. Similar studies led to the identification of the *MYC* oncogene, which is overexpressed in a wide range of human cancers. *MYC* oncogene is transcription factor that regulates the expression of several genes involved in cell proliferation, cell growth, and apoptosis [31]. Another example of oncogene is *BCL-2* which unlike *MYC* oncogene promotes cellular survival rather than proliferation [32].

Working in the opposite manner, tumor suppressor genes are known participants of several high conserved cellular functions such as regulation of cell cycle and apoptosis, differentiation, surveillance of genomic integrity and repair of DNA errors, signal transduction, and cell adhesion [33]. Consequently, inactivation of these genes confers tumor cell growth and survival advantages. Some authors defend the division of tumor suppressor genes in two major categories depending on their functions as gatekeeper or caretaker genes [34]. Gatekeeper genes are involved in the control of cell cycle progression, cell death, and differentiation while caretaker genes are involved in genomic stability maintenance and thus reducing the mutation rates of genes [34, 35]. Despite this simplified distinction between gatekeeper and caretaker tumor suppressor genes, one should take into account the fact that some genes may belong to both families, as the example of *TP53* (also *P53*) [36].

The first tumor suppressor gene was identified by studies in retinoblastoma and led to subsequent identification of the retinoblastoma gene *RB* (Fig.1.1) [37, 38]. This gene encodes a nuclear protein that plays a central role in cell cycle progression being responsible for an important G1 checkpoint, blocking S-phase entry, and cell growth, promoting terminal differentiation and cell cycle exit [39]. Another well-studied tumor suppressor gene is *TP53*. This protein is often referred to as the "guardian of the genome" and plays critical roles in genetic stability maintenance, cell cycle regulation, metabolism, induction of apoptosis, senescence and differentiation control, both through genomic and non-genomic mechanisms [40].

Clonal expansion initiation requires one or more mutations, somatic and/or inherited, which confer selective advantage to neoplastic cells over normal cells. Mutations in tumor suppressor genes can occur in the germ line while mutant versions of proto-oncogenes are rarely hereditary [26]. Although mutations that yield activated oncogenes might occur during gametogenesis, these usually disrupt normal tissue development due to their typical dominant nature. Consequently, embryos carrying these mutations are unlikely to be viable. In contrast, germ line mutations of tumor suppressor genes are often compatible with normal embryonic development, since these alleles are recessive at the cellular level [41]. It is however important to understand that germ line mutations in these genes do not cause cancer but rather predispose cells for further neoplastic development. Inheritance of these mutations increases the risk of tumor progression, as individuals often develop multiple tumors that occur at an earlier age than individuals whose cancer-gene mutations occurred somatically.

Taking all the above information into account, cancer should be understood as a highly complex and heterogeneous process, and as a disease resulting from the occurrence of a complex series of events [42, 43]. As referred, no single mutations causes cancer; in fact, it takes a stepwise accumulation of genetic alterations that affect discrete signaling pathways, each contributing for a specific aspect to the acquisition of a malignant phenotype.

Although one cannot define the exact number of mutations required to achieve malignancy, as it varies between and within cancer types, research in the past decades led to the identification of several features acquired during the multistep development of human tumors. In 2000, Douglas Hanahan and Robert A. Weinberg proposed six hallmarks of cancer that provided an organized view for a better understanding of the diversity and complexity of neoplastic disease [44]. These include the acquisition of sustained proliferative signaling, ability to evade growth suppressors and cell death, development of limitless replicative potential, sustained angiogenesis, and activation of tissue invasion and metastasis (Fig.1.2). A decade later, the same authors revised their previous work integrating new obtained information in the field [45]. The conceptual progress on cancer research came to support and broaden the range of tumor capabilities. The redesigned work proposes the inclusion of two new emerging hallmarks, the ability of cancer cells to evade detection and elimination by immune system, and cellular energy metabolism reprograming [45]. Moreover, the authors suggested tumor-promoting

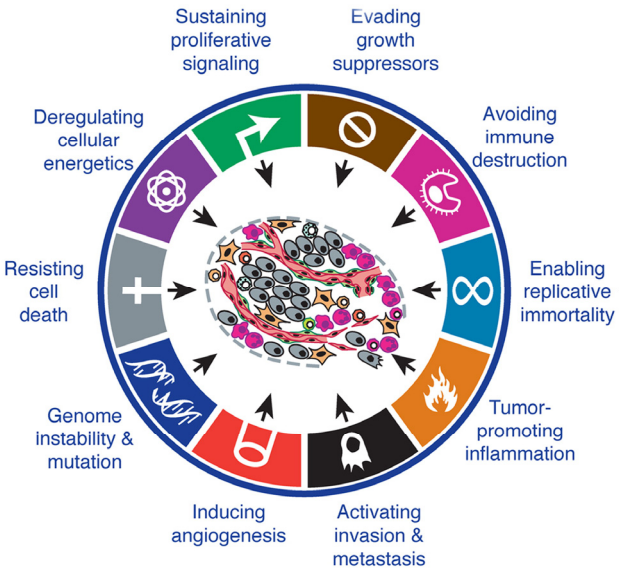

Figure 1.2 - The hallmarks of cancer. Acquired capabilities of cancer cells which allow them to survive, proliferate, and disseminate. These functions are acquired by different tumors through different mechanisms. Adapted from [45] with permission (Appendix A).

inflammation as an enabling characteristic. Additionally, the acquisition of the multiple hallmarks depends on the occurrence of alterations in the genomes of neoplastic cells, consequently genomic instability and mutations also constitute enabling characteristics for tumor progression [45]. Additionally, several studies also point out the importance of tumor microenvironment contribution to tumorigenesis, contrasting with the reductionist view of a tumor as nothing more than a group of fairly homogeneous cancer cells [46].

According to Hanahan and Weinberg the multistep pathway to malignancy involves the successive acquisition of these hallmark features by normal cells. The progressive development of such functional traits is thought to be common to most tumors albeit through different mechanistic strategies. The concept of cancer hallmarks is widely recognized and accepted throughout the scientific community as it provides useful basis for the understanding of cancer complexity. Moreover, considering the high heterogeneous nature of a tumor, its biology can only be addressed through the study of the individual specialized cell types within it.

1.2.1 Cancer therapies: overview

The remarkable progress of research into the mechanisms of cancer pathogenesis in the last decades led to important advances in the development of new therapies (Fig.1.1). The increased understanding on the pathophysiology of the disease allowed a clear evolution of traditional cancer treatments, such as surgery, radiotherapy, and chemotherapy and the rise of new emerging therapeutic approaches, namely hormone therapy, immunotherapy and targeted therapy.

For many centuries, surgery was the only available treatment for cancer and although a lot has changed since the first documented surgeries on cancer patients, this still constitutes one of the most important and widely used treatment methods. Today, surgical techniques and technologies are more precise, allowing a less invasive approach without sacrificing the efficiency of the process. These advances also contributed to the emergence of strategies to destroy tumors without removing them, including the use of cryosurgery and the use of lasers [47, 48]. Furthermore, robotic-assisted surgery has been introduced for treatment of several types of cancer, namely prostate and pancreatic cancer [49, 50]. However, surgery relies on prevention and early detection to minimize its impact and adverse effect as well as increases cure.

Radiation therapy was introduced not long after x-ray discovery in 1895 by Wilhelm Roentgen, soon undergoing a great evolution as the early protocol of a single massive dose of radiation was shown to have severe side effects [6]. Today, due to advances in radiation physics and computer technology, it is possible to aim radiation more precisely. In 1990, a computer technique termed three dimensional planning began to be employed, compiling computed tomography (CT) scan information into a special computer to precisely pinpoint the location of tumors [51]. A decade later, additional technological leaps and the development of highly sophisticated machines allowed several other radiation therapy techniques to emerge, including the intensity-modulated radiation therapy (IMRT) and stereotactic radiosurgery (SRS) [52, 53].

Chemotherapy still constitutes an efficient cancer treatment. The increasing number of new drugs as well as their proper combination revealed to be advantageous in the battle against cancer. Research has been made regarding new drug delivery techniques in order to target cancer cells more effectively and to reduce the side effects. These include drug attachment to monoclonal antibodies, which can be designed to guide chemotherapy

drugs directly to tumor cells, and liposomal therapy [54, 55]. In the latter technique, drugs are incorporated inside liposomes allowing drug penetration in cancer cells. A new emerging technology consists in a nanoparticle-based drug delivery system [56, 57]. Cancer nanotechnology basic rationale consists in the development of nanoscaled molecular platforms carrying therapeutic compounds, which allows a precise tumor cell target while avoiding harming normal cells, and high reduction of side effects caused by the treatment.

In the work developed by Thomas Beatson in 1896, the connection between ovaries and breast cancer development provided a foundation for the modern use of hormone therapy [58]. Later, in 1939, Charles Huggins discovered the importance of hormones in the development of certain cancers [59]. The better understanding of how hormones influence cancer growth provided insights to the development of a new class of drugs have been used to treat prostate and breast cancer [60, 61].

The increased knowledge on cancer biology led to the development of biological agents that mimic some of the natural signals that control cell growth to cancer therapy, including immunotherapy, which stimulates the immune system to fight cancer. Advances in the understanding of the molecular principles underlying the immune system role on cancer led to the development of several anti-cancer strategies that include immunostimulants, monoclonal antibodies, and cancer vaccines [62].

Research in molecular oncology has also increased the number of identified proteins whose malfunction contributes to the formation and maintenance of tumors. Some of these proteins constitute attractive targets for novel anti-cancer therapeutic agents. Targeted therapy refers to the systemic administration of drugs that specifically act on well-defined targets or biologic pathways which, when activated or inactivated, may cause regression or destruction of tumor cells, while minimizing adverse effects on nearby tissues [63, 64]. Moreover, the increased number of targeted anticancer therapeutics can be categorized according to their effects on the hallmark capabilities [45].

Considering cancer heterogeneity the appropriate combined use of several anticancer therapies may contribute more efficiently for treatment of the disease. Furthermore, the increased screening and the rise of more sensitive techniques results in a timely detection of tumors, which consequently increases therapeutic approach efficiency. Although there

is still no one cure for cancer, the advances on cancer knowledge so far led to remarkable improvements regarding cancer therapy and prevention.

1.3 Cancer Incidence and Statistics

Cancer is the leading cause of death worldwide accounting for 7.6 million deaths (or about 13% of all deaths) in 2008. Cancer has a higher incidence in economically developing countries (4.8 million) than in economically developed countries (2.8 million) [65]. In 2008, lung (1.37 million deaths), stomach (736,000 deaths), liver (695,000 deaths), colorectal (608,000 deaths), female breast (458,000 deaths), and cervical cancer (275,000 deaths) were the most prevalent cancer types accounting for about 40% of all diagnosed cases [66].

The global burden is expected to grow up to 21.4 million new cancers cases and 13.2 million cancer deaths by 2030, based on population growth and aging as cancer incidence rises dramatically with age [67]. However, these numbers may get even higher due to the adoption of western lifestyles, namely smoking, poor diet, and reduced physical activity.

Cancer occurrence varies geographically. The factors that contribute to these regional differences are related with the prevalence of major risk factors, availability and quality of cancer screening and treatment. For example, approximately 15% of all cancers are attributed to infections, this percentage being higher in developing countries (26%) than in developed countries (8%) [66]. Moreover, around 47% of cancer cases and 55% of cancer-associated deaths occur in less developed regions [68].

Cancer risk highly increases with age since around 78% of newly diagnosed cancers occur at the age of 55 or older in developed countries, this rate being lower in developing countries due to differences in age structure of the populations [66]. Although, inherited genetic alterations also contribute for increased cancer risk only about 5% of cancers are strongly hereditary.

Between the years of 2002 to 2008, an estimate 68% survival rate for all diagnosed cancers was observed compared with the 49% in the years comprised between 1975 and 1977 [1]. This improvement in survival reflects the progress in cancer diagnosis in an earlier

[1] Statistics available on the public domain http://www.cancer.org.

stage and improvement of available treatments. In fact, a substantial proportion of all cancers can be prevented with the acquisition of healthier lifestyles, i.e. avoiding risk factors such as cigarette smoking or heavy alcohol consumption. Tobacco is by far the most important cancer risk factor being responsible for 22% of overall cancer deaths and 71% of lung cancer deaths in 2008 [69, 70]. Other important risk factors include alcohol abuse, unhealthy diet and physical inactivity.

Infectious agents, such as human papilloma virus (HPV), hepatitis B virus (HBV), and *Helicobacter pylori*, constitute other major cancer risk factor with estimated 16.4% new cases in 2008 [71]. Cancer associated with specific infections may also be prevented through behavioral changes, vaccination and/or antibiotics.

In addition to prevention, regular screening tests allow early cancer detection and removal of pre-cancerous growths. Earlier detection results in less extensive treatment approaches allowing for better outcomes, and reduced mortality rates. However, screening has been proven to be effective in reducing mortality for only breast, cervical and colorectal cancers.

Cancer awareness campaigns have been largely contributing for society knowledge of risk factors and their avoidance, leading to the observed increase in survival rates and quality of life. This reveals the importance of raising "educated populations", meaning that the understanding of cancer complexity and how a healthy lifestyle and regular screening might contribute to a decrease in cancer incidence and mortality. Although the identification and study of factors that affect cancer development, cancer epidemiology, has revealed to be of extreme importance in the prevention of some types of cancer, the high complexity of this disease implies a multidisciplinary approach.

1.3.1 Lung Cancer

Lung cancer constitutes the most common deadly cancer, accounting for 13% of the total cancer cases diagnosed and 18% of the deaths in 2008 with a considerably higher incidence in men than in women [68]. In men, the highest lung cancer incidence rates were in Northern America, Europe, and Eastern Asia while the lowest rates were in sub-Saharan Africa (Fig.1.3). Among women, the highest lung incidence rates were in Northern America, Northern Europe, and Eastern Asia (Fig.1.3). Interestingly, despite the

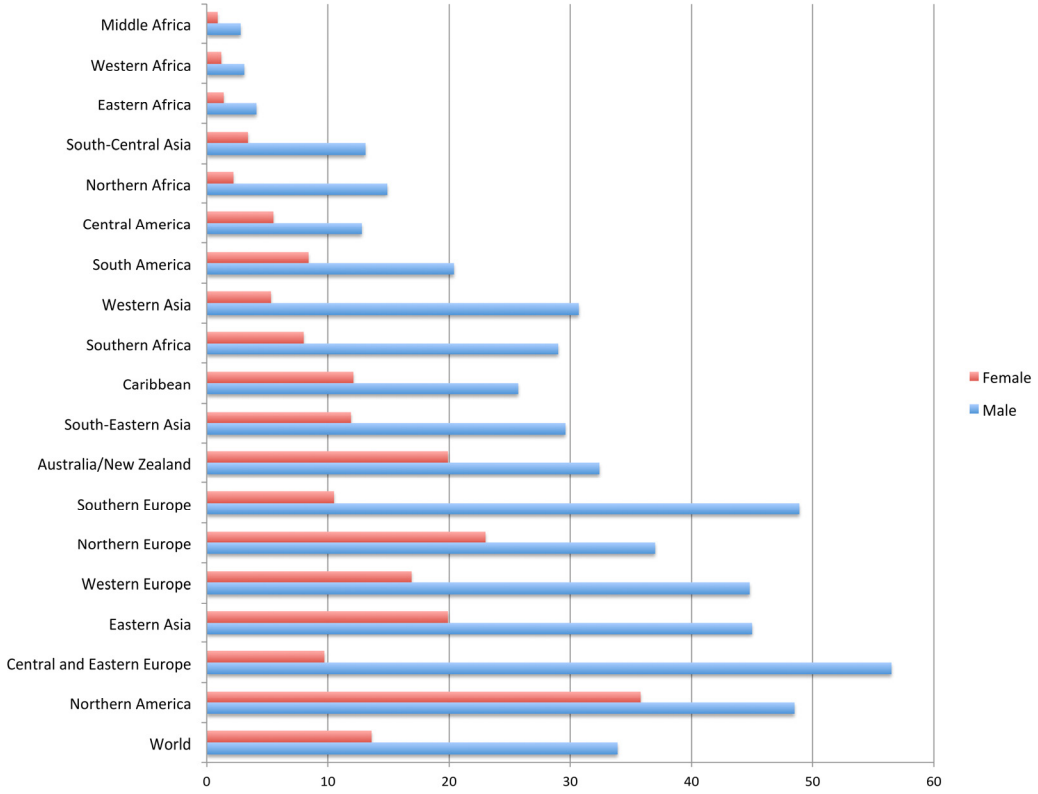

Figure 1.3 - Lung cancer incidence. World age-standardized lung cancer incidence rates by sex and world area. Source: GLOBOCAN 2008, in globocan.iarc.fr.

higher lung cancer rates, the prevalence of smoking is low among Chinese women. This apparent contradiction is explained by indoor air pollution from unventilated coal-fueled stoves and cooking fumes [72].

Geographic variations in lung cancer rates reflect differences in the stage and degree of tobacco consumption [73]. Moreover, the observed differences in lung cancer rates between genders are related with the fact that women only started smoking in large numbers decades later than men.

Cigarette smoking constitutes the most important risk factor for lung cancer. Tobacco smoke contains several carcinogens, which include complex aromatic hydrocarbons, and nitrosamines [74]. These carcinogens may induce cellular genetic alterations that in turn may lead to oncogenic transformation. Other risk factors include second-hand smoke, occupational or environmental exposures to radon and asbestos, as well as to air pollution

[75]. In addition, genetic susceptibility is also known to increase the risk of lung cancer development [76]. Moreover, some individuals might also spontaneously develop lung cancer without any exposure to carcinogens.

Overall, lung cancer is one of the most preventable cancers. Worldwide burden of lung cancer could be decreased by implementation of tobacco control interventions that include significantly increasing the price of cigarettes, banning smoking in public places, restricting advertisement, and counter advertising in order to achieve lower smoking rates.

Treatment and prognosis depend on the type of lung cancer (small *versus* non-small cell) and stage at diagnosis. Standard oncological therapies are effective in the treatment of some lung cancer cases. Localized carcinomas are usually removed through surgery. Moreover, survival with early detection of non-small cell lung cancer improved by combination treatment with chemotherapy followed by surgery. However, considering the rapid lung cancer cell division, by the time small cell lung cancers are detected, these are already disseminated resulting in a poorer prognosis when compared to early detection of non-small cell lung cancer [77].

Lung cancer is usually characterized by a poor prognosis with a five-year survival rate of around 15%. The five-year survival rate reaches the 53% for cases of early detection[2]. However, the majority of the cases are only diagnosed in an advanced stage of progression. Despite the advances in treatment methods, and combined therapies, lung cancer is still one of the most lethal cancers.

[2] Statistics from 1975 to 2007 available at http://seer.cancer.gov/csr/1975_2007/.

Chapter 2

Mitochondria in tumor cells: what is so different about them?

2.1 The Warburg Effect and mitochondrial metabolism in tumor cells
2.1.1 The Warburg effect
2.1.2Metabolic reprogramming provides a selective advantage for cancer cells
2.1.3 Targeting aerobic glycolysis
2.2 Altered mitochondrial oxidant production in cancer cells
2.2.1 Targeting mitochondrial oxidative stress in tumor cells
2.3 Mitochondrial DNA mutations and cancer
2.3.1 Mitochondrial DNA as a predictive marker in the diagnosis and staging of cancer
2.4 Altered mitochondrial transmembrane electric potential in cancer cells
2.4.1 Targeting mitochondrial hyperpolarization in tumor cells

Mitochondria have many roles in normal cells: they are the main producers of energy via oxidative phosphorylation, they produce many metabolic intermediates, and they mediate the intrinsic and extrinsic apoptotic pathways [78]. Mitochondria have these same essential roles in cancer cells. However, mitochondria undergo profound changes during oncogenesis, which commonly result in altered energy metabolism, resistance to apoptosis and increased production of reactive oxygen species (ROS). This section aims to review recent developments in cancer mitochondrial metabolism research, with the goal of better understanding the role of mitochondrial changes in the pathogenesis of cancer

and the potential for novel therapies targeting these changes. It starts by reviewing mitochondrial oncogenic alterations "Mitochondria in tumors cells". This will include alterations of mitochondrial metabolism (Section 2.1) and oxidative stress (Section 2.2) in cancer cells; followed by what is known about the role of mtDNA alterations in cancer progression (Section 2.3) and alterations in mitochondrial mitochondrial membrane potential in tumors (Section 2.4).

2.1 The Warburg Effect and mitochondrial metabolism in tumor cells

2.1.1 The Warburg effect

Often called the furnace of the cell, mitochondria synthesize the vast majority of chemical energy (in the form of adenosine triphosphate, ATP) that cells use for anabolism and catabolism. Under normoxic conditions, cells normally rely on aerobic respiration which makes use of both cytosolic and mitochondrial processes to generate energy via oxidation of glucose, fatty acids and amino acids. In this process, glucose is partially oxidized to pyruvate in the cytosol. Pyruvate is then imported into mitochondria where it is fully oxidized in two stages, including a first set of reactions in the tricarboxylic acid (TCA) cycle and then a stepwise oxidation of resulting metabolites through the electron transport chain (a process also known as oxidative phosphorylation or OXPHOS). Other metabolic substrates that feed into the TCA cycle are fatty acids via beta oxidation to acetyl coenzyme A (acetyl-CoA), and glutamine via serial deamination of glutamine to glutamate and then to alpha-ketoglutarate [79].

Although aerobic respiration in mitochondria is the most efficient method of energy generation, it requires non-limiting oxygen availability. When oxygen levels are low, untransformed cells rely on an alternative cytosolic process, glycolysis, followed by lactic acid fermentation. In this process, glucose is converted to pyruvate by means of glycolysis, but pyruvate is then reduced to lactate by lactate dehydrogenase in the presence of NADH (nicotinamide adenine dinucleotide) rather than being transported into the mitochondria. This process generates far less energy per molecule of glucose than OXPHOS, but allows the cell to continue generating energy under hypoxic conditions.

The initial observation linking altered mitochondrial metabolism to cancer was made by Otto Warburg in a classic study of tumor energy metabolism [80]. Using slices of living tissue, Warburg observed that whereas normal cells use lactic acid fermentation only in the absence of oxygen, tumor cells show increased levels of lactic acid production even under aerobic conditions [80]. Warburg proposed that neoplastic cells undergo a metabolic shift from aerobic respiration to aerobic glycolysis, involving lactic acid fermentation, which would occur even at normal oxygen tensions. This shift is now recognized as the Warburg effect. Warburg further proposed that cancer cells rely on less efficient aerobic glycolysis to achieve their energy requirements due to defects in the oxidative phosphorylation metabolic pathway [81]. According to this model the first step in cancer development is an irreversible defect in the OXPHOS pathway which stimulates an upregulation of lactic acid fermentation [81].

Subsequent work has confirmed that a shift from oxidative phosphorylation to glycolysis as primary energy source is prevalent among many types of cancers [82]. Further, this work has substantiated the key role of mitochondrial alterations in development of cancer [83]. However, the Warburg effect is now seen in the context of a set of concerted changes in energy metabolism and mitochondrial function that support oncogenesis. This process, often referred to as metabolic reprogramming [84], is proposed to support deregulated proliferation that is an essential feature of cancer cells.

2.1.2 Metabolic reprogramming provides a selective advantage for cancer cells

Metabolic reprogramming in cancer is commonly characterized by two major changes in energy metabolism: reliance on glycolysis rather than oxidative phosphorylation for oxidation of glucose, and increased use of glutamine as an energy source (Fig.2.1).

Glycolytic remodeling

Since glycolysis is far less efficient than oxidative phosphorylation in generating ATP, the question arises as to how glycolysis can provide a selective advantage for rapidly dividing cancer cells, which have high metabolic requirements. Warburg initially proposed that increased glycolysis is an adaptive response to tumor hypoxia, which is consistent with

the fact that tumor cells have to survive in adverse environments characterized by variable oxygen and nutrient supplies, pressuring these cells to adapt their metabolism to the new environment. However, as Warburg himself pointed out, tumors are often highly glycolytic before being exposed to low oxygen conditions suggesting hypoxia is not the only trigger for the metabolic shift [84].

An alternate explanation is that although glycolysis generates far less ATP per glucose than oxidative phosphorylation, it does generate ATP more rapidly. Even in severe pathology and malnutrition, the liver maintains serum glucose concentration within a narrow range. In a situation where glucose supply is not a problem, the more rapid generation of ATP by glycolysis may be better suited to supply the energy needs of rapidly proliferating cells than the arguably more "efficient" OXPHOS. In support of this idea, normal embryonic cells undergoing rapid proliferation display similar reliance on glycolysis [85]. Further, alterations that result in increased intracellular glucose levels are common in cancer cells (Fig.2.1). These include increased expression of glucose transporters [86], and alternate hexokinase isoforms [87] and increased transcription of glycolytic enzymes [88-90]. An additional selective advantage may be provided by export of lactate generated by increased glycolysis, which may contribute to oncogenesis via decreased extracellular pH, leading to increased activity of pro-invasion factors such as matrix metalloproteases and hyaluran, and, re-moving the physical barriers to tumor cell expansion and invasion into healthy tissue [91-93].

However, the most compelling explanation for metabolic remodeling of the glycolytic pathway is that it creates the capability to generate increased levels of biosynthetic intermediates via increased flux through several biosynthetic pathways. For example, the pentose phosphate pathway has an increased importance in cancer cells, because their rapid proliferation requires rapid generation of nucleotides as well as fatty acids and other components of cell membranes. As a result, glucose-6-phosphate is diverted from ATP production to the generation of ribose-6-phosphate and NADPH (nicotinamide adenine dinucleotide phosphate) [94, 95]. Increased use of the pentose phosphate pathway may be promoted by a tumor-specific pyruvate kinase isoform, PKM2, which catalyzes the final rate-limiting step in glycolysis. The increased expression of PKM2 in cancer cells is due to mutually exclusive exon splicing [96] and was shown to be required for aerobic glycolysis in tumor cells as well as for tumor growth [90]. The PKM2 isoform has a lower Km than the other three PK isoforms, and PKM2 is further inhibited by

phosphorylated tyrosines, which are abundant in cancer cells with hyperactive growth factor signaling pathways. Expression of the PKM2 isoform may promote the channeling of glycolytic intermediates through the pentose phosphate pathway. Tumor cells expressing the low-activity PKM2 isoform show an increase in upstream glycolytic metabolites [88], suggesting that the slower glycolysis promoted by less active PKM2 allows glycolytic intermediates to be used for alternate biosynthetic pathways as well as for the maintenance of redox balance needed for to support a rapid cell division [97].

Glutamine metabolism

Tumor cells undergo a second major shift in energy metabolism, a dramatic upregulation in glutamine consumption (Fig.2.1). Rossignol *et al* demonstrated that HeLa cells, which ordinarily show high rates of glycolysis typical of cancer cell, can survive using glutamine alone as a carbon source in a process that requires the TCA cycle and oxidative phosphorylation [98]. This work demonstrated that the shift to glycolysis could be reversed and thus that it was not necessarily due to mitochondrial defects. In addition, the work by Rossignol *et al* provided an indication of the importance of glutamine metabolism for growth of transformed cells. Conversion of glutamine into lactate via malate dehydrogenase produces NADPH, which is required for de novo synthesis of fatty acids, thus fulfilling an important metabolic need of cancer cells [99]. Glutamine has also been reported to be essential for RAS-mediated anchorage independent growth of HCT116 colorectal cancer cells. In this case, glutamine metabolism via the TCA cycle generates ROS that stimulate ERK (extracellular signal-regulated kinase) proliferation signaling pathways [100]. Similarly, glutaminase was found to be essential for transformed phenotype of NIH-3T3 cells and the human breast cancer cell lines MD-MBA-231 and SKBR3 [101]. These studies have established altered glutamine metabolism as a second metabolic alteration in cancer cells, thus supporting that the shift to glycolysis is only one part of a complex network of metabolic reprogramming (Fig.2.1).

Regulation of metabolic reprogramming

In many cases, metabolic reprogramming seems to be directed by oncogenic changes in several interconnected cell signaling pathways including phosphatidylinositol 3-kinase (PI3K) and AMP-activated protein kinase (AMPK) pathways. In normal cells these

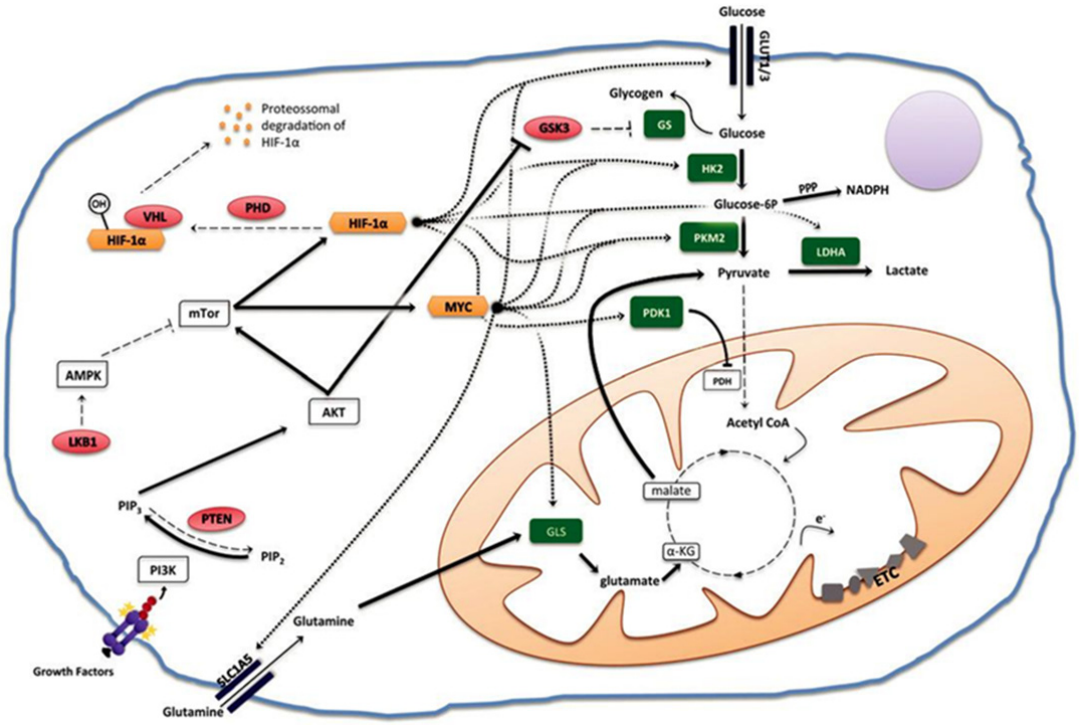

Figure 2.1 - Metabolic remodeling in cancer cells. Metabolic reprogramming in cancer is characterized by two major adjustments in energy metabolism, increased glycolysis and increased use of glutamine as an energy source. These alterations are due to oncogenic changes in several interconnected cell-signaling pathways, which seem to be responsible for the observed metabolic shift. PIK3 activation by various growth factors triggers (bold arrows) a signaling cascade that includes AKT and mTOR. Moreover, mutations in AMPK activator LKB1 are also known to contribute for AKT/mTOR pathway activation through repression (dash arrows) of mTOR inhibition. In turn, mTOR/AKT pathway activation results in GSK3 inhibition and consequent concomitant expression of GS, and also in the upregulation of MYC and HIF1α transcription factors, contributing to metabolic changes. In contrast to normal cells, HIF1α expression is stabilized in tumor cells even under normoxic conditions due to PTEN, VHL, and PHD loss of function mutations (in red). HIF1α constitutive expression promotes transcription (square dot arrows) of genes responsible for an increase in glycolytic pathway those include increased expression (in green) of GLUT1 and GLUT3 transporters; alternate isoforms of glycolytic pathway enzymes HK2 and PKM2; LDHA, and PDK1. Expression of MYC is also known to favor the glycolytic pathway through increased expression of glucose transporters and glycolytic enzymes (square dot arrows). PKM2 increased activity promotes a shuttle of glycolytic substrates through the pentose phosphate pathway. Furthermore, MYC promotes an increase in glutamine metabolism through increased transcription of transporters like SLC5A1, and through increased expression of GLS. Abbreviations: AKT — serine/threonine protein kinase; AMPK — AMP-activated protein kinase; GLS — glutaminase; GLUT — glucose transporter; GS — glycogen synthase; GSK-3 — glycogen synthase kinase 3; HIF1α — hypoxia inducible factor 1, alpha

subunit; HK2 — hexokinase 2; α-KG — alpha ketoglutarate; LDHA — lactate dehydrogenase A; LKB1 — serine/threonine kinase 11; mTOR — mechanistic target of rapamycin (serine/threonine kinase); MYC — v-Myc myelocytomatosis viral oncogene homolog; PDH — pyruvate dehydrogenase; PDK1 — pyruvate dehydrogenase kinase, isoenzyme 1; PHD — prolyl hydroxylase; PIK3 — phosphatidylinositol 3-kinase; PIP — phosphatidylinositol phosphate; PKM2 — pyruvate kinase, muscle 2; PTEN — phosphatase and tensin homolog; SLC5A1 — solute carrier family 5 (sodium/glucose cotransporter), member 1; VHL — Von Hippel–Lindau tumor suppressor.

pathways regulate metabolic pathways in response to environmental conditions including nutrient availability, O2 levels and growth factors. Cancer cells, however, accumulate mutations that remove environmental constraints (Fig.2.1). PI3 kinase is activated by various growth factors binding to their receptor tyrosine kinases. PI3 kinase in turn activates a signaling cascade including AKT and mTOR kinases. These kinases upregulate expression of the MYC and hypoxic transcription factor (HIF) transcription factors, which in turn, upregulate the glycolytic pathway as a whole [80].

In normal cells, HIF1α is rapidly degraded under normoxic conditions and only stabilized under hypoxic conditions. When stabilized, HIF1α, in complex with HIF1β, promotes increased transcription of genes necessary for normal cells to increase glycolytic capacity. These include GLUT1 and GLUT3 glucose transporters, nine of the ten glycolytic enzymes, lactate dehydrogenase (LDH), the enzyme that catalyzes conversion of pyruvate to lactate, and pyruvate dehydrogenase kinase (PDK), which inhibits pyruvate oxidation in mitochondria [102]. However, common oncogenic mutations inactivate PTEN (phosphatase and tensin homolog), a PI3 kinase inhibitor, and VHL (von Hippel-Lindau tumor supressor), required for oxygen-dependent destabilization of HIF1α. Thus, in tumor cells, HIF1α can be stabilized even under normoxic conditions so that glycolysis is enhanced even in the presence of oxygen [103].

Expression of MYC also favors the glycolytic pathway through increased expression of glucose transporters and glycolytic enzymes. MYC also promotes increased glutamine metabolism associated with oncogenesis through increased transcription of transporters SLC5A1 and SLC7A1, and through increased expression of the glutaminase GLS1 [80]. Increased expression of glutaminase occurs through transcriptional regulation and through repression of inhibitory miRNA23a and miRNA23b [104]. MYC is normally activated in response to signaling pathways initiated by growth factors binding to their

receptors. In cancer, MYC is commonly activated in the absence of growth factor signaling by mutations that cause constitutive activation of AKT and mTOR [80].

In contrast to PI3K, AMPK acts to limit glycolysis by acting as a cellular energy sensor. In response to elevated AMP/ATP ratios, AMPK promotes oxidative phosphorylation and inhibits proliferation, in part by inhibiting mTOR kinase. Interestingly, mutations in the up-stream AMPK activator, LKB1, are common in cancers [105].

Multiple mechanisms for activation of HIF1α and MYC point to the importance of the shift to glycolysis for cancer cells [80]. The fact that activation is triggered by common oncogenic signaling pathways suggests that this shift is an essential component of the oncogenic program.

Recently, HIF1α activation has been implicated in driving metabolic changes in cancer-associated fibroblasts. Cancer-associated fibroblasts have been found to be deficient in Caveolin-1 (Cav-1) [101]. Loss of Cav-1 combined with increased ROS produced by neighboring cancer cells results in stabilization of HIF1α. HIF1α-mediated upregulation of glycolytic enzymes results in the over-production of pyruvate and lactate that can be secreted into the medium and fuel the oxidative metabolism in adjacent tumor cells. This phenomenon is termed the "Reverse Warburg effect" [106-108].

Mitochondrial succinate dehydrogenase and fumarate hydratase as tumor suppressors

Although Warburg initially characterized cancer as an injury to respiration, until recently no respiratory chain oncogenes or tumor suppressors had been identified. However, the importance of HIF1α signaling was underscored by the discovery of succinate dehydrogenase (SDH) and fumarate hydratase (FH) as tumor suppressors [109]. Both SDH and FH are TCA cycle enzymes which act to convert succinate to fumarate and fumarate to malate, respectively. SDH is also a functional member of the electron transport chain (ETC) forming complex II [109]. Oncogenic mutations result in an accumulation of their substrates, succinate and fumarate, in the cytosol, leading to a pseudohypoxic response and activation of glycolytic enzymes [110] through inhibition of prolyl hydratase enzyme, the first step of HIF degradation [111]. Loss of function mutations in SDH lead to the development of paraganglioma and phaeochromocytoma [112], while mutations in FH have been implicated in leiomyoma, leiomyosarcoma, and renal cell carcinoma [111].

2.1.3 Targeting aerobic glycolysis

Since one of the main phenotypes presented in most cancer cells is their high glycolytic rate [113], the exploitation of the Warburg effect could represent an approach to perturb and efficiently kill malignant cells by using proper glycolytic inhibitors (Fig.2.2 and Table 2.1). 2-Deoxyglucose (2-DG), a glucose analog which is metabolically inactive, and 3-bromopyruvate, a lactic acid analog undergoing preclinical trials, constitute two examples of chemical compounds that inhibit glycolysis. Both 2-DG and 3-bromopyruvate treatment lead to ATP depletion which in turn results in dephosphorylation of the pro-apoptotic BAD protein, BAX migration to mitochondria, permeabilization of mitochondrial outer membrane and consequent cell death [114] with minimal toxic effects to normal cells [115]. Suppression of intracellular ATP level by 2-DG alone or in combination with glucose-free medium promotes Fas-induced phosphatidylserine externalization during apoptosis [116]. 2-DG compromises glycolytic metabolism through the ability to competitively inhibit hexokinase, decreasing its association with the outer mitochondrial membrane and decreasing the threshold for mitochondrial induction of apoptosis [117]. In addition, 2-DG enhances the anticancer activity of doxorubicin and paclitaxel [118], and acts synergistically with histone deacetylase inhibitors [119]. 3-Bromopyruvate also inhibits hexokinase, and when used in combination with mTOR inhibitors, displays synergistic effects on leukemia and lymphoma cells [120, 121]. Whether 3-bromopyruvate will move forward to clinical trials is still uncertain at this time.

Lonidamine, a derivative of indazole-3-carboxylic acid, inhibits glycolysis under hypoxic conditions [122] and has also been demonstrated to inhibit the mitochondrial adenine nucleotide translocase (ANT) [123]. Despite its anticancer efficacy, lonidamine is toxic to non-tumor tissues. In fact, toxicity was observed when lonidamine was co-administrated with doxorubicin, cyclophosphamide or cisplatin to a mouse xenograft model [124]. In a dog model, lonidamine was also shown to cause hepatoxicity [125]. Despite the potential liabilities to non-tumor tissues, lonidamine is currently undergoing phase III/IV clinical trials, after promising phase II–III trials [126, 127].

Dichloroacetate (DCA), a pyruvate analog, stimulates pyruvate dehydrogenase enzyme (PDH) through the inhibition of PDK1. DCA has an inhibitory impact in cancer cells with altered mitochondrial activity [128], while showing no effect on normal cells [129].

Table 2.1 - Summary of the anti-cancer agents and phase of their clinical development.

Agent	Cellular Target	Phase of clinical development						References
		Pre-Clinical		Clinical Trials				
		in vitro	*in vivo*	Phase I	Phase II	Phase III	Phase IV	
2-DG	HK2	✓	✓	✓	✓	–	–	NCT00633087 [a]
2-ME	Cu–ZnSOD MnSOD	✓	✓	✓	✓	–	–	[130]
3-Bromopyruvate	HK2	✓	✓	–	–	–	–	[115]
5-Aminolevulinic acid	OXPHOS	✓	✓	✓	–	–	–	[131]
ABT-263	BCL-2	✓	✓	✓	✓	–	–	[132]
ABT-737	BCL-2	✓	✓	–	–	–	–	[133]
Antimycin A	OXPHOS	✓	✓	–	–	–	–	[134]
As_2O_3	OXPHOS ANT, VDAC	✓	✓	✓	✓	✓	✓	[135]
Berberine	OXPHOS ANT	✓	✓	–	–	–	–	[136]
Bismaleimido-hexane	ANT	✓	–	–	–	–	–	[137]
Bullatacin	OXPHOS	✓	✓	–	–	–	–	[138]
Cisplatin	DNA	✓	✓	✓	✓	✓	✓	[139]
Curcumin	BAX, BCL-2, BCL-X_L	✓	✓	✓	✓	–	–	[140]
DCA	PDH	✓	✓	✓	–	–	–	[128]
Dithiodipyridine	ANT	✓	✓	–	–	–	–	[141]
Doxorubicin	OXPHOS	✓	✓	✓	✓	✓	✓	[142]
EGCG	HSP70, HSP90 p68	✓	✓	–	–	–	–	[143, 144]
F16	OXPHOS	✓	–	–	–	–	–	[145]
FGIN-1-27	PBR	✓	✓	–	–	–	–	[146]
Gossypol	BCL-2, BCL-X_L	✓	✓	✓	✓	–	–	[147]
HA14-1	BCL-2	✓	✓	–	–	–	–	[148]
Lonidamine	HK2 ANT	✓	✓	✓	✓	✓	✓	[126, 127]
Menadione	Redox-cycling agent	✓	✓	✓	✓	–	–	[149]
Metformin	AMPK	✓	✓	✓	✓	–	–	[150]
MKT-077	mtDNA	✓	✓	✓	–	–	–	[151]
Motexafin gadolinium	AKT	✓	✓	✓	✓	✓	–	[152]
Obatoclax	BCL-2, BCL-X_L	✓	✓	✓	✓	–	–	[153]
Oligomycin	OXPHOS	✓	–	–	–	–	–	[134]
PEITCs	GSH	✓	✓	–	–	–	–	[154]
Phloretin	GLUT2	✓	✓	–	–	–	–	[155]

Agent	Cellular Target	Phase of clinical development						References
		Pre-Clinical		Clinical Trials				
		in vitro	*in vivo*	Phase I	Phase II	Phase III	Phase IV	
PK11195	PBR	✓	✓	–	–	–	–	[156]
Resveratrol	OXPHOS	✓	✓	✓	✓	–	–	[157]
Rhodamine-123	OXPHOS	✓	✓	✓	–	–	–	[151, 158]
Ro5-4864	PBR	✓	✓	–	–	–	–	[159]
Rolliniastatin	OXPHOS	✓	✓	–	–	–	–	[160]
Rotenone	OXPHOS	✓	✓	–	–	–	–	[161]
Sanguinarine	OXPHOS	✓	✓	–	–	–	–	[162]
Thenoyltrifluoroacetone	OXPHOS	✓	–	–	–	–	–	[163]
Troglitazone	$PPAR_{\gamma}$	✓	✓	✓	✓	–	–	[164]
Vinblastine	DNA	✓	✓	✓	✓	–	–	[165]
α-TOS	OXPHOS	✓	✓	–	–	–	–	[166]
β-Lapachone	NQO1	✓	✓	–	–	–	–	[167]

* Clinical trials number identifier found in http://clinicaltrials.gov at April 16, 2012.

Abreviations: AKT – serine/threonine protein kinase; AMPK – AMP-activated protein kinase; ANT – Adenine nucleotide translocase; BCL-2 – B-cell CLL/lymphoma 2; BCL-XL – B-cell lymphoma extra large; BAX – Bcl-2 associated X protein; DCA – Dichloroacetate; 2-DG – 2-Deoxyglucose; DNA – Deoxyribonucleic acid; mtDNA – Mitochondrial DNA; EGCG – Epigallocatechin-3-gallate; GLUT – Glucose transporter; GSH – Glutathione; HK2 – Hexokinase 2; 2-ME – 2-Methoxyestradiol; OXPHOS – Oxidative phosphorylation; NQO1 – NAD(P)H quinone oxidoreductase 1; PBR – Peripheral benzodiazepine receptor; PDH – Pyruvate dehydrogenase; PEITC – Phenyl ethyl isothiocyanates; $PPAR_{\gamma}$ – Peroxisome proliferator activated receptor gamma; SOD – Superoxide dismutase; α-TOS – alpha tocopherol succinate; VDAC – Voltage-dependent anion channel.

DCA indirectly stimulates con-version of pyruvate to acetyl-CoA and up-regulates mitochondrial metabolism [128, 168]. It is suggested that mitochondria in several types of tumors are particularly susceptible to this transition as their metabolism is not able to quickly restart oxidative phosphorylation; instead, mitochondria suffer apoptotic alterations and trigger cell death [128, 168]. DCA is currently undergoing Phase I clinical trials after several *in vitro* studies and clinical trials for the improvement of mitochondrial diseases [128]. Despite this, doubts remain on the joint use of DCA with other conventional and clinically used chemotherapeutics [169].

Besides the effects of inhibition of the glycolytic pathway, suppression of glucose transport might also sensitize tumor cells to anti-cancer agents. For instance, phloretin, a glucose transporter inhibitor, was reported to profoundly enhance the anticancer effects of daunorubicin [170], although further studies need to be performed to even consider the use of that agent in clinical trials.

2.2 Altered mitochondrial oxidant production in cancer cells

Reactive oxygen species are a component of cell signaling pathways in normal cells, regulating proliferation, gene transcription and metabolism, among others [171]. Some species, especially hydrogen peroxide (H_2O_2), act as important intracellular messengers which can regulate both cell death and survival [172, 173]. The mitochondrial electron transport chain is considered one important site for ROS production, with ten different sites recognized to participate in ROS generation [174] and several more regulated by redox alterations [175]. Antioxidant mechanisms in mitochondria have both an enzymatic and non-enzymatic component. Enzymes such as manganese-superoxide dismutase (SOD2), glutathione peroxidase (GPx), glutathione reductase (GRed), peroxiredoxins, glutaredoxins and proteins such as cytochrome c itself can contribute to ROS detoxification [174]. Non-enzymatic defenses include reduced glutathione (GSH) and a high NAD(P)H/NAD(P) ratio. When ROS generation overloads antioxidant defenses, generalized oxidative stress occurs, which can trigger cell death [176].

In cancer cells, ROS production is often augmented [177], which in turn acts to induce genetic instability through the accumulation of mutations [178]. The exposure to a hypoxic environment enhances mitochondrial ROS production [179], although this appears to be counter-intuitive. Cells exposed to hypoxia respond acutely through production of endogenous metabolites and proteins that regulate metabolic pathways. However, when present in a continuous low oxygen microenvironment, cells activate adaptive mechanisms including HIF1α [180], which also result in increased ROS production by still fairly unknown mechanisms [181] and which contribute to metabolic remodeling. One particular source of mitochondrial ROS is p66Shc, which has been implicated in carcinogenesis. As an example, p66Shc-derived ROS has been implicated in

androgen-induced prostate cancer cell proliferation and early prostate carcinogenesis [182]. p66SHC was initially thought to use reducing equivalents derived from the mitochondrial ETC to produce H2O2 in the intermembrane space [183]. Recent evidence suggests that p66Shc increases mitochondrial oxidative stress by negatively regulating SOD2 activity [184]. p66SHC null fibroblasts were shown to be resistant to ROS-induced apoptosis in a TP53 dependent manner, indicating that p66Shc has a downstream effect from TP53 [184, 185]. Among the mitochondrial enzymatic systems described above, SOD2 is one of the most effective antioxidant enzymes with anti-tumor activity [186]. In fact, overexpression of SOD2 in several cell lines leads to tumor growth retardation [187]. Further, SOD2 activity was found to be rather low in many cancers [187], with evidence pointing to a defect in gene expression rather than to its deletion, most likely due to epigenetic silencing [186]. For certain tumor cells, the activity of total SOD has also been found to be reduced [188]. However, overexpression of mitochondrial SOD2 correlates with poor prognosis, advanced stages of progression, and an invasive and metastatic profile in cancers of the gastrointestinal tract while SOD expression and activity appear unchanged in some tumor cells [189, 190]. The heterogeneity of SOD expression levels suggests that different cancers or cancer stages may have different optimal levels of oxidative stress or may use alternate pathways to manage oxidative stress.

Another important contributor to ROS generation in mitochondria from cancer cells is the respiratory chain, namely proteins that are found mutated in cancer. For example, a mutation in SDH subunit C results in increased superoxide anion production, oxidative stress, increased glucose consumption and genomic instability [191]. The effects were mimicked by inhibitors of the respiratory chain and also resulted in increased glucose deprivation-induced stress on cancer cells [192]. Mutations of SDH gene, including those affecting subunit C, have been associated with rare paragangliomas [193], suggesting that mitochondrial oxidative stress resulting from SDH mutations may be one driving force for the development of this type of tumors.

Based on these observations, it appears that alterations in mitochondrial antioxidant machinery and free radical production exist in mitochondria from tumor cells, although differences vary according to the tumor type. One logical explanation is that antioxidant defenses must be regulated to a point in which ROS are high enough to be effective in generating a malignant phenotype, but controlled enough to avoid triggering cell death. Nevertheless, increased oxidative stress in cancer not only contributes to metabolic

remodeling via HIF1α, but also promotes the malignant phenotype via the activation of several survival pathways, disruption of cell-death signaling, and increased cell proliferation [178]. In addition, it has been proposed that increased mitochondrial and non-mitochondrial oxidative stress in the primary site may increase the likelihood of metastasis progression [194] and regulate angiogenesis [195].

2.2.1 Targeting mitochondrial oxidative stress in tumor cells

As described above, some types of tumors are characterized for having increased oxidative stress and altered modulation of antioxidant defenses. In some particular cases, it can be envisioned that overloading the antioxidant defenses by increasing mitochondrial oxidative stress over a certain threshold may lead to cell death. In normal cells, the same process would take longer to occur since basal mitochondrial oxidative stress would be lower. In fact, many anti-tumor agents have been reported to act as pro-oxidant agents, disturbing the mitochondrial respiratory chain and leading to further increase in mitochondrial oxidative stress [196], with example being cisplatin, vinblastine and doxorubicin [165] (Fig.2.2 and Table 2.1). These three agents were thought to inhibit cancer cell proliferation primarily through DNA-related mechanisms; however mitochondria is an important secondary target. Anthracyclines are chemotherapeutic agents that have multiple effects on mitochondria of both healthy and tumor cells [197]. For example, Oliveira and Wallace demonstrated that doxorubicin-induced cardiac toxicity relates with oxidative stress, inhibition of mitochondrial respiration and increased mitochondrial permeability transition (MPT), which also involved inhibition of ANT expression [142]. Other studies indicate that menadione (2-methyl-1,4-naphthoquinone), bismaleimido-hexane, and dithiodipyridine also act as ANT thiol oxidizing agents overcoming BCL-2 mediated protection [137]. Despite the interesting results *in vitro*, these three agents require further characterization before being tested under clinical trials.

In addition, agents such as motexafin gadolinium and β-lapachone (ARQ 501) are also known for triggering excessive ROS production. The former is characterized by a high oxidizing potential inhibiting antioxidant systems whereas the second undergoes several redox cycles catalyzed by NAD(P)H quinone oxidoreductase 1 (NQO1) [167]. From the two,

only motexafin gadolinium is currently undergoing Phase II clinical trials, although results were modest against refractory chronic lymphocytic leukemia [198].

Chemicals that resemble ubiquinone can act to inhibit complex II via competitive binding; examples are some benzoquinone derivatives, monoamine oxidase inhibitors and vitamin E analogs. For instance, agents such as α-tocopherol succinate (α-TOS) a vitamin E analog, represent excellent candidates for cancer therapy. α-TOS competes with ubiquinone in binding to Q sites on complex II of the respiratory chain. This connection disrupts the electron flux and destabilizes the mitochondrial membrane, consequently generating superoxide anion [166]. Furthermore, α-TOS promotes BAX translocation to the mitochondria and subsequent cytochrome c release resulting in programmed cell death [199]. Treatment with α-TOS seems to be selective for tumor cells since it is not toxic for normal cells due to their differential metabolism of the parent compound [200, 201]. Despite very promising *in vitro* data, still no clinical trials are being performed with α-TOS.

In addition to the mentioned drugs, arsenic trioxide also promotes ROS increase by increasing electron leakage in the mitochondrial electron chain [202]. Numerous results show that arsenic trioxide (As_2O_3) treatment of cultured cells decreased oxygen consumption and increased superoxide production, indicating a disturbance of mitochondrial respiration [202-204]. At low doses, arsenic trioxide exerts an anticancer effect on tumor cells with no acute toxic effects on normal cells [205]. Arsenic trioxide is currently undergoing phase III/IV clinical trials and human data shows that consolidation to standard induction and consolidation therapy significantly improves event-free and disease-free survival in adults with newly diagnosed acute promyelocytic leukemia (ACL) [135]. Also, arsenic trioxide was found to be effective when used alone in terms of durable response and safe in new cases of diagnosed ACL [206].

On the other hand, inhibition of antioxidant systems constitutes an alternative approach to increase ROS accumulation in tumor cells. High levels of GSH have been associated with tumor drug resistant phenotype therefore depletion of cellular GSH can restore sensitivity to the cytotoxic effect of an anticancer drug. Phenyl ethyl isothiocyanates (PEITCs) stimulates or activates phase II detoxification enzymes exerting a potent chemotherapeutic effect without elevated toxicity to normal cells [154]. PEITC's mechanism of action relies on the inhibition of glutathione antioxidant pool by modifying thiol groups in malignant cells [207]. Consequently, the excessive ROS output results in

oxidative mitochondrial damage and cell death. The idea looks attractive *in vitro* but clinical trials are needed to demonstrate the validity of this approach.

2-Methoxyestradiol (2-ME), an endogenous metabolite of 17β-estradiol, not only inhibits tumor angiogenesis but also inhibits both cytosolic Cu–ZnSOD and mitochondrial MnSOD, as well as enhances superoxide anion generation and induces apoptosis in leukemia cells through a ROS-mediated mechanism [208]. Preclinical studies showed 2-ME selective cytotoxicity for leukemia cells in comparison to normal lymphocytes [209]. 2-ME synergizes with rotenone, a complex I inhibitor and pro-oxidant under some conditions, that is responsible for increasing cellular free radical accumulation and trigger apoptosis [210]. 2-ME has been investigated against advanced, platinum-resistant ovarian cancer and primary peritoneal carcinomatosis in a small group of patients. Although the anti-tumor activity was modest in this particular study, toxicity was found to be low, opening the door to further developments of the molecule [211]. Oncogenic changes in mitochondria were originally thought to represent mitochondrial dysfunction which forced a shift to glycolysis. However, accumulated evidence now suggests that mitochondrial changes provide a selective advantage to cancer cells and that these changes are more complex and dynamic than a simple switch to glycolysis. For example, glutamine metabolism via the TCA cycle has been identified as a second major metabolic shift in cancer cells (see Section 2.1.2.2). In accord with this more recent model, mitochondrial inhibition has been widely used in cancer therapy.

In animal models, the complex I inhibitor rotenone by itself exhibits anti-tumor activity [212], which is a feature common to other inhibitors of mitochondrial respiratory chain, including antimycin A, a complex III inhibitor and oligomycin, a complex V inhibitor. The two latter agents were demonstrated to induce apoptotic cell death in cultured human lymphoblastoid cells [134]. Inhibition of the mitochondrial respiratory chain can induce other forms of cell death as well. Rotenone, by acting as a complex I inhibitor, can selectively induce autophagic cell death via a ROS-mediated mechanism in the transformed cell line HEK 293 and in cancer cell lines U87 and HeLa [213]. Mitochondrial dependence of effects of rotenone or other OXPHOS inhibitory drugs are supported by reports that cells lacking functional mitochondria are not as susceptible to those molecules [214, 215].

Understandably, the toxic nature of classic mitochondrial inhibitors limits their possible clinical application but can provide evidence that the concept works and serve as useful

experimental standards by which to judge the efficacy of other ETC targeted drugs. However, in addition to its inhibitory effect on mitochondrial respiration, rote-none has also microtubule-depolymerizing activity [216]. Therefore, this fact should be taken into account when interpreting data from cells with higher proliferation rates, including tumor cells. In fact, the use of rotenone to induce Parkinson's disease has already been questioned, since it appears that the mechanism involved in disease development does not involve complex I inhibition by rotenone but its anti-microtubule activity instead [217]. However, the microtubule and electron transport chain effects of rotenone may be linked. An interesting recent report also demonstrated that destabilization of tubulin by rotenone depolarizes mitochondria through VDAC (voltage-dependent anion channel) modulation, and consequently regulates not only respiration but also the metabolic status of cancer cells [216].

Acetogenins such as rollinistatin and bullatacin are among the most potent inhibitors of the mitochondrial complex I, and they are also effective inhibitors of tumor cell proliferation [218]. Thenoyltrifluoroacetone, a chelating agent, can slow tumor cell cycle progression, and increase ROS production and glutathione oxidation by inhibiting mitochondrial complex II [163]. The data appear to suggest that inhibition of complex II, the tumor suppressor succinate dehydrogenase, can be a good choice as a mitochondrial target in neuroblastoma cells, as inhibition by malonate also leads to increased ROS production, p38 MAPK activation and BAX mediated apoptosis [219]. None of the compounds described here has been tested in humans, being still in an early phase of the drug development process.

Natural compounds have long been studied for their anticancer properties; besides the vitamin E analogs referred to above, another example is epigallocatechin-3-gallate (EGCG), a green tea polyphenol known for its ability to induce apoptosis. Elevated concentration of EGCG causes ROS accumulation in malignant cells but not in normal cells; this characteristic makes the compound a good candidate for therapy [154]. Although extensive *in vitro* data exist, there is still the need for solid human data to demonstrate the preventive or chemotherapeutic effects of EGCG. This is further confirmed by some epidemiologic studies demonstrating that dietary green tea prevents the development of some types of cancer including colorectal [143] and prostate [144].

Resveratrol, a natural stilbene, was shown to act as a mitocan, i.e. a compound which specifically target mitochondria in tumor cells [220]. Resveratrol can act directly at

several different sites from complexes I to III, possibly competing with ubiquinone binding sites. Moreover, it interacts with complex V, the Fo–F1 ATP synthase [221]. Although resveratrol is generally considered a potent antioxidant, it can also act in favor of oxidant status in cells, inducing apoptosis through the mitochondrial pathway [222]. Although the balance between anti- and pro-oxidant can regulate distinct signaling pathways, it is generally accepted that the pro-oxidant activity of resveratrol is implicated in the anti-cancer mechanism [223]. Resveratrol is currently undergoing phase I/II clinical trials and the safety threshold was calculated to be under 5g/day, despite the occurrence of mild to moderate side effects [157]. Plans are underway to pursue clinical trials to investigate the effects of resveratrol against lymphoma and colorectal cancer, as well to confirm the role of resveratrol in the prevention of colon cancer [224].

Another interesting approach in cancer therapy involving increased oxidative stress in the tumor involves photodynamic therapy (PDT). This technique uses non-toxic molecules, called photosensitizers, which become pharmacologically active in the presence of specific wavelengths [225]. The delivery of a suitable light dose to photosensitized tissues can result in a localized eradication of neo-plastic lesions with reduced damage to healthy adjacent tissues. The efficacy of the process is dependent on the presence of oxygen, suggesting a role for ROS in the therapeutic mechanism [226]. This is strengthened by the observation that upon light absorption, the photosensitizer switches from its singlet state to a triplet state and consequently may react with molecular oxygen forming an excited-state single oxygen [227]. PDT may be used in superficial tumors where light penetration in tissues is more favored. The most common photosensitizers are porphyrin derivatives, although other molecules can also be used [226].

Mitochondria are thought to be a key target of PDT, since PDT-induced cell death seems to predominantly involve a mitochondrial-dependent apoptotic pathway [225]. The hydrophobicity and charge nature of certain porphyrins influence their cellular distribution, resulting in mitochondrial accumulation. In the mitochondrial inner membrane, porphyrin sensitizers have been described to significantly inhibit cytochrome c oxidase and FoF1 ATP synthase, thus disturbing oxidative phosphorylation [228]. In some cases photosensitizers specifically enter mitochondrial pathways. For example, the pre-photosensitizer 5-aminolevulinic acid enters the heme biosynthetic pathway leading

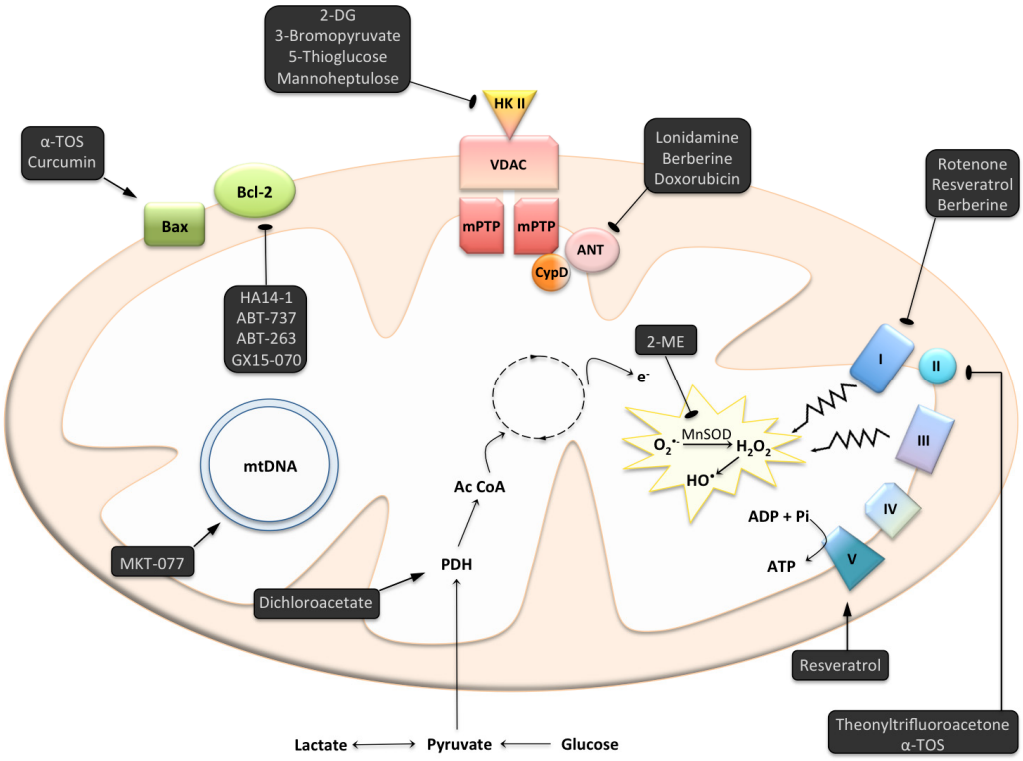

Figure 2.2 - Chemotherapeutic agents targeting mitochondrial alterations. Mitochondria in cancer cells present metabolic alterations, increased oxidative stress, aberrant apoptotic machinery, $\Delta\Psi_m$ alterations and structural changes. Inhibition of OXPHOS through targeting of complex I and/or complex II can be an anti-tumor approach. Besides inhibiting complex I, resveratrol was also described to interact with complex V. Other anti-tumor agents such as 2-DG, 3-bromopyruvate, 5-thioglucose, and mannoheptulose are known to inhibit HKII, decreasing its ability to bind to the outer membrane VDAC, compromising tumor cell glycolytic metabolism. ANT, other possible regulator of the mPTP, has also been considered a therapeutic target. Its inhibition may slow cellular glycolytic rate and prone mitochondria to apoptotic stimuli. Recently, several small molecules that mimic Bcl-2-like proteins BH3 domain have been developed, which act by binding to and/or antagonize Bcl-2 and Bcl-XL. α-TOS and curcumin were described to induce Bax translocation to mitochondria and outer mitochondrial membrane permeabilization. Alterations in the cell redox balance can also be a useful strategy. Antioxidant systems suppression can contribute for lethal oxidative stress in cancer cells. One example is 2-ME which inhibits mitochondrial MnSOD activity. Also shown in the figure is PDH stimulation by dichloroacetate, which increases mitochondrial capacity in cancer cells, decreasing the Warburg phenotype, and MKT-077, whose effects on mitochondria include direct damage to mtDNA.

to accumulation of PpIX in mitochondria [226]. In addition, some photosensitizers were shown to interact with specific mitochondrial molecules/proteins, such as cardiolipin or

the peripheral benzodiazepine receptor (PBR), leading to their mitochondrial accumulation [226]. PBR overexpression in tumor cells (see Section 3.1) may suggest enhanced mitochondrial porphyrin accumulation based on a specific interaction with that receptor.

An alternative and paradoxical approach relies on the use of anti-oxidants in anti-tumor therapeutics. Antioxidants have been described to counteract harmful effects of ROS and consequently contribute in the treatment of oxidative stress-associated diseases, such as cancer. The use of antioxidants as anti-cancer therapeutics has been controversial because it is thought that these agents may confer a protective advantage to cancer cells rather than inducing cell death. In fact, many antioxidant agents have been shown to be unsuccessful in tumor treatment (reviewed in [229]). Nevertheless, given the role of ROS in activating signaling pathways leading to metabolic remodeling, mitochondrial-directed antioxidants including MitoQ may contribute to normalizing the metabolic phenotype in cancer cells. This antioxidant agent has already been demonstrated to decrease the hypoxic induction of ROS and to destabilize HIF1α protein, reducing its transcriptional activity [230]. *In vitro* assays revealed that MitoQ was 30-fold more cytotoxic to breast cancer cells than to healthy mammary cells, apparently acting through Nrf2 negative regulation of autophagy and cell growth [231].

2.3 Mitochondrial DNA mutations and cancer

Mitochondrial DNA (mtDNA) is a 16,569 base pair super-coiled, double-stranded molecule that contains 37 genes coding for 13 polypeptides of mitochondrial electron transport chain, 22 tRNAs, and 2 rRNAs for protein synthesis [232]. mtDNA includes a non-coding DNA region which consists of three hypervariable regions and a displacement loop (D-loop). The D-loop region harbors regulatory elements required for replication and transcription [233, 234]. Proteins involved in the replication, transcription, and translation of mtDNA are encoded by nuclear genes and targeted to mitochondria [233]. The ETC consists of five multi-enzymatic complexes formed from gene products of 74 nuclear and the 13 mitochondrial genes [235]. Mitochondrial DNA is more susceptible to mutation than nuclear DNA. Besides being in close proximity to the electron transport system where ROS are produced, mtDNA, unlike nuclear DNA, has no protective histones and chromatin structure, has limited repair capabilities, and has no introns [236].

Consistent with these characteristics, many studies have identified mitochondrial DNA alterations in cancers including ovarian, thyroid, salivary, kidney, liver, lung, colon, gastric, and breast cancers [233, 236-239]. Welter *et al* described a 40 bp insertion localized in the COX I gene specific of renal cell oncocytoma [240], and later, deletion mutations in the gene coding for NADH dehydrogenase subunit III were observed in renal carcinoma [241]. In addition to mutations in protein-coding regions, mutations that may affect function have been identified in tRNA genes and the D-loop regulatory region [242, 243].

Consistent with the importance of metabolic remodeling to oncogenesis, cancer-specific mtDNA mutations have been reported and in some cases a functional defect has been identified. However, it has been difficult to determine the functional significance of mtDNA alterations in carcinogenesis for several reasons. First, there are as many as several hundred mitochondria in each cell and mtDNA in a cancer or normal cell may be the same (homeoplasmy) or different (heteroplasmy). Therefore to understand the significance of a mutation it is necessary not only to identify its sequence but also to determine its frequency relative to wild type. Second, there are no tools to experimentally manipulate specific mitochondrial DNA alterations. The traditional tools of genetics, such as transgenic mice, and molecular biology, such as RNA interference, cannot be used reliably. However, it may be possible to discern the significance of specific cancer mitochondrial genomes using mitochondrial swaps or cybrids, in which a cell depleted of mtDNA is repopulated with mtDNA from a different donor, although maintaining the same nuclear background [244]. In this context, cybrids harboring the mitochondrial DNA (mtDNA) polymorphism G10398A found in African-American women with aggressive breast cancer were shown to have slower proliferation rate and cell cycle, increased complex I activity and augmented production of ROS and more depolarized mitochondria. The G10398A cybrid also showed resistance to apoptosis triggered by etoposide and increased ability to form metastasis in vivo [245].

Finally, mitochondrial function, including DNA metabolism, is also determined by the nuclear genome raising the problem of separating nuclear and mitochondrial effects. Studies relating alterations in mtDNA and cancer risk or aggressiveness have just begun but they suggest that mtDNA alterations during development of cancer are more complex than previously suspected [246, 247].

2.3.1 Mitochondrial DNA as a predictive marker in the diagnosis and staging of cancer

As described above, mtDNA alterations have been identified in several cancers. This raises the question of whether these alterations can be used to stratify cancer patients according to distinct mitochondrial phenotypes, allowing for the development of tailored therapies.

Hsu *et al* demonstrated a lower mtDNA content in breast cancer tissues when compared to normal counterparts [248], with other work previously confirming the same observation [249]. Interestingly, cancer cells exhibiting low mtDNA content were more susceptible to anthracycline treatment [248]. The authors proposed that the low mtDNA content might lead to an increase in electron leakage during cancer cell respiration which culminates in an increase of oxidative stress and consequently, to an increased susceptibility to chemical agents that further increase ROS levels, such as anthracyclines. Thus, the low mtDNA content might constitute a biomarker for cancer detection and a sign that chemotherapeutics that act by increased oxidative stress should be used. Nevertheless, in clear contrast, an in-crease in mtDNA copy number was observed in patients with a higher risk for breast cancer [250]. The observed increase in mtDNA copy number was observed to be inversely correlated with antioxidant levels suggesting that increased oxidative stress leads to a compensatory production of mtDNA in order to protect mitochondrial genome from damage [250]. This apparent discrepancy may be resolved by recent results from Bai *et al*, who showed in a large clinical sample of breast cancer patients that the mtDNA content of stage II breast tumor was lower than both stage 0–I and more advanced stage III tumors [251]. These work and others [252-256] suggest that mtDNA content alterations are tumor and stage specific and clearly more research is required to gain a deeper knowledge of how these alterations impact the mitochondrial and redox phenotype of tumor cells.

Besides alterations in mtDNA copy number, numerous mutations on the mitochondrial genome have been reported in cancer. These mutations can occur in both the non-coding and the coding regions of mtDNA and may arise in the female germ line leading to cancer predisposition, or arise in somatic tissues. Mutations in mtDNA may be heteroplasmic, when both mutated and wild-type mtDNA coexist, or homoplasmic. Heteroplasmic, but not the correspondent homoplasmic, mtDNA mutations have been described to contribute

to tumor progression [257]. The most common somatic mtDNA deletion occurs between nucleotides 8470 and 13,477, mtDNA^{4977}, and it is known to accumulate during the aging process, being found in several tissues. Tumor cells were shown to have decreased mtDNA^{4977} content relative to cells in non-tumor tissues. A possible explanation raised by the authors is that this specific deletion may induce metabolic changes that, in the case of normal cells, are of minimal impact in contrast with cells under stress, such as tumor cells in which even low frequencies of this mutation are not tolerable, possibly resulting in bioenergetic failure and cell death [258]. Studies on non-melanoma skin cancer are consistent with previous results demonstrating accumulation of mtDNA^{4977} deletions in normal but not in tumor tissue. It was suggested that this may imply a protective role of mtDNA deletions in the process of tumor formation, since carcinogenesis would require a bioenergetic transformation in which the cells with high mutated mtDNA would be incompetent [259].

2.4 Altered mitochondrial transmembrane electric potential in cancer cells

In 1961, Peter Mitchell proposed a breakthrough hypothesis, the chemiosmotic theory [260], suggesting that in mitochondria, electrons from reducing equivalents are transported downstream of the electrochemical potential of specialized protein complexes, the ETC. Electron transfer allows generation of adequate free energy (∆G), so that some of those complexes pump protons from within the matrix to the intermembrane space (IMS). Ultimately, this establishes a separation of charges (∆Ψ) and chemical species (protons; ∆pH) both contributing to the generation of the proton motive force (∆p). Since the inner mitochondrial membrane is highly impermeable, the ∆p becomes a sink of energy to drive other biochemical reactions, namely ATP synthesis. ATP synthase (Complex V), a transmembranar protein, catalyzes ATP phosphorylation in the matrix side and uses ∆p to release the tightly bound nucleotides from the enzyme [261].

In the early 80's, Chen and his coworkers demonstrated that transformed cells and several carcinoma cell lines show increased uptake of rhodamine 123, a fluorescent probe used to measure $\Delta\Psi_m$, when compared to their control non-tumor counterparts [262]. Since then, it is considered that mitochondria from cancer cell are hyperpolarized.

However, explanations for such phenotype are scarce. In normal cells, the regulation of $\Delta\Psi_m$ depends on cellular energy demand and therefore ATP production; however, cancer cells suffer a metabolic shift towards glycolysis decreasing mitochondrial ATP production, which consequently can increase $\Delta\Psi_m$. This could explain the decrease in $\Delta\Psi_m$ upon DCA treatment which leads to pyruvate usage by mitochondria and shift of the Krebs cycle towards oxidative metabolism [263]. In the same work, it was shown that cancer cells have decreased activity and expression of Kv1.5 potassium channels. The resulted increase in $[K^+]_c$ could promote electroneutral exchange of potassium/protons in mitochondria and ultimately convert ΔpH to $\Delta\Psi_m$. Nonetheless, the detection of overexpressed uncoupling proteins in cancer [264] is apparently contradictory to the notion of mitochondrial hyperpolarization, although it has been widely described that uncoupling proteins have other functions besides mitochondrial uncoupling [265].

2.4.1 Targeting mitochondrial hyperpolarization in tumor cells

Another possible therapeutic approach takes advantage of the higher mitochondrial transmembrane electric potential of most cancer cells. Positively-charged lipophilic molecules can accumulate within mitochondria causing non-specific cell death (Fig.2.2 and Table 2.1) [266]. Rhodamine-123 is selectively toxic toward carcinoma cells [158, 267] and was shown to accumulate in mitochondria [268]. Kidney and breast cancer cells that also retained rhodamine-123 were also highly affected [269]. Although never tested in clinical trials, the data obtained with rhodamine-123 serve as proof of concept for further variations of the same theme.

Belonging to the cyanine dyes family, the analog MKT-077 (FJ-776) was demonstrated to damage mitochondrial DNA and to promote mitochondrial swelling of CX-1 carcinoma cells without significant ad-verse effects in nuclear DNA [270] and to inhibit the growth of five different human cancer cell lines [271]. MKT-077 was indeed a very promising anti-cancer agent, which was initially proposed to have mild and reversible toxicity in non-target organs [272], despite the fact that pre-clinical trials demonstrated that MKT-077 caused a reversible depletion of mtDNA in rat heart, as well as a reversible disruption of liver mitochondrial bioenergetics [272]. Phase I clinical trials revealed that the compound indeed accumulates preferentially in tumors [151], due to their higher $\Delta\Psi_m$ [273]. Despite this, the development of serious renal toxicity in some patients stopped further trials, and

its development as a promising anti-cancer drug was arrested [274]. Nevertheless, the studies demonstrated the concept of selective targeting of mitochondria in cancer cells in vivo, although new agents with decreased liabilities are clearly needed.

The compound F16 was demonstrated to accumulate to a greater extent in the mitochondrial matrix, without strongly binding to mitochondrial membranes. Mitochondrial damage, opening of the MPT pore, cell cycle arrest and cell death are observed after F16 treatment [145]; significantly, these effects are observed in cells resistant to apoptosis [275]. This compound so far has not progressed beyond *in vitro* studies.

Dequalinium, another lipophilic cation, can drastically alter the morphology of mitochondria [276]; in fact, when incubated with BT20 cells, dequalinium-DNA can be imported into the mitochondrial matrix, where most of the effects are caused [277]. No plans for clinical trials are available, which limits the development of this agent as a possible chemotherapeutic.

As described in the previous section, the phytochemical berberine accumulates primarily at lower doses in mitochondria in melanoma cells, although it can still be secondarily accumulated in the cytoplasm and nucleus at higher concentrations [278]. The accumulation of the cationic molecule berberine by mitochondria results into a series of alterations of mitochondrial function, including inhibition of respiration, lower calcium loading capacity, decreased mtDNA copy number and increased ROS generation [278, 279]. No clinical trials have been performed to explore if this effect is also observed *in vivo*, although this may well be a very important and promising compound for anti-cancer therapy.

Although the majority of the above mentioned compounds were shown to specifically target tumor cells in contrast to their normal counterparts, further pre-clinical in vivo studies are necessary to establish the rationale for further clinical trials. In addition, even compounds effective in animal models may prove to be unsafe in clinic as seen with MKT-077 [274].

Chapter 3

Cell quality control systems and tumorigenesis

3.1 Apoptosis
  3.1.1 Abnormal mitochondrial apoptotic signaling in cancer cells
  3.1.2 Targeting the aberrant mitochondrial apoptotic machinery
3.2 Autophagy
  3.2.1 Macroautophagy
  3.2.2 Chaperone-Mediated Autophagy
  3.2.3 The "Janus-faced" role of autophagy in cancer
  3.2.4 Targeting altered autophagy pathways in tumor cells

Cells are the basic building blocks of living organisms harboring a high complexity of functions and characteristics. The maintenance of cellular homeostasis is of great importance as it allows the preservation of tissue architecture and function, thus ensuring normalcy. In order to maintain an effective internal regulation the cell needs quality control mechanisms to identify, correct, and prevent the occurrence of mistakes. The consequences of deregulated quality control systems are disastrous and often associated with the development of different pathologies and acquisition of a malignant phenotype. This section constitutes a review of two of the major quality control systems, apoptosis (Section 3.1) and autophagy (Section 3.2) as well as their implications in cancer development.

3.1 Apoptosis

Apoptosis, also called programed cell death type I, has been a high focus of study since its discovery in 1972 [280] as it constitutes a mechanism of extreme importance, not only in tissue development and homeostasis, but also in the pathogenesis of different diseases such as cancer.

Cells undergo several changes during apoptosis, namely DNA fragmentation and chromatin condensation; along this process cells lose their attachment to the surroundings and shrink. A particular characteristic of the apoptotic mechanism is membrane blebbing, which precedes the formation of apoptotic bodies. These small cytoplasmic fragments encapsulated in cellular membranes are then eliminated by phagocytosis [281]. Due to this orderly disposal of cells, inflammation reactions do not generally occur in apoptosis.

Apoptosis is a complex process that occurs via multiple pathways and which is triggered in response to a variety of extrinsic or intrinsic signals (Fig.3.1). The apoptotic machinery is composed of upstream regulators and downstream effector components [282]. The regulators are divided into two major circuits, one receiving and processing extracellular signals, referred to as the extrinsic pathway, which is activated by the engagement of "death receptors", and another that senses and integrates internal signals, the intrinsic pathway, which involves mitochondria as a central crossroad for death signaling. Both extrinsic and intrinsic circuits then culminate with the activation of intracellular cysteine proteases, caspases 8 and 9 respectively, which in turn activate a proteolysis cascade that involves effector caspases, caspase 3, 6, and 7, responsible for apoptosis execution (Fig.3.1) [283]. All caspases exist as inactive zymogen which activation involves the proteolytic cleavage of their prodomains to attain a large catalytic subunit plus a small fragment.

Apoptosis activation is controlled by a balance between pro- and antiapoptotic proteins of the BCL-2 family that function as a "life/death switch" integrating inter- and intracellular signals [282]. The different members of the family might share two to four BCL-2-homology domains (BH) or can form a specific subgroup of the so called BH3-only proteins. Moreover, BCL-2-like proteins can also be sorted accordingly to their function. The antiapoptotic proteins include BCL-2, BCL-x_L, and BCL-w, and inhibit apoptosis mainly by binding to and consequently suppressing pro-apoptotic triggering proteins,

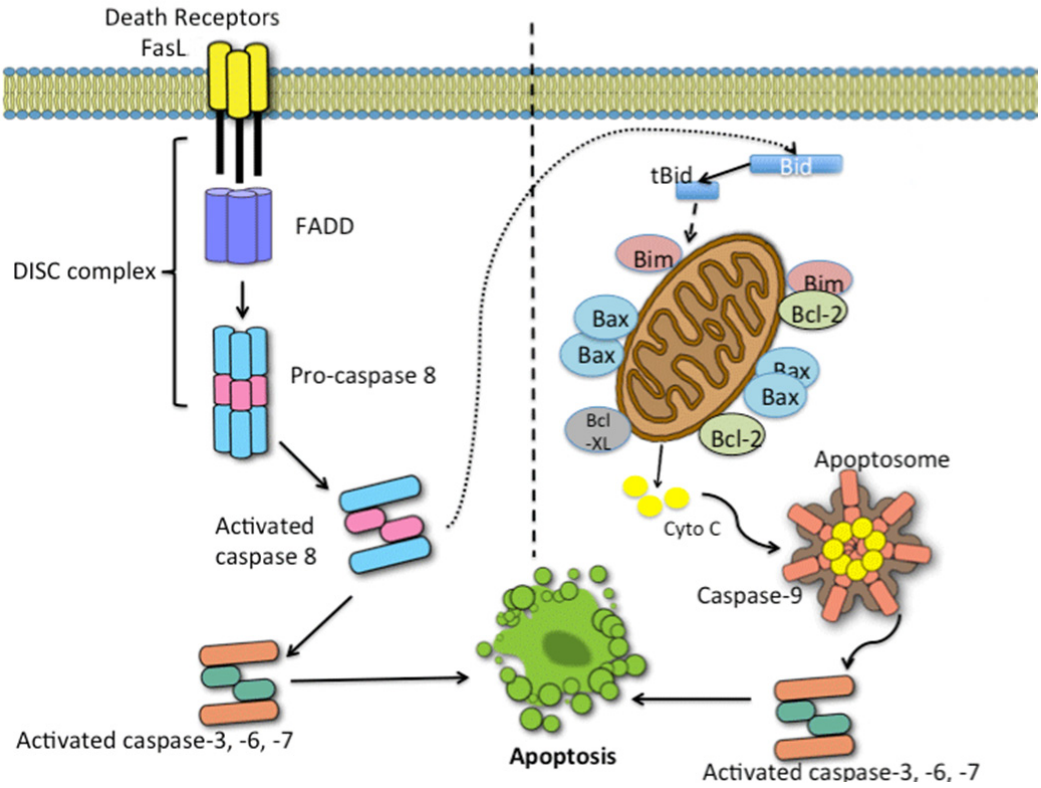

Figure 3.1 - Apoptotic pathways: extrinsic vs intrinsic. The left side of the figure depicts the extrinsic pathway beginning with the arrival of apoptotic stimuli, which are internalized by means of death receptors (Fas, TNFαR, DR3, DR4, and DR5). In this picture only Fas receptor is shown which forms trimmers upon ligand binding and recruits pro-caspase 8 via FADD adaptor protein. Active caspase 8 will trigger caspases cascade by activation of caspase 3, 6 and 7. On the right, the intrinsic pathway is shown in the right side with mitochondria being the hub for the mechanism of antiapoptotic/proapoptotic proteins. Stress signals will alter the ratio of these proteins and potentiate mitochondrial outer membrane permeabilization (MOMP) releasing cytochrome c into the cytosol. Cytochrome c interacts with APAF-1 and pro-caspase 9 to form the apoptosome and trigger caspase cascade by activation of caspase efectors (3, 6 and 7). Nevertheless, the two pathways are not independent as in some circumstances caspase 8 can activate Bid which will promote MOMP establishing the bridge between the extrinsic and intrinsic pathways. Adapted from [285]. Abbreviations: Cyto-c – cytochrome c; BAX – BCL-2 associated X protein; BCL-XL – B-cell lymphoma extra large; BID – BH3 interacting domain death agonist; BCL-2 – B-cell CLL/lymphoma; BIM – BCL2-like 11; FADD – Fas-Associated protein with Death Domain.

such as BAX, and BAK [282]. The group of proteins sharing a single BH, the BH3 motif (BH3-only proteins) which include PUMA, Noxa, BID, and BIM, bind and inhibit the antiapoptotic BCL-2 proteins acting as pro-apoptotic proteins [284]. Overall, BH3-only

proteins and antiapoptotic BCL-2 proteins are positive and negative regulators of BAX/BAK respectively and the overall cell fate depends ultimately on the ratio of those proteins.

Upon a death signal, pro-apoptotic proteins undergo post-translational modifications that include dephosphorylation and cleavage resulting in their activation and subsequent translocation to mitochondria. In mitochondria, these proteins disrupt the integrity of the mitochondrial outer membrane releasing pro-apoptotic signaling proteins including cytochrome *c* [281]. Released cytochrome *c* interacts and binds to apoptotic protease-activating factor 1 (APAF-1) inducing ATP-dependent activation and oligomerization of seven APAF-1/cytochrome *c* complexes (apoptosome) [286] which ultimately cleaves pro-caspase 9 and activates a cascade of caspases that acts to induce multiple cellular changes associated with apoptosis.

Important during embryonic development [287], programed cell death also constitutes a barrier to pathological development as it normally eliminates cells whose cell cycle control is disturbed by oncogenic mutations. Tumor cells develop a variety of strategies in order to overcome apoptosis including abnormal expression of some key regulatory factors. Impaired apoptosis potentiates malignant progression at multiple steps allowing cell survival and contributing to genomic instability.

3.1.1 Abnormal mitochondrial apoptotic signaling in cancer cells

Genotoxic stress and excessive oncogenic signaling initiate intracellular signaling pathways leading to apoptosis. Release of pro-apoptotic factors from the mitochondria is the decisive step in most apoptotic pathways. This release can be triggered by two processes, mitochondrial outer membrane permeabilization (MOMP) and mitochondrial permeability transition (MPT). Extrinsic or intrinsic signals can cause mitochondrial translocation of pro-apoptotic proteins such as BAK or BAX, which form hetero- and homodimer channels in the outer mitochondrial membrane resulting in MOMP (reviewed in [288]). These channels allow release of pro-apoptotic factors enclosed in the inter-membrane space, including cytochrome *c*, the apoptosis-inducing factor (AIF), OMI/HTRA2 and SMAC/Diablo, among others. Release of those factors leads to activation

of executor caspases and their translocation to the nucleus triggering death-dependent responses [289]. On the other hand, internal mitochondrial stress caused by calcium overload or oxidative stress can result in increased permeability of the inner mitochondrial membrane (IMM) often designated as MPT. The effect is due to formation of non-specific protein pores in the IMM which allow equilibration of solutes <1.5 KDa between the matrix and cytosol. The structural entity of the pore remains highly debated [290, 291], with recently findings suggesting the phosphate carrier [292] or ATP synthase dimers [293] as possible structural components of the pore. The classic model of the MPT pore has been thus remodeled to alter the role of ANT and VDAC from pore components to pore modulators [294, 295]. Nevertheless, cyclophilin D (Cyp-D) retains its role as a pore regulator by interacting with an intermembrane protein, probably the ANT or the ATP synthase, and inducing a conformational change upon calcium binding [291, 295]. The sudden increase of membrane permeability leads to osmotic readjustment with consequent mitochondrial swelling and damage to the outer membrane, resulting in uncontrolled release of pro-apoptotic factors [296].

The transcription factor TP53, the most frequently mutated tumor suppressor in human cancer, is a well-studied hub linking stress response to apoptosis. In addition to its well known role promoting transcription of pro-apoptotic factors such as APAF1, BAX, PUMA and Noxa, TP53 also plays a direct role in apoptosis. In response to stress, TP53 translocates to mitochondria, where it displaces inhibitors of pro-apoptotic channel-forming proteins such as BAK [297].

Uncontrolled growth of cancer cells leads to a series of cellular stresses that would trigger apoptotsis [298, 299]. In addition to transcriptional effects these mutations also affect activation of BAK and BAX at the outer mitochondrial membrane (OMM). Also, tumor mitochondria commonly display increased binding of the enzyme hexokinase II (HKII) to VDAC at the OMM. HKII–VDAC complexes appear to inhibit apoptosis by blocking binding of pro-apoptotic proteins to the OMM [121, 300]. Cancer cells display altered MPT regulation [301] that may involve HKII binding to the VDAC as well. In addition, cancer cells commonly display increased mitochondrial localization of several heat shock proteins, including HSP60, HSP90 [302] and the tumor necrosis factor receptor-associated protein 1 (TRAP1) [303]. These heat shock proteins inhibit apoptosis by binding Cyp-D, thus apparently blocking MPT in response to pro-apoptotic insults [302, 304].

The mitochondrial protein peripheral-type benzodiazepine receptor (PBR), also known as 18 kDa translocator protein (TSPO), is also implicated in oncogenesis. The PBR is primarily located in contact sites between the inner and outer mitochondrial membranes, where it associates with VDAC and ANT [305]. Paradoxically, the PBR promotes apoptosis via activation of VDAC [306] but also to promote oncogenesis. Elevated PBR expression in tumors is associated with increased metastatic potential in several cancers [307]. This oncogenic effect is likely due to non-apoptotic functions of PBR possibly dependent on nuclear localization which has been associated with tumor aggressiveness [308].

3.1.2 Targeting the aberrant mitochondrial apoptotic machinery

One anticancer strategy to target the increased mitochondrial resistance to apoptosis in tumor cells is to develop small molecules which mimic the BH3 dimerization domain that exists in all BCL-2 related proteins, leading to activation of pro-apoptotic BCL-2-like proteins (Fig.2.2 and Table 2.1). Two typical examples are the chromene derivative HA14-1, which binds to the BCL-2 protein and induces apoptosis [309] and ABT-737, which binds preferentially to BCL-2 and BCL-X_L and induces cell death through the intrinsic apoptotic pathway [310]. In various cultured leukemic cells and acute myeloid leukemia cells obtained from patients, the BH3 mimetic 072RB demonstrated mitochondrial localization followed by cell death [311]. Other examples of BH3 mimetics are ABT-263, gossypol (AT-101) and Obatoclax (GX15-070), which, similarly to gossypol, antagonizes BCL-2 and BCL-X_L [312]. Obatoclax is currently undergoing phase I/II trials against myelofibrosis [153], advanced chronic lymphocytic leukemia [313], solid tumor malignancies [314] and advanced hematologic malignancies [315] with results that range from disappointing to promising. Moreover, the great majority of BH3 mimetic proteins have been described as having a differential cytotoxic effect on cancer treatment and normal counterparts [316].

As described above the PBR has been implicated in mitochondrial-mediated apoptosis. This role in conjunction with the overexpression of PBR in some cancer cells has been exploited by developing specific ligands which induce cell death [308]. These ligands, such as PK11195, Ro5-4864 and FGIN-1-27, have been identified as anticancer modulators, and may either induce apoptosis directly, or through inhibition of BCL-2 antiapoptotic

effects [308]. The overexpression of PBR in neoplastic tissues combined with selective binding of high affinity PBR ligands has also led to the development of PBR ligands as tools for tumor imaging and diagnosis [317].

The chemotherapeutic properties of curcumin, the major constituent of tumeric powder, have been reported as inducing lung cancer cell death through BAX upregulation and BCL-2, BCL-X_L downregulation, causing AIF and cytochrome *c* release [154]. Several other intracellular targets for curcumin have also been described, including suppression of TP53 and inhibition of cyclooxygenase-2 (COX-2) [318]. Curcumin is currently undergoing phase II/III clinical trials in different types of cancer, including colon and cervical, with promising results in some cases [318].

Sanguinarine, a natural benzylisoquinoline alkaloid, was shown by our group to interfere with mitochondrial calcium loading capacity and to cause an increase in TP53 [319]. Barreto *et al* demonstrated that complex II is a mitochondrial target for sanguinarine, which may explain the effects on respiration [162]. Other studies confirmed that sanguinarine causes apoptosis via mitochondrial depolarization and cytochrome *c* release [320, 321], ROS-induced DNA damage [322], glutathione depletion, and cleavage of poly (ADP-ribose) polymerase and beta-catenin [323]. Berberine, an alkaloid derived from plants of the *Berberidaceae* family, has also been described to act as an anticancer agent, exerting several direct effects on mitochondria function, including inhibition of mitochondrial complex I and interaction with the ANT [279, 324]. Inhibition of mouse liver mitochondrial respiratory activity by berberine was confirmed by other experimental results [162, 325]. Berberine also induced apoptosis through alterations in the BCL-2/BAX ratio, ROS production, TP53 upregulation, a decrease in $\Delta\Psi$, cytochrome *c* release and activation of caspases [326-329]. Of particular interest is the fact that for low concentrations, berberine is accumulated by energized mitochondria in tumor cells [279] (see below). Clinical trials are still warranted for sanguinarine and berberine in order to confirm the promising efficacy shown *in vitro*.

3.2 Autophagy

Autophagy is an evolutionary conserved, tightly regulated lysosomal degradation pathway important in normal cell development and survival under changing

environmental conditions. This self-cannibalistic process is characterized by an extensive vacuolization of the cytoplasm and is generally activated in all cells at low basal levels [330].

Autophagy is essential for homeostasis maintenance contributing to protein and organelle turnover, and it is rapidly upregulated upon stress conditions, such as starvation, growth factor deprivation, oxidative stress or whenever cells undergo situations that require high energy demands [331, 332]. Thus, autophagy is activated for structural remodeling and developmental transitions allowing cells to dispose of damaged cytoplasmic components in return of fresh *building blocks*.

Due to its importance in cell-physiologic response, autophagy constitutes a method of cellular adaptation enabling cells to break down cellular organelles allowing the resulting catabolites to be recycled and used for biosynthesis and energy metabolism under new internal and external environments. Despite its role in survival, promoting cell flexibility to overcome environmental changes that ranges from adaptation to nutrient deprivation to severe cellular damage, autophagy can lead to the elimination of entire cells [333]. This occurs when adaptive mechanisms are insufficient to circumvent the damage caused to the cells. Consequently, autophagy molecular mechanism can be an alternative form of cell death, the so-called programed cell death type II [334]. Considering autophagy role in housekeeping, stress responses and cell death, defects in this cellular quality control process have been implicated in the development of several human diseases, including cancer (see Section 3.2.3) [332, 335].

So far three different autophagic routes have been identified, namely macroautophagy, microautophagy and chaperone mediated autophagy (CAM), which differ in their physiological function and mode of cargo delivery to lysosomal lumen (Fig.3.2) [332]. This section will focus on macroautophagy, regerred here as autophagy, and chaperone-mediated autophagy.

3.2.1 Macroautophagy

The term autophagy often refers to macroautophagy processes. This form of autophagy is characterized by the formation of a double-membrane vesicle, which encapsulates cytoplasmic cargo and then fuses with lysosomes where the sequestered material is

degraded and recycled (Fig.3.2). Macroautophagy constitutes a high-capacity process that allows the simultaneous sequestration of multiple cytoplasmic components, including organelles, for degradation in the lysosomal lumen [336].

Although autophagosome formation occurs in close proximity to the endoplasmic reticulum (ER), the direct involvement of ER membrane in this process remains unclear. In addition to ER, recent works suggest that the Golgi complex, mitochondria, and plasma membranes may also provide a membrane source for autophagosome formation [337-339]. In 1990, the identification of a series of autophagy-related (ATG) genes in yeast resulted in an increased understanding of the mechanism and function of autophagy [340, 341].

The first step of the autophagic pathway is the induction phase, which is initiated by cellular stresses mediated by signaling cascades. Thus, stress stimuli, such as starvation, induce autophagy through inhibition of mTOR, which is the major autophagy inhibitory signal. Conversely, in response to growth factors or other autophagy inhibitory signals that stimulate the class I phosphatidylinositol 3-kinase (PI3K)-AKT signaling pathway, mTOR negatively regulates autophagy. mTOR inhibition allows the activation of the complex consisting of UNC-51–like kinase 1 (ULK1), ATG13, FIP200, and ATG101, crucial for autophagy initiation. Once activated, the ULK1 complex regulates the class III phosphatidylinositol 3-kinase (PI3K) complex, which includes BECLIN-1, the class III phosphatidylinositol 3-kinase (VPS34), and ATG14L [342]. Antiapoptotic BCL-2 homologs exert an antiautophagic function through inhibition of VPS34-BECLIN-1 complex [343]. Stimulation of this complex generates phosphatidylinositol-3-phosphate (PI3P), which promotes vesicle nucleation and serves as signal to the recruitment of proteins required for vesicle elongation [343].

Moreover, autophagosomal elongation requires two ubiquitin-like conjugation pathways, the ATG5-ATG12 and the light chain 3 (LC3) conjugation systems (Fig.3.2). In the former, ATG12 protein is activated by the E1 ubiquitin-like enzyme ATG7, and then is further transferred to the E2 ubiquitin-like enzyme ATG10 to be finally conjugated with ATG5. The ATG12-ATG5 complex is important for the elongation of the isolation membrane during autophagosome formation and is required for efficient LC3 lipidation [344]. In the second conjugation system, LC3 is first proteolyzed in its C-terminus by the cysteine protease ATG4 and activated afterwards by the E1 ubiquitin-like enzyme ATG7 to be further transferred to the E2 ubiquitin-like enzyme ATG3 allowing phosphatidyl-

ethanolamine (PE) connection to LC3-I (18KDA) and finally giving rise to LC3-II (16KDa) that stably associates to the autophagosomal membrane [345]. The next step involves autophagosome fusion with lysosomes, called autophagolysosomes, and consequent degradation of autophagic cargos by lysosomal proteases, such as cathepsins D, and B [346]. Cathepsins are considered an important class of lysosomal enzymes and are characterized by a cysteine at the active group, which may be susceptible to oxidative modification and redox regulation [347]. After fusion with lysosomes, both autophagosome cargo and inner limiting membrane are degraded and the resulting monomeric structures are exported to cytosol for reuse in biosynthesis or energy production [348]. Upon degradation, autolysosomes may either become lysosomes that are able to undergo another fusion with autophagosomes or, if the degradation of the cargo was not complete, autolysosomes may become residual bodies containing indigestible material [348].

Although this quality control process may occur in a non-selective manner increasing evidence indicates selectivity in the recognition of autophagic substrates, through which misfolded or aggregate-prone proteins (aggrephagy), organelles (e.g. mitophagy), and invading microorganisms (xenophagy) are degraded [349]. The identification of autophagic adaptors, such as p62/SQSTM1 (sequestosome 1) and neighbor of BRCA1 (NBR1), provided new insights on autophagy selectivity. These adaptors are both selective autophagy substrates and cargo receptors for degradation of ubiquitinated substrates by autophagy [350].

A particular case: Mitophagy

As mentioned in Section 2, mitochondria are highly central organelles for energy production and critical in the regulation of numerous signaling cascades. Consequently, the accumulation of dysfunctional mitochondria results in significant damage to the cell. Thus, mitochondrial biogenesis and degradation must be tightly regulated allowing an appropriate mitochondrial response to stress stimuli.

In response to environmental stress, ATP synthesis is disrupted, with excessive production of ROS by mitochondria and loss of $\Delta\Psi_m$ which can precede autophagy induction [351]. Elimination of aberrant mitochondria through both non-selective and selective autophagy pathways (mitophagy) constitutes a critical process as it allows

mitochondrial quality control, and cell viability maintenance. Damage to mitochondria often leads to the activation of apoptosis (Section 3.1.1). In an attempt to prevent cell death, mitochondria are sequestered by autophagosomes and degraded before cell death is triggered. In fact, increased ROS production plays an important role in autophagy activation through regulation of ATG4 activity [352]. Although there is an extensive similarity between general autophagy and mitophagy pathways, mitochondrial-specific mechanisms have been identified.

One mechanism of mitochondrial clearance involves the autophagy ubiquitin-binding adaptor p62, which recruits autophagic membranes to mitochondria by binding to LC3. In this model, dysfunctional mitochondria are recognized by the E3 ubiquitin ligase Parkin which ubiquitinates specific protein substrates in the mitochondria to which p62 binds. Subsequently, this complex is selectively tethered to the autophagosome through p62 binding to LC3. Although this model is supported by numerous studies [353, 354], others show that depletion of p62 by RNAi has no effect on mitophagy [355] suggesting the involvement of other adaptor proteins in mitochondrial autophagy pathway.

Recent works led to the identification of AMBRA1 as a mitophagy regulator [356, 357]. AMBRA1 is a BECLIN-1 interacting protein, which positively regulates autophagy. Under normal conditions, AMBRA1 binds preferentially to mitochondrial BCL-2, after autophagy induction AMBRA1 is released from BCL-2 and is recruited to BECLIN-1 promoting its activity and leading to mitophagy initiation [356]. Moreover, AMBRA1-mediated mitophagy was shown to be dependent on its interaction with Parkin [357]. The activation of the phosphoinositide 3-kinase complex (see Section 3.2.1) by AMBRA1 in mitochondria, allows the formation of the autophagosome directly around depolarized organelles, contributing for the selective nature of mitophagy.

Considering that LC3 only associates with already formed autophagosomes, and p62 inability to induce the formation of new autophagosomes, these two Parkin-mediated mitophagy models seem to have complementary effects; AMBRA1 induces autophagosome formation at mitochondria, which, after incorporation of LC3, may be then linked to ubiquitinated mitochondria via p62 [351].

The identification of ATG11 and its receptor ATG32 as important factors for mitochondrial degradation in yeast [358] led to the understanding that damaged mitochondria can also be eliminated via an ubiquitin-independent pathway involving the direct binding of LC3

to autophagy receptors on the mitochondria. In mammalian cells, mitochondrial NIX (mammalian ATG32 homolog) and BNIP3 (BCL-2 /E1B 19KDa-interacting protein 3-like protein) are known to promote mitophagy [359, 360]. Both of these proteins target mitochondria for degradation by directly binding to LC3 on the autophagosome and BNIP3-mediated autophagy is associated with Parkin translocation to mitochondria.

Other key player in the regulation of mitophagy is the serine/threonine kinase PTEN-induced putative kinase 1 (PINK1), which plays a central role in communicating the loss of $\Delta\Psi_m$ to Parkin [361, 362]. In healthy mitochondria, PINK1 is preferentially located in the inner membrane at low levels as it is rapidly cleaved by mitochondrial proteases. After $\Delta\Psi_m$ loss, PINK1 accumulates in the outer membrane, where it is protected from degradation, and is involved in Parkin recruitment to mitochondria [363]. Parkin is then able to polyubiquitinate proteins residing in the OMM, namely VDAC, and mitofusins MFN1 and 2 [364].

Additionally, segregation of mitochondria by fission and inhibition of their fusion machinery is thought to be a pre-requisite for mitophagic degradation. Accordingly, PINK1 and Parkin were shown to play an essential role in mitochondrial dynamics [365] supporting the idea of a close relation between mitochondrial dynamics and mitophagy. Mitofusins MFN1 and 2 degradation as result of Parkin activation prevents damaged mitochondria to fuse with functional mitochondria and constitutes an essential step in their clearance through mitophagy [351]. Furthermore, mitochondrial depolarization was shown to cause loss of OPA1 (optic atrophy 1) and MFN1 and 2, proteins necessary for the fusion of mitochondrial inner and outer membranes. Consequently, overexpression of these proteins results in excessive fusion, which in turn protect mitochondria from degradation. In accordance with the essential role of fission in mitophagy, inhibition of mitochondrial fission mediated by dynein-related protein 1 (DRP1) prevents mitochondrial degradation through autophagy [366].

Basal levels of mitophagy are important for maintenance of cellular homeostasis and protection against accumulation of dysfunctional mitochondria. During cellular stress, an activation of mitophagy occurs, which consists in an early response to promote survival. However, the pathways of mitochondrial quality control are limited in their capacity and eventually become overwhelmed by an accumulation of damaged mitochondria, which ultimately culminates in cell death.

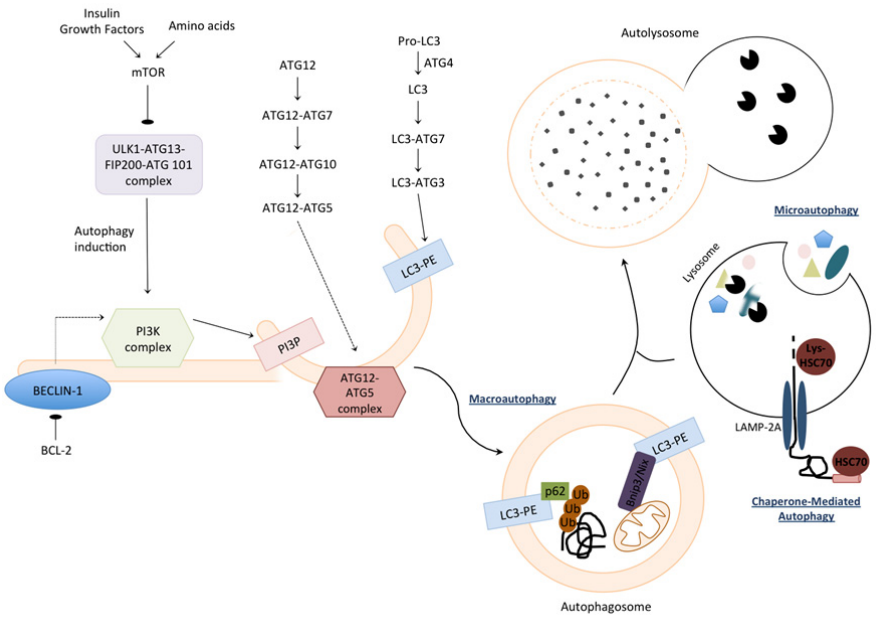

Figure 3.2 - Different types of autophagy and autophagosome formation during macroautophagy. Macroautophagy occurs at basal levels and can be induced upon environment alterations. The regulatory pathway includes mTOR, which inhibits macroautophagy. Under macroautophagy induction, the ULK1 complex (includes ULK1, ATG13, FIP200, and ATG101) is activated regulating the class III PI3K complex (includes ATG14, VPS34, and AMBRA) and BECLIN-1 recruitment. Under nutrient-rich conditions BECLIN-1 is associated with BCL-2 and is released after BCL-2 phosphorylation by JNK. Stimulation of this complex generates PI3P, which promotes vesicle nucleation and serves as signal to the recruitment of proteins required for vesicle elongation. The elongation process requires two ubiquitin-like conjugation pathways, the ATG12-ATG5 complex, and LC3-PE. The ATG12-ATG5 is required for efficient LC3 lipidation. In the cytoplasm, p62 interacts with polyubiquitinated proteins and this complex binds to LC3 in the autophagosome. Autophagy receptors on the mitochondria such as BNIP3 and NIX interact directly with LC3. This is followed by fusion of the autophagosome with a lysosome, autolysosome, where captured material and inner membrane are degraded. Chaperone mediated autophagy involves cytosolic HSC70 recognition of a KFERQ motif presented by unfolded substrate proteins. Then these are translocated into lysosomal lumen after binding to LAMP-2A, this process requires lysosomal HSC70 (lys-HSC70). Mircoautophagy refers to sequestration of cytosolic components directly into the lysosome through invagination of lysosome membrane. Abbreviations: ATG – autophagy related gene; BCL-2 – B-cell CLL/lymphoma; BNIP3 – BCL-2 /E1B 19KDa-interacting protein 3-like protein; HSC70 – 70KDa heat shock cognate; LAMP-2A – lysosome-associated membrane protein type 2A; LC3 – light chain 3; mTOR – mechanistic target of rapamycin (serine/threonine kinase); NIX – BCL2/adenovirus E1B interacting protein 3-like; PE – phosphatidylethanolamine; PI3K – Phosphatidylinositol 3-kinase; PI3P – phosphatidylinositol-3-phosphate; ULK1 – UNC-51–like kinase 1.

3.2.2 Chaperone-Mediated Autophagy

Chaperone-mediated autophagy (CMA) constitutes a type of selective autophagy that differs from other subtypes due to the unique way through which substrates, mainly cytosolic proteins, are recognized for lysosomal delivery and enter this organelle (Fig.3.2). The proteins internalized in lysosomes through CMA contain in their aminoacid sequence a pentapeptide motif, KFERQ, which selectively targets proteins to the lysosome [367]. This motif is then recognized by a cytosolic chaperone, the heat shock cognate protein of 70KDa (HSC70), which, along with its modulatory co-chaperones (BAG1, HIP, HOP, and HSP40), delivers the substrate protein to the surface of lysosomes. Unlike other degradation tags, such as ubiquitin, that are added to substrates targeting them for degradation, the KFERQ motif is always present. However, in properly folded proteins this sequence is "hidden" from its recognition by CMA machinery. Conformational alterations may favor the recognition of the KFERQ motif and consequently target unfolded proteins to degradation through CMA [368]. Other mechanisms that mask tag motifs may involve interaction with other proteins and binding to intracellular membranes. Moreover, further studies revealed that post-translational modification of some proteins might also be necessary to complete the CMA-targeting motif [369].

After the recognition step, the substrate protein-chaperone complex docks at the lysosomal membrane where it interacts with the lysosome-associated membrane protein type 2A (LAMP2A), which functions as a receptor for CMA pathway [370]. One-by-one translocation of the substrate protein into the lysosomal lumen requires its unfolding in a process through which cytosolic HSC70 and its co-chaperones are thought to be involved [371]. Substrate binding to LAMP2A is a limiting step for CMA through which proteins are translocated one-by-one to the lysosomal lumen [372].

LAMP2A organizes in dynamic defined protein complexes at the lysosomal membrane and was shown to undergo conformational changes along CMA process. Substrates bind preferentially to LAMP2A monomers while their translocation across the lysosomal membrane requires the formation of LAMP2A complexes. HSC70 plays a role in the disassembly of LAMP2A complexes whereas HSP90, at the lysosomal membrane, is important for the maintenance of LAMP2A stability [373].

Translocation to the lysosome lumen also requires the presence of a luminal from of HSC70 (lys-HSC70), which assists in this process [374]. In fact, lys-HSC70 levels increase

in response to stressors leading to an increase of CMA fluxes, and its presence or absence in lysosomal lumen allows the identification of CMA-active lysosomes [375]. Finally, in the lysosomal lumen, a wide range of lysosomal hydrolases rapidly degrades substrate proteins.

Overall, CMA contributes to maintenance of energy homeostasis, by providing aminoacids resultant from protein degradation, and protein quality control, by elimination of damaged and prone-to-aggregate proteins [370].

3.2.3 The "Janus-faced" role of autophagy in cancer

Disturbance in the autophagy flux has been associated with cancer development and progression [332]. Numerous lines of evidence point out to an anticancer role for autophagy. The tumor suppressive role of autophagy was first established from studies with BECLIN-1 [376]. Experiments revealed that mice with heterozygous disruption of *BECLIN-1* exhibited decreased autophagy and were more susceptible to develop tumors [377], further studies showed that BECLIN-1 is monoallelically depleted in several human cancers [378]. Similarly, the antiapoptotic BCL-2 and BCL-X_L proteins, which are often overexpressed in human cancers, inhibit autophagy by binding to BECLIN-1 (see Section 3.2.1) [379]. Consequently, BECLIN-1 overexpression leads to increased autophagy and inhibition of tumor development [380]. Additionally, loss of the autophagy gene *ATG5* was shown to promote tumorigenesis [381]. Moreover, tumorigenesis and autophagy share several signaling pathways. The activation of the signaling pathway involving PI3K and the mTOR is one of the most common events in cancer cells and leads to autophagy inhibition [332]. Another example is related with the TP53 tumor suppressor, which was shown to positively regulate autophagy in DNA-damage cells through mTOR inhibition [382].

All of the above works establish a role of autophagy as a mechanism of tumor suppression; however, the question of how autophagy depletion leads to cancer development remains debatable. A possible link between tumorigenesis and autophagy impairment may involve the accumulation of protein aggregates, damaged mitochondria, and misfolded proteins which in turn leads to increased ROS production and consequently to DNA damage [383]. Furthermore, defective autophagy may also contribute to tumor formation via decreased cell death. As previously mentioned in Section 3.2, autophagy has been proposed as a cell

death mechanism; in fact autophagy and apoptosis share regulatory circuits, namely the signaling pathway involving PI3K, AKT and mTOR which blocks apoptosis and inhibits autophagy [332]. In addition, BECLIN-1 is a member of BH-3–only subfamily of antiapoptotic regulatory proteins whose expression is decreased in tumor cells [343]. Moreover, autophagy prevents necrotic death reducing the risk of inflammatory responses which can be actively tumor-promoting [384, 385]. Another possibility is that autophagy negatively regulates cell growth by degrading specific organelles and/or proteins essential for growth regulation. This hypothesis is supported by studies demonstrating that overexpression of BECLIN-1 slows the proliferation of tumor cell lines [386].

Conversely, autophagy activation in advanced cancer was shown to facilitate tumor progression by providing nutrients during starvation [332]. Similarly to what happens in normal cells, autophagy is activated in tumor cells by stress. Accordingly, autophagy activation in these cells potentiates cell survival in some cases [387], as it promotes a cell death escape by conferring superior stress tolerance in tumor cells. CMA was also shown to be upregulated in several human cancers allowing cell proliferation and tumor growth [388]. Moreover, autophagy induction by hypoxia-inducible transcription factor 1α (HIF1α) enables tumor cells to tolerate hypoxic conditions [389]. Autophagy activation under prolonged stress conditions may enable a state of dormancy in cancer cells, which contributes to tumor relapse and progression [390].

Taking all the above information into account, autophagy seems to have a “Janus-faced” role in neoplastic development. Although the importance of autophagy modulation in tumor cells is clear, the question of whether the promotion or inhibition of autophagic pathways is an effective cancer therapy, remains a challenge. The role of autophagy in cancer development is complex and seems to depend on cell type, stage and genetic context [391].

Recently, an important role was attributed to autophagy activation in tumor microenvironment by epithelial cancer cells. The importance of tumor microenviroment in tumorigenesis has been a topic of great discussion in the last years, revealing that tumor biology can no longer be understood solely by the enumeration of traits acquired by cancer cells alone [45]. Accordingly, the autophagic tumor stromal model of cancer was proposed based on the observation that epithelial cancer cells induce oxidative stress in neighboring cancer-associated fibroblasts (CAFs), and in other stromal cell types which

results in autophagy activation [392]. Autophagy activation in these cells works as a "battery" providing tumor cells with energy sources favoring tumorigenesis. In addition, increased oxidative stress also potentiates mutagenesis. Thus, ROS production in CAFs was shown to induce DNA damage and aneuploidy in adjacent epithelial cancer cells constituting an important driving force to tumor evolution as it potentiates random mutagenesis [392]. Furthermore, autophagy in CAFs was also seen to protect cancer cells from apoptotic cell death through the maintenance of a constant flow of energy-rich nutrients that help to fulfill their high metabolic demands [393].

Although not consensual, these findings can provide great alterations in our understanding of tumor metabolism. Contributing to these advances, Lisanti and collaborators showed that CAFs are forced to undergo aerobic glycolysis due to loss of their mitochondria through mitophagy [394]. This phenomenon was termed "The Reverse Warburg Effect" through which substrates resulting from the Warburg effect occurring in CAFs can be transferred to adjacent tumor cells and used as fuels for oxidative mitochondrial respiration [394]. The autophagy stroma model of cancer and the reverse Warburg effect are characteristic of tumor microenvironment, providing new insights for autophagy role on cancer progression as well as a new target for cancer therapy.

3.2.4 Targeting altered autophagy pathways in tumor cells

Autophagy inducers were shown to have the potential to induce tumor cell death and may therefore be a potential strategy for cancer therapy [395]. Rapamycin, a natural occurring inhibitor of the autophagy regulator mTOR, along with its analogs temsirolimus (CCI-779), everolimus (RAD-0014), and deforolimus (AP-23573) selectively inhibit mTOR resulting in autophagy stimulation [396]. However, rapamycin and its analogs have had limited successes in the treatment of neuroendocrine carcinomas and lymphoma, which results from their inability to inhibit mTORC2 [397]. These limitations led to the development of ATP-competitive mTOR inhibitors of both mTORC1 and mTORC2 and the dual PI3K-mTOR inhibitor NVP-BEZ235 [398].

Moreover, the anti-diabetic drug metformin was shown to modulate autophagy through activation of the mTOR upstream mediator AMPK [399]. However, in prostate cancer cells, metformin inhibited 2-DG-induced autophagy, decreased BECLIN-1 expression and led to cell death [400], suggesting that AMPK autophagy induction might depend on the

cell type. Other autophagy inducers include the BCL-ABL tyrosine kinase inhibitor, imatinib, which modulates autophagy through regulation of lysosomal components and was shown to be effective in chronic myeloid leukemia treatment [401]. In addition, some antidepressants, such as fluoxetine and maprotiline, were shown to induce autophagy in chemoresistant Burkitt lymphoma cell lines [402]. Furthermore, several conventional cytotoxic drugs showed autophagy induction as an important anticancer effect [398].

Conversely, autophagy inhibitors may provide the means to overcome treatment resistance caused by the induction of a post-treatment dormancy state in cancer cells that often contributes to cancer recurrence and metastasis [403]. Additionally, enhanced autophagy can target hypoxic tumors, which are usually more resistant to therapy [404].

Autophagy inhibitors can be divided in early- and late-stage inhibitors depending on the stage of the autophagic pathway they target. Early-stage inhibitors include 3-methyladenine, wortmannin, and LY294002 that target class III PI3K (VPS34) interfering with its recruitment to the membranes [405]. Late-stage inhibitors include chloroquine (CQ), hydroxychloroquine (HCQ), and monensin that prevent acidification of lysosomes impairing cargo degradation by digestive hydrolases [405]. Another late-stage inhibitor is bafilomycin A1, which is a specific inhibitor of vacuolar-ATPase [406]. The use of microtubule-disruption agents, such as taxanes, and colchicine, was shown to inhibit autophagosome fusion with lysosomes [407].

Considering the dual role of autophagy as a tumor suppressor and as an adaptive stress response in tumor cell, discussed in Section 3.2.3, the understanding of autophagy function in different tumor cells is critical to improve therapy. Autophagy modulation for cancer therapy should take into account that tumors with enhanced autophagy will respond differently to therapy when compared to those with suppressed autophagy. Consequently, the question of whether to activate or inhibit autophagy remains a challenge and implies a better knowledge of how this process works in neoplastic *versus* normal cells.

Chapter 4

Heat Shock Proteins in cancer

4.1 HSP90 family
  4.1.1 TRAP1: the mitochondrial HSP90
  4.1.2 Targeting the mitochondrial complex of HSP90, TRAP1 and CypD in cancer cells

As described in Section 3.2, accumulation of misfolded proteins and aggregates results in a cytotoxic effect in cells and is associated with the development of numerous diseases. Consequently, protein quality control is essential for homeostasis and cellular integrity maintenance. In normal cells, proteins often misfold as a result of stochastic insults, presence of destabilizing mutations, stress conditions, and metabolic challenges. In order to overcome these deleterious effects, cells developed different mechanisms to monitor and maintain the viability of their proteome. HSPs are stress proteins that play essential roles in protein homeostasis maintenance.

Heat shock proteins assist the folding of newly synthesized polypeptides, avoid the formation of aggregates and promote the refolding of stress-denature proteins [408]. Besides these functions, HSPs also aid the translocation of proteins to their correct intracellular localization and target misfolded proteins for degradation [409]. Under normal conditions, HSPs are expressed at low levels. However, when exposed to cellular stressors, which leads to impaired proteome, damaged proteins bind to chaperones and induce the release heat shock factor (HSF) that consequently induces HSP expression [410].

Mammalian HSPs have been categorized in two groups depending on their size, the high molecular weight HSPs, and small molecular weight HSPs. The former includes three major families, HSP90, HSP70, and HSP60, which localize in different cellular compartments. These high molecular weight HSPs are ATP-dependent and require co-chaperones to function. Conversely, small weight HSPs, such as HSP27, are ATP-independent [411]. HSPs are often overexpressed in several human carcinomas [412] as an adaptive response to promote cell survival under an unfavorable environment. Increased HSPs expression allows tumor cells to tolerate stress levels participating in alterations that define cancerous growth [45].

4.1 HSP90 family

HSP90 proteins are highly conserved molecular chaperones that comprise up to 1-2% of all cellular proteins and their expression can be further stimulated under stress conditions [413]. The human HSP90 family includes seventeen genes from which only six (*HSPAA1*, *HSP90AA2*, *HSP90N*, *HSPAB*, *HSP90*, and *TRAP1*) are considered to be functional whereas the remaining eleven are thought to be pseudogenes. HSP90 members can be divided into four different classes, the cytosolic HSP90AA (or HSP90α), and HSP90AB (or HSP90β), the HSP90B (or GRP94) from ER, and mitochondrial TRAP1 [213]. These isoforms are closely related sharing high structural homology [213]. There are two major cytosolic HSP90 isoforms, the inducible HSP90AA1 and the constitutive form HSP90AB1, which are usually not differentiated in most works being generally referred to as HSP90 [414].

Heat shock protein 90 is an ubiquitously expressed molecular chaperone essential for the correct folding, maturation, stability, and function of a wide range of client proteins. HSP90 client proteins, namely protein kinases (HER2, AKT, Raf-1, CDK4, SRC) and transcription factors (steroid hormone receptors, TP53, HIF1α) are involved in many cellular processes such as cell signaling, growth and/or survival, angiogenesis, metastasis, and play important roles in tumor development and progression. HSP90 also escorts mitochondrial pre-proteins synthesized in the cytosol to the TOM70 complex and assists in their translocation across the outer mitochondrial membrane [415].

Heat shock protein 90 exists as a homodimer, which is constituted by three domains; the N-terminal domain contains an ATP-binding site, the middle domain, which is highly charged and has a high affinity for co-chaperones and client proteins, and the C-terminus the second ATP-binding site is located [416]. The dimeric structure of the chaperone is crucial for ATP hydrolysis, and the association of the amino-terminal domains during the ATPase cycle is required for maximum ATPase activity [417]. The inherent ATPase activity of HSP90 is essential for its function as protein folding mediated by this molecular chaperone is dependent on an "active" ATP-coupled mechanism [418]. Moreover, C-terminal mutations were found to influence ATPase activity, which suggests the involvement of these regions in the ATPase cycle [419].

Additionally, HSP90 alters its conformation depending on the nucleotide occupancy of its N-terminal nucleotide-binding pocket to attract different co-chaperone proteins, such as p23, and Cdc37. Co-chaperones are critical components of the HSP90 folding pathway as their functions include targeting client proteins and HSP90 ATPase activity modulation. When ATP is bound to the N-terminus, p23 and Cdc37 (p50) proteins bind to HSP90 leading to the stabilization and protection of its client proteins. However, when ADP is bound, HSP70 and HOP (p60) bind to HSP90, which results in client protein degradation by the proteasome [420].

As previously mentioned (Section 1.2), genetic instability allows cells to acquire some capabilities that are characteristic of most cancer cells, such as self-sufficiency in growth signaling, insensitivity to anti-growth signaling, ability to evade cell death, sustained angiogenesis, tissue invasion and metastasis, and limitless replicative potential. The fact that HSP90 plays a pivotal role in the acquisition and maintenance of each of these capabilities makes it an excellent target for anti-cancer therapies.

HSP90 inhibitors interfere with the chaperone activity of HSP90, and consequently client proteins are targeted to the proteasome where they are degraded [421]. However, if the proteasome is inhibited, client proteins accumulate in a misfolded, inactive form in detergent-insoluble subcellular complexes [422]. These evidences demonstrate the anti-tumor clinical potential of these agents.

The HSP90 inhibitor NVP-AUY922 has been shown to exhibit significant antiproliferative properties against human breast cancer cell lines [423] and in HCT116 colon carcinoma cells where it induced a G_1 and G_2-M arrest [424, 425]. NVP-AUY922 interferes with the

HSP90-p23 complex [423] and exhibits an extremely high affinity for the N-terminal nucleotide-binding site of human HSP90 [424]. IPI-504, another HSP90 inhibitor, significantly inhibits growth of a series of pancreatic tumors revealing that it might have a potent anti-tumor activity in pancreatic cancer [426].

Moreover, HSP90 is required for the stability and function of multiple mutated, chimeric, and/or overexpressed signaling proteins that are involved in the oncogenic process. BCL-ABL protein and mutated B-RAF as well as mutated epidermal growth factor receptor (EGFR) are some examples of chimeric HSP90 client proteins, which show sensitivity to its inhibitors [427].

The fact that HSP90 plays an essential role in the maintenance of many oncogenic client proteins stability and function, contributing to all of the hallmark traits of malignancy, makes this a good therapeutical target for the treatment of cancer. HSP90 inhibition constitutes a promising therapeutical approach.

4.1.1 TRAP1: the mitochondrial HSP90

TRAP1, an HSP90-like chaperone, was first identified by yeast-two-hybrid assay as a novel interacting partner of the tumor necrosis factor receptor 1 (TNFR1) [428, 429]. Additionally, an independent screening identified a 75KDa protein (HSP75) with structural homology to HSP90 family members that bound to the Rb protein [430]. This HSP75 was implicated in the maintenance of RB conformation during mitosis and after heat shock [430]. Later, sequence analysis determined that HSP75 and TRAP1 were identical molecules. Although these initial reports suggest its predominant extra-mitochondrial localization, TRAP1 was shown to be primarily a mitochondrial matrix protein [431, 432]. Nevertheless, TRAP1 was found to localize at specific extramitochondrial sites, namely on the cell surface of blood vessel endothelial cells, insulin and zymogen granules in pancreatic cells, nuclei of pancreatic and heart cells, cardiac sarcomeres, and in the ER [432]. Regarding tissue distribution, TRAP1 was detected in normal tissues and, with higher expression, in tumor cell lines [304, 433].

TRAP1 structure

Despite being a member of HSP90 family, sharing 34% sequence identity and 60% homology with members of the HSP90 family [429], TRAP1 has distinct functional properties [431]. Sequence analysis revealed that TRAP1, similarly to other members of the HSP90 family, contains an ATP-binding domain at its N-terminus [434]. Thus, TRAP1 ATPase activity is affected by HSP90 inhibitors [431]. Moreover, TRAP1 molecule lacks a C-terminal MEEVD sequence, which is characteristic of cytosolic HSP90 and is critical for its binding to several tetratricopeptide repeat-containing co-chaperones [431, 435]. Consequently, TRAP1 does not bind to typical HSP90 co-chaperones p23 and HOP, and cannot substitute HSP90 in promoting the maturation of the progesterone receptor hormone-binding state [431]. TRAP1 was shown to form stable homodimers with melting temperature of 55 °C, and its ATPase activity is induced by 200-fold in response to heat shock [436]. Another functional difference between TRAP1 and other HSP90 members regards its ATPase cycle. ATP-binding results in conformational alterations, shifting to a more closed configuration, though with slower kinetics in TRAP1 when compared to HSP90 [436]. Despite the conformational trapping, ATP hydrolysis occurs at a slower rate than chaperone configuration re-opening, i.e. ATP-binding to TRAP1 is insufficient to commit to nucleotide hydrolysis revealing the lower ATPase activity of these chaperone [436].

TRAP1 subcellular localization

TRAP1 subcellular localization was confirmed by the identification of a mitochondrial targeting sequence at its N-terminal [431]. Further work demonstrated that TRAP1 predominantly accumulates in the mitochondrial matrix [432], although it has been recently suggested it may also be found in the intermembrane space [437]. TRAP1 putative mitochondrial import sequence is removed upon organelle import. Notwithstanding, TRAP1 is also found in extramitochondrial sites, suggesting that a pool of mitochondrial TRAP1 is exported out of the organelle matrix allowing chaperone interaction with proteins in other subcellular compartments. The presence of an LxCxE motif allows this chaperone binding to RB, being absent in other members of the HSP90 family [430].

TRAP1 functions and regulators

With respect to its cellular functions, TRAP1 was first shown to be involved in the protection against apoptosis, through regulation of both intrinsic and extrinsic pathways [438]. Masuda and colleagues found that treatment of tumor cells with the ATP non-competitive inhibitor of protein-tyrosine kinases, β-Hydroxyisovalerylshikonin (β-HIVS), or with the DNA-damaging chemotherapeutic VP-16, resulted in suppression of TRAP1 expression and enhanced mitochondrial apoptosis [438]. These results suggest the important role of TRAP1 in the protection against apoptosis. Similar conclusions were achieved in studies regarding Granzyme M mediated apoptosis in Natural Killer cells [439]. Granzyme M, a serine protease stored in granules of immune system effector cells, causes mitochondrial swelling, loss of $\Delta\Psi_m$, generation of ROS, and cytochrome *c* release in a TRAP1-dependent manner [439].

In addition to its antiapoptotic function, TRAP1 also exerts an antioxidant function, allowing cells to cope with oxidative stress. Accordingly, several lines of evidence support the important role of ROS in TRAP1 regulatory network [438-440]. Moreover, Im and colleagues demonstrated that TRAP1 overexpression attenuated the effects of deferoxamine, through the reduction of ROS production [440]. An independent study identified TRAP1 as one of the target genes upregulated by the MYC oncogene [441]. The concept of TRAP1 as a stress-responsive chaperone that protects cells against oxidative stress and apoptosis following DNA damage, ROS production, or oncogene expression, gained further support [442-444]. TRAP1 cytoprotective effects seem to be important for cells to overcome oxidative stress through inhibition of ROS-mediated cell death.

Further evidences of the role of TRAP1 in tumorigenesis came from studies regarding the role of TNFα/TNFR1 signaling in cell adhesion of neuronal cells. TRAP1 was shown to modulate the expression of N-cadherin cell adhesion molecule, through the regulation of the signal transducer and activator of transcription 3 (STAT3) phosphorylation status [445]. These observations seemed to point-out the involvement of TRAP1 in the processes of cell invasion and motility. Later, the identification of TRAP1-regulated pathways in an hypoxic model, demonstrated that TRAP1 regulates the expression of genes involved in cell cycle and metastasis [446]. In this study, TRAP1 depletion in lung cancer cells resulted in an increase of genes involved in cell motility and metastasis suggesting that TRAP1 activates proliferation while inhibiting cell invasion [446]. In addition, Leav and

collaborators identified TRAP1 as a novel molecular target in localized and metastatic prostate cancer [433].

As previously mentioned, TRAP1 expression is increased in numerous cancer cells and tissues when compared with their normal counterparts [433, 447, 448]. TRAP1 overexpression in cancer cell lines is associated with multi-drug resistance phenotype [442, 447]. However, the full mechanism for such resistance remains to be elucidated. For instance, Montesano and colleagues demonstrated that TRAP1 upregulation is associated with cell resistance to H_2O_2-induced DNA damage and apoptosis upon cisplatin treatment [442]. These observations were later supported by independent works showing a link between TRAP1 overexpression and the acquisition of a multi-drug resistance phenotype in colorectal cancer cells [447].

Studies in Parkinson Disease (PD) brought great contributions to the knowledge of some TRAP1 regulation mechanisms [437]. Pridgeon and colleagues found that phosphorylation of TRAP1 by PINK1 protects against ROS-mediated cell death whereas variants of PINK1 exhibiting loss of function mutations in PD patients were unable to reverse cell death [437]. TRAP1 phosphorylation by PINK1 seems to be required to enable its cytoprotective effect and preserve mitochondrial integrity, at least in neuronal cells.

Despite these advances in the understanding of TRAP1 role in apoptosis protection, the mechanisms behind TRAP1 cytoprotective effect in tumor cells are still unknown. Following this line of thought, recent studies regarding HSP90 protective role in tumor cells led to the identification of a mitochondrial chaperone network implicated in this process [304]. TRAP1 directly interacts with CypD, inhibiting mPTP opening and consequent cytochrome *c* release upon apoptotic stimuli [304]. The authors also identified a pool of HSP90 localized in mitochondria and demonstrated that both of these two chaperones physically associate with CypD and are required to oppose its function [304]. Later, works developed by Ghosh and collaborators led to the identification of HSP60 as an additional CypD interacting partner [302]. Altogether, CypD modulation seems to occur through its interaction with a multi-chaperone complex comprising HSP60, HSP90, and TRAP1 (Fig.4.1). Furthermore, the antagonistic functions of these chaperones regarding mPTP opening require their ATPase activity suggesting that protein folding/refolding is critical in regulating CypD functions [304]. These data support the mPTP model proposed by Lemasters [449] composed of clusters resulting from oxidized and misfolded proteins, which would expose hydrophilic residues to the lipid membrane

creating therefore the channel. Accordingly, pore closure would be determined by chaperone proteins, which would bind to the cluster blocking channel conductance [449].

In addition to CypD and PINK1, Sorcin, a mitochondrial localized low molecular weight (18KDa) calcium-binding protein, was recently identified as a novel TRAP1-interacting molecule [450]. In this work, the authors propose that Sorcin interaction with TRAP1 is implicated in stabilization of this chaperone through post-translational mechanisms. Functionally, this interaction was shown to be important for Sorcin-induced multidrug resistance phenotype and antiapoptotic activity whereas Sorcin mitochondrial localization and stability seems to be crucial for TRAP1 regulation of cell survival [450]. The crucial role of this 18-KDa Sorcin isoform in mitochondrial Ca^{2+} homeostasis maintenance, contributing to the regulation of mPTP opening, and the relevance of the TRAP1/Sorcin complex in TRAP1 cytoprotective pathway contribute for a better understanding of TRAP1 mPTP modulation.

The most recent function attributed to TRAP1 is its involvement in ER stress protection [451]. TRAP1 expression regulates ER stress levels, i.e. TRAP1 expression decreases upon strong ER stress, resulting in the activation of the ER stress-induced unfolded protein response (UPR) pathway protecting cells against ER stress-induced cell death [451]. However, these results were quite inconclusive regarding the mechanisms through which TRAP1 is involved in ER stress protection. Nevertheless, Altieri's group showed that selective targeting of mitochondrial HSP90 chaperones in tumor cells triggers compensatory autophagy and an UPR based on the upregulation of CCAAT enhancer binding protein (C/EBP) transcription factor and its dimerization partner C/EBP homology protein (CHOP) [452]. Simultaneous works led to the identification of TBP7, an AAA-ATPase component of the 19S proteasome subunit, as a TRAP1-interacting partner whose role is determinant in protein quality control (Fig.4.1) [452]. Moreover, TRAP1/TBP7 was shown to regulate ubiquitination of the 18KDa Sorcin isoform.

4.1.2 Targeting the mitochondrial complex of HSP90, TRAP1 and CypD in cancer cells

The above data highlight TRAP1 cytoprotective functions in cells [438]. These results together with TRAP1 differential expression in cancer as opposed to normal tissue [447]

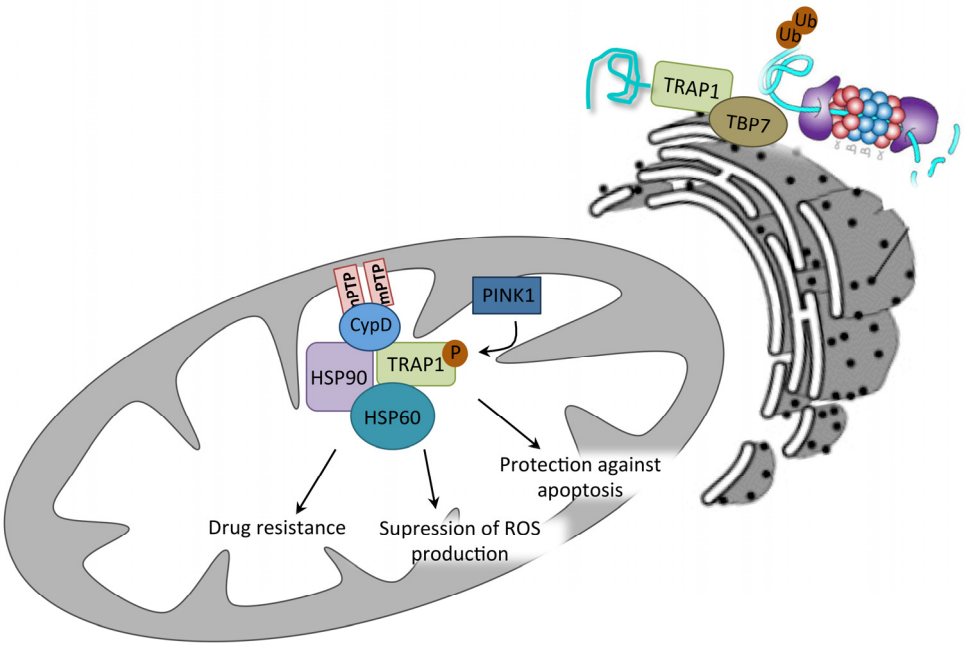

Figure 4.1 - TRAP1 cytoprotective functions in tumor cells. The differential expression of TRAP1 in tumor cells as opposed to normal cells has been associated with the acquisition of resistance to chemotherapeutic agents, inhibition of apoptosis, and suppression of ROS production, to which TRAP1 phosphorylation by PINK1 is thought to be required. A possible mechanism through which TRAP1 exerts its protective functions may be by interacting with CypD modulating mPTP. In addition, other molecular chaperones, namely HSP90 and HSP60, also seem to be involved in this function. More recently, TRAP1 was described to form a complex with TBP7 on the outside of the ER. This complex is involved in the control of stability and ubiquitination of several mitochondrial proteins. Abbreviations: CypD – cyclophilin D; HSP – heat shock protein; mPTP – mitochondrial permeability transition pore; PINK1 – PTEN induced putative kinase 1; ROS – reactive oxygen species; TRAP1 – TNF receptor-associated protein 1.

suggests TRAP1 involvement in tumor maintenance and the ability of tumor cell growth and survival under stress conditions, making it a potentially attractive target for cancer therapy. Moreover, the identification of a mitochondrial chaperone network, comprising HSP90, TRAP1 and CypD, brought new insights on TRAP1 mitochondrial integrity maintenance function [304]. As previously mentioned (Section 4.1.1), HSP90 and TRAP1 bind to and antagonize CypD allowing cancer cells to circumvent apoptosis. Therefore, inhibition of this complex seems to provide an efficient approach of targeting cancer cells.

Two types of drug candidates have shown high efficacy, shepherdin and gamitrinibs. Shepherdin was the first drug designed to target HSP90-like mitochondrial pool, and it

was shown to interact with the N-terminal region of HSP90 and TRAP1, which harbors their ATPase activity [453]. In the mitochondrial matrix of tumor cells, shepherdin rapidly induces apoptotic cell death in a CypD-dependent manner [454]. Further evidence of this inhibitor efficacy came from studies with TRAP1 overexpressing colorectal cancer cells. Treatment with shepherdin overcame cells resistance to chemotherapeutic agents [447].

A novel class of small molecule inhibitors of HSP90 that has been studied provide a less toxic alternative than the classic inhibitor Geldanamycin (GA) which binds to the ATP binding pocket, preventing ATP hydrolysis and revealed high hepatotoxicity in mammals [423, 424, 455]. Gamitrinibs (GA mitochondrial matrix inhibitors) are provided with a mitochondrial targeting sequence, which allows their accumulation in tumor mitochondria. Unlike gamitrinibs, non-GA derivatives such as NVP-AUY922 are not able to specifically accumulate in tumor mitochondria. Several studies show that gamitrinibs reveal a unique mechanism of action (revised in [454]). Within mitochondria, these mitochondria-targeted HSP90-like protein inhibitors lead to higher mitochondrial stress, namely the activation of the mitochondrial UPR, which in turn results in increased mitophagy [456]. In addition, tumor cell treatment with gamitrinibs causes a decline in mitochondrial and cytosolic energy production initiating the energy-sensing AMPK pathway and subsequent mTOR inhibition [457]. As a consequence of mTOR inhibition, there is an increase in the autophagy pathway in tumor cells. Importantly, these studies revealed high selectivity of gamitrinibs towards tumor cells showing no toxicity to their normal counterparts.

Gamitrinibs effect on tumor cells has been widely studied and has revealed a high potential for anticancer therapy emphasizing the important role of TRAP1 and HSP90 in tumorigenesis. Furthermore, gamitrinibs potential tumor selectivity may be justified not only by the differences observed in TRAP1 expression between tumor and normal mitochondria, but also by a possible increase in ATPase activity in transformed cells similarly to what happens with HSP90 [458].

Chapter 5

Hypothesis and Aims

As described in Chapter 4, TRAP1 is a highly expressed mitochondrial chaperone, in tumor cells, with antioxidant and antiapoptotic functions. The last decade of investigation added valuable information regarding TRAP1 network, unveiling the high complexity and wide range of mechanisms involved in TRAP1 role in tumorigenesis. However, despite the increasing knowledge on TRAP1 function in tumor cells there are still gaps that need to be filled for a better understanding of its mechanisms of action. Therefore, deeper investigation of TRAP1 role in mitochondria homeostasis and quality control is of great interest as it may contribute to the development of new therapeutic strategies.

Hence, **this work aspires to contribute with new insights on TRAP1 role in mitochondria protection and in quality control systems regulation**. Based on previous observations indicating TRAP1 as a mediator of tumor homeostasis through protection against mitochondrial dysfunction **we hypothesize that TRAP1 pro-survival actions are mediated by its interaction with critical cellular quality control systems upregulating survival under stress conditions and preventing mitochondrial disruption**. Thus, this study first aims the better understanding of the extent of TRAP1 role in mitochondrial integrity maintenance with special focus on the identification of the mitochondrial phenotype resulting from TRAP1 silencing. The second aim regards TRAP1 presumable involvement in the activation/suppression of quality control systems as a mechanism to achieve its cytoprotective role. In addition, this project intends to predict, the possible clinical significance of TRAP1 regulated quality control systems for tumor progression and maintenance.

This dissertation was divided in two independent chapters considering the two cell models used in our investigation. Alterations regarding mitochondrial function and morphology in TRAP1-depleted A549 lung cancer cells, a cell model which expresses high TRAP1 levels, are described in Chapter 7. Furthermore, the information which will be presented here will test whether TRAP1 impacts mitochondrial dynamics in this cell line. Also, studies concerning TRAP1 involvement in autophagy and apoptosis modulation are presented here, since stress-responses in the context of cancer are of high relevance for onco therapy.

The same scientific approaches were independently performed in MRC-5 normal human lung fibroblast cell line, and are present in Chapter 8. As this cell line revealed low TRAP1 content, this study aimed the deeper understanding of cell (in)dependence on TRAP1 in terms of mitochondrial dynamics and cell quality control. This work provided further information on TRAP1 function and effects of its inhibition in cells with low expression, which can mimic, saving the obvious differences, a pre-transformed cellular condition.

Finally, Chapter 9 integrates all the obtained results with information previously provided in the literature. This dissertation provides relevant and new information on how TRAP1 exerts its cytoprotective functions in tumor cells. Moreover, this work also brings novel interesting information on TRAP1-silencing effect in cells with low TRAP1 content providing new material for the eventual need of implementation of different therapeutic approaches.

Part II

Experimental Procedures & Results

Chapter 6

Material and Methods

6.1 Materials
6.2 Cell Culture
6.3 Experimental design
6.4 Sulforhodamine B assay
6.5 Material harvesting
6.6 Protein Quantification
6.7 Protein quantification and cellular localization
6.8 Quantitative RT-PCR
6.9 Evaluation of oxygen consumption
6.10 Evaluation of mitochondrial membrane potential
6.11 Evaluation of oxidative stress
6.12 Evaluation of mitochondrial permeability transition pore opening
6.13 Caspase-like activity assay
6.14 Fluorescence detection of lysosomal bodies
6.15 Statistics

6.1 Materials

6.1.1 Standard solutions and buffers

All aqueous solutions and buffers were prepared with Milli-Q water. Whenever needed buffers' pH was determined using a pH meter, which was regularly standardized with the following standard buffer solutions pH 7.0, 4.0, and 10.0. The solutions of siRNA

oligonucleotides to desired concentration were prepared in RNase DNase free water contained in the respective kits. All agents used in drug toxicity assays were diluted into the desired concentration directly in complete cell growth medium (see Section 1.2).

6.1.2 Reagents and kits

Reagents used in cell culture, such as 0.05% Trypsin-EDTA (Catalog# 25300-062), fetal bovine serum (FBS; Catalog# 16000-044), Penicillin-Streptomycin (Catalog# 15140-122), and Iscove's Modified Dulbecco's Medium (IMDM; Catalog# 12440-046), as well as 1x Opti-MEM (Catalog# 31985-047), and 10x Hank's Balanced Salt Solution, calcium, magnesium (HBSS/Ca^{2+}/Mg^{2+}; Catalog# 14065-049) were purchased from Invitrogen (Carlsbad, CA, USA).

The TRAP1 (Catalog# SI03066364) and the scrambled (Catalog# D-001810-03-20) siRNA oligonucleotides were obtained from Qiagen (Madrid, Spain) and Thermo Fisher Scientific (Lafayette, CO, USA) respectively, while Lipofectamine 2000 (Catalog# 11668-019) transfection reagent was from Invitrogen (Carlsbad, CA, USA). Additionally, 5x siRNA buffer (Catalog# B-002000-UB-100), used for oligonucleotide dilution during cell transfection protocol, was purchased from Thermo Fisher Scientific (Lafayette, CO, USA).

Agents used in drug toxicity assays such as Doxorubicin (Catalog# D1515), 3-Methyladenine (Catalog# M9281), and Rapamycin (Catalog# R8781) were obtained from Sigma-Aldrich (St. Louis, MO, USA). Total RNA harvesting RNeasy mini kit (Catalog# 74104) as well as the RNase-Free DNase set (Catalog# 79254) were acquired from Qiagen (Madrid, Spain), while the Recombinant RNasin ribonuclease inhibitor (Catalog# N2111) used was from Promega (Madison, WI, USA).

Reagents used for total protein harvesting such as RIPA buffer (Catalog# 89900), and the protease inhibitor cocktail (Catalog# P83490) were purchased from Thermo Fisher Scientific (Lafayette, CO, USA) and Sigma-Aldrich (St. Louis, MO, USA) respectively. The protein quantification bicinchonic acid assay (BCA) was performed using the Pierce BCA assay kit (Catalog# 23250) from Thermo Fisher Scientific (Lafayette, CO, USA).

Moreover, for Western Blot, precision plus protein dual color (Catalog# 161-0374) molecular weight standard and the blotting-grade blocker non-fat dry milk (Catalog# 170-6404) from BioRad (Hercules, CA, USA) were chosen. In addition, membrane protein

detection was achieved using the Enhanced Chemi-Fluorescence system (ECF; Catalog# RPN3685) from GE Healthcare (Buckinghamshire, UK). All primary antibodies used are listed in Table 6.2 as well as their respective catalog number and brand; the secondary antibodies used were all purchased from Santa Cruz biotechnology (Heidelberg, Germany). Moreover, when mounting coverslips during immunocytochemistry assay, ProLong Gold antifade reagent with DAPI (Catalog# P36935) from Invitrogen (Carlsbad, CA, USA) was used.

All primers used were purchased from Integrated DNA Technologies (Coralville, IA, USA) and can be found listed in Table 6.3. Reverse transcription was performed using the iScript cDNA Synthesis kit (Catalog# 170-8891) while the SsoFast EvaGreen Supermix (Catalog# 172-5201) was chosen for quantitative PCR, all from BioRad (Hercules, CA, USA). For classic PCR the HotStarTaq Master Mix (Catalog# 203443) from Qiagen (Madrid, Spain) was used.

In order to confirm primer specificity, agarose gel electrophoresis was performed using BlueJuice Gel loading buffer (Catalog# 10816-015) and a 100bp DNA ladder (Catalog# 10380-012) all from Invitrogen (Carlsbad, CA, USA) while 10x Tris Acetate-EDTA buffer (TAE; Catalog# T9650) was obtained from Sigma-Aldrich (St. Louis, MO, USA). DNA amplification products were purified with the MiniElute PCR Purification kit (Catalog# 28004) from Qiagen (Madrid, Spain).

All probes used in the present work, which include the Tetramethylrhodamine, methyl ester (TMRM; Catalog# T-668), MitoTracker Green FM (MTG; Catalog# M-7514), H_2DCFDA (Catalog# D-399), MitoSOX Red (Catalog# M-36008), LysoTracker Green (Catalog# L-7526), and the MitoProbe Transition Pore Assay kit (Catalog# M-34153), were purchased from Molecular Probes, Invitrogen (Carlsbad, CA, USA).

Caspase 3/7 and 9-like activities were analyzed with caspase Glo 3/7 (Catalog# G8090) and caspase Glo 9 (Catalog# G8210) assay kits respectively, from Promega (Madison, WI, USA), whereas caspase 12-like activity was measured with the fluorimetric Caspase 12 assay kit (Catalog# ab65664) from AbCam (Cambridge, UK). Caspase 8-like activity was accessed using the granzyme B substrate I (Catalog# 368057) from Millipore (Billerica, MA, USA).

All general chemicals used were of the highest grade of purity commercially available.

6.2 Cell Culture

6.2.1 Cell lines

In the present work, the A549 lung cancer and MRC-5 normal lung fibroblast cell lines were used. The A549 cell line was first developed in 1972 by D.J. Giard, *et al* through explant culture of lung carcinomatous tissue from a 58-year-old Caucasian male [459]. A549 cells are a monolayer human adenocarcinomic alveolar basal epithelial hypotriploid representative with a modal chromosome number of 66 occurring in 24% of cells. Although most of the cells contain two X and two Y chromosomes, 40% of the cell population may have lost one or both Y chromosomes.

The MRC-5 cell line was initially derived by J.P. Jacobs from normal lung tissue of a 14-week-old male fetus aborted for psychiatric reasons from a 27-year-old physically healthy woman [460]. Cells show a fibroblast-like morphology and present normal diploid human cell line with 46,XY karyotype without any known alterations in the X and Y chromosomes.

Both cell lines were purchased from ATCC (LGC Standards, Middlesex, UK), stored frozen in liquid nitrogen vapor phase and expanded following manufacturer's instructions. For routine subculturing, cells were first rinsed with 1x Phosphate Buffered Saline (1x PBS; 0.137 M NaCl, 2.7 mM KCl, 1.4 mM KH_2PO_4, 0.01 M Na_2HPO_4) and then incubated with 1 volume of trypsin-EDTA for 3 min at 37°C. Trypsin activity was inhibited by the addition of 1 volume of complete growth medium and the final volume centrifuged at 300x*g* for 3 min at room temperature. An appropriate aliquot of the cell suspension was added to new culture flasks to obtain cultures between $2x10^3$ and $1x10^4$ viable cells/cm^2. This procedure was repeated when cultures reached 80-90% confluence. Cells were used between passages 5 and 25.

Unless stated otherwise, the normal culture medium was Iscove's Modified Dulbecco's Medium (IMDM) supplemented with 5% FBS and 1% penicillin-streptomycin (all from Invitrogen) at 37°C in humidified air with 5% CO_2 (all concentrations in vol/vol).

6.2.2 siRNA Transfection

TRAP1 silencing was performed using a commercial available small interfering RNA (siRNA). siRNA are a class of double-stranded RNA, of short length (20-25 base pairs), present in nature as a mechanism to inhibit gene expression [461] The rationale behind it is that in normal cells, mRNA can only exist as a single strand. Because siRNA is complementary to the mRNA sequence, it binds to it and lead to its destruction. The RNAi pathway is depicted in Fig.6.1; briefly, the double-strand RNA is unwound through an ATP-dependent step by the RNA-induced silencing complex (RISC) where one of the strands is degraded and the other assists in the identification of RNAs that are complementary to this single stranded siRNA. Next, an endoribonuclease cleaves the referred RNA, which is then degraded by exoribonucleases [461].

Cells were transfected with 50nM of either TRAP1 siRNA oligonucleotide, antisense strand 5'- UGG AUG AGG ACU UUG CGG CTG -3' (Qiagen), or with a scrambled siRNA (Thermo Fisher Scientific). Oligonucleotides were prepared following the manufacturer's instructions in order to obtain a 20μM stock solution.

Transfection was performed using Lipofectamine 2000™ transfection reagent (Invitrogen) according to the manufacturer's instructions. Twenty-four hours prior to transfection, cells were seeded at a concentration of $1x10^5$ cells/mL in standard 60mm dishes and incubated overnight under normal growth conditions. In the transfection day, two sets of three tubes were prepared, tubes **1** to **3**, and **1'** to **3'**, as represented in Fig.6.2. The TRAP1 and control oligonucleotides were diluted to the desired concentration (50nM) in 1x siRNA buffer (Thermo Fisher Scientific) in the first set of tubes, tubes **1** and **2** respectively (see Fig.6.2), reaching the final volume of 250μL. In **tube 3**, only 250μL of the referred buffer was added. Additionally, in the second set of tubes, namely tubes **1'** and **2'**, Lipofectamine 2000™ was diluted in Opti-MEM (Invitrogen) without serum to a final volume of 500μL. Moreover, 500μL of Opti-MEM was added to tube **3'**. Both sets of tubes were incubated for 5 min at room temperature before addition of 250μL of Opti-MEM to the first set of tubes (**1** to **3**).

Next, the content of **tubes 1** to **3** was combined with **tubes 1'** to **3'** respectively and incubated for 20 min at room temperature allowing complexes to form. Once the incubation was complete, complexes were added to dishes containing cells and 1.5mL of Opti-MEM and incubated for 5 hours under growth conditions until the addition of 2.5mL

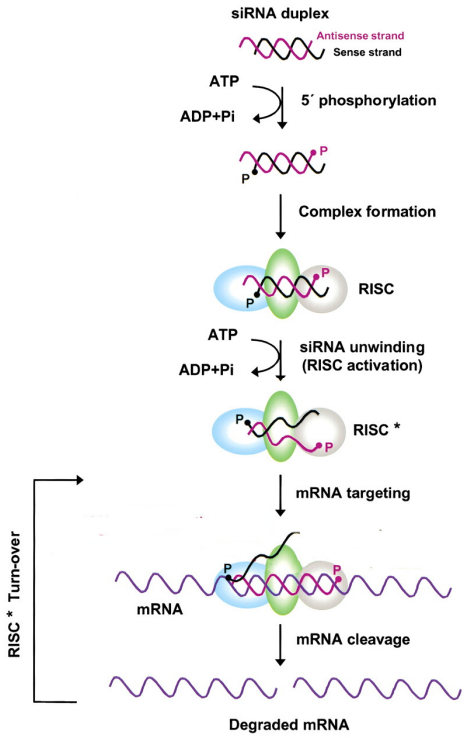

Figure 6.1 - siRNA pathway. The double-strand RNA (dsRNA) is unwound through an ATP-dependent step by the RNA-induced silencing complex (RISC). Upon dsRNA loading onto RISC the passenger (sense) strand is cleaved so that active RISC contains the guide (antisense) strand. Consequently, the siRNA guide strand recognizes target sites to direct mRNA cleavage. Adapted from [460].

of complete growth medium. The cell culture medium was changed 24 hours after transfection to remove unloaded oligonucleotides and transfection reagent from solution and cells were allowed to grow for 48 hours before further experiments.

6.3 Experimental design

The overall experimental design is shown in Fig. 6.3. Twenty-four hours before the transfection protocol, cells were seeded in 60mm dishes. The time of transfection was designated as *time zero* and cells were kept in culture for 48 hours for an efficient transfection. However, at that time, and depending on the final objective of the experiment, cells were harvested and seeded into proper plastic ware or glass coverslips

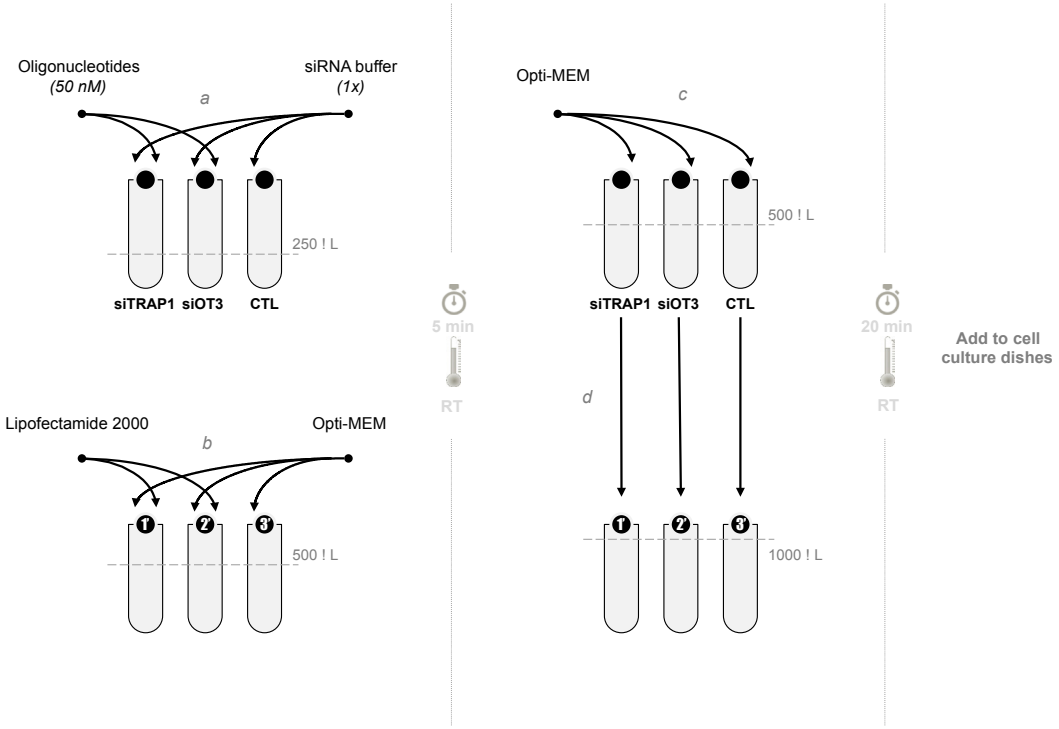

Figure 6.2 - Cell transfection scheme. Two sets of three sterile RNase DNase free tubes were prepared (tubes 1 to 3 and 1' to 3'). Firstly, 250μL of 1x siRNA buffer was added to tubes 1 to 3 and 500μL of Opti-MEM to tubes 1' to 3'. Moreover, 50nM of either TRAP1 siRNA or scrambled RNA oligonucleotides were added to tubes 1 and 2 respectively while Lipofectamine was added to tubes 1' and 2'. Tubes were incubated for 5 min at room temperature before addition of 250μL of Opti-MEM to tubes 1 to 3. After incubation time, the content of tubes containing the diluted oligonucleotides was combined with the respective tube containing the transfection reagent. Tubes were incubated for 20 min at room temperature. In the mean time, cells were washed three times with pre-warmed 1x PBS and 1.5mL of Opti-MEM was added to each plate. After the incubation period, the content of each tube was added in different cell plates and let incubate for 5 hours under normal growth conditions.

24 hours before the assay (live imaging, immunocytochemistry, caspases 3/7 and 9-like activity and Sulforhodamine B, SRB assay), or otherwise kept in culture (mRNA and protein harvest, flow cytometer, caspases 8 and 12-like activity) until 72 hours post-transfection.

A relevant note should be made regarding the incubation times in SRB assay to clarify the reader. Although the results are expressed as percentage of *time zero*, this designation

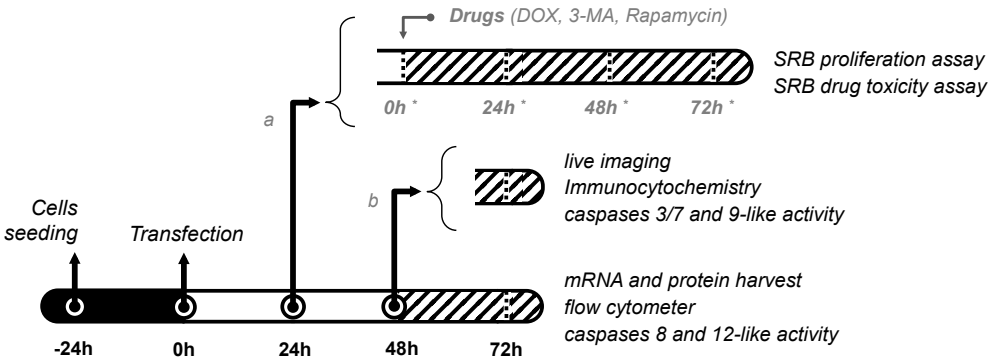

Figure 6.3 - Experimental design. Twenty-four hours prior to transfection 1x105 cells/mL were seeded in a standard 60mm dish and incubated overnight under normal cell culture conditions. Cells were then transfected with either a TRAP1 siRNA (siTRAP1) or a scrambled siRNA (siCTL) for control, another control group of non-treated cells (CTL) was added to the experiment. The medium from cells used for mRNA and protein harvest as well as for flow cytometry assays was replaced twenty-four hours post-transfection and cells were leave to rest for 48 hours under growth conditions until used. However, when performing SRB proliferation assays, transfected cells were transferred to a 48-well plate 24 hours post-transfection. Moreover, at 48 hours post-transfection, these same cells were either drugged or allowed to grow and medium from cells corresponding to time zero was removed. The experimental protocol was conducted until stopping cell growth at the pretended time point. To perform live imaging, immunocytochemistry and caspase 3/7 and caspase 9-like activity assays, transfected cells were transferred to the respective plates 48 hours post-transfection while assay was performed 72 hours post-transfection.

does not refer to the time when transfection was performed but to 24 hours post-cell plating. In fact, the *SRB time zero* refers to 48 hours post-transfection (please consult Fig.6.3 to visualize the protocol).

6.4 Sulforhodamine B assay

Skehan introduced the sulforhodamine B (SRB) assay in 1990[462]. This method is based in the ability of the bright pink aminoxanthene SRB dye with two sulfonic groups to bind to cell proteins under mildly acidic conditions. Under these conditions, SRB binds to protein basic amino acid residues in acid-fixed cells to provide an estimate of total protein

mass, which is related to cell number. Accordingly, this assay allows to indirectly access cell proliferation and viability. Moreover, once pH is alkalinized, basic amino acids became protonated and the SRB dye is released into the solution allowing its measurement through a conventional spectrophotometer.

The protocol used in the present work follows the initial method with minor modifications. Since in most situations the experiment was performed in such a way that a single microplate contained wells for different time points, cells were first dried before being methanol fixed in order to stop cell growth. For that purpose and at the required time points, wells were washed twice with 1x PBS and allowed to dry in the incubator at 37°C for the remaining time of the experiment. Once all wells were processed, cells were fixed with ice-cold 1% acetic acid in methanol overnight at -20°C and covered with parafilm. Microplates containing fixed cells were then dried at 37°C and 0.5% SRB in 1% acetic acid was added to each well and incubated for 30 min at 37°C and subsequently washed three times with 1% acetic acid to remove unbound staining. Plates were then allowed to dry before the addition of 10mM Tris (pH 10), which was incubated at room temperature for 15 min in an orbital shaking platform in order to solubilize bound-protein stain. Finally, 200µL of the solubilized solution was transferred to a standard 96-well plate and its absorbance read in a VITOR X3 microplate reader (Perkin Elmer, Waltham, MA, USA) working at room temperature with a 544/15 nm filter.

Note that the volume of solution added was always the standard advised volume for the plate in use.[3]

6.4.1 Cell proliferation assay

For evaluation of cell growth, cells were seeded at a concentration of $2x10^5$ cells/mL in 48-well plates. Note that the referred seeding time corresponds to 24 hours post-transfection (see Fig.6.3). Twenty-four hours later, one of the wells was used as *time zero* to normalize cell proliferation and reduce inter-plate and inter-day variability associated with the assay. Then, every 24 hours, wells were processed as described in the previous section to estimate cell growth.

[3] Recommended volumes for plastic labware material used can be found in the manufacturer's website: http://catalog2.corning.com/Lifesciences/media/pdf/an surface areas reco med vol for cc vessels.pdf.

Table 6.1 - Drug concentrations and combinations used in SRB proliferation assays.

Name	Concentration	Incubation Time *
Doxorubicin	0.5 µM	0 to 72 h
Rapamycin	100 nM	0 to 72 h
3-methyladenine	5 mM	0 to 72 h
Doxorubicin + Rapamycin	0.5 µM + 100 nM	0 to 72 h
Doxorubicin + 3-methyladenine	0.5 µM + 5 mM	to 72 h

*Note that incubation time is relative to SRB time zero and not post-transfection period, corresponding to 48h to 120h post-transfection.

Drug toxicity assay

To evaluate cells susceptibility to different chemical compounds, the following setup was used: cells were seeded at a concentration of $2x10^5$ cells/mL in 48-well plates, 24 hours post-transfection (see Fig.3). After 24 hours, one well was used as *time zero* and the agents were added to cells. For this purpose, a solution with the compound in study was prepared in complete growth medium and then added to wells. Every 24 hours, wells were processed as described before (Section 2) to estimate cell growth. Table 6.1 shows agent concentrations applied in this study as well as the time of addition.

6.5 Material harvesting

6.5.1 Total RNA

Total RNA was isolated using the RNeasy Mini Kit (Qiagen) with minor alterations. In the day of the harvesting (72 hours post-transfection) cells grown in 60mm dishes were rinsed once with 1x PBS and incubated with 1 volume of trypsin during 3 min at 37°C to detach cells. Then, 1 volume of complete growth medium was added to stop the reaction and cells were centrifuged for 3 min at 300x*g* at room temperature, with the supernatant being discarded.

To disrupt cells and remove the nuclei, the pellet was resuspended in 350µL of RLN [50mM Tris pH 8.0, 140mM NaCl, 1.5mM $MgCl_2$, 0.5% NP-40, 1mM DTT supplemented with 175 U RNAsin (Catalog# N2111, Promega)] and incubated on ice for 5 min. Tubes were then spun at 300x*g* for 2 min at 4°C and pellets discarded.

RNA extraction was initiated with the addition of 600µL of Buffer RLT (supplemented with 1% of β-mercaptoethanol) and vigorously vortexing the tubes. Once mixing was complete, 430µL of 100% biomolecular grade ethanol was added to the tubes and the resulting solution was transferred to a RNeasy spin column placed in a 2mL microtube and centrifuged at 8,000x*g* for 15 sec. After discarding the flow-through, the column was washed with RW1 buffer at 8,000x*g* for 15 sec followed by an in-column DNase digestion performed by adding 80µL DNase I incubation mix (RNase-Free DNase Set, Qiagen) directly to the column and incubating for 15 min at room temperature. Finally, columns were washed once with RW1 buffer (8,000x*g* for 15 sec) and twice with RPE (firstly, 8,000x*g* for 15 sec; secondly, 8,000x*g* for 2 min).

RNA was eluted twice from the columns with 30µl RNase-free water to two separate new 1.5mL RNase DNase-free microtubes. RNA was quantified using a NanoDrop spectrophotometer (Thermo Fisher Scientific) to measure the absorbance at 260nm (A260). Finally, RNA quality and purity was tested by spectral scan observation and considered when a single prominent A260 peak and an A260/A280 ratio with a minimum value of 2, was found.

6.5.2 Total protein

Two different buffers were used to extract total protein depending on its final applications. Extracts for western blot were collected with RIPA buffer (Thermo Fisher Scientific; 25mM Tris-HCl pH 7.6, 150mM NaCl, 1% NP-40, 1% sodium deoxycholate, 0.1% SDS) as it detergent composition allows efficient extraction of water-soluble and membrane-inserted proteins. On collection day, cells grown in 60mm dishes were washed once with 1x PBS, detached with 1 volume of trypsin followed by its inactivation with 1 volume of complete growth medium. Cells were transferred to a 15mL tube and centrifuged at 300x*g* for 3 min; supernatant was discarded and pellet rinsed in 1x PBS. Cells underwent another centrifugation at 300x*g* for 3 min and the supernatant was

discarded. Finally, cells were lysed in 1mL of RIPA supplemented with protease inhibitors cocktail (Sigma-aldrich) and 1mM DTT.

The suspension was kept on ice for 20 min, mixed with a pipette every 5 min. Lysates were then sonicated three times 1.5 sec at 60 A with 18 W output. Protein content was determined by BCA assay (Section 4) using Bovine Serum Albumin (BSA) as standard.

Extracts for caspase 8-like activity assay (Section 11.2) were collected using a mild-detergent buffer composition that allows proteins to retain their activity. On collection day, cells grown in 60mm dishes were washed once with 1x PBS, detached from the dishes with 1 volume of trypsin followed by its inactivation with 1 volume of complete growth medium. Cells were then transferred to a 15mL tube and centrifuged at 300x*g* for 3 min; supernatant was discarded and pellet rinsed in 1x PBS. Cells underwent another centrifugation at 300x*g* for 3 min and the supernatant was discarded. Finally, cells were lysed in a buffer containing 100mM NaCl, 0.1% CHAPS, 1mM DTT, 0.1mM EDTA, 50mM HEPES pH7.4, and kept on ice for 20 min. Protein was quantified by BCA assay (Section 4), using BSA as standard.

6.6 Protein Quantification

6.6.1 Bicinchonic acid assay (BCA)

Protein was quantified using the bicinchonic acid assay (BCA) as it is less prone to errors resulting from the high detergent concentrations found in RIPA buffer. The commercial Pierce BCA assay kit (Thermo Fisher Scientific) was used and the complete protocol was as follows.

Working Reagent was prepared in a proportion of 50 parts of BCA reagent A to 1 part of reagent B. The reaction was initiated by adding 200µL of working reagent to 8µL of sample diluted 1:5 in ultrapure water, in a standard polystyrene flat bottom 96-well microplate. After 30 min incubation at 37°C, absorbance was read in a VICTOR X3 plate reader (Perkin Elmer Inc.) using a 544/15 nm filter. The standard curve ranging from 25 to 2,000 µg/ml was made using a solution of BSA standard ampules included in the referred kit. Standards and unknown samples were performed in duplicates.

6.7 Protein quantification and cellular localization

6.7.1 Immunoblotting

After protein quantification, samples were diluted in a 5:1 ratio with a homemade 5x concentrated Laemelli Buffer [62.5mM Tris pH 6.8 (HCl), 2% SDS, 50% Glycerol, 5% β-mercaptoethanol, 0.04% bromphenol blue] to achieve a working concentration of 1µg/mL. Protein lysates were then boiled at 95ºC for 5 min. The previous steps led to protein denaturation and therefore loss of quaternary, tertiary and secondary protein structure. Moreover, proteins obtained a uniform negative charge, which masks the intrinsic charges on the amino acids side-chain. Consequently, after this point, proteins can be separated solely as a function of their molecular size [463].

To accomplish that, samples (15 to 25µg of protein) were loaded in a discontinuous vertical polyacrylamide gel electrophoresis system. Polyacrylamide gels were formed by copolymerization between acrylamide and bis-acrylaminde through a vinyl addition polymerization reaction initiated with the addition ammonium persulfate (APS) and catalyzed by tetramethylethylenediamine (TEMED). The separating gel consisted in 12% acrylamide/bis, 375mM Tris pH 8.8 (HCl), 0.1% SDS, 0.05% TEMED and 0.05% APS while stacking gel consisted in 4% acrylamide/bis, 126mM Tris pH 6.8 (HCl), 0.1% SDS, 0.1% TEMED and 0.05% APS. Different final acrylamide/bis percentages were used depending on the molecular size of the proteins of interest allowing a maximum separation resolution (see Table 6.2).

Casted gels were fitted in a Mini-PROTEAN 3 Cell (Bio-Rad) filled with running buffer (25mM Tris, 192mM glycine, 0.1% SDS) and connected to a PowerPac Basic Power Supply (Bio-Rad) outputting a constant voltage of 150V. Separation was carried out at room temperature and until the front of the run reached the bottom end of the gel. Note that in every gel, a molecular weight standard (Precision Plus Protein Dual Color Standards, from Bio-Rad) was included to allow molecular weight estimation.

Once protein separation was complete, proteins were transferred to a thin surface layer of pre-activated (5 sec in 100% methanol followed by 15 min in 25mM Tris, 190mM glycine and 20% methanol) polyvinylidene difluoride membrane (PVDF, 0.45µm, Millipore, Billerica, MA, USA), by an electric current passed through the gel. For that, gels were

placed in a 'transfer sandwich' (filter paper-gel-membrane-filter paper), cushioned by pads and pressed together by a support grid/cassette. The supported gel sandwich was then placed vertically in a Mini Trans-Blot Cell (Bio-Rad) tank between stainless steel/platinum wire electrodes and filled with transfer buffer (25mM Tris, 190mM glycine and 20% methanol). Protein transference was performed at a constant voltage (100mV) during 90 min with a PowerPac Basic Power Supply (Bio-Rad). An ice pack was placed inside the tank to mitigate the heat produced during the transference.

Once protein transfer was complete, the membrane was labeled for future identification and incubated with blocking solution, 5% non-fat dry milk (Bio-Rad) in Tris-buffered saline Tween-20 (TBS-T; 154 mM NaCl, 50 mM Tris pH 8.0 (HCl) and 0.1% Tween-20) overnight (<18 hours) at 4°C under continuous stirring (Stuart SRT6 tube roller, VWR, Leuven, Belgium), to block non-specific binding. On the next day, membranes were washed three times for 5 min each with TBS-T prior to incubation with a primary antibody directed against the respective protein (listed in Table 6.2) overnight (>18 hours) at 4°C under continuous stirring (Stuart SRT6 tube roller), except for anti-actin antibody which was incubated for 2 hours only at room temperature. All primary antibodies were prepared in 1% non-fat dry milk in TBS-T supplemented with 0.02% sodium azide to a final volume of 5 ml and stored at 4°C for no longer than 4 months or used for a maximum of 4 times. Alternatively, antibodies were prepared in 1% BSA solution in TBS-T depending on manufacturer's instructions.

Once incubation was complete, membranes were washed three times for 5 min with TBS-T and incubated with alkaline phosphatase conjugated secondary antibodies (1:5,000 dilution) for 1 hour at room temperature under continuous agitation (Stuart SRT6 tube roller). Finally, membranes were washed three times in TBS-T for 5 min before immunodetection.

Membranes were dried and placed with the protein side down on a flat plastic plaque pre-filled with small droplets of Enhanced Chemi-Fluorescence system (ECF; GE Healthcare) substrate ensuring no air bubbles were trapped and was incubated for no longer than 5 min at room temperature. Alkaline phosphatase present in secondary antibody dephosphorylates the ECF substrate leading to the formation of a fluorescent product at 540 to 560nm when excited at the appropriate wavelength (UV), which localizes at the site of catalysis.

Table 6.2 - List of primary antibodies used in Western Blot protein analysis.

Code	Dilution	Host Species	MWt (KDa)	Gel (%)	Catalog Number	Manufacturer
Actin	1:10,000	Mouse	43	var.	MAB1501	Millipore
ATG12	1:300	Rabbit	16.53	12	4180	Cell Signaling
ATG3	1:500	Rabbit	40	10	3415	Cell Signaling
ATG5	1:500	Rabbit	55	10	2630	Cell Signaling
ATG7	1:300	Rabbit	78	10	2631	Cell Signaling
ATP sub c	1:500	Rabbit	14	8	ab96655	abcam
BAX	1:1,000	Rabbit	20	12	2774	Cell Signaling
BCL-2	1:500	Rabbit	26	12	2870	Cell Signaling
BCL-xL	1:1,000	Rabbit	30	12	2764	Cell Signaling
BECLIN-1	1:600	Rabbit	60	10	3495	Cell Signaling
CypD	1:10,000	Mouse	18	12	ab110324	abcam
DRP1	1:500	Mouse	80	10	611113	BD Biosciences
FIS1	1:500	Rabbit	17	14	IMG-5113A	IMGENEX
HSP90	1:600	Rabbit	90	10	4877	Cell Signaling
LAMP2A	1:500	Rabbit	100	10	ab18528	abcam
LC3	1:600	Rabbit	16/18	14	PD014	MBL
MFN1	1:200	Rabbit	87	10	sc50330	Santa Cruz
OPA1	1:200	Goat	132	9	sc30573	Santa Cruz
p62	1:1,000	Rabbit	62	10	PM045	MBL
PINK1	1:300	Rabbit	60	10	ab23707	abcam
SHC1	1:1,000	Mouse	66/52/46	10	610878	BD Biosciences
SOD-2	1:1,000	Rabbit	25	12	ab13533	abcam
TOM20	1:500	Rabbit	20	14	sc11415	Santa Cruz
TRAP1	1:750	Mouse	75	10	612344	BD Biosciences
Ubiquitin	1:750	Rabbit	10	14	3933	Cell Signaling

*also used in immunocytochemistry assay. Abbreviations: MWt – molecular weight; var. – variable.

Chemi-fluorescence data was collected using a UVP Biospectrum 500 Imaging System equipped with a BioChemi HR Camera (UVP, Upland, CA, USA) through UV (365 nm) epi-illumination. Camera settings, namely exposure time, were set-up in preview mode to optimize exposure and determine the appropriate final exposure settings using 4x4

binning with real-time exposure compensation. Data processing was performed with on-chip integration ensuring maximum exposure without signal saturation.

Densitometry analysis was carried out using Quantity One software (Bio-Rad Laboratories) where a rectangle with the maximum size similar to the band of greater length present in the blot was considered as the region of interest (ROI) which was then repeated for all the bands in the membrane. The parameter "adjusted volume", which represents the sum of all pixels intensity in ROI corrected for the local mean background, was used for analysis. The software calculates "local mean background" as the intensities of added pixels in a 1-pixel border around ROI and divided by the total number of border pixels. For each blot, data was first normalized as the percentage of the sum of the total density of all bands and then normalized to its respective actin immunoreactivity to achieve even amounts of protein loading in gels.

6.7.2 Immunocytochemistry

Twenty-four hours prior to the beginning of the experiment, $1.5x10^5$ cells/mL were seeded in 6-well plates containing sterile glass 18x18mm coverslips and were grown under normal culture conditions. For some experiments, mitochondria were first labeled using MitoTracker® Red CMXRos (MTR; Invitrogen) prior to fixation. The culture medium was removed and cells were washed with warm 1x PBS. Cells were then incubated with 125nM MTR for 45 min under normal growth conditions. After staining, cells were washed with fresh pre-warmed 1x Hank's Balanced Salt Solution, calcium and magnesium (HBSS/Ca^{2+}/Mg^{2+}; Invitrogen) and fixed with 3.7% formaldehyde in 1x PBS for 15 min at 37°C.

After fixation, coverslips were washed three times for 5 min each with 1x Phosphate Buffered Saline Tween-20 (1x PBS-T; 0.137 M NaCl, 2.7 mM KCl, 1.4 mM KH_2PO_4, 0.01 M Na_2HPO_4, 0.1% Tween-20) followed by cell permeabilization with 0.2% Triton X-100 in 1x PBS for 10 min at room temperature. Coverslips were washed again three times for 5 min each with 1x PBS and blocked with 1% BSA in 1x PBS-T solution for 60 min at room temperature in an orbital shacking platform. The volume used was enough to cover the entire well surface to ensure an efficient blocking. After blocking, coverslips were again washed three times for 5 min each with 1x PBS-T and transferred to a humid chamber, consisting in a squared glass container (20 x 20 cm) with filter paper soaked in ultrapure

water underneath the tray, in where the coverslips were incubated with the primary antibodies at 37°C for 90 min.

Primary antibodies (listed in Table 6.2) were used in a 1:250 dilution in 1% BSA in PBS-T solution. Coverslips were then washed three times for 5 min each with 1x PBS-T, and incubated with 1:250 diluted secondary antibodies in PBS-T containing 1% BSA solution in humid chamber for 60 min at 37°C. For dual immunofluorescence staining, antibodies were simultaneously incubated under the conditions described above. In this case, the only additional care was to make sure that the hosts of primary antibodies were distinct to allow fluorescent detection using different fluorophores (Texas Red or FITC).

All samples were mounted in microscope slides using ProLong® Gold antifade reagent with DAPI (Invitrogen) according to manufacturer's instructions. If visualization was not performed at the end of the protocol, slides were stored at -80C and analyzed as soon as possible. Slides were examined by confocal microscopy. Images were obtained in a Zeiss LSM510 META (Carl Zeiss Microscopy LLC, Thornwood, NY, USA) confocal scan head mounted on an inverted based-microscope Zeiss Axiovert 200M with a 63x objective. Sequential excitation at 350nm (DAPI), 490nm (FITC), 579nm (MTR) and 589nm (Texas Red) was provided by diode, argon gas and diode-pumped solid-state lasers, respectively. Emission filters BP500-550 and LP560 were used for collecting green and red channel images, respectively. After sequential excitation, all fluorescent images of the same cell were saved with LSM 510 software and then analyzed with ImageJ (NIH). The term colocalization refers to the simultaneous presence of green and red fluorescence in the same pixel, as measured by the confocal microscope.

6.8 Quantitative RT-PCR

6.8.1 Primer design

All primers were designed using the web-based Primer–Basic Local Alignment Search Tool (Primer-BLAST) after obtaining nucleotide accession numbers from the database. Both services are public and supported by the National Center for Biotechnology Information (NCBI).

Table 6.3 - List of primers used in the present work.

Accession Number	Code	Sequence	Amp. (bp)	T_m (°C)
NM_016292.2	TRAP1	5' - GTC GCG CAG GCT CAC GAC AA -3'	203	60
		5' - CGC AGC CAC TTG GGC AGG AT -3'		
NM_001017963.2	HSP90AA1	5' - CCC AGA GTG CTG AAT ACC CG -3'	191	60
		5' - GTG GAA GGG CTG TTT CCA GA -3'		
NM_001017963.2	HSP90AA1.1	5' - CAGT GAAG CATT TTTC AGTT GAAG G -3'	201	60
		5' - CCG AGT CTA CCA CCC CTC TA -3'		
NM_002156.4	HSP60	5' - TCT TTC GCC AGA TGA GAC CG -3'	191	60
		5' - ACT TCC CCA ACT CTG CTC AAT -3'		
NM_005729	PPIF	5' - CTC CGG GAA CCC GCT CGT GTA -3'	198	60
		5' - TCG CCC GCC TGG CAC ATG AA -3'		
NM_001130040.1	SHC1	5' - CTC ATT TGC ATC CGG CGG GGA -3'	111	60
		5' - GCA AGC CCT TCG GGA CAC TCC -3'		
	18S	5' - TCAA CTTT CGAT GGTA GTCG CCGT -3'		60
		5' - TCCT TGGA TGTG GTAG CCGT TTCT -3'		

Note: Amp -amplicon in base pairs; T_m - temperature of melting in Celsius.

The accession numbers used for the transcripts of interest analyzed are shown in Table 6.3. The default settings were used with the following exceptions: amplicon was set to a minimum of 70 bp and a maximum of 200 bp; primers should span an exon-exon junction and intron inclusion options were selected to allow specific amplification of mRNA over DNA or pre-mRNA.

Although the algorithm aims to design the best primer set, the operator should always double-checked the top five entries for: priming towards the *3'* of the target, optimal melting temperature close to 60°C and primers specificity amplifying no off-target gene sequences in the targeting genome. Additionally, secondary structure of the primer set was checked in OligoAnalyzer 3.1 web-based software from IDT. There, low intra-primer and between-primer complementary (low meting temperature and high $\triangle G$) were preferred.

All primers were synthesized by Integrated DNA Technologies (Coralville, IA, USA) and diluted in DNase RNase-free water to a working concentration of 10 μM upon arrival.

Primers were tested through a standard PCR and agarose gel and discarded if non-specific products were detected (none for the current design).

Primers for the HSP90 family

There are two subfamilies of the cytoplasmic HSP90A which differ by being constitutively or inducible expressed [213]. For the current study, the HSP90AA inducible family was chosen as the most relevant. This protein is encoded by two different genes, HSP90AA1 and HSP90AA2, which generating

HSP90-α_1 and HSP90-α_2 isoforms respectively. Moreover, the HSP90AA1 mRNA can occur as two transcripts variants due to alternative splicing increasing therefore the complexity of this analysis.

Running a *blastn suite-2sequences* to find similarity over the above mentioned sequences, besides the already expected 100% identity without gaps of HSP90AA1 variant 2, HSP90AA2 also shares 97% of homology with only 8 gaps in a total of 2868 bp when compared to HSP90AA1 variant 1. It was also evident from this screening that primers targeting position below the 711th bp would solely target the HSP90AA1 variant 1 transcript.

Therefore our strategy was to design one set of primers that would target both subfamilies and another that was able to detect specifically the HSP90AA1 variant 1 (HSP90AA1.1), following the above mentioned specifications.

6.8.2 Step one: reverse transcription

mRNA levels were analyzed through a two-step quantitative real-time polymerase chain reaction (PCR). The first step involves the reverse transcription of total mRNA into cDNA using the iScript cDNA Synthesis Kit (Bio-Rad). The kit contained a modified moloney murine leukemia virus (MMLV)-derived ribonuclease H plus (RNase H+)-type reverse transcriptase enzyme that synthesizes a complementary DNA strand up to 7 kb from single-stranded RNA. It also specifically degrades the RNA in RNA:DNA hybrids but not unhybridized RNA, also lacking endonuclease activity.

Additionally, the kit mix contained oligo(dT) and random hexamer primers to maximize the sensitivity (towards mRNA) and extension (increasing the probability that 5' ends of the mRNA would be converted to cDNA) of the reverse transcription reaction. Oligo(dT) is a short sequence of deoxy-thymine nucleotides that targets the poly-A tail only present in mRNA. The random hexamer priming consisted in the use of a mixture of oligonucleotides representing all possible nonamer sequences (5'–NNN NNN–3' with 4^6 = 4096 permutations).

The iScript mix was diluted in 1:5 with nuclease-free water and 1µg of total RNA to a final volume of 20µL, which was then loaded in PCR strip tubes recommended by vendor. Reactions were performed in a Bio-Rad S1000 thermal cycler running a single cycle programmed as follows: 5 min at 25ºC, 30 min at 42ºC and 5 min at 85ºC. In order to dilute the total cDNA for downstream PCR but also to dilute the salts present in the RT mix, the final product was diluted to one-tenth of the reaction volume.

6.8.3 Step two: real-time PCR

mRNA transcript levels were quantified in real-time PCR using 2µl of the cDNA samples and amplified with SsoFast™ EvaGreen® Supermix (Bio-Rad) in 20µl total reaction volume using 500nM of genetic-specific forward and reverse primers. SsoFast supermix uses Bio-Rad's Sso7d fusion protein technology in which the antibody-mediated hot-start feature sequesters the enzymatic activity prior to the initial PCR denaturation step and the dsDNA-binding protein stabilizes the polymerase:template complex and provides greater speed reducing reaction time [464].

Amplification and quantification of generated products were performed in a Multiplate® low-profile 96-Well unskirted PCR plate (Bio-Rad) sealed with an optically clear Microseal 'B' adhesive seal (Bio-Rad) and then loaded in a CFX96 Real-time PCR detection system (Bio-Rad) under the following cycling conditions: a single step of 95°C for 30 sec, 30 to 40 cycles of 95°C for 5 sec followed by another 5 sec at 60°C with single-point fluorescence acquisition at the end. Finally, a melting curve program was performed at the end of the amplification program in order to ascertain that only the expected products were generated. The melting curve program ranged from 65°C to 95°C for 5 sec per step with increments of 0.5°C.

Samples were run in duplicates, together with a standard curve for that respective transcript across 5 $\log_{10}$, which covered the range in the sample unknowns without extrapolating. This allowed calculating the efficiency of the reaction, which is of extreme importance in expression analysis. Additionally, a non-template control (NTC) and a negative control lacking cDNA template (NRT) were also included to ensure no contamination. None of the runs showed expression on these conditions and none was discarded.

6.8.4 DNA standards preparation

Standard curves were prepared by serial dilutions of a characterized DNA standard prepared from cDNA from either A549 or MRC-5 cells amplified through a simple PCR reaction using the HotStartTaq Master Mix Kit (Qiagen) and genetic-specific primers. For this purpose, the master mix was diluted with 0.3µM of forward and reverse primers and 10µL of cDNA template to a final volume of 50µL. The reaction was amplified in a Bio-Rad S1000 thermal cycler running a pre-incubation step at 95°C for 15 min, followed by 35 cycles of denaturation at 94°C for 30 sec, annealing at 60°C for 30 sec and extension at 72°C for 20 sec plus an additional final extension step at 72°C for 10 min.

In order to check primer set specificity and temperature reaction efficiency, the amplification product (10µL) was first diluted 4:1 with BlueJuice™ Gel loading buffer (Invitrogen) and then loaded in a 4% agarose (Invitrogen, Catalog# 16520-050) gel prepared in 1x Tris Acetate-EDTA buffer (TAE; Catalog# T9650, Sigma, St Louis, MO, USA) supplemented with 0.02% of ethidium bromide together with 5µL 100bp DNA ladder (Invitrogen). DNA fragments were separated through a horizontal electrophoresis system consisting in a multiSUB Midi (Cleaver Scientific Ltd, Rugby, Warwickshire, UK) connected to a PowerPac Basic Power Supply (Bio-Rad) running at 100mV for 1 hour at room temperature. In the end, the gel was imaged by UV (365nm) transillumination using a UVP Biospectrum 500 Imaging System equipped with a BioChemi HR Camera (UVP, Upland, CA, USA).

If a single product was detected the remaining PCR reaction product was purified using the MinElute® PCR Purification Kit (Qiagen) for efficient recovery of DNA fragments and removal of contaminants such as enzymes, primers, unincorporated nucleotides and salts. Briefly, the remaining PCR reaction was diluted 1:5 with PBI buffer, transferred to a

MiniElute column and centrifuged at 8,000x*g* for 1 min. The column was then washed with PE buffer by being first spin at 8,000x*g* for 1 min and then at 10,000x*g* for 1 min after discarding the flowthrough. The DNA standard was eluted by applying 10 µL of EB buffer to the center of column and incubation for 1 min at room temperature before centrifugation at 10,000x*g* for 1min and thereafter quantified in a NanoDrop 2000 (Thermo Fisher Scientific).

A standard stock solution of $5x10^9$ copies/mL was prepared using the following equation:

$$number\ of\ copies = \frac{Concentration_{Standard} \times Avograd o's\ number}{length_{amplicon} \times 650}$$

and stored at -20°C where *number of copies* is in copies/mL, the concentration of DNA standard in g/mL and 650 is the average molecular weight of a DNA base pair in g/mol.

6.8.5 mRNA expression analysis

Expression analysis was performed in CFX Manager Software (version 2.1) to normalize the relative differences in a target concentration between samples, where a reference gene was used to account for loading differences or other variations represented in each sample, thus used to normalize the expression levels of the gene of interest. In the present study 18S was used as the reference gene.

The software was set to calculate the normalized expression using the 'delta-delta C_t' ($\Delta\Delta C_t$) [465]. This is an efficiency corrected calculation model based on multiple samples and a single reference gene and is expressed by the following equation:

$$ratio = \frac{(E_{target})^{\Delta C_t(\ Control_{Mean} - Treatment_{Mean}\ )}}{(E_{reference})^{\Delta C_t(\ Control_{Mean} - Treatment_{Mean}\ )}}$$

where E is the efficiency of the reaction and C_t is the crossing-point value of the sample. Efficiencies were automatically calculated using the amplification rate, which is calculated on the basis of a linear regression slope of a serial dilution of standards:

$$Efficiency = 10^{-\frac{1}{slope}}$$

Additionally, the software was set to normalize expression relative to siOT3 control group. Depending on the comparison being made, the *control group* was defined as siOT3 for intra-cell line comparisons and A549 for between-cell line comparisons.

6.9 Evaluation of oxygen consumption

In the present work, cellular oxygen consumption was measured using a novel oxygen-sensitive fluorescent probe. While Clark-type electrodes sensors detect a current flow caused by oxygen reduction, this new optical oxygen sensors operate on the principle of fluorescence quenching of the excited-state lifetime of a fluorescent indicator dye. A complete comparison of both methodologies and their inherent pros and cons has been previously described [466].

The oxygen-sensitive Oxoplate (model numb. OP96U) microplates were obtained from PreSens (Regensburg, Germany). The oxygen sensor is based on the use of the luminescent probe Pt(II)-pentafluorophenylporphyrine which is incorporated in hydrophobic oxygen-permeable particles containing sulforhodamine B as a reference fluorophore. These oxygen-sensitive microspheres are dispersed in a hydrogel matrix with thickness of about 10µm and fixed at the bottom of each well of a round bottom 96-well plate [467].

For the assay, cells were washed once with 1x PBS, trypsinized and centrifuged. The supernatant was discarded and the pellet resuspended in complete growth medium in order to count cells using a Bio-Rad TC10 automated cell counter (Bio-Rad). Preliminary studies showed that a final concentration of $3.75x10^3$ cells/mL was found to give the best oxygen consumption rates for A549 cells. For this purpose, $8.25x10^5$ cells were pippeted to a microtube, centrifuged (300x*g*, 3 min) and resuspended in 220µL of DMEM (no phenol red and no FBS). Then, 200µL of cell suspension was added to each well and covered by 100µL of pre-warmed heavy mineral oil (Sigma-aldrich) to prevent oxygen from air to diffuse back to the reaction medium.

Plates were read in a SpectraMax Gemini EM multiplate reader (Molecular Devices, Sunnyvale, CA, USA) working in time-resolved fluorescence dual kinetic mode. The complete setup program comprised the following entries: 49 reads every 1 min and 15 sec up to 1 hour, excitation and emission wavelengths set to 540/650nm for the indicator dye

and 540/590nm for the reference dye. To increase the resolution of the assay, integration start was set to 0µsec and integration time to 500µsec, for both wavelength pairs combination. Each condition was run at least in duplicate.

A two-point calibration was also performed using air-saturated and oxygen-free water using 1mg/mL of sodium sulphite to deplete oxygen. This calibration allowed the conversion of absolute fluorescence values to oxygen partial pressure (pO_2) given as % of air saturation, following manufacturer's instructions.

6.10 Evaluation of mitochondrial membrane potential

The $\Delta\Psi_m$ was evaluated using different fluorescent probes and different methods, which differed at a cell manipulation extent and end-point measurement after fixation or live imaging.

6.10.1 Microplate assay

For this protocol, tetramethylrhodamine methyl ester (TMRM; Invitrogen) was used in quench mode, i.e. higher dye concentrations were applied so accumulation within mitochondria is enough to form aggregates, thus quenching some of the fluorescent emissions of the aggregated dye. Under these conditions, mitochondrial depolarization is followed by probe release and thus increasing fluorescent signal [468].

Forty-eight hours post transfection cells were seeded in 24-wells plate at a concentration of $2.5x10^4$ cells/mL. In the next day, cells were washed with 1x PBS and loaded with 1µM of TMRM dissolved in warm 1x HBSS/Ca^{2+}/Mg^{2+} and incubated for 30 min at 37°C in cell culture incubator. Then, plates were read in a SpectraMax Gemini EM multiplate reader (Molecular Devices, Sunnyvale, CA, USA) working with 573nm emission and 549nm excitation wavelengths with a time course of 45 min read every 5 min at 37°C. In the end, 2µM of the uncoupler FCCP was added to each well and fluorescence read as previous described. Mitochondrial membrane potential was indirectly calculated as the difference between TMRM fluorescence after FCCP addition and dye fluorescence before the addition of the uncoupler.

6.10.2 Flow cytometer

For this protocol, TMRM was used in non-quenching mode, i.e. low dye concentrations were applied so accumulation within mitochondria does not allow dye aggregation and quenching. Under these conditions, depolarized mitochondria contain lower dye concentration and therefore display a lower TMRM signal [468].

On the day of the assay, transfected cells were harvested by trypsin treatment and resuspended in microscopy medium (120mM NaCl, 3.5mM KCl, 0.4mM KH_2PO_4, 20mM HEPES, 5mM $NaHCO_3$, 1.2mM $NaSO_4$, 10mM sodium pyruvate at pH 7.4) supplemented with 1.2mM $MgCl_2$, 1.3mM $CaCl_2$ and incubated with 150nM TMRM (Invitrogen) for 30 min at 37°C in cell culture incubator. A sample of non-labeled cells was also analyzed in order to calibrate the system, taking cell self-fluorescence into account.

Samples were kept on ice until use and 10,000 cells were analyzed on a FACSCalibur flow cytometer (BD Biosciences, San Jose, California, USA) at a low (12 µL/min) sample flow rate. The blue laser was used for excitation and the filter 3 for red was used for emission; for forward scatter detection, a photodiode with 488/10nm bandpass filter was used. During preliminary tests, all cell groups were incubated with FCCP in order to ascertain the sensitivity, reliability and best analysis to perform. Data was analyzed using BD CellQuest Pro software package (version 5.2).

6.10.3 Confocal microscopy

Mitochondrial transmembrane potential changes were also analyzed through live imaging confocal microscopy by co-labeling cells with TMRM and MitoTracker® Green (MTG). In contrast to TMRM that is accumulated by polarized mitochondria, MTG stains mitochondria independently of membrane potential [469]. When co-labeled TMRM reversibly quenches MTG fluorescence of functional mitochondria. Furthermore, the addition of an uncoupler, such as FCCP, results in mitochondria depolarization and consequent loss of TMRM but not MTG fluorescence. At this point, MTG fluorescence becomes visible allowing the identification of all mitochondria in the cell.

Twenty-four hours prior to the assay, $1.5x10^5$ cells/mL were seeded in µ-Slide 8 well ibiTreat (ibidi Martinsried, Germany) (Fig.3). At the time of experiment, the medium was

removed from all wells and cells were washed with warm 1x PBS. Cells were then incubated with 100nM MTG in warm 1x HBSS/Ca^{2+}/Mg^{2+} for 30 min under normal growth conditions followed by labeling with 1μM TMRM for 30 min under the previously referred conditions. Note that control samples stained with either TMRM or MTG were also analyzed in order to assure correct probe staining and concentrations. Moreover, $\Delta\Psi_m$ was monitored by serial imaging before and after depolarization with 2 μM FCCP. Samples were examined by confocal microscopy using Zeiss LSM510 META and image analysis performed in the LSM 510 software. An argon/2 laser was used for MTG fluorescence detection, and a DPSS 561-10 laser for TMRM.

6.11 Evaluation of oxidative stress

Oxidative stress evaluation was addressed through flow cytometry and confocal microscopy by using two different probes, H_2DCFDA (Invitrogen) and MitoSOX™ Red (Invitrogen). The probe H_2DCFDA is used as a general indicator for reactive oxygen species (ROS) as the probe can be oxidized by different radicals while MitoSOX is specifically accumulated in mitochondrial matrix and allows the unique identification of superoxide generated in mitochondria in live cells [470].

6.11.1 Flow cytometry

On the day of the assay, transfected cells were harvested by trypsin treatment and resuspended in a solution of 5μM H_2DCFDA (Invitrogen) in 1x HBSS/Ca^{2+}/Mg^{2+} for 60 min at 37°C in a CO_2 incubator. A sample of non-labeled cells was also analyzed in order to set up the assay settings considering cells self-fluorescence. Samples were kept on ice until use and 10,000 cells were analyzed in a FACSCalibur flow cytometer (BD Biosciences, San Jose, California, USA) at a low (12 μL/min) sample flow rate. When measuring DCFDA fluorescence, the red laser was used for excitation together with filter 1 for detection of green emission. For MitoSox fluorescence, the blue laser was used for excitation together with filter 3 for detection of red emission. Data was analyzed using BD CellQuest Pro software package (version 5.2).

6.11.2 Confocal microscopy

Twenty-four hours prior to live imaging assay, $1.5x10^5$ cells/mL were seeded in µ-Slide 8 well ibiTreat (ibidi Martinsried, Germany). At the time of experiment, medium was removed from all wells and cells were washed with warm 1x PBS. Cells were then incubated with either 7.5µM of H_2DCFDA or 5µM MitoSOX in warm 1x HBSS/Ca^{2+}/Mg^{2+} for 30 min under normal cell culture conditions. Regarding H_2DCFDA, a positive control was performed by incubating cell with 50µM of tert-butylhydroperoxide (tBHP) in 1x HBSS/Ca^{2+}/Mg^{2+} for 60 min under normal cell culture conditions before incubation with the probe. The pro-oxidant compound tBHP is commonly used as an oxidative stress inducer [471].

Finally, samples were examined by confocal microscopy using a Zeiss LSM510 META device and image analysis performed in the LSM 510 software. More detailed information about the microscope is presented in Section 5.2. An argon/2 laser was used for H_2DCFDA fluorescence detection, and a DPSS 561-10 laser for MitoSOX.

6.12 Evaluation of mitochondrial permeability transition pore opening

The mPTP opening was measured using the MitoProbe™ Transition Pore Assay Kit (Invitrogen) with slight alterations to the manufacturer's instructions. This assay includes calcein-AM, a non-fluorescent esterase substrate, and $CoCl_2$, a quencher of calcein fluorescence [472]. Briefly, calcein-AM passively diffuses across cell membranes accumulating in cytosolic compartments including mitochondria. Once inside the cell, calcein acetoxymethyl esters are cleaved by intracellular esterases releasing the fluorescent dye calcein that does not cross cellular membranes. Moreover, $CoCl_2$ quenches calcein cytoplasmic fluorescence while mitochondrial fluorescence is maintained due to the fact that $CoCl_2$ is not able to cross the mitochondrial inner membrane. As a control, cells were treated with ionomycin, a calcium ionophore which allows Ca^{2+} accumulation in cell and, in triggering pore opening and consequent loss of mitochondrial calcein fluorescence due to $CoCl_2$ influx. Additionally, cells were also treated with cyclosporin A (CsA), a mPTP inhibitor through its interaction with Cyclophilin D (CypD) [473].

To perform the assay, cells were first trypsinized and centrifuged 300x*g* for 3 min. Pellets were resuspended in pre-warmed 1x HBSS/Ca^{2+}/Mg^{2+}. Cells were counted using a Bio-Rad TC10 automated cell counter (Bio-Rad) and 1mL of 1x HBSS/Ca^{2+}/Mg^{2+} containing $3.5x10^5$ cells was transferred to a FACS tube. For each treatment group, five aliquots were prepared as follows: one containing 10nM calcein-AM only; one containing calcein-AM plus 0.4mM $CoCl_2$; one containing calcein-AM, $CoCl_2$ and 0.5µM ionomycin; one containing calcein-AM, $CoCl_2$ and 2µM cyclosporin A (CspA); and one containing calcein-AM, $CoCl_2$, ionomycin and CspA. Cells were incubated under one of the referred conditions for 15 min at 37°C protected from light followed by removal of excess staining through addition of 1x HBSS/Ca^{2+}/$Mg^{2+}$and centrifuged 300x*g* 3 min at room temperature. Finally, the pellet was resuspended in 400µL 1x HBSS/Ca^{2+}/$Mg^{2+}$and samples were analyzed on a FACSCalibur flow cytometer.

6.13 Caspases-like activity

6.13.1 Caspase 3/7 and Caspase 9-like activities

Caspase 3/7 and Caspase 9-like activities were measured using the Caspase Glo® 3/7 and Casapse Glo® 9 Assay Kits (Promega, Madison, WI, USA) respectively. Both kits provide a simple, sensitive and one-step only approach to measure caspase-like activity based on cell lysis followed by caspase cleavage of the substrate (DEVD and LEDH derivatives for caspase 3/7 and 9, respectively) and generation of a "glow-type" luminescent signal.

Four hours prior to the assay, $2x10^4$ cells/well were seeded in a cell culture compatible white-walled 96-well plate in 100µL of complete growth medium. Prior to initiating the assay, the 96-well plate containing the cells was removed from incubator and equilibrated at 25°C. Cells were then incubated with 100µL of either Caspase Glo® 3/7 or Caspase Glo® 9 Reagent for 60 min at 25°C. A negative control consisting of non-transfected cells and a background control to measure luminescence associated with the culture medium and caspase-reagent was included to each assay and subtracted from experimental values. Luminescence was read in a VICTOR X3 plate reader (Perkin Elmer) working in luminometer mode. Caspase-like activity was expressed as relative units of luminescence (RLU).

6.13.2 Caspase 8-like activity

Caspase 8-like activity was accessed using a colorimetric assay base on the proteolytic cleavage of granzyme B substrate I (Calbiochem, Millipore) composed by the chromophore, *p*-nitroanilide (*p*NA), and a synthetic tetrapeptide, IETD. The assay is sensitive to caspase 8 and other proteases that recognize the amino acid sequence, IETD (Ile-Glu-Thr-Asp). Upon cleavage of the substrate, free *p*NA light absorbance can be quantified at 400 or 405 nm following manufacturer's instructions.

Cells extracts were collected as previously described in Section 3.2. The reaction was performed in a standard 96-well plate equilibrated at 37°C with 40µg cell extract per well and assay buffer (100mM NaCl, 0.1% CHAPS, 10mM DTT, 0.1mM EDTA, 10% glycerol, 50mM HEPES pH 7.4) supplemented with 200µM Granzyme B Substrate I. For quantitative measurement, a *p*NA standard curve and a control with no cell extract were included in the experiment. Absorbance was measured at 405nm in VICTOR X3 plate reader (Perkin Elmer) after 2 hours incubation at 37°C and capase 8-like activity was expressed as µM of pNA.

6.13.3 Caspase 12-like activity

Caspase 12-like activity was accessed using a fluorimetric Caspase 12 assay kit (Abcam, Cambridge, UK). Cells were trypsinized, centrifuged at 300x*g* for 3 min as previously described in Section 3.2, the supernatant was discarded and cells were resuspended in complete cell culture medium. Thereafter, either $4x10^6$ A549 or $2x10^6$ MRC-5 cells were transferred to a new microtube and centrifuged 300x*g* for 3 min at room temperature. The supernatant was once again discarded and the pellet was resuspended in 50µL cell lysis buffer following manufacturer's instructions. The lysates were then transferred to a standard 96-well plate where 1x Reaction Buffer containing 10mM DTT and 50µM ATAD-AFC substrate were added to each sample. Samples were read in a fluorimeter under kinetic conditions bottom read every 10 min to a total of 120 min at 37°C with 400nm excitation filter and 505nm emission filter with cut off at 475nm. Caspase 12-like activity was expressed as relative units of fluorescence (RFU).

6.14 Fluorescence detection of lysosomal bodies

Twenty-four hours prior to live imaging assay, $1.5x10^5$ cells/mL were seeded in μ-Slide 8 well ibiTreat (ibidi Martinsried, Germany). At the day of the experiment growth medium was removed and cells were incubated with 75nM Lysotracker® Green (Molecular Probes), a weakly basic amine that selectively accumulates in cellular compartments with low internal pH, in pre-warmed growth medium for 45 min under growth conditions. After incubation period, medium was replaced by fresh growth medium. Cells were examined by confocal microscopy using Zeiss LSM510 META and image analysis performed in the LSM 510 software. Argon laser was used for lysotracker detection.

6.15 Statistics

For statistical analysis of two means, including for comparison of control groups between both cell lines, the Student's t test was used while for comparisons of more than two groups an analysis of variances (ANOVA) with matched-pairs was used instead. In both cases, data was checked for normality using the Kolmogorov-Smirnorv with Dallal-Wilkinson-Lillie for correction and equality of variances using the F test or Bartletts's test in order to apply the statistical tests. If data deviated from normality, a simple squared or log transformation was applied and normality checked once again. If transformed data revealed to be normal, the parametric statistical test was applied. Otherwise the respective non-parametric test was chosen: Mann-Whitney for t test and Friedman test for ANOVA. For ease of comprehension, data is presented to the reader as non-transformed.

In situations where one wanted to evaluate the effect of two variables, namely transfection effect and time points, a two-way ANOVA was applied following the same assumptions as mentioned earlier. Differences were considered significant at 5% level and p value was categorized accordingly to their interval of confidence. For one- and two-way ANOVA, corrections for multiple comparisons were made using Bonferroni post-hoc test using predefined comparisons, in order to decrease both type I and type II errors.

Chapter 7

TRAP1 regulates of mitochondrial function and dynamics, as well as cellular quality control systems in A549 lung cancer cells

Tumor necrosis factor receptor associated protein 1 (TRAP1) is a mitochondrial heat shock protein with antioxidant and antiapoptotic functions determined to be overexpressed in several tumor cells. Although our knowledge on TRAP1 functions has been increasing, the mechanisms of TRAP1 cytoprotective effect still remain to be fully defined. In the present work, we have used transient TRAP1 silencing in A549 lung cancer cells to show how TRAP1 modulates mitochondrial function and how its depletion influences different quality control pathways. This work brings new insights on TRAP1 regulation of ROS production and mPTP modulation, as well as it describes, for the first time, TRAP1 involvement in the regulation of autophagy pathways. Overall, the preferential mitochondrial localization of TRAP1 in A549 cells appears to be important in the maintenance of normal mitochondrial physiology, morphology and organelle quality control.

7.1 Introduction

TRAP1 is a member of HSP90 family with prevalent mitochondrial localization, and whose cytoprotective role has been widely documented. Several studies suggest that TRAP1 preserves cellular function by decreasing ROS-mediated oxidative stress [439, 440, 442], and by regulating mPTP opening through its interaction with HSP90 and CypD [304, 474]. Together, these functions seem to contribute for TRAP1 protective effect against mitochondrial apoptosis. Additionally, TRAP1 expression increases in numerous human malignancies [433, 447, 475] and its antiapoptotic functions confer tumor cells resistance against several chemotherapeutic agents [447, 450]. For these reasons, TRAP1 has been proposed as a cancer biomarker and consequently a potential target for anticancer therapies. In this context mitochondrial-targeted agents have been developed to selectively inhibit HSP90-like chaperones inducing cell death and reverting tumor cell multi-drug resistant phenotype [454].

Despite the increased information regarding its cytoprotective functions, the characterization of TRAP1 antiapoptotic effects is far from being complete. Research on TRAP1 role in tumorigenesis led to numerous pieces of evidence whose conections are, in our opinion, still not well established. For example, although several papers suggest TRAP1 involvement on mPTP modulation [304, 474], none of these works directly evaluated the basal state of the mPTP through any of the available techniques [472, 476, 477], which can cloud the established concept of TRAP1 as a protective heat shock protein. Moreover, although TRAP1 cytoprotective functions in cancer cells have been largely attributed solely to its mitochondrial functions, recent reports indicate its involvement in the extramitochondrial control of cell death [452, 478]. These evidences point out for a higher complexity of TRAP1 functions.

Recent findings point out new tumor protective role for TRAP1, focusing on the regulation of the unfolded protein response (UPR) in the ER [451, 452, 456]. Therefore, inhibition of mitochondrial HSP90-family proteins induces an organelle-specific UPR triggering compensatory autophagy and activates ER stress responses [456]. Further evidence came from the demonstration that TRAP1 downregulation increases caspase-4 expression and activates UPR-related signaling molecules [451]. As a mitochondrial protein, TRAP1 regulation of ER stress was soon thought to constitute evidence for the relationship between the two organelles, which was later demonstrated by the identification of TRAP1

localization at the interface between ER and mitochondria [452]. These works constituted the first link to TRAP1 involvement in the regulation of protein quality control mechanisms.

While these studies focused on TRAP1 role in the crosstalk between ER and mitochondria, the relationship between TRAP1 mitochondrial maintenance and quality control is still unknown. In this work we hypothesize that TRAP1 contributes to mitochondrial function maintenance through regulation of the main mechanisms of cell quality control, namely autophagy and apoptosis. This hypothesis was investigated in A549 lung cancer cells, which overexpress TRAP1 [446]. Hence, we first aimed the identification of TRAP1 silencing-induced mitochondrial alterations and, additionally, we aimed at obtaining for the first time a functional assessment of mPTP opening resulting from manipulating TRAP1 levels. Finally, we addressed TRAP1 role in mitochondrial dynamics and its silencing repercussion on autophagy pathways and expression and activity of several apoptosis regulators.

7.2 Results

7.2.1 TRAP1 silencing efficiency

TRAP1 silencing efficiency was evaluated by assessing *TRAP1* mRNA content by qRT-PCR. After 72 hours post-transfection, the results showed an 18-fold decrease on *TRAP1* mRNA content normalized to 18S upon silencing when compared to the two control (siCTL and CTL) groups (Fig.7.1A). In addition, no differences were found in *TRAP1* mRNA content between siCTL and CTL groups demonstrating the lack of effect resulting from the transfection reagents per se. In order to address silencing efficiency at the protein level, TRAP1 content was semi-quantified through western blot. In accordance with mRNA analysis, TRAP1 protein content, normalized to actin as loading control, was significantly decreased ($p<0.001$) in A549 siTRAP1 cells when compared with the siCTL and CTL control groups (Fig.7.1B), with the two latter groups again showing no differences between themselves.

The above mentioned effects were assessed only at 72 hours post-transfection, the time point chosen for the characterization of TRAP1-silenced effects in the present work.

However, considering that siRNA-mediated gene knockdown consists in a transient silencing method, TRAP1 silencing stability was also evaluated. After cell transfection, protein was harvested every 24 hours up to 144 hours post-transfection. As can be seen in Fig. 7.1 panel C, 24 hours post-transfection were not sufficient to observe a decrease in TRAP1 at the protein level; however, 48 hours after the silencing protocol, a clear and dramatic decrease in TRAP1 expression in siTRAP1 cells was observed. This difference remained stable up to 144 hours post-transfection (Fig.7.1C). Consequently, the effects to be described in the upcoming sections were evaluated during the early stages of TRAP1 low expression/content (72 hours).

7.2.2 TRAP1 silencing effect on cell growth and susceptibility to DOX-induced toxicity

In order to characterize TRAP1 silencing effect on A549 cell growth, cell mass was evaluated through the SRB dye-binding assay, used as an indirect method to infer cell proliferation. Cell growth was assessed every 24h up to 72h post-seeding. As described in the previous section, this time frame corresponds to the period when TRAP1 transcript and protein are permanently decreased. As can be seen in Panel A of Fig. 7.2, the growth profile of TRAP1-silenced cells is clearly slower when compared to the control groups. TRAP1 silencing led to a decrease in cell growth within 24 hours post-seeding (corresponding to 72 hours post-transfection, see Section 6.2.3, Material and Methods) (Fig.7.2A). These differences in cell proliferation were more visible for 48 and 72 hours post-seeding time points. Thus, TRAP1 silencing resulted in a maximal 62% reduction of cell mass during the 72 hours the assay lasted (Fig.7.2A). Note that no differences were observed regarding cell proliferation between siCTL and CTL groups.

Because TRAP1 overexpression confers tumor cell resistance against several chemotherapeutical agents [447], we next addressed TRAP1 silencing effect on the susceptibility of A549 cells to DOX-induced toxicity. DOX is a chemotherapy drug used in the treatment of numerous types of cancer, inducing tumor cell death through multiple mechanisms, including induction of DNA damage [479]. A preliminary experiment was performed in order to address the optimal DOX concentration for the assay. The aim here was to obtain the highest DOX concentration that would still allow for some cell proliferation. CTL cells were incubated with different drug concentrations (0μM, 0.1μM,

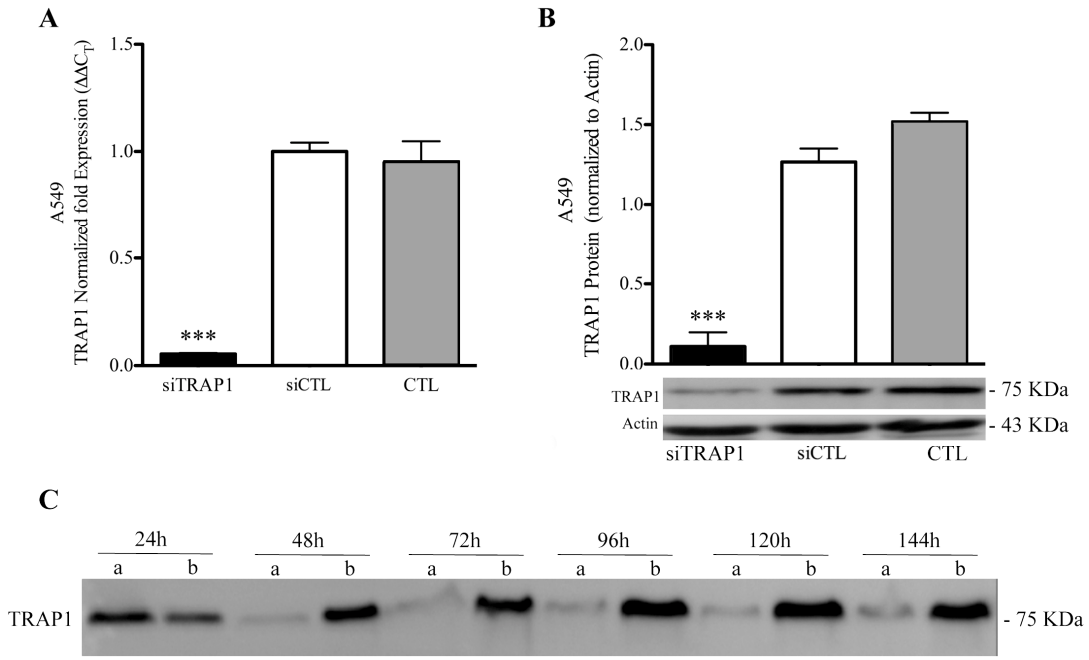

Figure 7.1 - TRAP1 silencing efficiency in A549 cells. A549 cells were either transfected with a TRAP1 siRNA oligonucleotide (siTRAP1) or a scrambled siRNA as a control (siCTL), CTL cells correspond to non-transfected cells. Silencing efficiency was confirmed through qRT-PCR and western blot. (A) Results show a significantly lower TRAP1 content in siTRAP1 cells when compared with the controls groups. mRNA levels were normalized to 18S (N=12) and results were calculated by ΔΔCT method. Bars show mean ± SEM (*** $p<0.001$ to siCTL, one-way ANOVA followed by Dunnett's post-hoc test). (B) TRAP1 protein content analysis shows a large decrease in TRAP1 protein upon silencing when compared with the controls. Protein levels were normalized to actin (N=4), bars show mean ± SEM (*** $p<0.001$ to siCTL, one-way ANOVA followed by Dunnett's post-hoc test). (C) Transfection stability was evaluated by using western blot in a time period ranging from 24 hours to 144 hours post-transfection. Data shows that silencing is efficient at 48 hours post-transfection remaining stable at least up to 144 hours post-transfection (a – siTRAP1 cells, and b – siCTL control cells).

0.2μM, 0.5μM, and 1μM of DOX) for up to 48 hours. Fig. 7.2B summarizes the obtained results and shows that except for the concentration of 0.5 μM DOX, all other concentrations resulted in unaltered growth rates. Therefore, 0.5 μM of DOX was used in the following assays.

After TRAP1 silencing, cells were plated as previously described (Section 6.3, Materials and Methods), incubated with 0.5 μM DOX, and allowed to grow up to 72 hours. DOX

effect on siTRAP1, siCTL, and CTL cell proliferation was analyzed through the SRB assay. All cell groups were susceptible to DOX toxicity, showing a decreased cell proliferation pattern when compared with non-treated cells described in Fig.7.2B. Despite these observations, cell proliferation seems to be more inhibited in TRAP1-depleted cells than in control groups suggesting that TRAP1 loss results in a higher cell predisposal to DOX-induced toxicity (Fig.7.2C). Comparing the two control groups (siCTL and CTL), no differences in cell proliferation in any of the analyzed time-points were found, confirming that the variations regarding TRAP1-depleted cell growth were not due to the transfection protocol (Fig.7.2C).

Although the above results seem to indicate a link between TRAP1 depletion and increased DOX susceptibility, siTRAP1 cells previously showed decreased proliferation rates under non-treatment conditions (Fig.7.2A), which may be masking the real effects of DOX in cell growth. In order to overcome this issue, an alternative data analysis approach in which variances in cell proliferation between the different groups were considered was performed. For this, the percentage of difference between each cell group non-treatment growth and DOX-treatment growth was calculated. The new data analysis revealed that both siTRAP1 and siCTL cell groups are statistically equally susceptible to DOX toxicity, showing a 75.5±2.2 % (N=6) decrease in siTRAP1 cell growth against the 78.7±1.0 % (N=6) observed for siCTL cell group ($p>0.05$).

7.2.3 TRAP1 modulation of mitochondrial function

After general evaluation of TRAP1 effects on cell growth, we moved on to analyze its cellular effects. Considering its subcellular localization we hypothesize that TRAP1 silencing might affect mitochondrial physiology. This section aims to assess this issue with a special interest on $\Delta\Psi_m$, oxygen consumption, global and mitochondrial oxidative stress and mPTP regulation.

TRAP1 preferentially localizes to mitochondria

TRAP1 subcellular localization was verified through immunocytochemistry by co-staining cells with both TRAP1 and OMM marker TOM20 antibodies, and imaging cells by confocal fluorescence microscopy. In agreement with the literature [431], immunofluorescence

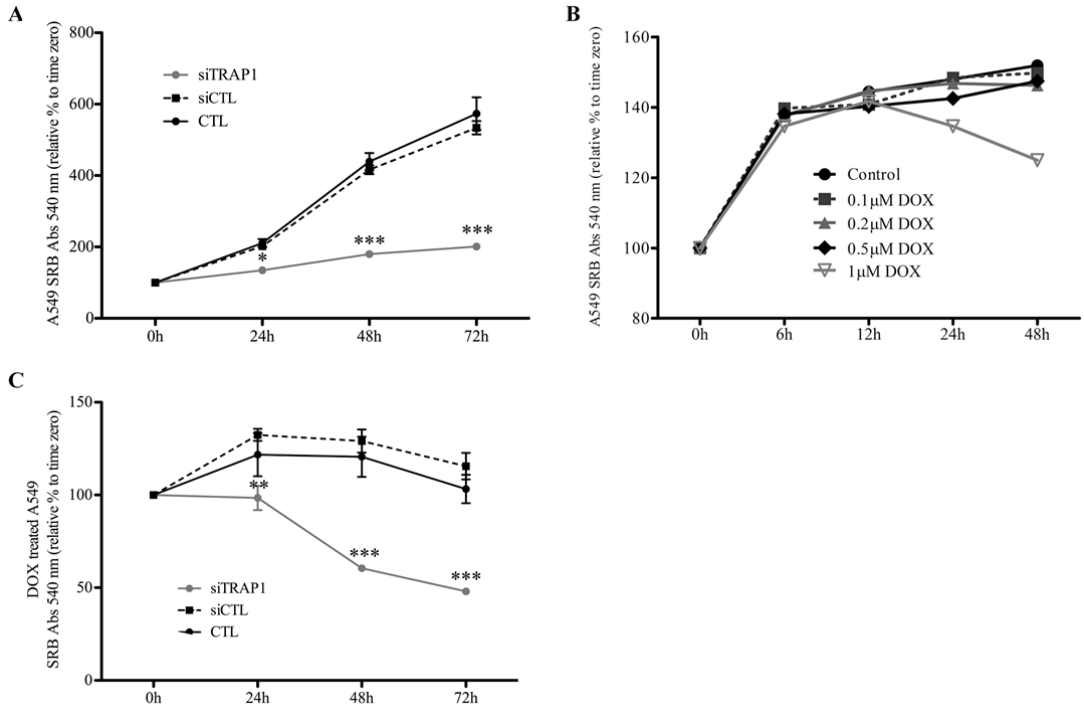

Figure 7.2 - TRAP1 silencing effect on cell growth and susceptibility to DOX treatment. (A) Cell growth curves show a decrease in TRAP1 silenced cells proliferation when compared with control groups (N=6). (B) Control cell susceptibility to different DOX concentrations. (C) DOX-treated TRAP1-silenced cells show lower cell proliferation when compared with the controls (N=6). Data are presented as mean ± SEM (* $p<0.05$, ** $p<0.01$, and *** $p<0.001$ to siCTL; two-way ANOVA followed by Bonferroni post-test).

showed TRAP1 co-localization with TOM20 in both siCTL and CTL groups suggesting TRAP1 preferential mitochondrial localization (Fig.7.3A). Nevertheless, both controls showed TRAP1 staining that did not co-localize with TOM20 fluorescence and was disperse throughout the cell, also in accordance with previously reported non-mitochondrial TRAP1 localization [432]. Interestingly, it appears that the remaining TRAP1 staining upon chaperone silencing may reside in those non-mitochondrial targets. These results also reinforced the efficiency of our transfection by showing a significant decrease in TRAP1 staining in siTRAP1 cells when compared with the control groups (Fig.7.3A). Additionally, the immunofluorescence analysis did not show decreased staining (either signal and/or extension) for TOM20, suggesting that mitochondrial network content appear to remain constant despite TRAP1 silencing. This idea was

further assessed by measuring the levels of TOM20 through western blot, which showed no change in this protein levels in TRAP1-silenced cells (Fig.7.3B).

These findings indicate that TRAP1 localizes to A549 mitochondria, and that its depletion has no effect on overall mitochondrial mass.

TRAP1 silencing results in $\Delta\Psi_m$ depolarization

To assess the possible impact of TRAP1 depletion on mitochondrial function, alterations in $\Delta\Psi_m$ were evaluated in all experimental groups through flow cytometry using the probe TMRM, which is accumulated by polarized mitochondria. TRAP1-silenced cells showed lower TMRM fluorescence, suggesting a decrease in $\Delta\Psi_m$ when compared with siCTL cells (Fig.7.4A). The same experimental conditions were repeated using TMRM in quenching [468] and further analyzed fluorimetrically in a microplate reader. Once again, siTRAP1 cells showed decreased $\Delta\Psi_m$ when compared with the control group (Table 7.1).

A third technique based in the co-labeling of cells with Mitotracker Green (MTG) and TMRM was also performed. The former probe stains mitochondria in a $\Delta\Psi_m$- independent fashion whereas TMRM loads into polarized mitochondria. When co-labeled, TMRM reversibly quenches MTG fluorescence to obtain a relative balance between total mitochondrial content and depolarized mitochondria [469]. Results showed higher TMRM fluorescence and consequent MTG quenching in siCTL cell group in contrast with TRAP1-depleted cells (Fig.7.4B), suggesting once more the higher depolarization status of siTRAP1 cells. To further confirm the sensitivity of the technique, cells were then incubated with 2 μM FCCP to collapse $\Delta\Psi_m$. As expected, a higher uncoupler-related difference was found in control cells while no significant alterations were observed in siTRAP1 cells, demonstrating once again the lower mitochondrial polarization in this cell group (Fig.7.4B). It should also be noted that since MTG stains mitochondria in a $\Delta\Psi_m$-independent fashion it provides an indirect measurement of mitochondrial mass, which once again appears to be similar to control.

The fact that TRAP1 depletion results in decreased $\Delta\Psi_m$ supports the hypothesis of a wider role for this chaperone in mitochondrial physiology maintenance.

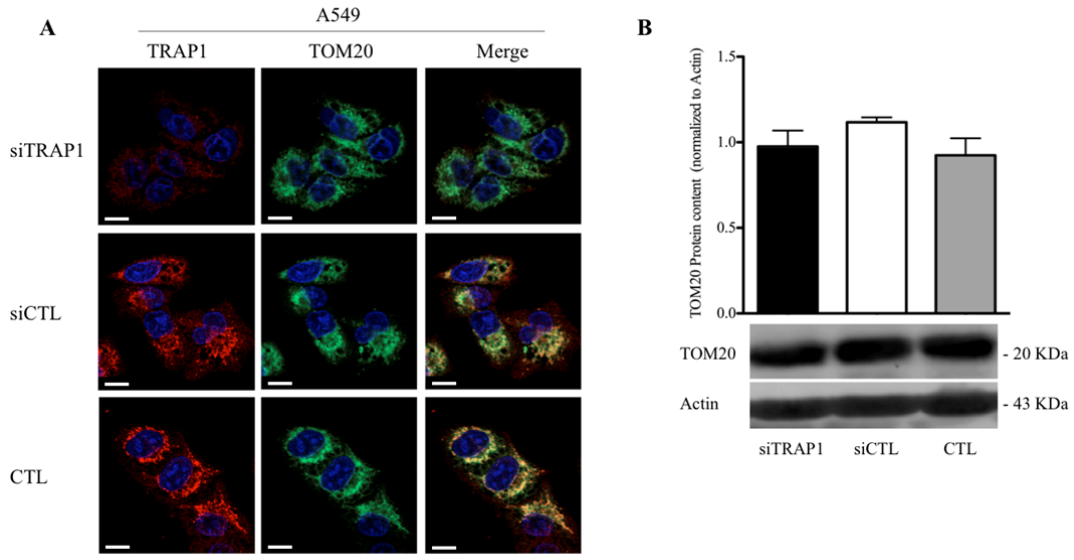

Figure 7.3 - TRAP1 subcellular localization. (A) Red fluorescence labels TRAP1 while green fluorescence labels TOM20 (mitochondrial outer membrane marker), nuclei were counterstained with DAPI and are shown in blue. The merged figures show a large overlap between TRAP1 and TOM20 labeling in siCTL and CTL cell groups while TRAP1 silenced cells show decreased red fluorescence when compared with controls. Images were acquired by confocal microscopy using a 63x objective, scale bar = 8μm. (B) TRAP1 silencing did not affect TOM20 expression levels (N=4). Bars show mean ± SEM (one-way ANOVA).

TRAP1 silencing results in a higher closed-conformation of the mPTP

Considering that mitochondrial depolarization constitutes one of the end-point effects of mPTP opening [291], and that TRAP1 has been described to modulate mPTP by binding to and antagonizing CypD function conferring tumor cells protection against apoptosis [304], we next aimed the understanding of whether the observed mitochondrial depolarization (Section 7.2.2) was associated with alterations in mPTP flickering. Thus, the effect of TRAP1 silencing was for the first time investigated using the calcein-cobalt quench assay [480]. Transfected A549 cells were co-loaded with calcein-AM and cobalt chloride and either incubated with CsA, ionomycin (Io) or both. Calcein-AM readily crosses cellular and mitochondrial membranes whereas cobalt is spatially restricted to the cytosol. In the cell cytosol, cobalt quenches cytoplasmic calcein fluorescence revealing the mitochondrial calcein fluorescence staining and thus an intact IMM.

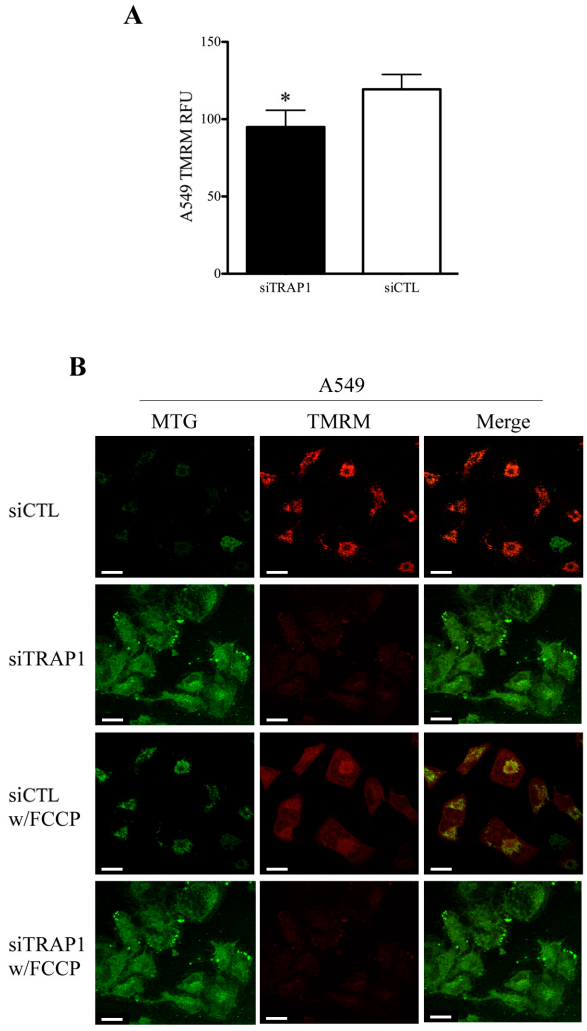

Figure 7.4 - Mitochondrial membrane potential alterations upon TRAP1 silencing. (A) Mitochondrial membrane potential ($\Delta\Psi_m$) alterations were evaluated using TMRM probe and analyzed through flow cytometry. Cells showed a significant decrease in TMRM fluorescence when compared with siCTL (N=10). Bars show mean ± SEM (*p<0.05, two-tailed t-students test). (B) Quenching of MTG by TMRM in siCTL and siTRAP1 cell groups (two upper panels). A549 siCTL cells show a large MTG quenching (upper left panel) while no MTG quenching was observed in siTRAP1 group. In addition siCTL cells show higher TMRM fluorescence when compared with siTRAP1 cells. Mitochondrial de-energization with FCCP caused red TMRM fluorescence (two lower panels) to disappear and green MTG fluorescence to recover in siCTL cells whereas no alterations were seen in siTRAP1 cells. Images were acquired by confocal microscopy using a 40x objective, scale bar = 22μm.

When co-loaded with calcein-cobalt, TRAP1-silenced cells showed higher mitochondrial calcein fluorescence than siCTL control (Fig. 7.5A, first group of bars) whereas treatment with Io led to a decrease in calcein fluorescence, with no differences between cell groups being observed (Fig.7.5A). When the assays were performed in the presence of the mPTP inhibitor CsA, although the fluorescence increased in all groups as expected, it was higher in siTRAP1 cells compared with the control (Fig.7.5A). In order to determine the percentage of mPTP closure, we normalized the values obtained after CsA as 0% open probability and after Io as 100% open probability. Surprisingly, TRAP1 depletion resulted in a higher percentage of mPTP closed state than siCTL group (Fig.7.5A right graph). In

fact, siTRAP1 cells showed that 70% of their mitochondria had the mPTP in a closed state comparing to 50% in the control group.

To elucidate about TRAP1 regulation of mPTP modulation, CypD mRNA content was analyzed in all cell groups. Data showed a significant increase in *PPIF* mRNA (CypD) content in A549 siTRAP1 cells after 72 hours post-transfection when compared with siCTL cell group (Fig.7.5B). However, for the same time-point and despite the increase in CypD mRNA, protein expression analysis by western blotting showed no differences in CypD content between cell groups (Fig.7.5C). Recent findings point out the possible role of subunit c of the ATP synthase in mPTP structure [481]. Considering this novel information, expression of the subunit c of the ATP synthase was evaluated, showing similar protein levels between both groups (Fig.7.5D).

As referred in Section 4.1.1, TRAP1 is part of a mitochondrial chaperone network. Therefore, we investigated whether TRAP1 silencing leads to the activation of compensatory mechanisms which may result in increased HSP90 and HSP60 levels. Thus, transcript content of the both chaperones was measured. Regarding *HSP60* mRNA content, no alterations were observed between siTRAP1 and siCTL cell groups after 72 hours post-transfection (Fig.7.6A). Similarly, TRAP1 silencing had no effect on *HSP90AA1* (HSP90) mRNA content (Fig.7.6B). In addition, the mRNA content for the HSP90 splicing variant 1 (*HSP90AA1.1*, see Section 6.7.1.1 Material and Methods), often described as the canonical sequence, was analyzed. Although no differences were found when analyzing HSP90 mRNA, where primers were constructed to target both splicing variants (*HSP0AA1.1* and *HSP90AA1.2*), TRAP1 silencing resulted in an increased *HSP90AA1.1* mRNA content (Fig.7.6C). Subsequently, HSP90 protein content was evaluated by western blotting, with no alterations in its expression between cell groups being found (Fig.7.6D).

In conclusion, the data showed a transient mPTP opening in all cell groups, however, a normalization with pore inducer/inhibitor, suggests that TRAP1 silencing seems to induce a more closed mPTP conformation without alterations in the expression of the analyzed modulators/components of mPTP: CypD and subunit c of the ATP synthase. Moreover, data also suggest that mitochondrial HSPs are not upregulated upon TRAP1 silencing.

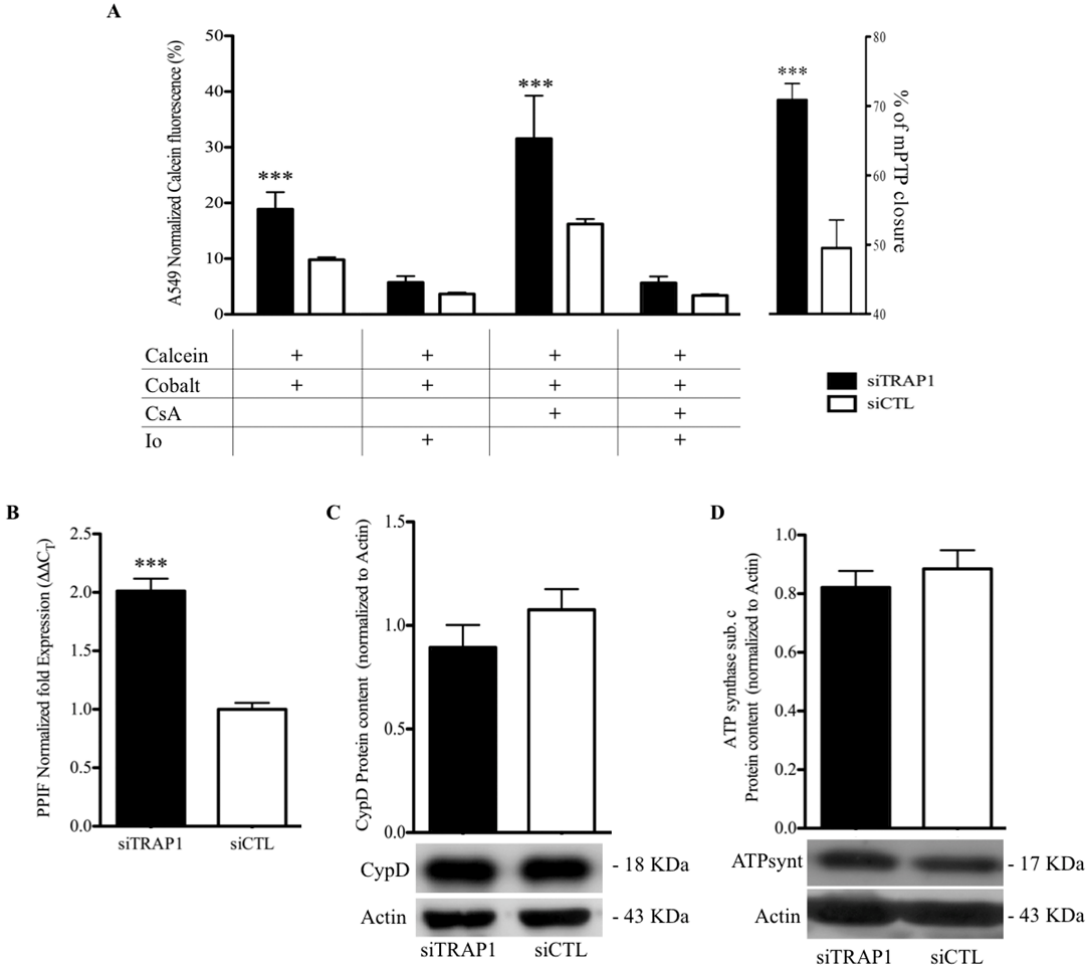

Figure 7.5 - TRAP1 expression and mitochondrial permeability transition pore (mPTP) modulation. The mPTP was monitored by quantifying calcein fluorescence in cell mitochondria by flow cytometry. The cells were loaded with calcein AM and cobalt, a cytosolic calcein quencher, in order to determine the basal calcein fluorescence in mitochondria. The cells were also incubated with Ionomycin (Io) which triggers calcium overload and pore opening and consequent loss of mitochondrial calcein fluorescence. Additionally, cells were incubated with cyclosporin A (CsA) which blocks pore opening. (A) siTRAP1 cells show higher basal calcein fluorescence when compared with siCTL cell group. No alterations were observed in calcein fluorescence between all cell groups upon treatment with Io only, and Io and CsA. siTRAP1 cells incubated with CsA also showed higher mitochondrial calcein fluorescence than the one observed for siCTL control (N=6). In the panel, we calculate the % of mPTP closure based on the values for CsA (0% mPTP opening), and Io (100% mPTP opening). (B) PPIF content was increased in siTRAP1 cells when compared to siCTL. mRNA levels were normalized to 18S (N=12), results were calculated by ΔΔCT method. (C) Evaluation of CypD protein expression showed no differences between cell groups. Protein levels were normalized to actin (N=8). (D) No differences were found in

the subunit c of the ATPsynthase expression levels between siTRAP1 and siCTL cells. Bars show mean ± SEM (***p<0.001, two-tailed t-students test).

Table 7.1 - Mitochondrial membrane potential and basal O2 consumption in A549 cell groups.

	Units	siTRAP1	siCTL	CTL	n
ΔΨm	RUF	0.023*±0.0034	0.032±0.0056	0.032±0.0040	5
O2 basal cons.	RUF/min	0.0065*±0.0008	0.0186±0.0004	0.0179±0.0016	2

$\Delta\Psi_m$ values were calculated as the difference between TMRM fluorescence after FCCP addition and dye fluorescence before the addition of the uncoupler. Data is presented as mean ± SEM (*p<0.05, one-way ANOVA followed by Dunnets' post-hoc test).

TRAP1 silencing decreases oxygen consumption

Another possible explanation for the decreased $\Delta\Psi_m$ (Section 7.2.2) may reside in alterations in the mitochondrial ETC, resulting in inhibition of electron transfer. This was addressed by evaluation of oxygen consumption. Therefore, oxygen consumption was evaluated for all A549 cell groups using fluorescent based oxygen-sensitive Oxoplates (see Section 6.8, Materials and Methods). The basal oxygen consumption assay was performed in two independent cell groups. TRAP1-silenced non-permeabilized cells respiring using endogenous substrates showed lower basal oxygen consumption rates (about 65% decrease) when compared with siCTL cells (Table 7.1). Data strongly suggests that TRAP1 silencing may decrease electron transfer in the respiratory chain, which may result in decreased $\Delta\Psi_m$.

TRAP1 silencing results in increased ROS production

Possible inhibition of respiratory chain suggested by the results obtained in the previous sections (Sections 7.2.2 and 7.2.4) may results in an increased ROS production. Since, the role of TRAP1 in oxidative damage has been previously described [439], we aimed at identifying whether TRAP1 silencing would alter the redox state in A549 cells. Cells were first labeled with the general oxidative stress indicator CM-H_2DCFDA to verify the effect of TRAP1 silencing on ROS generation. Differences in CM-H_2DCF fluorescence were evaluated using confocal microscopy and also quantified through flow cytometry. TRAP1

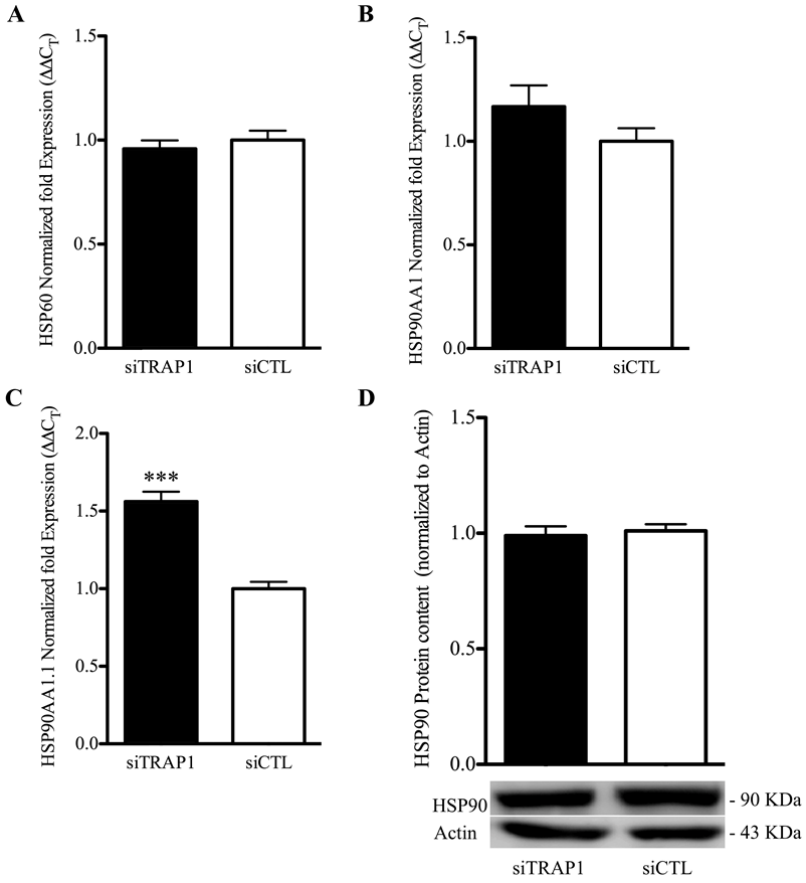

Figure 7.6 - Mitochondrial HSP90 and HSP60 chaperone content. HSP60 and HSP90 mRNA content was analyzed by qRT-PCR. Results show no alterations in either HSP60 (A) or HSP90AA1 (B) mRNA content in siTRAP1 cells when compared with control cells. (C) siTRAP1 cells showed higher HSP90AA1 variant 1 mRNA content than siCTL cells. mRNA levels were normalized to 18S (N=12), results were calculated by ΔΔCT method. (D) HSP90 protein expression analysis by western blotting, showed no alterations in this protein expression between siTRAP1 and siCTL cells. Protein levels were normalized to actin (N=8). Bars show mean ± SEM (*** $p<0.001$, two-tailed t-students test).

depletion resulted in a small increase in CM-H_2DCF fluorescence and a more punctuated staining pattern as can be seen in the representative micrograph in Fig.7.7A. A549 CTL cells were incubated with the pro-oxidant compound tert-butyl hydroperoxide (tBHP), which promotes lipid peroxidation and which was used as a positive control. As expected, control cells treated with tBHP showed higher fluorescence indicative of probe oxidation (Fig.7.7A). Confirming microscopy results, flow cytometry analysis showed higher CM-H_2DCF fluorescence in A549 siTRAP1 cells when compared with siCTL cells.

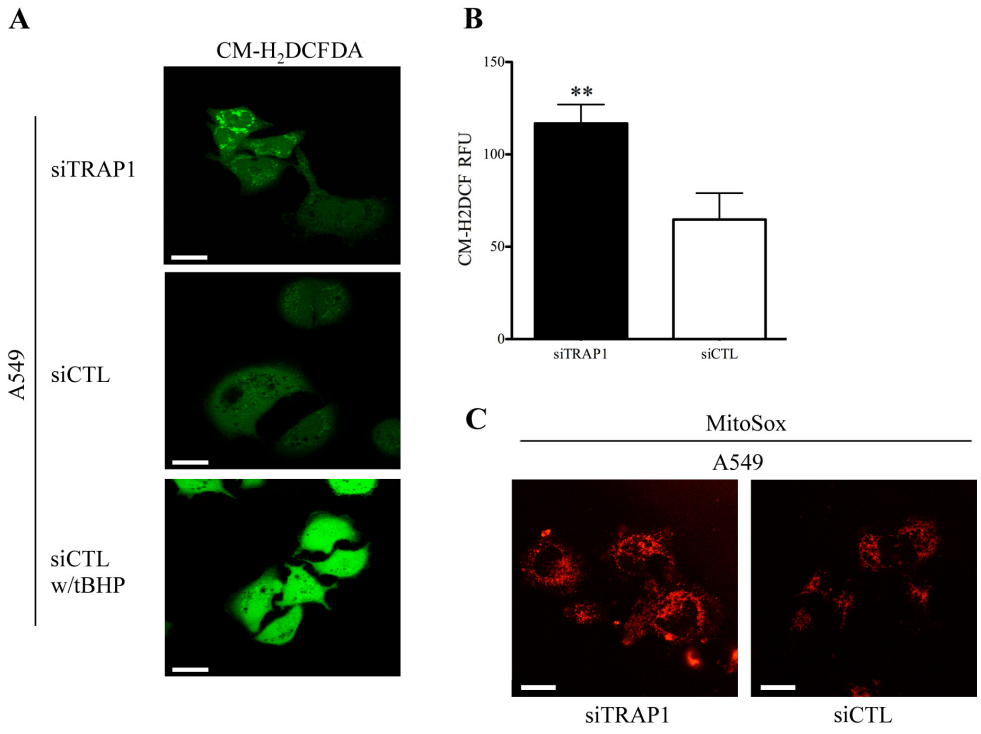

Figure 7.7 - TRAP1 silencing effect on intracellular and mitochondrial reactive oxygen species (ROS). Detection of intracellular ROS was performed using the CM-H_2DCFDA green fluorescence probe through both live imaging confocal microscopy (A) and flow cytometry (B) in A549 cells. (A) A549 siTRAP1 cells show higher DCFDA fluorescence when compared with siCTL. siCTL control cells incubation with tert-Butyl hydroperoxide (tBHP) led to an increase in probe fluorescence. (B) Results were then confirmed by flow cytometry, showing higher cell fluorescence in siTRAP1 when compared with siCTL cells (N=4). Bars show mean ± SEM **p<0.01, two-tailed t-students test. (C) Mitochondrial superoxide anion was monitored using the red fluorescent MitoSOX Red probe. A549 siTRAP1 cells show a higher MitoSOX fluorescence comparing with siCTL cells. Images were acquired by confocal microscopy using a 63x objective, scale bar = 8μm.

However, because CM-H_2DCFDA is a general marker of oxidative stress it is not suitable for discriminating between ROS types or site of origin. Therefore, considering that mitochondria constitute an important intracellular source of ROS [482], the next question raised was whether TRAP1 silencing in A549 cells led to a higher mitochondrial superoxide anion generation. Thus, A549 cell groups were loaded with the mitochondrial superoxide anion indicator MitoSOX Red. Confocal microscopy imaging performed 72 hours post-transfection demonstrated significant increase in MitoSOX fluorescence

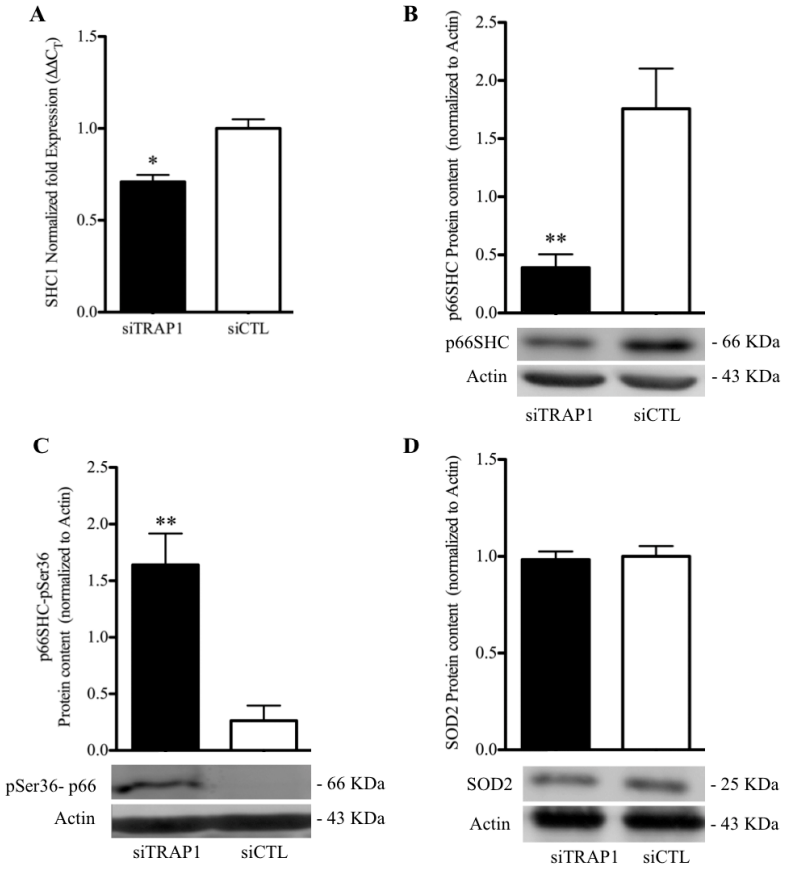

Figure 7.8 - TRAP1 silencing effects on SHC1 gene and p66Shc and SOD2 protein content. SHC1 mRNA content alterations were analyzed by qRT-PCR. (A) A549 siTRAP1 cells show lower SHC1 content than siCTL cells. mRNA levels were normalized to 18S (N=12), and results were calculated by ΔΔCT method. (B) Protein expression of p66SHC showed a decrease in siTRAP1 when compared to siCTL cells. (C) TRAP1-depleted cells showed increased pSer36-p66SHC content. (D) No differences in SOD2 protein measured by western blotting were detected between cell groups. Band densities were normalized to actin (N=4). Bars show mean ± SEM (*p<0.05, **p<0.01, two-tailed t-students test).

intensity in A549 TRAP1-silenced cells when compared with siCTL cell group (Fig.7.7C). As for CM-H_2DCFDA, MitoSOX fluorescence evaluation by flow cytometry was also attempted; however, the use of this technique with this particular probe proved to be unreliable (data not shown). Overall, TRAP1 silencing appears to induce a higher oxidative stress status with a probable mitochondrial origin; still, the entity behind the increased ROS production upon TRAP1 silencing still remains elusive, even in the literature.

Considering p66SHC role in oxidative stress modulation and its regulation of SOD2, *SHC1* mRNA content as well as the expression of these two proteins were evaluated. *SHC1* gene encodes three main isoforms designated according to their molecular weights, p66SHC, p52SHC, and p46SHC, and which differ in activity. P66SHC translocates to mitochondria upon phosphorylation of its Serine 36 residue and increases mitochondrial oxidative stress through an impairment of mitochondrial antioxidant responses [184]. Interestingly, despite the increase on mitochondrial ROS TRAP1 silencing led to a decrease in *SHC1* mRNA levels (Fig.7.8A). These results were then confirmed at protein level with A549 siTRAP1 cells showing a significant decrease in p66SHC content when compared with siCTL group (Fig.7.8B). Interestingly, the expression of p66SHC phosphorylated in Serine 36 residue was increased in TRAP1-depleted cells establishing a possible correlation between ROS increase in these cell group and p66SHC activation and possible translocation to mitochondria (Fig.7.8C). In fact, the ratio between the phosphorylated form over total p66SHC, which gives a better indication of protein activation, showed to be 4.2±1.43 (N=4) in siTRAP1 cells against 0.15±0.08 (N=4) in siCTL cell group (p=0.03). However, the expression of mitochondrial antioxidant protein SOD2 was not altered by TRAP1 silencing (Fig.7.8D).

Therefore, described results are in accordance with TRAP1 antioxidant protection in tumor cells. Data supports the idea of TRAP1 role in mitochondrial ROS maintenance probably through a p66SHC-dependent mechanism.

7.2.4 TRAP1 silencing affects mitochondrial morphology and dynamics

Altogether, results described in the previous sections indicate that TRAP1 silencing results in mitochondrial dysfunction. As damage to mitochondria is often accompanied by the activation of fusion and fission processes, contributing for trigger mitochondrial quality control processes, we next aimed at the evaluation of TRAP1 silencing effect on mitochondrial morphology and dynamics.

TRAP1 silencing results in mitochondrial fragmentation

To examine the effect of TRAP1 silencing in mitochondrial morphology, Mitotracker Red (MTR) and TOM20 labeling combination was used to stain for mitochondrial bodies, and results were analyzed by confocal microscopy. Similarly to TMRM, MTR is dependent on $\Delta\Psi_m$; however, mitochondrial morphology analysis with the former probe revealed inconclusive results due to the observed decrease in $\Delta\Psi_m$ in A549 siTRAP1 cells (Fig.7.9A). Although MTR fluorescence was, as expected, decreased in siTRAP1 cells, analysis of mitochondrial morphology with this probe allowed a better assessment of polarized mitochondria than with TMRM by increasing the contrast of the image. Immunofluorescent microscopy showed that A549 siTRAP1 transfected cells contained highly fragmented, smaller, rounder and dot-like shaped mitochondira, whilst siCTL control cells exhibited more tubular shaped mitochondria with a longer interconnected networks (Fig.7.9B). The same pattern was observed with the OMM marker TOM20, which labels mitochondria in a $\Delta\Psi_m$-independent fashion, regardless of the cell-line in study.

The results here obtained may indicate a role for TRAP1 in the maintenance of mitochondrial morphology, which is pertinent for cell homeostasis under stress, which occurs during the carcinogenic process.

Effects of TRAP1 silencing on mitochondrial dynamics

Considering the observed morphological alterations in TRAP1-depleted cell mitochondria (Fig.7.9), the identification of possible alterations on proteins involved in TRAP1 mitochondrial dynamics modulation seemed pertinent. In this regard, the expression of proteins involved in mitochondrial fusion and fission was further investigated.

Mitochondrial fusion proteins. Mitochondrial fusion is a process dependent on proteins from the MFN family, MFN1 and MFN2, located in the OMM, and OPA1 protein, located in the mitochondrial intermembrane space [483]. During mitochondrial fusion, MFN1 or MFN2 form homo-oligomeric or hetero-oligomeric complexes with juxtaposed mitochondria. This is followed by OMM and IMM fusion through a GTP dependent process and regulated by OPA1 [484]. Changes in MFN1 and OPA1 mitochondrial fusion

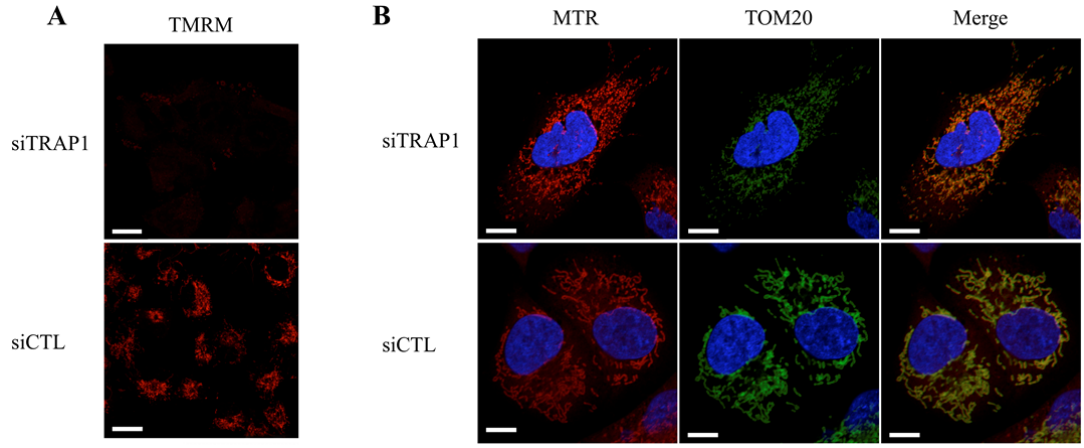

Figure 7.9 - Mitochondria morphology alterations upon TRAP1 silencing. (A) Mitochondria were labeled with TMRM red fluorescent probe. Results were inconclusive regarding A549 cells due to the decrease in siTRAP1 $\Delta\Psi_m$. Images were acquired by confocal microscopy using a 40x objective, scale bar = 22μm (B) A549 mitochondria were stained with Mitotracker Red (MTR) and with TOM20 (green) while nuclei were counterstained with DAPI and are shown in blue. Images show mitochondrial morphology alterations in A549 cells upon TRAP1 silencing. These cells show more fragmented mitochondria than siCTL cell group. Images were acquired by confocal microscopy using a 63x objective, scale bar = 8μm. Note that contrast in siTRAP1 MTR staining was increased in order to better show the morphology alterations. The staining intensity was, in this case, not relevant for the study.

proteins were addressed by western blot analysis. TRAP1 silencing revealed no alterations in both MFN1 and OPA1 protein content after 72 hours post-transfection (Fig.7.10A and B).

Mitochondrial fission proteins. Mitochondrial fission requires the recruitment of the DRP1 from the cytosol to the OMM. In the OMM, DRP1 interacts with fission 1 protein (FIS1) leading to the constriction of mitochondria and consequent separation of the IMM and OMM [484]. Mitochondrial fission proteins FIS1 and DRP1 were evaluated in all cell groups. TRAP1 silencing did not alter expression of the fission protein FIS1 (Fig.7.10C). However, in the siTRAP1 group, significant increased DRP1 levels were observed when compared with control (Fig.7.10D). These findings suggest an important role for TRAP1 in maintaining mitochondrial morphology through regulation of DRP1. Interestingly, both increased fission and mitocondrial depolarization may signal mitochondrial for autophagic removal [485].

7.2.5 TRAP1 silencing affects autophagy pathways

Previous results show that TRAP1 silencing affects mitochondrial function (Section 7.2.3) and dynamics (Section 7.2.4). Taking the above observations into account and considering that mitochondrial damage often triggers the activation of autophagy pathways (Section 3.2.1.1) the next question regarded how TRAP1 silencing affects these processes of quality control in cells.

TRAP1 silencing decreases macroautophagy levels

Macroautophagy is initiated in the cytoplasm by the formation of an isolation membrane, the autophagosome, which is promoted by the class III PI3PK binding to BECLIN-1 and other cofactors [332]. Autophagosome expansion is mediated by two ubiquitin-like conjugation systems, the ATG12, and LC3 protein systems [332]. The first consists in a process that leads to ATG12 covalently binding to ATG5 and is mediated by the ubiquitin-E1-like enzyme ATG7 and the E2-like enzyme ATG10. The second complex involves LC3-I activation by ATG7 and ATG3 through its conjugation with PE, originating LC3-II, which is intimately associated with autophagosome membranes [341].

In the present study, several autophagy markers were evaluated through western blot in all A549 cell groups. After 72 hours post-transfection, TRAP1 depletion resulted in a marked decrease in BECLIN-1 protein levels (Fig.7.11A). Next, alterations in the content of proteins from the ATG12 system were evaluated. TRAP1 silencing significantly decreased ATG5 levels when compared with siCTL group (Fig.7.11B). Similarly, ATG12 expression was decreased in TRAP1-silenced cells when compared with the control (Fig.7.11C). Additionally, as ATG12 antibody allows identification of the ATG12-ATG5 complex by means of different molecular weights, this complex content was also evaluated in both cell groups. Also, the ATG12-ATG5 complex content showed a significant decrease in siTRAP1 cells when compared with control (Fig.7.11D).

The following step was to evaluate the content of proteins from the LC3 conjugation system. It was observed that not only ATG3 (Fig.7.11E) but also ATG7 content were decreased in siTRAP1 cells (Fig.7.11F). Finally, total LC3 content was evaluated, showing that this protein was considerably decreased in siTRAP1 cells when compared to control (Fig.7.11G). In fact, both mature (high molecular weight; LC3-I) and cleaved form

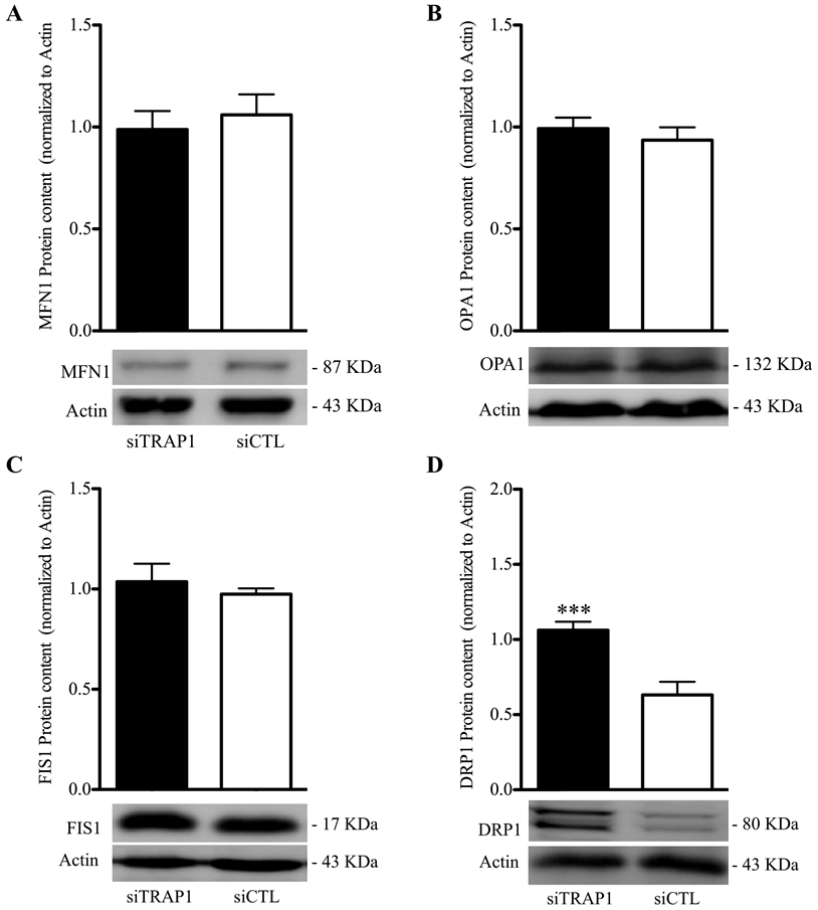

Figure 7.10 - Measurement of mitochondrial dynamics-related proteins. Proteins associated with mitochondrial fusion (MFN1 and OPA1) and fission (FIS1 and DRP1) were evaluated by western blot. (A-B) There were no alterations in MFN1 and OPA1 proteins between cell groups. (C) FIS1 protein analysis also showed no differences between siTRAP1 and control. (D) DRP1 protein levels were increased in siTRAP1 cells when compared with siCTL. Protein levels were normalized to actin (N=4), bars show mean ± SEM (***p<0.001, two-tailed t-students test). Abbreviations: MFN1 – mitofusin 1; OPA1 – optic atrophy 1; FIS1 – fission protein 1; DRP1 – dynamin-related protein 1.

(low molecular weight; LC3-II) of LC3 were decreased to same extent, showing a LC3-II/LC3-I ratio of 1.12±0.14 (N=3) in siTRAP1 cells against 0.94±0.06 (N=3) in siCTL (p=0.29).

Analysis of the serine/threonine protein kinase PINK1 expression, which plays a key role in the removal of damaged mitochondrial through autophagy, showed no alterations

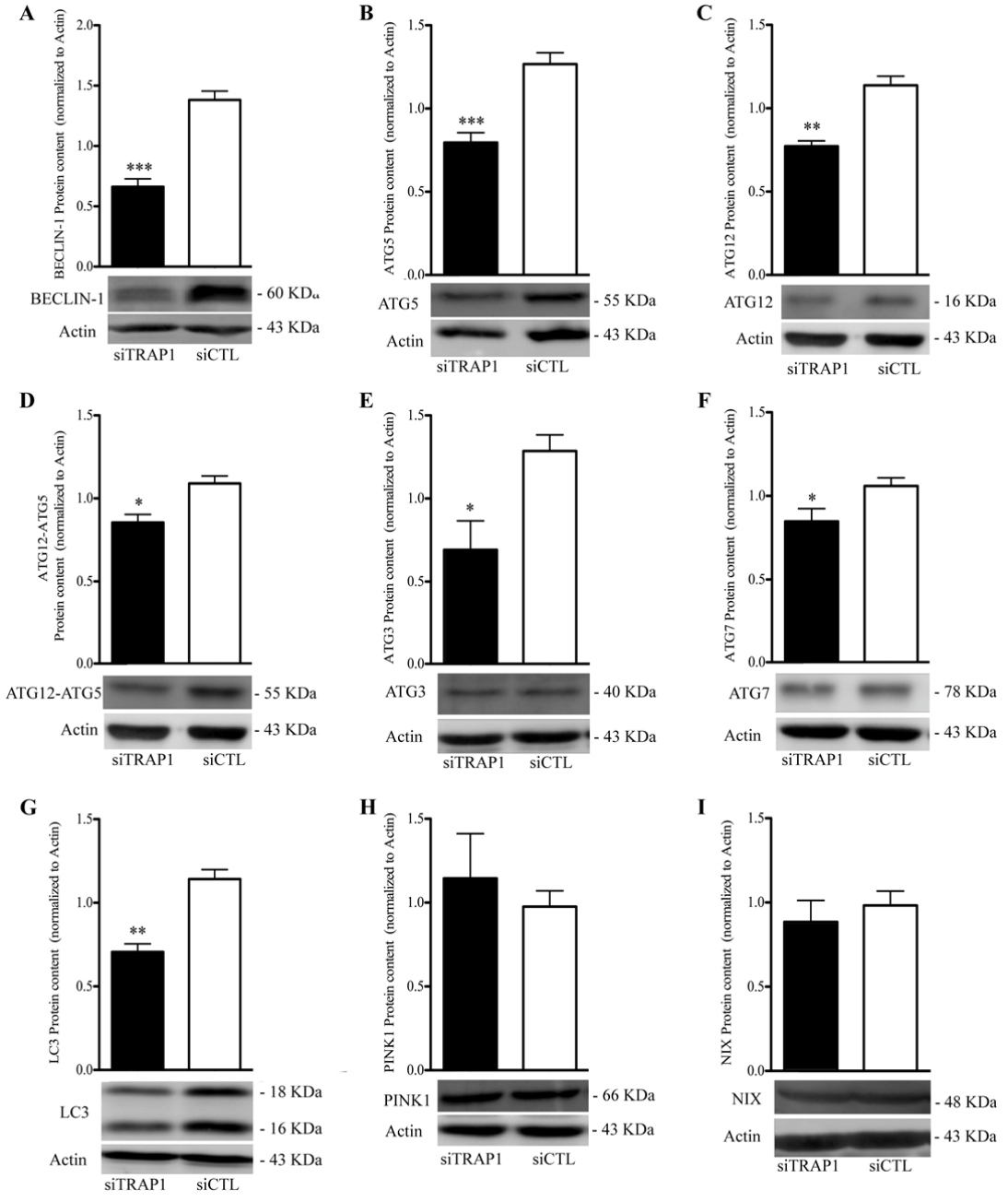

(continues on the next page)

Figure 7.11 (Previous page) - Alterations in macroautophagy-related proteins during TRAP1 silencing. Proteins associated with autophagosome formation, namely in nucleation (BECLIN1-) and elongation (ATG5, ATG12, ATG3, ATG7, LC3) were evaluated by western blot. (A) BECLIN-1 protein content in siTRAP1 cells was decreased. (B-D) ATG5, ATG12, proteins as well as ATG12-ATG5 protein complex content were decreased in siTRAP1 cells when compared with the control. (E-F) TRAP1 silencing led to a decrease in both ATG3 and ATG7 protein expression. (G) LC3 protein content was also decreased upon TRAP1 silencing. (H-I) No alterations were observed regarding the expression of PINK1 and NIX mitophagy related proteins. Protein levels were normalized to actin (N=4), bars show mean ± SEM (* $p<0.05$, ** $p<0.01$ and *** $p<0.001$, two-tailed t-students test).

between siTRAP1 and control (Fig.7.11H). Similarly, no differences were observed between cell groups regarding the expression of NIX, a receptor protein for mitophagy (Fig.7.11I).

Altogether, TRAP1 silencing results in a general decrease in the levels of several autophagy markers, indicating this chaperone involvement in the control of the autophagy flux.

Autophagic flux. In order to confirm that TRAP1 silencing decreases autophagic flux, lysosome content and p62 protein levels were evaluated. Lysosomes constitute key executors of autophagy as they fuse with the autophagosome during the maturation process [348]. The p62 protein recognizes toxic cellular waste through its interaction with polyubiquitinated cargo. Furthermore, p62 is targeted to the autophagosome formation site where it directly interacts with LC3. Considering its role in autophagy, p62 is often analyzed as a marker for autophagy flux in cells. Suppression in autophagy leads to an accumulation of p62 as well as a large formation of ubiquitinated aggregates [486]. Lysosome content was evaluated by incubating cells with the Lysotracker Green probe and imaged through confocal fluorescent microscopy. As can be seen in Fig.7.12A (left panels), TRAP-silenced cells presented higher lysosomal content in comparison to siCTL group. Surprisingly, immunocytochemistry showed a decrease in p62 levels in TRAP1-depleted cells when compared to both controls (Fig.7.12A right panels). The decreased p62 content in siTRAP1 cells was further confirmed through protein analysis by western blot, which corroborated the confocal microscopy results by showing a significant decrease in p62 levels in siTRAP1 cells (Fig.7.12B).

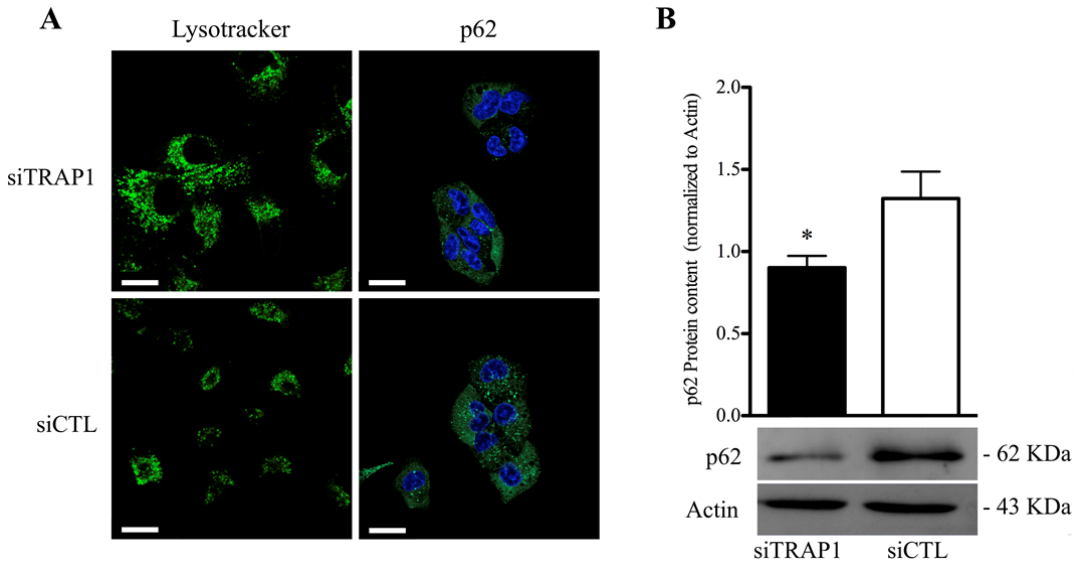

Figure 7.12 - p62 and lysosome content after TRAP1 silencing. (A, left panel series) Cells were incubated with Lysotracker (green fluorescence) and imaged by confocal microscopy. Increased lysosomal content was observed in siTRAP1. p62 protein content was evaluated both by confocal microscopy (A, right panel) and western blot (B and C). Regardless the methodology used, TRAP1 silencing always induced a decrease in p62 content. In micrographs, nuclei are marked in blue (DAPI), images were acquired by confocal microscopy using a 40x objective, scale bars = 22μm. Protein levels were normalized to actin (N=4), bars show mean ± SEM (* $p<0.05$, two-tailed t-students test).

Although findings regarding the decreased expression of main autophagy markers together with the increased lysosomal content observed in siTRAP1 cells may suggest a reduced autophagy flux, p62 decreased levels indicate otherwise. One explanation for these apparently contradictory results may imply the activation of alternative autophagy pathways in these cells.

TRAP1 silencing and macroautophagy modulation. In order to better understand the significance of the decreased macroautophagy pathway on cell proliferation, transfected cells were treated with either rapamycin or 3-methyladenine (3-MA) for up to 72 hours. Rapamycin constitutes an autophagy inducer as it inhibits the autophagy negative regulator mTOR [487]. In contrast, 3-MA inhibits the formation of the PI3K–BECLIN-1 autophagosomal promoting complex leading to autophagy inhibition [488].

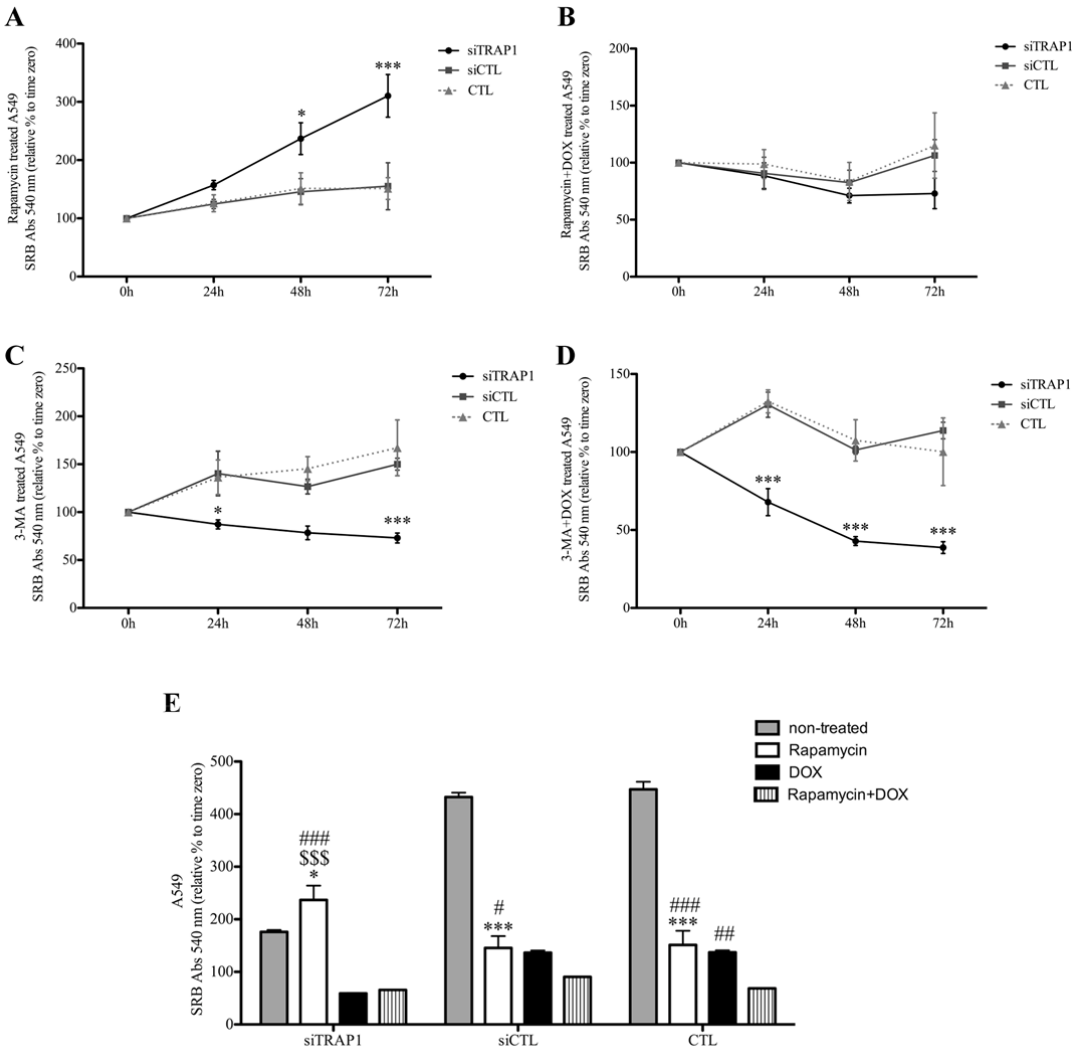

Figure 7.13 - Effect of macroautophagy modulators in the proliferation of TRAP1 silenced cells. Cell proliferation in the presence of the chemical compounds was accessed by SRB dye-binding assay during a period of 72 hours. (A) Data shows increased cellular proliferation for siTRAP cells compared to siCTL cell group with no differences in curves between the two control groups. (B) The same experiment was also conducted in the presence of the anticancer agent doxorubicin (DOX). No differences were observed in rapamycin and DOX-treated A549 cell mass between groups. (C) When treated with 3-MA siTRAP1 cells showed lower proliferation rates than control cells. (D) A549 siTRAP1 cells treated with 3-MA and DOX show a large decrease in cell mass when compared with siCTL control, with no differences being observed between CTL and siCTL cell mass. Data is presented as mean ± SEM (*p<0.05 and ***p<0.001 to siCTL for the respective time-point, N=5; two-way ANOVA followed by Bonferroni's *post hoc* analysis for correction for multiple comparisons). (E) Summarized data from previous images for the 48 hours time-point in order to compare cell viability with and without treatment with the following agents:

rapamycin, DOX, and rapamycin and DOX. Bars show mean ± SEM, two-way ANOVA followed by Bonferroni's *post hoc* analysis for correction for multiple comparisons (* represents comparison with non-treated, $ represents comparison with DOX-treated cells, # represents comparison with rapamycin and DOX-treated cells; all comparisons where made within the same cell group, symbol number represent statistical significance, i.e. one symbol – $p<0.05$, two symbols – $p<0.01$ and three symbols – $p<0.001$).

As can be seen in Fig.7.13A, A549 cell proliferation analysis upon rapamycin treatment showed differences between siTRAP1 and control groups regarding cell growth at the 48 and 72 hours post-seeding time points. In fact, when treated with rapamycin TRAP1-silenced cells showed a surprisingly higher growth rate when compared to siCTL group. In order to better understand whether autophagy has a protective role in these cells, A549 cell groups were incubated with both rapamycin and DOX (Rapamycin+DOX). In this case, data shows similar growth rates for all A549 cell groups with no statistically significance between them (Fig.7.13B).

In contrast to the effect observed upon rapamycin treatment, cell incubation with the autophagy inhibitor 3-MA resulted in decreased cell proliferation in TRAP1-depleted cells (Fig.7.13C). Additionally, cell groups were also treated with 3-MA plus DOX (3-MA+DOX). The presence of both drugs in TRAP1-silenced cells resulted in lower cell proliferation when compared with siCTL for all the time points in study (Fig.7.13D).

Based on the previous data, another analytic approach was used with the purpose of clarifying the alterations measured with rapamycin treatment. For this reason, results were analyzed in order to compare cell viability in untreated and treated conditions (rapamycin, DOX, and rapamycin+DOX) at the 48 hours post-transfection time point. Fig.7.13E summarizes this analysis and shows that rapamycin treatment in A549 siCTL nd CTL groups led to a decrease in cell mass similar to the one observed upon DOX treatment. Conversely, rapamycin-treated siTRAP1 cells showed higher proliferation than the one observed under both no-treatment and DOX-treatment conditions. In addition, no alterations were observed between DOX and rapamycin+DOX treatment in these cells. Moreover, treatment combination with the two agents, rapamycin+DOX, had synergistic suppression on cell growth in the control groups, which was significant in CTL group (Fig.7.13E).

Results suggest that autophagy levels in A549 control cells are maintained in a way that favors tumor progression. Additionally, the effect of rapamycin treatment in TRAP1-silenced cells growth reinforces the role of this chaperone in autophagy maintenance.

TRAP1 silencing decreases ubiquitin content and increases CMA

Because p62 binds to polyubiquitinated cargos targeting them for autophagic removal, and TRAP1 as been reported to regulate cellular ubiquitination, we hypothesize that the observed decrease in p62 levels upon TRAP1 silencing results from differences in protein ubiquitination. Consequently, alterations in ubiquitin expression were analyzed in order to understand the previously observed differences in p62 content. Proteins were separated by SDS-PAGE and ubiquitin labeling was evaluated through western blot. Ubiquitin binds to several proteins and therefore it creates a smear-like pattern after western blot membrane imaging, as seen in Fig.7.14C. A semi-quantitative analysis of ubiquitin labeling, which comprised proteins from high to low molecular weight, showed that TRAP1 silencing resulted in a lower ubiquitin content when compared with siCTL group (Fig.7.14A and C).

Considering the apparently contradictory results previously described regarding the decrease in macroautophagy markers and decreased p62 content in TRAP-depleted cells, the activation of alternative autophagy pathways, namely the chaperone-mediated autophagy (CMA), was evaluated. This constitutes a selective lysosomal mechanism of protein degradation through which proteins are singularly identified by a cytosolic chaperone, the HSC70, and delivered to the lysosome surface through binding to the LAMP2A [370]. Once bound to this receptor, proteins targeted for degradation unfold and cross the lysosomal membrane assisted by a lysosomal form of the HSC70 (lys-HSC70), with substrates being completely degraded by the lysosomal proteases in the lumen [370]. LAMP2A expression was analyzed revealing a higher content of this protein in A549 TRAP1-silenced cells when compared with siCTL cells (Fig.7.14B and C).

The results suggest that TRAP1 silencing leads to an activation of CMA pathway. In addition to these observations, the decreased ubiquitin content in this cell group is also in accordance with the decreased p62 content described previously.

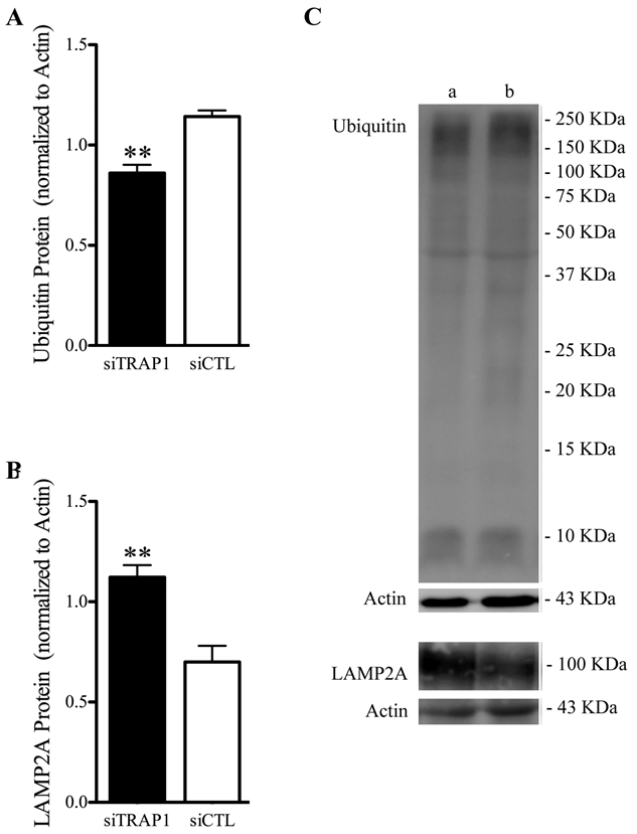

Figure 7.14 - Effect of TRAP1 silencing in both ubiquitin and LAMP2A content. (A-C) The extent of protein ubiquitination was evaluated in total protein extracts. TRAP1 silencing decreased the overall ubiquitin content when compared to siCTL cell group. (B-C) Protein content of LAMP2A, a receptor for chaperone-mediated autophagy, showed increased levels on siTRAP1. Protein levels were normalized to actin (N=4), bars show mean ± SEM (**p<0.01; two-tailed t-students test). Panel C show representative western blot for the above mentioned proteins together with their respective loading controls (actin). a – siTRAP1 and b – siCTL.

7.2.6 TRAP1 silencing affects apoptosis regulators

The previous sections showed that TRAP1 affects mitochondrial homeostasis and cellular quality control processes. The next question regarded the effect of TRAP1 silencing on yet another cell/tissue quality control mechanism, apoptosis. Apoptosis constitutes a highly regulated process of programed cell death in which caspases constitute central regulators. Initiator caspases, such as caspase 8, 9, and 12, are closely associated with pro-apoptotic signals. When activated, these caspases cleave and activate downstream effector caspases, namely caspase-3 and -7, which in turn execute apoptosis by substrate cleavage [489]. The decision to proceed with cell death upon intrinsic pathway activation is usually dependent on the balance between pro-apoptotic and pro-survival BCL-2 family proteins.

Taking into account TRAP1 silencing effect on cell proliferation and mitochondrial physiology, it still remains to be known whether silencing of TRAP1 results in increased

apoptotic signaling. In order to elucidate this issue, caspase-like activity, as well as the content in proteins from the BCL-2 family were analyzed.

TRAP1 silencing results in increased caspase 3-like activity while not affecting initiator caspases-like activities

After 72 hours upon TRAP1 silencing, no alteration was observed on initiator caspases 8-, 9- and 12-like activities, which are involved in the extrinsic-, intrinsic- and ER-related pathways (Fig.7.15A, B and C). However, suprisingly, effector caspase 3/7-like activity was dramatically higher in TRAP1-silenced cells when compared with siCTL control group (Fig.7.15D).

TRAP1 silencing shifts the balance BAX/BCL-xL in favor of apoptosis

Additionally, expression of BAX and BCL-xL pro-apoptotic and pro-survival proteins was analyzed. Note that it was not possible to evaluate BCL-2 protein content in this cell line because A549 cells do not express this protein [490]. TRAP1 silencing induced a slight yet significant increase in BAX content along with a marked decrease of BCL-xL (Fig.7.15E and F). Moreover, considering that the BAX/BCL-xL ratio was of 2.10±0.18 (N=6) for siTRAP1 cell group and 0.79±0.03 (N=6) for siCTL cells ($p<0.001$), TRAP1 seems to protect cells from apoptosis through regulating BCL-xL pro-apoptotic protein expression.

7.3 Discussion

Sustaining proliferative signaling is presumably the most fundamental trait of cancer cells [45]. Contrarily to normal cells, where growth is highly controlled by the release of growth-promoting signals, cancer cells overcome these controls and acquire the capability to circumvent these tight regulatory systems and show unlimited replicative capacity. Thus, A549 lung cancer cells are no exception, showing high cell proliferation rates and high TRAP1 content making A549 cells a good model for the study of TRAP1 role in tumorigenesis [446]. In this study, we initially showed that TRAP1 loss interferes with the high replicative capability of A549 cells, leading to a significant decrease in cell proliferation rates, therefore suggesting TRAP1 important role in tumor phenotype.

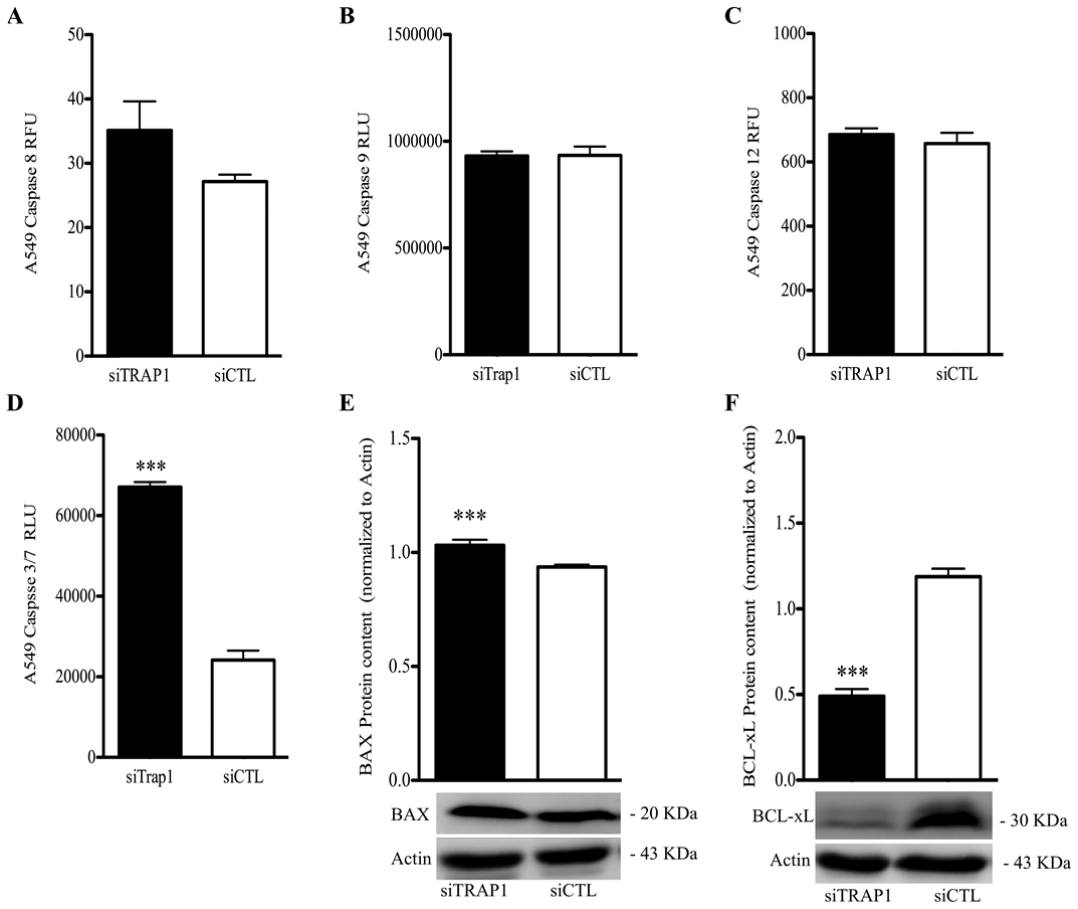

Figure 7.15 - TRAP1 silencing effect on caspase-like activities and BCL-2 family protein levels. The activities of initiator caspases (8, 9 and 12) and effector caspases (3/7) were evaluated. (A-C) There were no differences in activity of any initiator caspases between cell groups. (D) Alterations were only observed in caspase 3/7-like activity. Moreover, (E) BAX content was increased whereas (F) BCL-xL was decreased in siTRAP1 cells. Protein levels were normalized to actin (N=4). Bars show mean ± SEM (***p<0.001, two-tailed t-students test).

Since several lines of evidence support a role for TRAP1 in tumor cell acquisition of a multi-drug resistant phenotype [447, 450, 478]. Although in our work all cell groups were equally susceptible to DOX-induced toxicity, TRAP1-depleted cells presented lower cell proliferation than controls. These findings may indicate that TRAP1 silencing synergizes with DOX-induced toxicity which agrees with the observations made by Wu and colleagues whose work shows that TRAP1 loss combined with DOX may constitute a useful therapeutic strategy [491].

TRAP1 cytoprotective functions have been largely attributed to its mitochondrial localization. In agreement with previous studies [431] we found that TRAP1 co-localizes with A549 cell mitochondria labeled by TOM20. Cancer cell mitochondria undergo profound changes that often culminate in altered energy metabolism, hyperpolarization, increased ROS production, and resistance to apoptosis [492]. Considering its subcellular localization and cytoprotective roles, it did not take long for TRAP1 to be associated with mitochondrial function maintenance in tumor cells. Accordingly, TRAP1-depleted cells exhibit multiple markers of mitochondrial dysfunction, including loss of $\Delta\Psi_m$, increased ROS production, and low oxygen consumption. In the present dissertation, part of those hallmarks were evaluated in A549 cells in order to confirm the phenotype before exploring new mechanisms and roles of TRAP1 in tumor cells. During this characterization, new insights on previous reported alterations were detected and will be now further discussed.

Several groups had previously demonstrated that TRAP1 plays an important role in inhibiting cell death caused by ROS and thus conferring tumor cells with a selective advantage [438, 439, 442]. Although TRAP1 role in mitochondria protection against oxidative stress is consensual, the mechanisms behind this protective function are still unclear [439, 440, 442]. The present work suggests the involvement of p66SHC on TRAP1 regulation of mitochondrial ROS generation.

p66SHC is a pro-apoptotic protein involved in mitochondrial ROS production and oxidative stress response [493]. Studies on p66SHC subcellular localization have identified it as a cytoplasmic protein able to translocate to mitochondria upon different pro-apoptotic stimuli (e.g. H_2O_2 and UV exposure) [494, 495]. The mechanism behind the signaling pathway includes p66SHC phosphorylation at Ser36 (pSer36-p66SHC) by protein kinase c beta (PKCβ). Although Ser36 phosphorylation is critical for its apoptotic potential, mitochondrial-translocated p66SHC is not phosphorylated [183]. In mitochondria, p66SHC was shown to operate as a redox enzyme that transfers electrons from reduced cytochrome c to molecular oxygen [183], although doubts remain whether p66SHC really crosses the OMM.

The present study reveals that TRAP1 silencing increases Ser36 phosphorylation of p66SHC, which has been shown to exert a pro-apoptotic effect in different cell types [496]. Thus, it is plausible that TRAP1 controls ROS generation through regulation of p66SHC phosphorylation, thereby protecting mitochondria against oxidative stress-

induced apoptosis. However, the question of whether the observed increase in pSer36-p66SHC is cause or consequence of increased ROS production is still unclear and would require further investigation on this topic. In addition to increasing ROS generation in mitochondria, down-regulation of expression of antioxidant enzymes has been considered another mechanism for p66SHC-dependent increase in oxidative stress [497]. Because previous research has shown that p66SHC reduces SOD2 expression [498], we investigated the content of this antioxidant enzyme in TRAP1-depleted cells. Although our results showed no alterations in SOD2 expression in TRAP1-silenced cells, contradicting previous observations, several other publications support these observations by showing that p66SHC activity does not alter the levels of antioxidant enzymes [183, 499].

The increased intracellular ROS production can trigger cell death by the opening of mPTP, which in turn results in the $\Delta\Psi_m$ loss. Moreover, mPTP opening has been reported to constitute a pre-requisite for induction of mitochondrial apoptosis [500]. Although mPTP exact structure is still debatable, a series of knockout studies demonstrated that CypD is indeed required for mPTP modulation, regulating mPTP opening in a positive manner [295, 501]. TRAP1, the HSP90 mitochondrial pool, and HSP60, were all described to physically interact with CypD modulating its activity resulting in mPTP inhibition [304, 474]. Considering our observations regarding TRAP1 role in $\Delta\Psi_m$ maintenance and oxidative stress regulation, we addressed this chaperone function in mPTP regulation in A549 cells.

Surprisingly, our data revealed that TRAP1-depletion resulted in having the mPTP preferentially in the closed conformation under basal conditions. Although these results go against previously suggested mechanism of TRAP1-dependent mPTP inhibition in cancer cells, none of the referred works included studies on mPTP open/closed status after TRAP1 silencing and/or overexpression. In fact, in these previous works, the impact of TRAP1 on mPTP was extrapolated either by analysis of $\Delta\Psi_m$ alterations [304] or by evaluation of cell viability [474] in the presence or absence of CsA. Although those methodologies are well established when using isolated mitochondrial fractions, the use of whole cells may result in other confounding factors. For example, CsA is not specific for mPTP inhibition (contrarily to NIM811) as it also inhibits calcineurin and multidrug resistance protein. Therefore, incubating the drug for long periods of time may impact mPTP-independent effects. In our assays, CsA was incubated solely during the assay and for a short period of time. Additionally, caution should be taken when using $\Delta\Psi_m$ to

characterize mPTP status as mitochondrial depolarization can occur due to ETC inhibition or together with mPTP opening, giving rise to false positives. Although not explored in the present study, we hypothesize that if CsA was used in $\Delta\Psi_m$ experiments, a higher value in siTRAP1 group would also be obtained, since CsA was shown in the calcein-cobalt technique to be able to fully close mPTP. Finally, one should understand the differences between the end-points used to characterize the mPTP status in intact cells. In the present work, the parameter used reports qualitatively the percentage of mitochondria/cells with closed mPTP under basal conditions, i.e. without cells experiencing any challenge (e.g. calcium increase) or exogenous stimuli. Therefore, it better depicts the mPTP opening extent in normal growth conditions. However, by using the same technique, but instead following the loss of mitochondrial calcein fluorescence over time after calcium challenging, it would be possible to observe that TRAP1-depleted cells show a faster calcein loss, suggesting a sensitized mPTP. Such outcome would suggest that TRAP1 increases the threshold for mPTP opening protecting cells during stressful events, although the mPTP would be in a more closed conformation during basal conditions.

Nevertheless, our observations corroborate the hypothesis that TRAP1 is somehow involved in mPTP modulation. Additionally, our results showed that TRAP1 silencing resulted in no alterations in overall *HSPD1* (HSP60) and *HSP90AA1* (HSP90) content while significantly increasing *PPIF* (CypD) levels. However, this increase was not observed at protein level suggesting that the time needed for CypD mRNA translation is higher than the time the assay lasted. Thus, differences at protein content level would only become visible at latter post-transfection times. This hypothesis can also help us understand the discrepancy in our results regarding previous observations of a more open state of the mPTP in TRAP1 depleted cells [304, 474]. In fact, in these previous works, studies on TRAP1 function in mPTP modulation were developed after longer periods of transfection time or incubation with HSP90-like inhibitors. However, further studies are needed to clarify the interplay between TRAP1 and the mPTP. Notwithstanding, our observations of a more closed mPTP state in cells lacking TRAP1 are interesting and suggestive of a more complex role of TRAP1 in mPTP modulation.

In agreement with previous observations, our results suggest that TRAP1 contributes for tumor cell mitochondria homeostasis through regulation of ROS generation and $\Delta\Psi_m$ maintenance, which is likely protective under stressful environments. TRAP1 homeostatic role may involve indirectly controlling CypD levels, as a decreased

expression of CypD have been shown to desensitize cells to mPTP opening [502]. Accordingly, TRAP1 depletion, which results in mitochondrial impairment, would increase CypD levels and thus sensitizing the mPTP. Although our results support this hypothesis, they also suggest that alterations in CypD protein levels might only emerge after several days of TRAP1 silencing. However, further work would be required to understand whether the increased mPTP inhibition observed in TRAP1-depleted cells is directly related to TRAP1 loss or if it only reflects an early compensatory mechanism in an attempt of maintaining mitochondrial viability.

Alternatively, loss of $\Delta\Psi_m$ in TRAP1-depleted cells could reflect alterations in the mitochondrial ETC. Here we showed that TRAP1 depletion resulted in decreased oxygen consumption. Together, a reduced oxygen consumption and decreased $\Delta\Psi_m$, suggest inhibition of the ETC. In agreement with this hypothesis, several works suggest a key role for TRAP1 in the regulation of the ETC [444, 503]. TRAP1 has been reported to preserve complex IV activity under stress conditions with no effect on the activity of other ETC complexes [444]. Although these observations were later supported by the identification of TRAP1 interaction with complex IV [503], this study did not provide further detail regarding TRAP1-dependent complex IV regulation. Moreover, in contrast to Xu *et al*, Sciacovelli and co-workers showed that TRAP1 interacts with SDH, part of Complex II, inhibiting its activity, which in turn results in HIF1α stabilization and increased cell glycolytic potential [503]. Similarly, an independent work using the same cell lines showed that TRAP1 promotes a metabolic switch between mitochondrial respiration and aerobic glycolysis via c-Src activity modulation [504]. Therefore, our observations regarding oxygen consumption in TRAP1-depleted cells are discrepant from the ones reported by both Sciacovelli [503], and Yoshida [504]. Notwithstanding, the reduced oxygen consumption may possibly be explained by a decrease in complex IV activity supported by Xu and collaborators work [444]. Moreover, according to Sciacovelli and colleagues HIF1α stabilization resulting from increased succinate accumulation can inhibit PHD. However, HIF1α stabilization is far more complex and might be regulated through other mechanisms, namely HSP90 [505-507]) and ROS [508, 509] have also been implicated in HIF1α stabilization. TRAP1 depletion leads to an increment in ROS generation within the cell, which might be contributing for HIF1α stabilization and, if so, could also help justify the observed reduction of oxygen consumption. Moreover, it is becoming evident that different cancer cells are metabolic diverse [510]. This

heterogeneity may also explain the discrepancy in cell metabolic responses to TRAP1 depletion. Altogether, these findings demonstrate that TRAP1 role in tumorigenesis is likely more complex than previously appreciated. TRAP1 function seems to be more nuanced and variable depending on the cell type and its basal TRAP1 levels and possible localization.

As mentioned above, decreased oxygen consumption together with the observed decrease in $\Delta\Psi_m$ suggests an inhibition of the ETC. Although these conditions may contribute, under specific circumstances, to ROS production [511], our data indicates p66SHC as the most probable mitochondrial ROS source. In fact, the published studies associate the increased oxygen consumption and mitochondrial depolarization with an increase in ROS [504], although other authors defended that mitochondrial uncoupling can decrease ROS produced by the ETC [512]. This apparent contradiction, further suggests that the source of ROS in TRAP1-depleted cells may result from activation of the p66SHC pathway upon TRAP1 depletion.

Accumulation of depolarized mitochondria and oxidative damage has been associated with the occurrence of mitochondrial fusion and fission processes in an attempt to either restore homeostasis or eliminate mitochondria that are beyond repair [513]. In this report, TRAP1 silencing shifted the balance towards a fission-prone phenotype, characterized by the accumulation of smaller and rounder mitochondria. In order to assess whether TRAP1 affected mitochondrial fusion or fission the expression of fusion and fission proteins was evaluated. TRAP1 was shown to have no effect on both MFN1 and OPA1 fusion proteins levels. Conversely, TRAP1 depletion led to a significant increase in DRP1 levels without affecting FIS1. This effect of TRAP1 depletion on mitochondrial morphology reported in our study is in accordance with the observations made by Butler and colleagues [514], and although not coherent with the tubular mitochondria observed by Takamura and colleagues [515], our findings also support the hypothesis that TRAP1 controls mitochondrial dynamics through DRP1 expression. In addition, Takamura and collaborators suggested that DRP1 is regulated by TRAP1 in a non-transcriptional manner. Post-translational modifications of DRP1, for example through ubiquitination, regulate its function in mitochondria by affecting DRP1 mitochondrial pool [516]. Considering that TRAP controls cellular ubiquitination and expression levels of mitochondrial proteins [452] it seems reasonable to think that it might also be involved in DRP1 regulation through this pathway. In fact, when analyzing overall protein ubiquitination, TRAP1-

depleted cells showed considerably lower ubiquitin levels, which may explain DRP1 stabilization in these cells. However, more specific assays are needed to verify to what extent DRP1 protein ubiquitination is affected by TRAP1 silencing.

Increased mitochondrial fragmentation is often related with damaged-mitochondria elimination through autophagy (mitophagy) as defective mitochondria can become toxic to the cell [485]. Indeed, DRP1 inhibition resulted in inhibition of mitochondrial autophagy, suggesting that fission is required for mitophagy [485]. Moreover, loss of $\Delta\Psi_m$ has been reported to induce mitophagy [517]. In this work, TRAP1 silencing resulted in a generalized decrease of the proteins involved in the autophagic pathway, such as BECLIN-1, part of class III PI3K complex and important for vesicle nucleation, and proteins that make part of both ATG12 and LC3 ubiquitin-like systems, which play crucial role in autophagosome elongation and cargo engulfment [335].

Interestingly, although both soluble (LC3-I) and membrane-bound (LC3-II) LC3 forms, were decreased in siTRAP1, no differences were found regarding the LC3-II/LC3-I ratio, an indicator of autophagosome formation [518]. This approach suggests that there are no alterations in the autophagic flux, i.e. according to this analysis autophagy does not seem to be defective or blocked although it may occur in a lesser extent considering that the overall machinery is downregulated. Alternatively, due to the limitations associated with LC3 analysis to infer autophagy flux (reviewed in [519]), measurement of p62 degradation may constitute an important tool. p62 binds to LC3 and constitutes a selective substrate of autophagy [520]. Therefore, p62 decreases upon autophagy stimulation and increases when autophagy is suppressed. Our data demonstrated that TRAP1 silencing resulted in decreased p62 levels, thus indicating an increased autophagic flux. However, the expression levels of p62 can also be changed in an autophagy-independent manner, namely by alterations in the levels of ubiquitinated proteins [521]. As previously mentioned, TRAP1 plays a role in cellular ubiquitination through its interaction with the regulatory proteasome protein TBP7 [452]. In fact, we observed reduced global cellular ubiquitin levels in TRAP1-depleted cells, which suggests that the observed decrease in p62 levels is not a consequence of a higher autophagy flux but is actually influenced by low cargo ubiquitination.

In addition to being regulated by autophagy adaptor proteins, such as p62 binding to ubiquitinated proteins on mitochondria, mitophagy may also be mediated *via* autophagy receptors, namely the ubiquitin-independent pathway that includes the mitochondrial

NIX/BNIP3 receptors [351]. However, results showed that NIX protein levels were not altered in TRAP1-depleted cells, thus indicating that TRAP1 does not affect this pathway. Another pathway involved in damaged-mitochondria removal by autophagy involves the activation of the PINK1/Parkin pathway, which is extensively studied in neuronal systems. Following $\Delta\Psi_m$ collapse, PINK1 accumulates in the OMM resulting in Parkin recruitment and activation [362, 363]. Parkin activation leads to ubiquitination of mitochondrial proteins signaling them for mitophagy [354]. In neuronal cells, TRAP1 was shown to be a downstream phosphorylation target of PINK1 [437]. Moreover, PINK1 was also shown to regulate TRAP1 levels [522]. However, while some studies developed in *Drosophila* indicate that TRAP1 expression compensates for the mitochondrial defects in Parkin mutant flies [523], others suggest that PINK1-dependent TRAP1 role in mitochondrial integrity maintenance is parallel or upstream of Parkin [524]. However, in this work, TRAP1 silencing did not affected PINK1 protein levels suggesting that the observed alterations regarding autophagy are independent of this pathway.

Because, TRAP1 depletion resulted in a significant decrease in several key components of the autophagic machinery, it is thought that TRAP1 plays a role in the control of autophagy levels in tumor cells. In order to understand whether the regulation of autophagy by TRAP1 manipulation constitute an advantage to tumor growth, cells were incubated either with an autophagy inducer, rapamycin, or inhibitor, 3-MA, and alterations at cell proliferation level were measured. Interestingly, when incubated with rapamycin siTRAP1 cells showed higher proliferation rates than control cells, whereas autophagy inhibition with 3-MA led to a decrease in the growth of these cells. In fact, TRAP1-depleted cells proliferation after rapamycin treatment was higher than their basal growth, suggesting that autophagy stimulation confers a growth advantage to TRAP1-silenced cells. Moreover, cell incubation with both rapamycin and DOX, with the purpose of understanding the advantage conferred by increased autophagy upon TRAP1 depletion, showed no differences in cell proliferation between groups indicating a lack of synergistic effect of autophagy stimulation and DOX in control cells.

Altogether, these findings suggest that TRAP1 plays a role in the maintenance of autophagy levels possibly through regulation of the expression of several components of the autophagic machinery. Moreover, mitochondria permeability transition has been implicated in the signaling for the induction of mitochondrial autophagy [525, 526]. In accordance with these works, we observed lower autophagy levels and a more closed

mPTP conformation. Although the referred works suggested mitochondrial depolarization as a bridge between mPTP and autophagy our current data may suggest a $\Delta\Psi_m$-independent mPTP regulation of autophagy. In these cells, autophagy levels seem to be kept at an "optimal" level conferring growth advantage to tumor cells, as stimulation or suppression of autophagy in these cells leads to a significant drop in cell proliferation.

In addition to the reduced autophagy levels, we showed in this work that TRAP1-depletion resulted in increased lysosomal content and increased LAMP2A. Similarly to previous studies showing a compensatory activation of CMA in response to autophagy impairment [527] our results suggest the activation of CMA pathway upon TRAP1 silencing. However, the activation of this compensatory mechanism presents its limitations as CMA lacks (macro)autophagy selectivity. Consequently, CMA would only be able to degrade cytosolic proteins and could not compensate for (macro)autophagy removal of organelles [527]. In the absence of (macro)autophagy, CMA can be responsible for enhanced oxidative stress resistance reflecting the advantage of its activation as a compensatory mechanism for autophagy impairment [528]. Moreover, substrate binding to LAMP2A transporter is a limiting step for CMA through which proteins are translocated one-by-one to the lysosomal lumen. Accordingly, levels of LAMP2A at lysosomal surface determine rates of CMA activity [373]. Despite the advantages conferred by CMA activation, when the gradual accumulation of damaged components overcomes cell repair/buffering capacity, cell death becomes inevitable.

When protective/adaptative mechanisms fail, stressed cells trigger apoptosis. High levels of cell stress often result in mitochondrial fission and apoptosis. The process of mitochondrial fragmentation has been reported to occur almost simultaneously with pro-apoptotic BCL-2 family member BAX translocation to mitochondria but before caspase activation [484]. Before caspase activation, BAX accumulates in the OMM in compacted foci that colocalize with DRP1 and mitofusin proteins [529]. Moreover, DRP1 stimulates BAX oligomerization and thus OMM permeabilization [530]. In addition to the increased mitochondrial fragmentation, TRAP1-depleted cells showed elevated BAX and reduced BCL-xL levels, thus indicating the higher sensibility of these cells to apoptosis. Surprisingly, caspase 3/7 was shown to be activated independently of caspase 8, 9, or 12. This further suggests that, in these cells, caspase 3/7 undergo activation through other alternative pathways or that we did not measure the right time-point for initiator caspases activation. Nevertheless, it was previously shown that caspase 3 activation

might occur independently of other initiator caspases, one example being through cathepsins' cleavage [531, 532]. Although the current work did not address this issue, considering the observed increment in lysosomal content, the overall increase in cellular stress may contribute to enhanced lysosomal membrane permeabilization (LMP) therefore leading to cathepsin release resulting in caspase 3 activation [533]. In fact, although lysotracker fluorescent pattern is more prominent in TRAP1-depleted cells which would suggest that LMP is not occuring, previous reports have shown that LMP and selective cathepsins release may occur in a subset of lysosomes, still allowing organelle labeling [534]. Several cellular constituents can promote LMP: lysosomal free iron, ROS-induced lysosomal lipid peroxidation, free fatty acids, sphingosine, oxidized cholesterol and BCL-2 family of proteins such as BAX or BAK [535]. In the context of the present work, ROS and BAX would be the most promising agents although the former appears to be of mitochondrial origin and with an inherent chemical character, which is not compatible with a high diffusion radius.

7.4 Conclusions

In agreement with previous reports, TRAP1 plays an important role in the mitochondrial physiology maintenance of A549 cells by decreasing oxidative stress, preserving $\Delta\Psi_m$, and modulating mPTP. Our present results suggest the participation of p66SHC in TRAP1 mechanisms of ROS regulation in these cells, although p66SHC silencing would help clarify this. Here we confirmed that TRAP1 indeed modulates mPTP, however, on the contrary to what was expected, TRAP1 depletion led to a more closed mPTP conformation under basal conditions. Although the knowledge on the implication of these observations is still unknown, this finding suggests the re-evaluation of TRAP1 mPTP protective function indicating a far more complex involvement of this chaperone in this function. Nevertheless, the understanding of the mechanisms underlying TRAP1 modulation of mPTP requires further investigation. Moreover, our findings suggest that TRAP1 controls these mitochondrial functions by regulating mitochondrial morphology. Furthermore, here we describe for the first time TRAP1 involvement in the regulation of autophagy levels. In A549 cells, TRAP1 seems to maintain an adaptive autophagy flux conferring a growth advantage to tumor cells. Altogether, these findings provide new insights for

TRAP1 role in tumor cells and contribute to increase our understanding of the mechanisms behind this chaperone complex function.

Chapter 8

TRAP1 regulates autophagy in MRC-5 lung cells but has reduced effects on mitochondrial function

TRAP1 is a mitochondrial chaperone of the HSP90 family which is differentially expressed in tumor versus normal cells. These differences in TRAP1 expression led to its characterization as an anticancer molecular target. However, current inhibitors available are not able to distinguish between TRAP1 and HSP90 making them not ideal drugs for targeting specifically TRAP1 in tumor cells. Furthermore, even if TRAP1 targeting is specific to this chaperone, it remains to be determined whether TRAP1 inhibition in non-tumor cells would have deleterious effects to those non-target cells. To investigate this, we have used transient TRAP1 silencing in MRC-5, a model for non-tumor cell line. Our results from this and previous sections suggest that besides TRAP1 levels, differences in its subcellular localization might also be important to understand the differential effect of TRAP1 inhibition between normal and tumor cells. TRAP1 was shown to preferentially accumulate in extramitochondrial sites, which may explain the fact that its silencing did not greatly affect mitochondrial function. Nevertheless, as in previously studied lung cancer cell line, TRAP1 silencing in MRC-5 cells affected autophagy levels.

8.1 Introduction

TRAP1 was first identified by yeast two-hybrid assay as a TNFR interacting partner. Although the presence of a mitochondrial targeting sequence at its N-terminus indicates TRAP1 primarily mitochondrial localization, further studies led to the identification of this chaperone in cytosol [430], nucleus [430], and more recently in the ER [452]. TRAP1 soon became high focus of study in cancer cells not only because of its high expression but also due to its cytoprotective functions (revised in [536]). Conversely, normal cells have been reported to have low TRAP1 expression [433]. To the author's knowledge, TRAP1 function in non-tumor cells has not been yet fully described. Despite these observations regarding TRAP1 differential expression in tumor *versus* normal cells, further studies show that this chaperone expression is also variable in cancer cells [446]. Indeed, lower TRAP1 expression levels observed in some cancers have been associated with the acquisition of a higher malignancy phenotype by increasing cell metastatic capability [441, 446]. Thus, TRAP1 functions in normal and transformed cells seem to be far more complex than initially thought.

Recently, a novel generation of mitochondrial targeted HSP90 inhibitors were developed and are considered to constitute promising drugs for anticancer therapy due to their ability to efficiently inhibit TRAP1 within mitochondria (revised in [454]). In addition, such agents showed high efficacy in reducing tumor cell growth with no major effects on their normal counterparts. However, these inhibitors are not able to distinguish between TRAP1 and HSP90 making them less suitable for TRAP1-specific studies.

TRAP1 expression and function in normal cell lines has been, in our opinion, highly disregarded, as most studies only focus on the therapeutic implications of HSP90-inhibitors in these cells without an extensive evaluation of TRAP1 loss implications in these cells. However, judging by the increased information on TRAP1 in the last decade and considering that we cannot address TRAP1 function in such a linear and clear manner as previously appreciated, the study of this chaperone function in normal lung fibroblasts seemed pertinent. Therefore, this study aims to explore the consequences of TRAP1 gene inhibition on mitochondrial physiology and morphology in the human MRC-5 normal lung fibroblast cell line. We hypothesized that in this non-tumor cell line, TRAP1 does not play a crucial role in mitochondrial function and dynamics as well as in cellular and organelle quality control. Hence, we first aimed the identification of TRAP1 silencing-consequences

in terms of mitochondrial dysfunction including, loss of $\Delta\Psi_m$, mPTP induction, and oxidative status. Finally, we addressed TRAP1 role in mitochondrial dynamics and its silencing repercussion on autophagy pathways and expression and activity of several apoptosis regulators. The results have implications not only how we perceive TRAP1 roles in the different cell types but also to understand the consequences of off-targeting TRAP1 in non-tumor cells.

8.2 Results

8.2.1 TRAP1 expression and silencing efficiency

In order to address TRAP1 levels in MRC-5 human lung fibroblasts *TRAP1* mRNA expression as well as its protein content were first investigated. Analysis of *TRAP1* mRNA normalized to 18S showed that the transcript content was two-fold lower in MRC-5 normal lung fibroblasts compared to A549 tumor cells, used in the previous section (Fig.8.1A). Moreover, TRAP1 protein expression normalized to actin confirmed its lower expression in MRC-5 cells (Fig.8.1B). It is important to mention that no differences regarding 18S mRNA content were found between both cell lines, indicating that this is a good internal reference for comparisons between cell lines (Fig.8.1C). However, in agreement with the fact that cell morphology differs, actin content was higher in MRC-5 cells, suggesting that this protein may not be an ideal loading control to compare different cell lines (Fig.8.1D). Thus, these results show that MRC-5 cells have low TRAP1 expression, making it a useful model for the understanding of the importance of TRAP1 functions in normal cells where its expression is less noted than in tumor cells.

The efficacy of TRAP1 inhibition by siRNA in MRC-5 cells was verified through qRT-PCR and results showed a 4-fold decrease in *TRAP1* mRNA content when compared with both control groups with no differences observed in the latter (Fig.8.2A). Furthermore, silencing efficiency was verified at protein level showing that TRAP1 protein content, normalized to actin, was significantly decreased after 72 hours post-transfection in MRC-5 siTRAP1 cells when compared with the siCTL and CTL control groups (Fig.8.2B), with the two latter groups showing no differences between themselves.

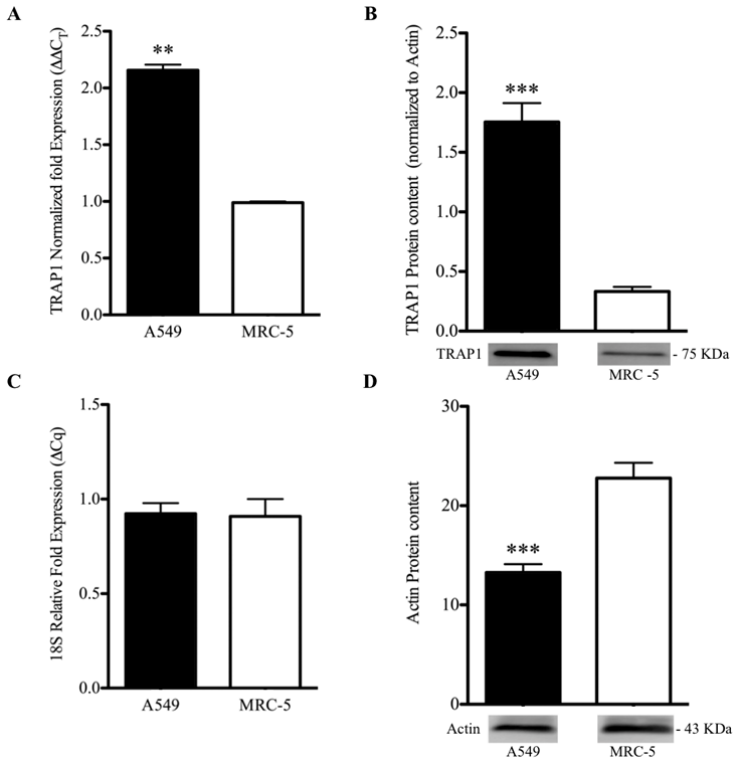

Figure 8.1 - TRAP1 differential expression. TRAP1 mRNA content in A549 and MRC-5 cells was determined through qRT-PCR. (A) TRAP1 mRNA content was lower in MRC-5 fibroblasts when compared with A549 cells. mRNA levels were normalized to 18S (N=12), with results being calculated through the ΔΔCT method. (B) These differences were confirmed at protein level through western blot. (C) No differences were observed regarding 18S reference gene mRNA content between both cell lines. (D) A higher actin content was found in MRC-5 cells when compared with A549 cells. TRAP1 protein content was normalized to actin (N=7). Bars show mean ± SEM (**p<0.01, ***p<0.001; two-tailed Student's t-test).

In order to evaluate TRAP1 silencing stability in MRC-5 cell line, cells were transfected and protein was harvested every 24 hours up to 144 hours post-transfection. Results showed no change in TRAP1 protein content 24 hours post-transfection; however, after 48 hours post-transfection there is a decrease in TRAP1 expression in siTRAP1 cells (group *a*) compared with siCTL control (group *b*), which remains stable up to 120 hours post-transfection (Fig.8.2C). Although at 144 hours post transfection siTRAP1 cells still show lower TRAP1 content this is not as clear as for the remaining time points revealing an apparent recovery of TRAP1 expression in these cells.

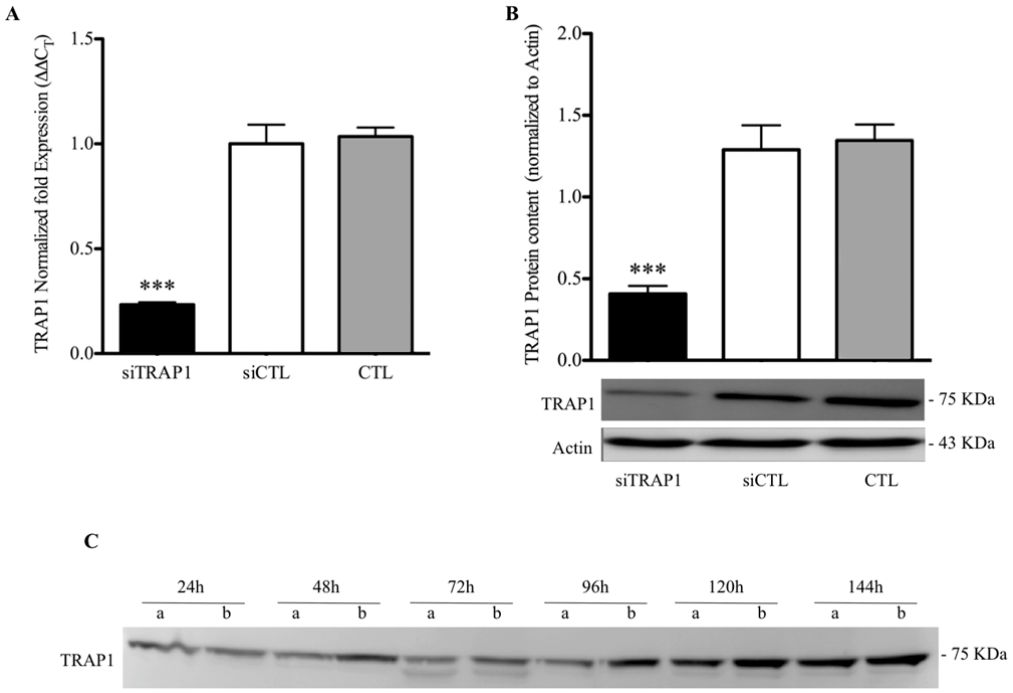

Figure 8.2 - TRAP1 silencing efficiency in MRC-5 cells. Cells were either transfected with a TRAP1 siRNA oligonucleotide (siTRAP1) or a scrambled siRNA as a control (siCTL), CTL cells correspond to non-transfected cells. Silencing efficiency was confirmed through qRT-PCR and western blot. (A) Results show a significantly lower TRAP1 content in siTRAP1 cells when compared with the controls groups. mRNA levels were normalized to 18S (N=12) and results were calculated by ΔΔCT method. Bars show mean ± SEM (*** $p<0.001$ to siCTL, one-way ANOVA followed by Dunnett's post-hoc test). (B) TRAP1 protein content analysis shows a large decrease in TRAP1 protein upon silencing when compared with the controls. Protein levels were normalized to actin (N=4), bars show mean ± SEM (*** $p<0.001$ to siCTL, one-way ANOVA followed by Dunnett's post-hoc test). (C) Transfection stability was evaluated by using western blot in a time period ranging from 24 hours to 144 hours post-transfection. Data shows that silencing is efficient at 48 hours post-transfection remaining stable at least up to 144 hours post-transfection (a – siTRAP1 cells, and b – siCTL control cells).

8.2.2 TRAP1 silencing effect on cell proliferation and susceptibility to DOX-induced toxicity

In order to assess TRAP1 role in MRC-5 cell growth in, cell proliferation was evaluated in TRAP1 naïve and silenced cells by the SRB method (see Section 6.2.3, Material and Methods). Results presented in Fig.8.3A show that TRAP1 silencing decreases cell mass

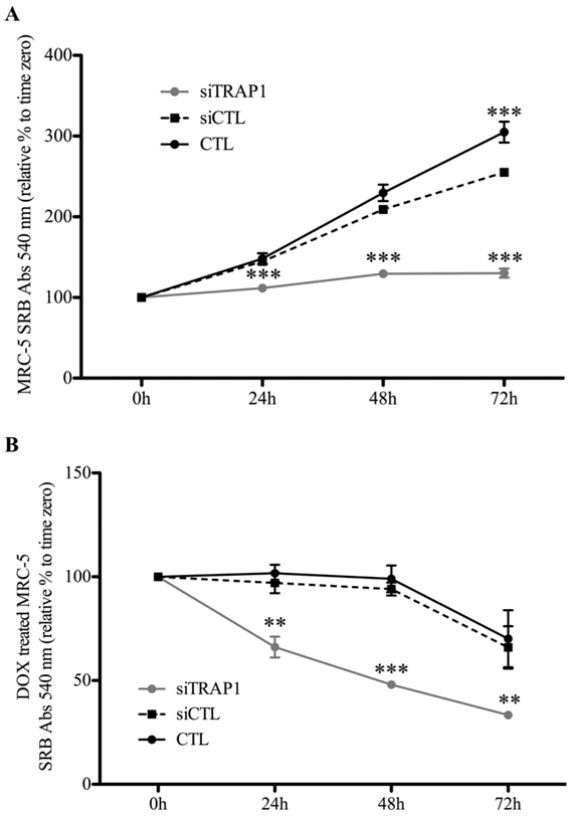

Figure 8.3 - TRAP1 silencing effect on cell growth and susceptibility to DOX treatment. (A) Cell growth curves show a decrease in TRAP1 silenced cells proliferation when compared with control groups (*N*=6). (B) DOX-treated TRAP1-silenced cells show lower cell proliferation when compared with the controls (*N*=6). Data are presented as mean ± SEM (** p<0.01, and *** p<0.001 to siCTL; two-way ANOVA followed by Bonferroni post-test).

within 24 hours post-seeding (corresponding to 72 hours post-transfection). These differences in cell growth continued for 48 and 72 hours post-seeding while controls showed a liner growth over the same period of time. Therefore, TRAP1 silencing led to a maximal 49% drop in MRC-5 proliferation (relative to siCTL cell group) during the 72 hours of the assay. Overall, no differences were observed regarding cell proliferation between siCTL and CTL groups with the exception of the 72 hours time point where cell mass was shown to be higher in the CTL cell group (Fig.8.3A).

We next addressed TRAP1 silencing effect on MRC-5 cell susceptibility to DOX-induced toxicity. After TRAP1 silencing, cells were plated as previously described, treated with 0.5ΕM DOX, and allowed to grow up to 72 hours. Doxorubicin-effects on cell proliferation were analyzed through the SRB assay and showed an overall growth inhibition in all cell groups and time points analyzed (Fig.8.3B). However, regarding inter-group comparisons, a high decrease in cell proliferation was observed in siTRAP1 cells within the first 24 hours of DOX incubation was shown, while no differences in both controls cell mass resulting from DOX treatment were detected. Although these findings reveal that all

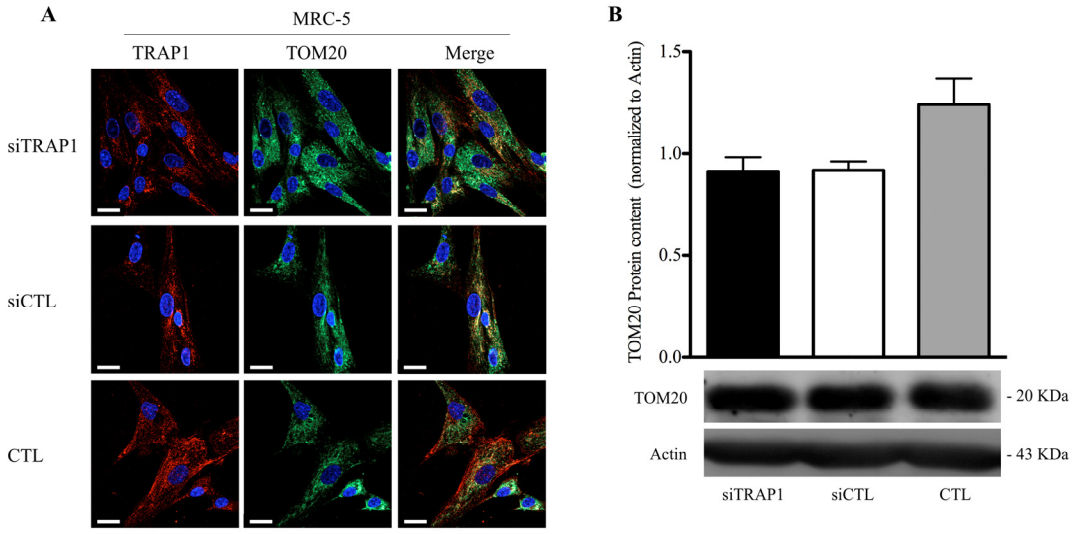

Figure 8.4 - TRAP1 subcellular localization. (A) Red fluorescence labels TRAP1 while green fluorescence labels TOM20 (mitochondrial outer membrane marker), nuclei were counterstained with DAPI and are shown in blue. The merged images show a sparse TRAP1 labeling, with no predominant co-localization with TOM20. In addition, siTRAP1 cells also show a decrease in red fluorescence when compared with the controls. Images were acquired by confocal microscopy using a 40x objective, scale bar = 22μm. (B) TRAP1 silencing did not affected TOM20 expression levels (N=4). Bars show mean ± SEM (one-way ANOVA).

cell groups were similarly susceptible to DOX toxicity, they suggest a higher susceptibility in the siTRAP1 group.

An additional analysis of the above data regarding DOX toxicity was performed taking into account the differences in cell proliferation between the different groups shown in Fig.8.3A. To achieve this, the percentage of difference between non-treatment growth and DOX-treatment growth for each correspondent cell group was calculated at 72 hours post-seeding. Interestingly, TRAP1-silenced cells showed a 59.4±0.61 % (N=3) inhibition of cell growth against the 78.2±3.84 % (N=3) inhibition in the siCTL group, which revealed to be statistically significant ($p<0.01$) and thus, indicating a higher susceptibility of siCTL cells to DOX toxicity.

8.2.3 TRAP1 modulation of mitochondrial function

After general evaluation of TRAP1 effects on cell growth, we moved on to analyze its silencing consequences on mitochondrial physiology. As a non-tumor cell line, and considering TRAP1 low levels in MRC-5 cells we hypothesize that mitochondrial function would not be extensively affected by TRAP1 depletion. This section aims to assess this issue with a special focus on $\Delta\Psi_m$, mPTP regulation, and cellular oxidative stress.

TRAP1 is highly localized in extramitochondrial sites

TRAP1 subcellular localization in MRC-5 cells was assessed through immunocytochemistry by co-staining cells with both TRAP1 and the OMM marker TOM20, followed by imaging trough using confocal fluorescence microscopy. TRAP1 co-localized with TOM20 in siCTL and CTL MRC-5 cells although to a less extent than what would be expected taking into account what was described before [431] (Fig.8.4A). In fact, TRAP1 seems to have a sparse and diffused distribution within the cells instead of the expected specific mitochondrial localization. These results suggest that TRAP1 preferentially localizes in extramitochondrial sites in MRC-5 cells. Mitochondrial mass was indirectly evaluated by measuring TOM20 protein content through western blot, the results showed that TRAP1 depletion had no impact on mitochondrial mass (Fig.8.4B).

In order to investigate whether TRAP1 silencing results in increased compensatory expression of HSP90 and HSP60 transcript levels were measured. TRAP1-silencing led to a significant decrease in *HSP60* mRNA content while not affecting *HSP90AA1* (Fig.8.5A and B). Additionally the mRNA content for the HSP90 splicing variant 1 (*HSP90AA1.1*, see Section 6.2.3 Material and Methods) was also analyzed. Although no differences were found when analyzing HSP90 mRNA, in which primers were designed in order to target both splicing variants (*HSP0AA1.1* and *HSP90AA1.2*), results showed an increase in *HSP90AA1.1* mRNA content in siTRAP1 cells when compared with siCTL cells (Fig.8.5C). Despite these alterations, TRAP1 silencing had no effect on HSP90 protein expression levels (Fig.8.5D).

In summary, cellular localization of TRAP1 in MRC-5 appear to be mostly extramitochondrial and chaperone silencing does not greatly affects other HSPs expression.

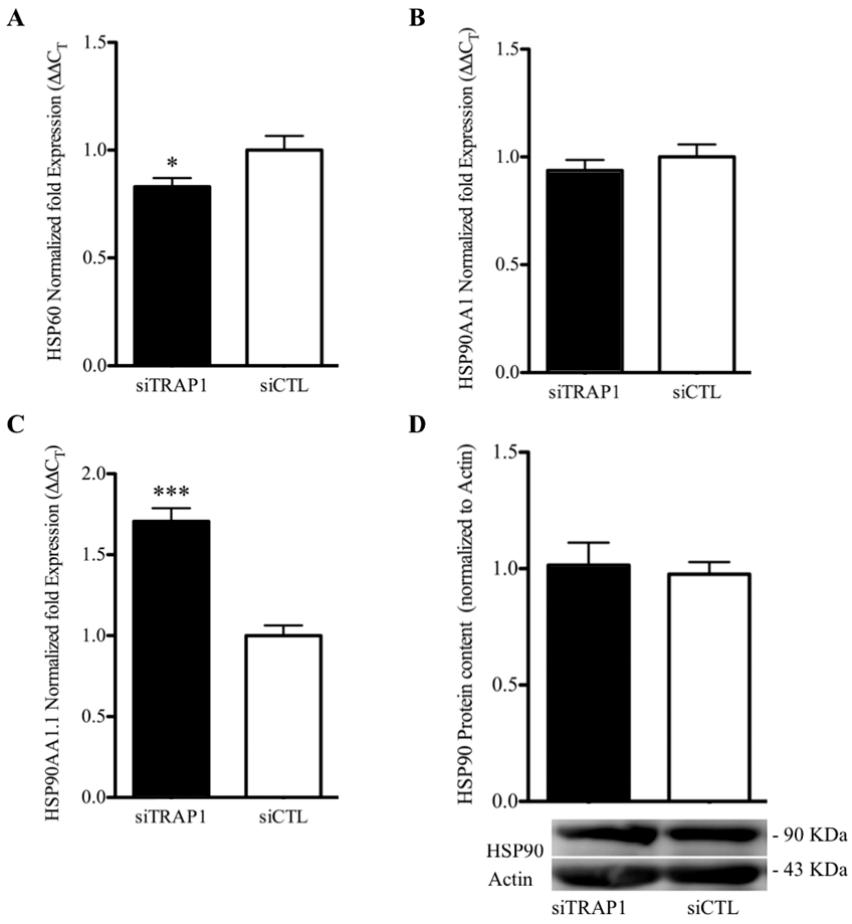

Figure 8.5 - Mitochondrial HSP90 and HSP60 chaperones content. HSP60 and HSP90 mRNA content was analyzed by qRT-PCR. Results show a decrease in HSP60 content (A) while HSP90AA1 content was not altered (B) in siTRAP1 cells when compared with control cells. (C) siTRAP1 cells showed higher HSP90AA1 variant 1 mRNA content than siCTL cells. mRNA levels were normalized to 18S (N=12), results were calculated by ΔΔCT method. (D) HSP90 protein expression analysis showed no alterations in this protein expression between siTRAP1 and siCTL cells. Protein levels were normalized to actin (N=8). Bars show mean ± SEM (*p<0.05, *** p<0.001; two-tailed Student's t-test).

TRAP1 silencing does not affect $\Delta\Psi_m$

To address the role of TRAP1 in mitochondrial function modulation in MRC-5 cells, alterations in $\Delta\Psi_m$ were initially evaluated through flow cytometry using TMRM, a fluorescent probe which is accumulated by polarized mitochondria. TRAP1-silenced cells showed no differences regarding TMRM fluorescence when compared with the control

(Fig.8.6A). In a second approach, cells were co-labeled with Mitotracker Green (MTG) and TMRM. The former probe stains mitochondria independent of $\Delta\Psi_m$ whereas TMRM loads into polarized mitochondria. As described in the previous sections, when co-labeled, TMRM reversibly quenches MTG fluorescence to obtain a relative balance between total mitochondrial content and depolarized mitochondria [469]. Both cell groups (siTRAP1 and siCTL) showed similar TMRM uptake, MTG quenching and response to FCCP-induced mitochondrial depolarization (Fig.8.6B), supporting the notion that TRAP1 silencing in MRC-5 cells does not impact $\Delta\Psi_m$.

TRAP1 silencing effect on mPTP modulation

TRAP1 has been described to modulate mPTP by binding to and antagonizing CypD function [304]. With the purpose of further verify TRAP1 silencing effect on mitochondrial function we next evaluated mPTP status. Thus, the effect of TRAP1 silencing was investigated using the calcein-cobalt quench assay, as described before [480]. Cells were co-loaded with calcein-AM and cobalt chloride and either incubated with CsA, Io or both. Calcein-AM readily crosses cellular and mitochondrial membranes whereas cobalt is spatially restricted to the cytosol. In the cell cytosol, cobalt quenches cytoplasmic calcein fluorescence revealing the mitochondrial calcein fluorescence staining. Calcein fluorescence in represented in Fig.8.7A showing that all cell groups equally responded to CsA and ionomycin by changing to a closed or open mPTP conformation, respectively. Normalization as described in previous section resulted in equivalent percentage of mPTP-closed state in both groups.

Therefore, the above data suggests that mPTP is open/closed to the same extent in all treatment groups. Analysis of *PPIF* (CypD) mRNA level showed an increase in siTRAP1 cells when compared to the control group (Fig.8.7.B). However, despite these differences in *PPIF* expression TRAP1 depletion did not affect CypD protein content (Fig.8.7C). Moreover, subunit c of the ATP synthase content, measured by western blotting, was also not affected by TRAP1 depletion (Fig.8.7D).

Overall, cell groups showed similar transient mPTP opening with no alterations in CypD and ATP synthase subunit c expression. These observations emphasize the hypothesis that TRAP1, in these cells, does not have a preponderant role in the maintenance of mitochondrial function with respect to $\Delta\Psi_m$ and mPTP.

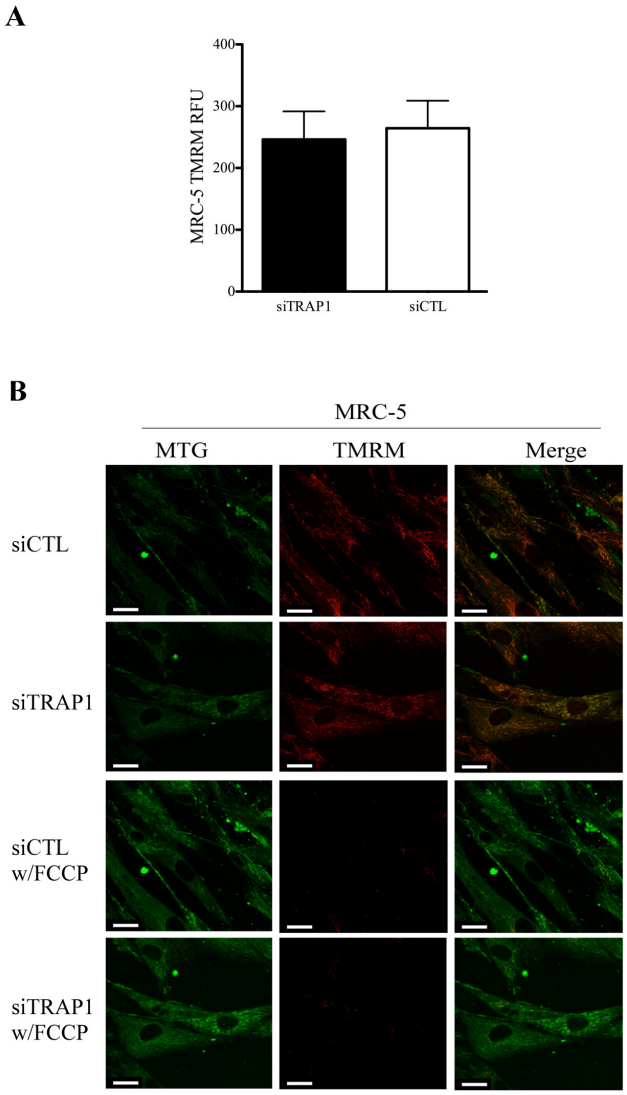

Figure 8.6 - Mitochondrial membrane potential alterations upon TRAP1 silencing. (A) Mitochondrial membrane potential ($\Delta\Psi_m$) alterations were evaluated using TMRM probe and analyzed through flow cytometry. No differences were observed regarding TMRM fluorescence. (B) Quenching of MTG by TMRM in siCTL and siTRAP1 cell groups (two upper panels). Both cell groups showed MTG quenching (upper left panel). In addition no differences were found in TMRM fluorescence intensity. Mitochondrial de-energization with FCCP caused red TMRM fluorescence (two bottom panels) to disappear and green MTG fluorescence to recover in both cell groups. Images were acquired by confocal microscopy using a 40x objective, scale bar = 22μm.

TRAP1 silencing does not alter cellular oxidative stress

Considering that mitochondria constitute an important intracellular source of ROS [482], and taking into account TRAP1 antioxidant role [442], the next question raised was whether TRAP1 silencing affected mitochondrial ROS generation. Consequently, MRC-5 cells were loaded with the mitochondrial superoxide anion indicator MitoSOX Red. Confocal microscopy imaging demonstrated that cell groups showed very low levels of fluorescence staining with no variations between siTRAP1 cells and the control (Fig.8.8A).

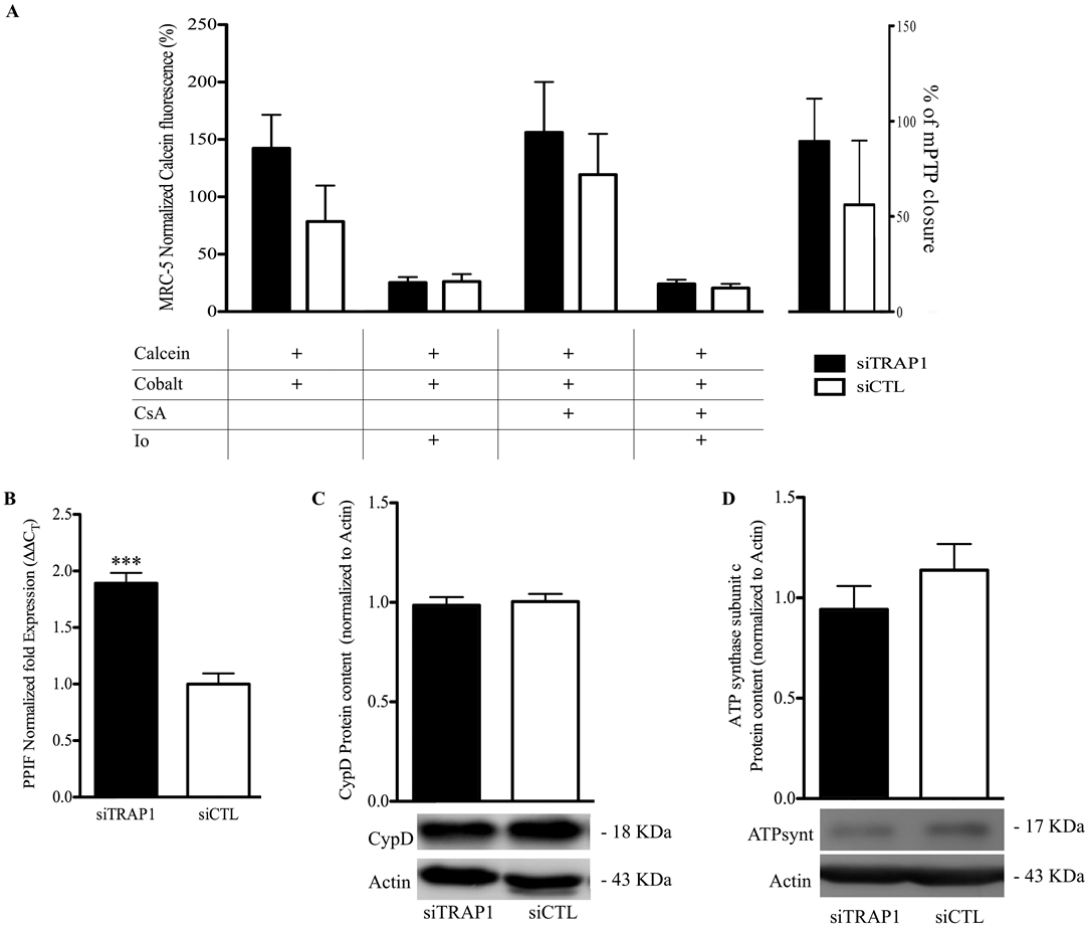

Figure 8.7 - TRAP1 expression and mitochondrial permeability transition pore (mPTP) modulation. The mPTP was monitored by quantifying calcein fluorescence in cell mitochondria by flow cytometry. The cells were loaded with calcein AM and cobalt, a cytosolic calcein quencher, in order to determine the basal calcein fluorescence in mitochondria. The cells were also incubated with Ionomycin (Io) which triggers calcium overload and pore opening and consequent loss of mitochondrial calcein fluorescence. Additionally, cells were incubated with cyclosporin A (CsA) which blocks pore opening. (A) Cell groups showed statistically similar basal calcein fluorescence. In addition, no alterations were observed in calcein fluorescence between all cell groups upon treatment with Io only, and Io and CsA (N=6). In the right panel, we calculated the % of mPTP closure based on the values for Io (100% mPTP opening) and CsA (0% mPTP opening). (B) PPIF content was increased in siTRAP1 cells when compared to siCTL. mRNA levels were normalized to 18S (N=12), results were calculated by ΔΔCT method. (C) Evaluation of CypD protein expression showed no differences between cell groups. Protein levels were normalized to actin (N=8). (D) No differences were found in the subunit c of the ATPsynthase expression levels between siTRAP1 and siCTL cells. Bars show mean ± SEM (***p<0.001, two-tailed Student's t-test).

We further evaluated *SHC1* mRNA expression as well as the content of p66SHC and SOD2 proteins. *SHC1* mRNA expression revealed no alterations in *SHC1* gene expression between cell groups (Fig.8.8B). However, p66SHC protein content was significantly lower in siTRAP1 and CTL cell groups when compared with the siCTL cell group (Fig.8.8C). Interestingly, analysis of the active phosphorylated form of p66SHC (pSer-p66SHC) also showed a decrease in siTRAP1 cells when compared to the controls (Fig.8.8D). These alterations reflected a pSer36-p66SHC/p66SHC ratio of 1.10±0.06 (N=4) against the 0.95±0.05 (N=4) observed in siCTL cells ($p>0.05$). Regarding SOD2 content no differences were found between siTRAP1 cells and siCTL group when measured by western blotting (Fig.8.8E).

These findings indicate that MRC-5 cells have low oxidative stress levels which are not affected by TRAP1 silencing. Also, the p66SHC appears not to be activated in TRAP1-silenced cells.

8.2.4 TRAP1 silencing effect on mitochondrial morphology and dynamics

Altogether, previous results indicate that TRAP1 silencing does not affect MRC-5 mitochondrial function. To further confirm the lack of effect of TRAP1 silencing on mitochondrial function of MRC-5 cells, we next evaluated silencing effects on mitochondrial morphology and dynamics.

TRAP1 silencing does not alter mitochondrial morphology

To examine the effect of TRAP1 silencing in mitochondrial morphology, mitochondria were stained with TMRM and analyzed by confocal microscopy. Live-cell imaging showed an evenly spread tubular mitochondrial network in MRC-5 cells with no differences in mitochondrial shape between TRAP1-silenced cells and the respective controls (Fig.8.9A), revealing that TRAP1 loss does not affect MRC-5 mitochondrial morphology.

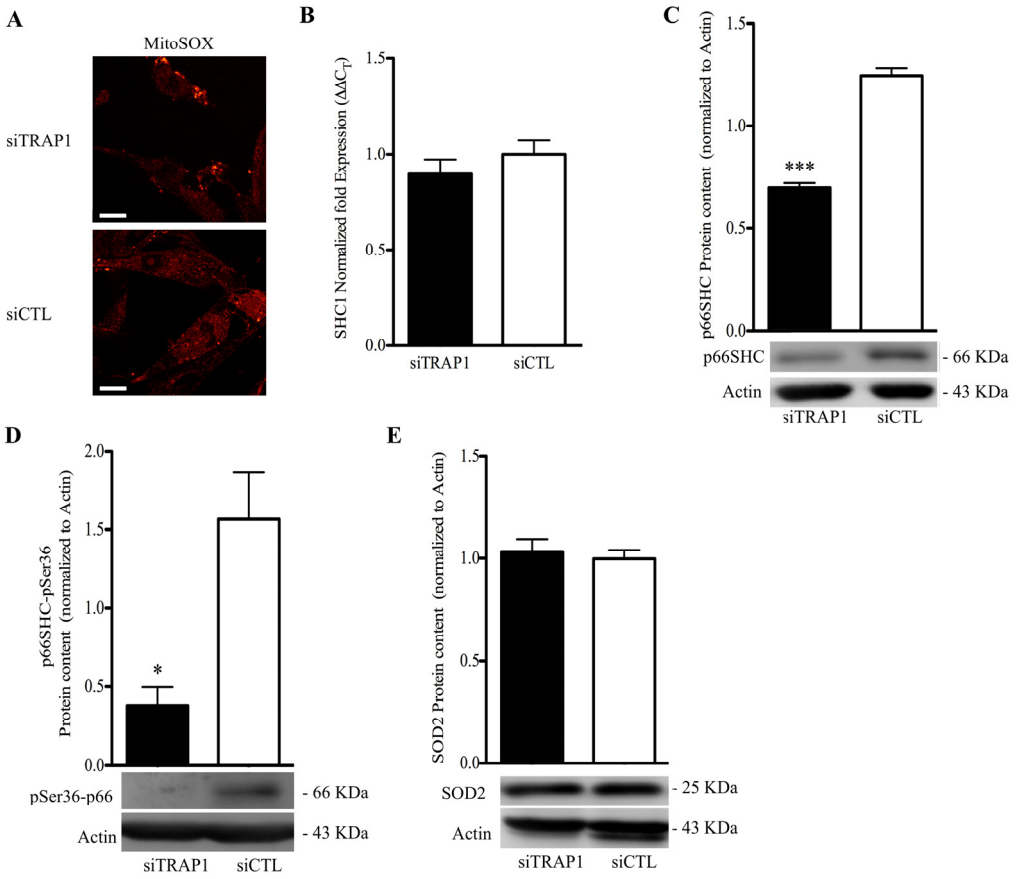

Figure 8.8 - TRAP1 silencing and oxidative stress. (A) Mitochondrial superoxide anion was monitored using the red fluorescent MitoSOX Red probe. Both cell groups showed low detectable levels of MitoSOX fluorescence. Images were acquired by confocal microscopy using a 63x objective, scale bar = 8μm. (B) SHC1 content was not altered by TRAP1. mRNA levels were normalized to 18S (N=12), and results were calculated by ΔΔCT method. (C) Protein expression of p66SHC showed a decrease in siTRAP1 when compared to siCTL cells. (D) TRAP1 depleted cells showed a decreased pSer36-p66SHC content. (E) There were no differences in SOD2 protein between cell groups. Band densities were normalized to actin (N=4). Bars show mean ± SEM (*p<0.05, ***p<0.001, two-tailed Student's t-test).

TRAP1 silencing does not affect the expression levels of proteins involved in mitochondrial dynamics

Considering that TRAP1 silencing did not affect mitochondrial morphology, we next aimed to confirm these results by evaluating the expression of different mitochondrial dynamics markers. In this regard, the expression of proteins involved in mitochondrial

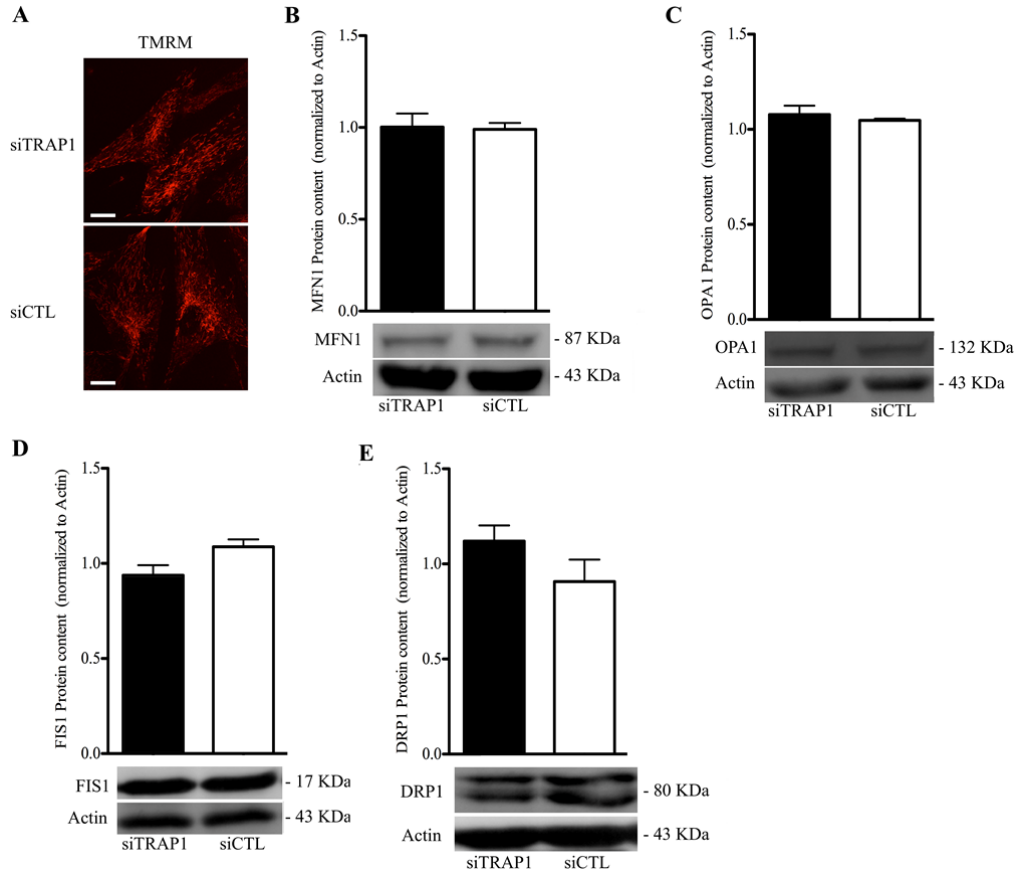

Figure 8.9 - Mitochondria morphology and dynamics in TRAP1-depleted cells. (A) Mitochondria were labeled with TMRM red fluorescent probe. Results showed no alterations in mitochondrial morphology between siTRAP1 and siCTL cells. Both groups showed a complex interconnected mitochondrial network. Images were acquired by confocal microscopy using a 40x objective, scale bar = 22μm. (B-E) Proteins associated with mitochondrial fusion (MFN1 and OPA1) and fission (FIS1 and DRP1) were evaluated by western blot. Protein levels were normalized to actin (N=4), bars show mean ± SEM (***p<0.001, two-tailed Student's t-test). Abbreviations: MFN1 – mitofusin 1; OPA1 – optic atrophy 1; FIS1 – fission protein 1; DRP1 – dynamin-related protein 1.

fusion and fission was investigated. Accordingly, the expression of mitochondrial fusion proteins, MFN1 and OPA1, was not altered in siTRAP1 cells when compared to the control (Fig.8.9B and C). In addition, expression of mitochondrial fission proteins FIS1 and DRP1 was also evaluated in all cell groups showing no alterations in the expression levels of both fission proteins between cell groups (Fig.8.9D and E). These findings are in

agreement with the previous observations regarding the absence of mitochondrial morphology alterations after TRAP1 silencing.

8.2.5 TRAP1 silencing effect on autophagy pathways

Previous results corroborate the hypothesis that TRAP1 does not play an essential role in the maintenance of mitochondrial function in MRC-5 cells. However, we further investigated if TRAP1 silencing in this cell line would alter the mechanisms of regulation of quality control.

TRAP1 silencing decreases macroautophagy levels

The protein content of several autophagy markers was evaluated through western blot in all MRC-5 cell groups. Although TRAP1 depletion did not alter the protein levels of both BECLIN-1 and ATG5 autophagy-related proteins (Fig.8.10A and B), expression of ATG12 was surprisingly decreased in siTRAP1 cells when compared with control groups (Fig.8.10C). Accordingly, levels of ATG12-ATG5 complex were also decreased in TRAP1-depleted cells when compared with siCTL group (Fig.8.10D). The following step was to evaluate the content of proteins from the LC3 conjugation system. The expression of both ATG3 and 7 was not altered in TRAP1-depleted cells when compared with siCTL cell group (Fig.8.10E and F). However, total LC3 content was considerably decreased in siTRAP1 cells (Fig.8.10G). In fact, both the mature (high molecular weight; LC3-I) and cleaved form (low molecular weight; LC3-II) of LC3 were decreased to same extent, showing a LC3-II/LC3-I ratio of 1.01±0.06 in siTRAP1 cells and 1.01±0.03 in siCTL ($p>0.05$).

Analysis of serine/threonine protein kinase PINK1 expression, which plays a key role in removal of damaged mitochondrial through autophagy, showed no alterations between siTRAP1 and the controls (Fig.8.10H). Similarly, no differences were observed between cell groups regarding the expression of NIX, a receptor protein for mitophagy (Fig.8.10I).

To further evaluate TRAP1 loss implications on autophagy, lysosome content and p62 protein levels were evaluated. Lysosome content was evaluated by incubating cells with the Lysotracker Green probe and imaged through confocal fluorescent microscopy. As can be seen in Fig.8.11A (left panels) no differences existed in lysosomal content between all cell groups. Although, immunocytochemistry analysis of p62 expression did not show

major alterations in this protein levels (Fig.8.11A right panels), protein analysis by western blot revealed a lower p62 content in siTRAP1 cells (Fig.8.11B).

Although p62 decreased levels suggest an increased autophagic flux, autophagy markers, with the exception of ATG12 and LC3, did not suffer any alterations upon TRAP silencing indicating otherwise.

TRAP1 silencing and macroautophagy modulation. In order to understand the significance of autophagy modulation on cell proliferation, transfected cells were treated with either rapamycin (autophagy inductor) or 3-MA (autophagy inhibitor) for up to 72 hours. Interestingly and contrarily to the effect observed in A549 cells, cell proliferation was shown to be statistically similar between all cell groups upon rapamycin treatment for all time points in study (Fig.8.12A). MRC-5 cell groups were also incubated with both rapamycin and DOX (Rapamycin+DOX), resulting in a higher decrease in cell proliferation of siTRAP1 group when compared with the siCTL control cells while no differences were found between the controls (Fig.8.12B). Moreover, treatment with the autophagy inhibitor 3-MA resulted in lower cell proliferation in siTRAP1 cells at 48 and 72 hours post-seeding (Fig.8.12C). Additionally, the response to co-incubation with 3-MA and DOX of MRC-5 cells was the same regardless of the applied treatment (Fig.8.12D).

Based on the previous data, another analytic approach was used with the purpose of clarifying the alterations measured with rapamycin treatment. For this reason, results were analyzed in order to compare cell viability in untreated and treated conditions (Rapamycin, DOX, and Rapamycin+DOX) at the 48 hours post-transfection time point and are represented in Fig.8.12E. Rapamycin treatment in siCTL and CTL groups induced a decrease in cell mass when compared to the respective non-treated cell groups whereas siTRAP1 cell mass remained similar. Moreover, no differences were observed when comparing rapamycin-treated with DOX-treated cells for both control groups. In contrast, rapamycin treatment in siTRAP1 cells resulted in a higher cell proliferation than the one observed when treating this same cell group with DOX. In addition, rapamycin and DOX combination treatment appears to have a synergistic effect on decreasing cell mass when compared with DOX treatment alone, and it was statistically significant for both siCTL and CTL groups. Therefore, these results indicate that despite not affecting mitochondrial physiology, TRAP1 does play a role in autophagy levels maintenance in MRC-5 cells.

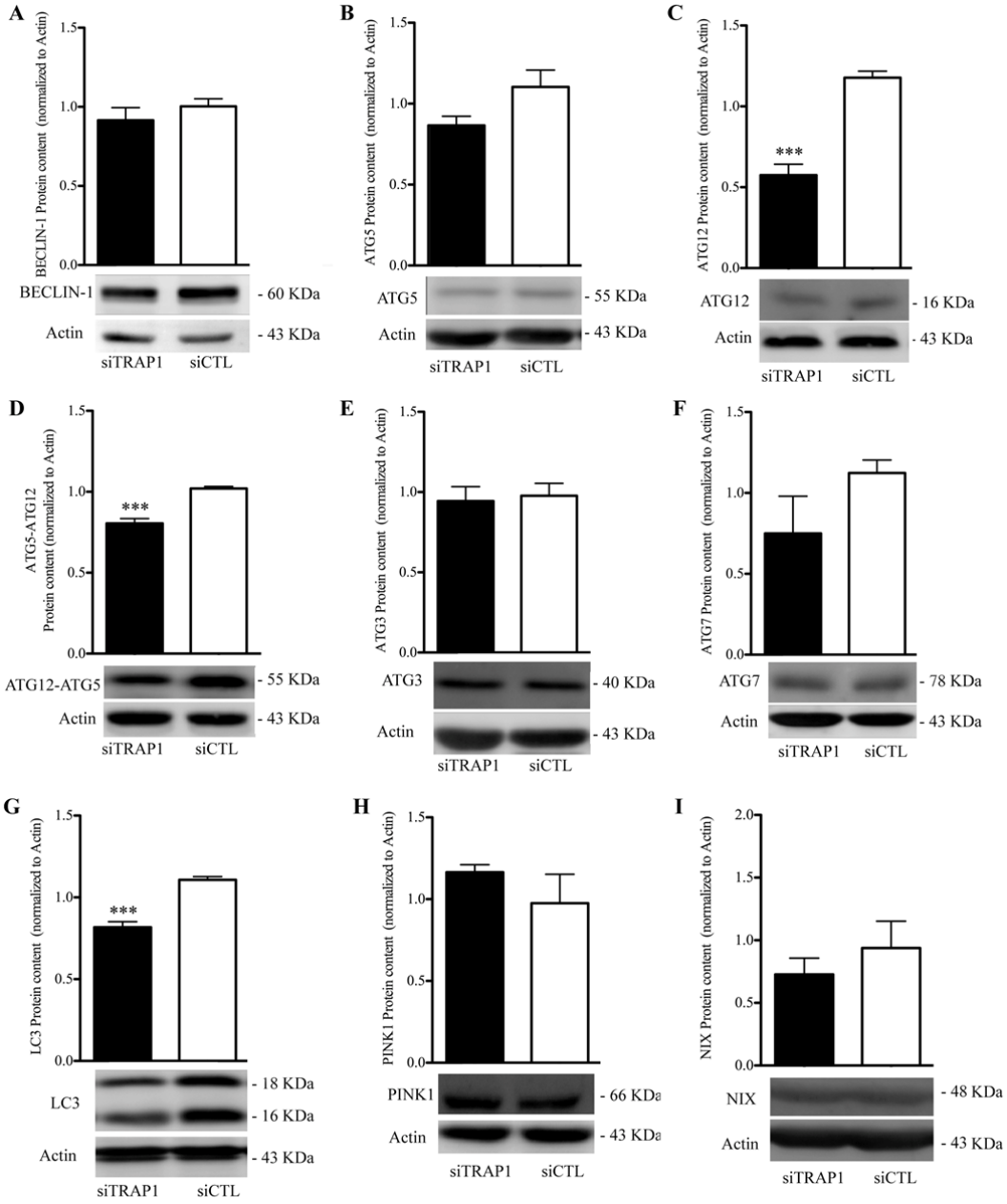

Figure 8.10 - Alterations in macroautophagy-related proteins during TRAP1 silencing. Proteins associated with autophagosome formation, namely in nucleation (BECLIN-1) and elongation (ATG5, ATG12, ATG3, ATG7, LC3) were evaluated by western blot. (A) BECLIN-1 protein content was not altered in TRAP1 silenced cells. (B-D) Although no differences were found in ATG5 levels, ATG12 content as well as ATG12-ATG5 protein complex were decreased in siTRAP1 cells when compared with the control. (E-F) No alterations were found in both ATG3 and ATG7 protein expression. (G) LC3 protein content was decreased upon TRAP1 silencing. (H-I) No alterations were observed regarding the expression of PINK1 and NIX mitophagy-related proteins. Protein levels were normalized to actin (N=4), bars show mean ± SEM (*** $p<0.001$, two-tailed Student's t-test).

TRAP1 silencing does not affect ubiquitin content and CMA levels

Because p62 binds to polyubiquitinated cargos targeting them for autophagic removal, and since TRAP1 has been reported to regulate cellular ubiquitination, we hypothesized that the observed decrease in p62 levels upon TRAP1 silencing results from differences in protein ubiquitination. Consequently, alterations in ubiquitin expression were analyzed in order to understand the previously observed differences in p62 content. Proteins were separated by SDS-PAGE and ubiquitin labeling was evaluated through western blot. Ubiquitin binds to several proteins, therefore creating a smear-like pattern after western blot membrane imaging, as can be seen in Fig.8.13C. A semi-quantitative analysis of ubiquitin labeling showed no alterations in ubiquitin content between cell groups (Fig.8.13A and C).

In order to better clarify TRAP1 role in MRC-5 cells autophagy modulation, we next investigated its silencing effect on LAMP2A expression. TRAP1 did not affect LAMP2A expression levels (Fig.7.14B and C).

8.2.6 TRAP1 silencing affects apoptosis regulators

Considering the previously reported antiapoptotic TRAP1 role [450], we next investigated the effects of silencing this chaperone in the activity of different initiator and effector caspases, as well as TRAP1 silencing implications on the expression of pro- and anti-apoptotic proteins from BCL-2 family.

TRAP1 silencing results in increased caspase 3-like activity and decreased caspase 12-like activity

After 72 hours upon TRAP1 silencing no alterations were observed on initiator caspases 8- and 9-like activities, which participate in extrinsic- and intrinsic- pathways respectively (Fig.8.14A and B). However, caspase 12-like activity decreased in siTRAP1 cells when compared with the control (Fig.8.14C). Moreover, effector caspase 3/7-like activity was dramatically elevated in TRAP1-silenced cells when compared with siCTL cells (Fig.8.14D).

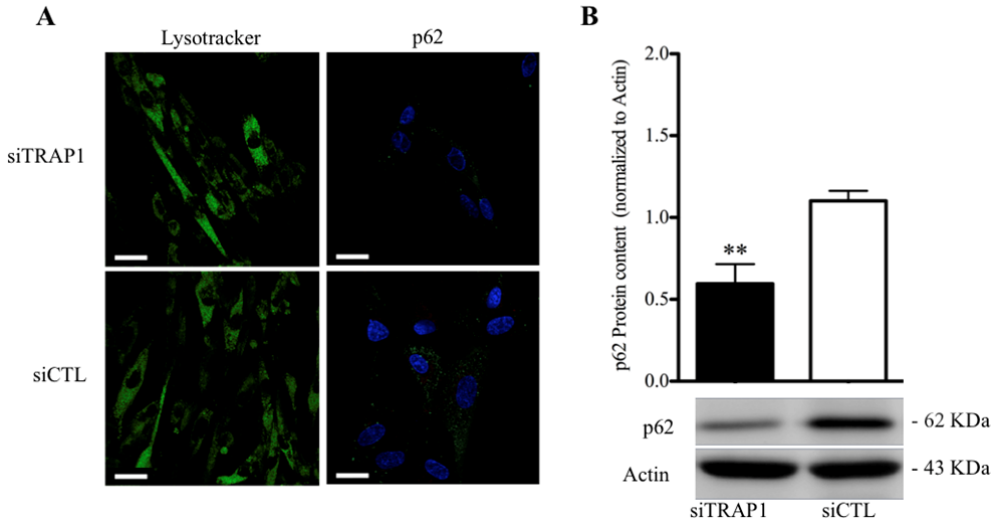

Figure 8.11 - p62 and lysosome content after TRAP1 silencing. (A, left panel series) Cells were incubated with Lysotracker (green fluorescence) and imaged by confocal microscopy. There were no differences in lysosomal content between cell groups. p62 protein content was evaluated both by confocal microscopy (A, right panel) and western blot (B and C). Regardless the methodology used, TRAP1 silencing was shown to induce a decrease in p62. In micrographs, nuclei are marked in blue (DAPI), images were acquired by confocal microscopy using a 40x objective, scale bars = 22μm. Protein levels were normalized to actin (N=4), bars show mean ± SEM (** p<0.01, two-tailed Student's t-test).

TRAP1 silencing did not affect pro-apoptotic and pro-survival BCL-2 family proteins

Additionally, expression of pro-apoptotic protein BAX and pro-survival BCL-2 and BCL-xL proteins was analyzed. TRAP1 depletion was shown to have no effect on any of these proteins (Fig.8.14E-G). Moreover, BAX/BCL-2 ratio was of 1.06±0.07 (N=4) for siTRAP1 and 1.00±0.15 (N=4) to siCTL group (p>0.05), further confirming that TRAP1 did not alter the balance between pro- and anti-apoptotic protein levels.

8.3 Discussion

Cell treatment with several HSP90 inhibitors inhibits cell proliferation and promotes cell death in several cancer cells without affecting their normal counterparts [454]. However, these inhibitors do not distinguish between HSP90 and TRAP1, making them not suitable

for specific TRAP1-function studies. Also, there is still a lack of knowledge on the effects of targeting TRAP1 in non-tumor cells, which could be an off-target consequence of a possible anti-cancer strategy. In this chapter we evaluated TRAP1 silencing effect on MRC-5 mitochondrial physiology and morphology, as well as its involvement in cellular quality control mechanisms.

MRC-5 cells are well-characterized normal human diploid fibroblasts with capability of 46 population doublings and limited lifespan [537]. Several lines of evidence led to the observation that TRAP1 is differentially expressed in normal *versus* cancer cells [433]. In accordance, MRC-5 express low TRAP1 levels. TRAP1 silencing in this cell line did not affect $\Delta\Psi_m$, oxidative stress, or did sensitize cells to mPTP opening. In addition, TRAP1 silencing resulted in a decrease in p66SHC expression levels, which was accompanied by a decrease in its activation through phosphorylation in Ser36 residue. Despite these differences between TRAP1-depleted cells and control, p66SHC activity, extrapolated with pSer-p66SHC/p66SHC ratio, was found to be statistically similar. Together, these results indicate that although TRAP1 somehow regulates p66SHC levels, it does not lead to p66SHC phosphorylation on its Ser36 residue confirming the lack of redox stress observed in these cells after TRAP1 silencing.

Notwithstanding, despite not affecting mitochondrial function, TRAP1 silencing resulted in a significant decrease of cell proliferation rates. These observations were interesting considering that most works report that TRAP1 inhibition affects tumor growth with no detectable alterations in normal cells [434]. Although our results seem apparently contradictory to these observations, it is important to mention that these studies were performed using HSP90 inhibitors that specifically inhibit the mitochondrial pool of both TRAP1 and HSP90. However, we observed that TRAP1 seems to preferentially localize in extramitochondrial sites in MRC-5 cells; therefore, considering its low levels within mitochondria, TRAP1 organelle-specific inhibition would also have low impact on cell growth. Altogether, these findings suggest that different responses to HSP90 inhibitors may be due to TRAP1 distinct intracellular localization between tumor and normal cells. In support of this hypothesis several works showed that cytoplasmic TRAP1 regulates cell cycle by interacting with TNF pathway, thus promoting cell growth and proliferation [446]. Although MRC-5 cells do not express high levels of TRAP1, this protein is still present in these cells, and extramitochondrial TRAP1 seems to play an important role in MRC-5 cell proliferation probably through TNF pathway.

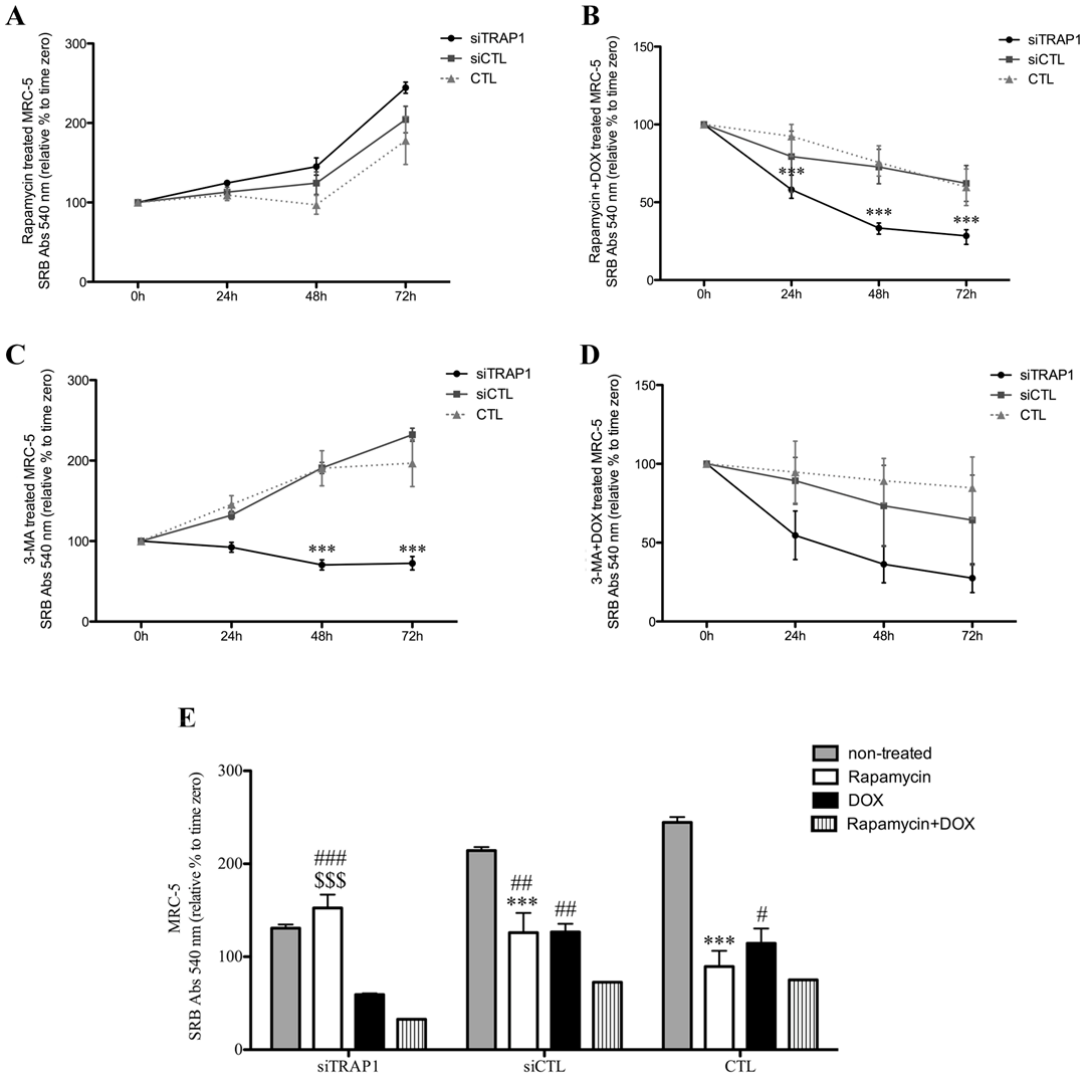

Figure 8.12 - Effect of macroautophagy modulators in the proliferation of TRAP1 silenced cells. Cell proliferation in the presence of the chemical compounds was accessed by SRB dye-binding assay during a period of 72 hours. (A) Data shows similar cellular proliferation for all cell groups analyzed. (B) The same experiment was also conducted in the presence of the anticancer agent DOX. In this case, siTRAP1 showed depressed cell growth throughout the 72 hours in comparison to controls. (C) When treated with 3-MA siTRAP1 cells showed lower proliferation rates than control cells. (D) MRC-5 siTRAP1 cells treated with 3-MA and DOX did not show significant decrease in cell mass in comparison to controls. Data is presented as mean±SEM (*** $p<0.001$ to siCTL for the respective time-point, N=5; two-way ANOVA followed by Bonferroni's *post hoc* analysis for correction for multiple comparisons). (E) Summarized data from previous images for the 48 hours time-point in order to compare cell viability with and without treatment with the following agents: rapamycin, DOX, and rapamycin and DOX. Bars show mean±SEM, two-way ANOVA followed by Bonferroni's *post*

hoc analysis for correction for multiple comparisons (* represents comparison with no-treated, $ represents comparison with DOX-treated cells, # represents comparison with rapamycin and DOX treated cells; all comparisons where made within the same cell group, symbol number represent statistical significance, i.e. one symbol – $p<0.05$, two symbols – $p<0.01$ and three symbols – $p<0.001$).

In addition to mitochondrial function, we also investigated possible mitochondrial morphology changes resultant from TRAP1 loss. Our data showed that TRAP1 silencing had no effect on mitochondrial morphology as all cell groups showed a filamentous mitochondrial network concomitant with the absence of alterations in the expression levels of different fusion and fission proteins. These results were coherent with our previous observations and further emphasize the idea of a less preponderant role of TRAP1 in regulating mitochondrial homeostasis in these cells.

Interestingly, TRAP1 depletion resulted in a decrease of ATG12 and LC3 levels while not affecting any of the other analyzed autophagy proteins. Moreover, both soluble (LC3-I) and membrane-bound (LC3-II) forms were decreased to the same extent in TRAP1-depleted cells. Despite these changes no differences were found regarding the LC3-II/LC3-I ratio between TRAP1-silenced cells and the control, which suggests that autophagy is not defective in these cells although it might occur in a lesser extent that in control cells. Alternatively, due to the limitations associated with LC3 analysis to infer autophagy flux (reviewed in [519]), measurement of p62 degradation may is an important tool. Our data demonstrated that TRAP1 silencing resulted in decreased p62 levels, thus suggesting an increased autophagic flux. Surprisingly, although p62 expression levels can also reflect alterations in ubiquitinated proteins [521] ubiquitin content was not altered in these cells indicating that changes in p62 expression are not dependent on ubiquitin levels. During autophagy, p62 binds to LC3-II being engulfed by the autophagosome and degraded along with polyubiquitinated cargos. Under normal circumstances, low LC3-II levels accompanied by low p62 levels could indicate elevated autophagic flux. However, our results suggest LC3-II decreased levels may result from the decreased ATG12-ATG5 expression, which is required for efficient LC3 lipidation. Consequently, changes in p62 levels in TRAP1-depleted MRC-5 cells can only be the result from the decreased LC3-II protein content.

TRAP1 depletion results in decreased cell growth and reduction of the autophagy levels, consequently, cell treatment with the mTOR inhibitor, rapamycin, was shown to restore

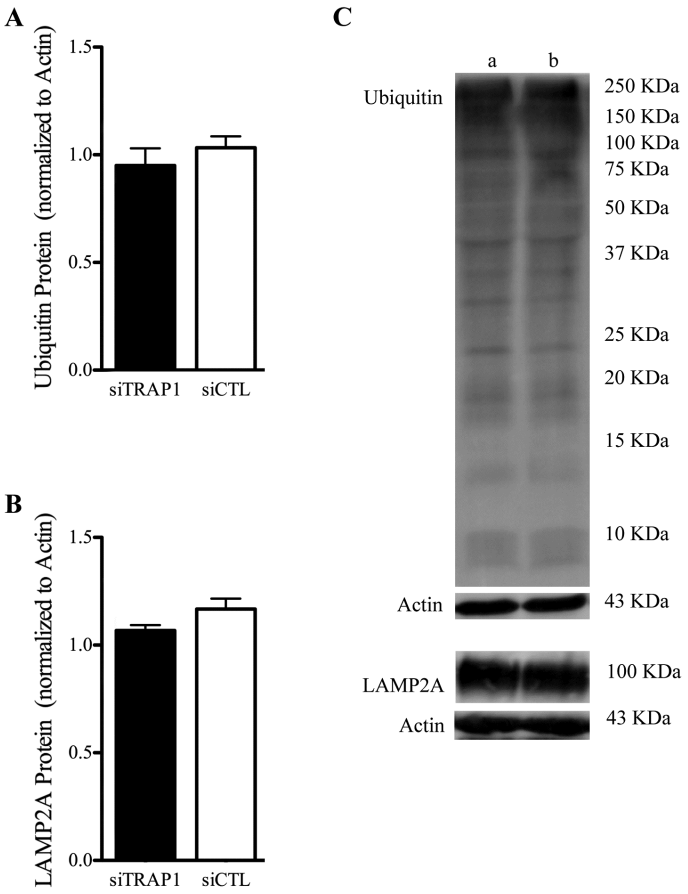

Figure 8.13 - Effect of TRAP1 silencing in both ubiquitin and LAMP2A content. (A and C) The extent of protein ubiquitination was evaluated in total protein extracts of MRC-5 cells. TRAP1 silencing showed similar ubiquitin content when compared to siCTL cell group. (B-C) Protein content of LAMP2A, a receptor for chaperone-mediated autophagy, was similar between both groups. Protein levels were normalized to actin (N=4), bars show mean±SEM. Panel C show representative western blot for the above mentioned proteins together with their respective loading controls (actin). a – siTRAP1 and b – siCTL.

cell proliferation rates in these cells. Conversely, autophagy inhibition in these cells resulted in an accentuated decrease in cell proliferation, whereas control cells proliferation was not affected by either rapamycin or 3-MA treatment. Altogether, these findings suggest that TRAP1 plays a role in the maintenance of the autophagy levels. Autophagy occurs at low basal levels in virtually all cells and plays an important role in cellular homeostasis and genomic integrity [538]. Therefore, autophagy disruption often results in the accumulation of abnormal proteins and organelles. Our results suggest that TRAP1 plays a role in the regulation of autophagy levels, which is necessary to maintain cell proliferation levels. In addition TRAP1 loss did not altered lysosomal content and LAMP2A protein levels, thus it seems TRAP1 has only a mild effect on autophagy, which is not enough to activate compensatory pathways.

Our results showed that TRAP1 depletion did not affect the apparent activity of the initiator caspases 9 and 8; however, surprisingly caspase 12-like activity was decreased in

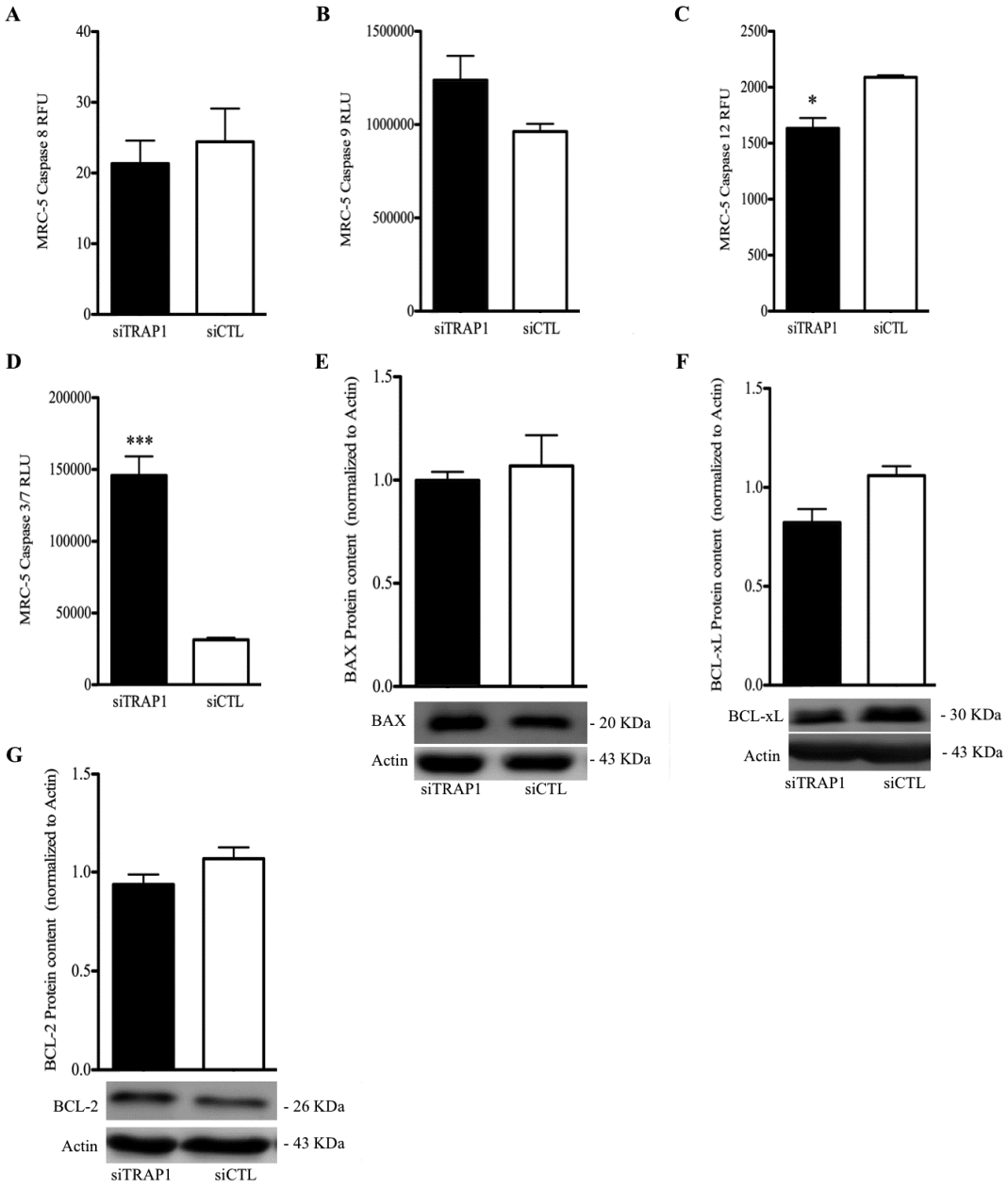

Figure 8.14 - TRAP1 silencing effect on caspase-like activities and BCL-2 family protein levels. The activities of initiator caspases (8, 9 and 12) and effector caspases (3/7)-like were evaluated 72 hours post-transfection. (A-C) There were no differences in activity of initiator caspases 8 and 9 but caspase 12 activity was lower in siTRAP1 group. (D) Effector caspase 3/7 activity was increased upon TRAP1 silencing. Moreover, no alterations in protein content were observed regarding BH3 family of pro-apoptotic protein BAX (E) or anti-apoptotic BCL-xL (F) and BCL-2 (G). Protein levels were normalized to actin (N=4). Bars show mean±SEM (* $p<0.05$; *** $p<0.001$, two-tailed Student's t-test).

TRAP1 silenced MRC-5 cells. Alterations in cellular homeostasis that result in the accumulation of unfolded proteins and aggregates in the ER trigger a signaling pathway called the UPR. TRAP1 has been previously implicated in the regulation of the UPR in the ER, and its depletion was shown to promote caspase 4 activity and induce cell death [451]. Therefore, it is unclear how TRAP1 depletion in our setup resulted in a decreased caspase 12 activity. Nevertheless, since previous works were mainly performed in tumor cell lines the divergence between results further suggests that TRAP1-depletion effects may be dependent on its expression levels, subcellular localization and type of cell. Moreover, TRAP1 depletion resulted in apparent increased caspase 3/7 activation, although there were no changes in the pro- and anti-apoptotic proteins balance therefore suggesting these cells do not undergo apoptosis resulting from TRAP1 silencing.

8.4 Conclusions

Several works reported the efficacy of HSP90 inhibitors in promoting tumor cell death without affecting the normal counterparts. Our findings suggest that in addition to the distinct levels of TRAP1 found in tumor versus normal cells, differences in its intracellular distribution may also contribute for HSP90 inhibitors efficacy. TRAP1 was shown to localize predominantly in extramitochondrial sites and its depletion did not affected mitochondrial physiology or morphology. Despite not affecting mitochondrial function, TRAP1 appears to play an important role in autophagy levels maintenance, which in turn seems to be important for cell growth. However, the TRAP1 role in autophagy is not yet fully understood and requires further investigation. Moreover, TRAP1 seems to mildly regulate autophagy in MRC-5 cells, as its loss did not resulted in activation of compensatory autophagy mechanisms or cell death.

Part III

Final Remarks

Chapter 9

Final Conclusions

Heat shock proteins are highly conserved molecular chaperones that are required for cell survival under stress. HSPs have important cytoprotective properties, which are closely related with their primary functions as molecular chaperones. HSPs play key roles in processes of protein quality control by assisting protein folding, prevent aggregation of un- or mis-folded proteins and assist in the translocation of proteins to their correct intracellular localization. In addition to these functions HSPs also have essential anti-apoptotic properties allowing cell survival and proliferation in unfavorable environments. Therefore, considering that apoptosis evasion and unlimited proliferative capability constitute two core characteristics of tumor development, it is not surprising to think that HSPs are important components of the oncogenic process. In fact, HSPs are overexpressed in a wide range of human carcinomas contributing to the several of the malignant traits that define cancerous growth proposed by Hanahan and Weinberg [45]. Furthermore, members of the HSP90 family are thought to promote tumor cell survival due to their role in maintaining stability and activity of a diverse range of client proteins [435].

TRAP1 was identified as a mitochondrial member of the HSP90 family which is generally overexpressed in tumor cells. An increasing amount of knowledge on TRAP1 role in tumorigenesis has been generated. The present dissertation first aimed at the identification of the several classic traits of mitochondrial dysfunction resultant from TRAP1 loss [536], in the two cell lines. In accordance with previous works, our results indicate that TRAP1 plays an important role in maintaining mitochondria homeostasis and thus conferring tumor cells a growth advantage. Similarly to what has been described in

other cell models TRAP1 depletion led to mitochondrial depolarization and increased ROS production in A549 cells (Fig.9.1). However, this study brought new clues on how TRAP1 modulates oxidative stress in tumor cells as its loss resulted in increased p66SHC Ser36 phosphorylation with no alterations in SOD2 expression. Although more work needs to be done to better understand whether increased p66SHC Ser36 phosphorylation is cause or consequence of ROS increase, our data suggests that TRAP1 is somehow involved in the regulation of p66SHC levels as TRAP1-silencing in MRC-5 cells also resulted in alteration in the levels of this protein without affecting ROS production.

Another important characteristic of TRAP1 that has been broadly explored for cancer therapy is its differential expression in normal *versus* tumor cells. In this regard, several studies have identified mitochondrial-targeted HSP90 inhibitors, gamitrinibs, as powerful anti-cancer tools. Suppression of TRAP1 and HSP90 activities by such agents causes inhibition of cell proliferation and cell death in tumor cells while not affecting non-neoplastic cells (revised in [454]). However, in addition to variations in its expression levels, our data suggests that TRAP1 may also differentially localize in normal (e.g. MRC-5 cells) *versus* tumor cells (e.g. A549 cells), which further explains the level of success of gamitrinibs in cancer therapy. In accordance, TRAP1-depletion in MRC-5 cells had no implications in mitochondrial physiology, which may be due to the fact that in these cells, and in contrast to what was observed in A549 cells, TRAP1 seems to preferentially localize in extramitochondrial sites and thus not have such an important role in the maintenance of mitochondrial homeostasis.

Since its discovery, several works linked TRAP1 cytoprotective functions to its role in mPTP modulation [304, 474]. Mitochondrial TRAP1, along with HSP90 and HSP60, was shown to bind CypD, which has been proposed to impair mPTP opening [302, 304]. Although our findings support the hypothesis that TRAP1 modulates mPTP these suggest a far more complex involvement of this chaperone in this process. Unlike what was expected TRAP1 loss in A549 cells resulted in pore closure under normal growth conditions. Nevertheless, these apparently contradictory results are interesting as, to our knowledge, this is the first study directly exploring TRAP1 role in mPTP modulation. However, the significance of this mPTP closure as well as a deeper knowledge on how TRAP1 is actually involved in its modulation needs to be further explored. A more closed status of the mPTP under basal conditions may result from an adaptive response to

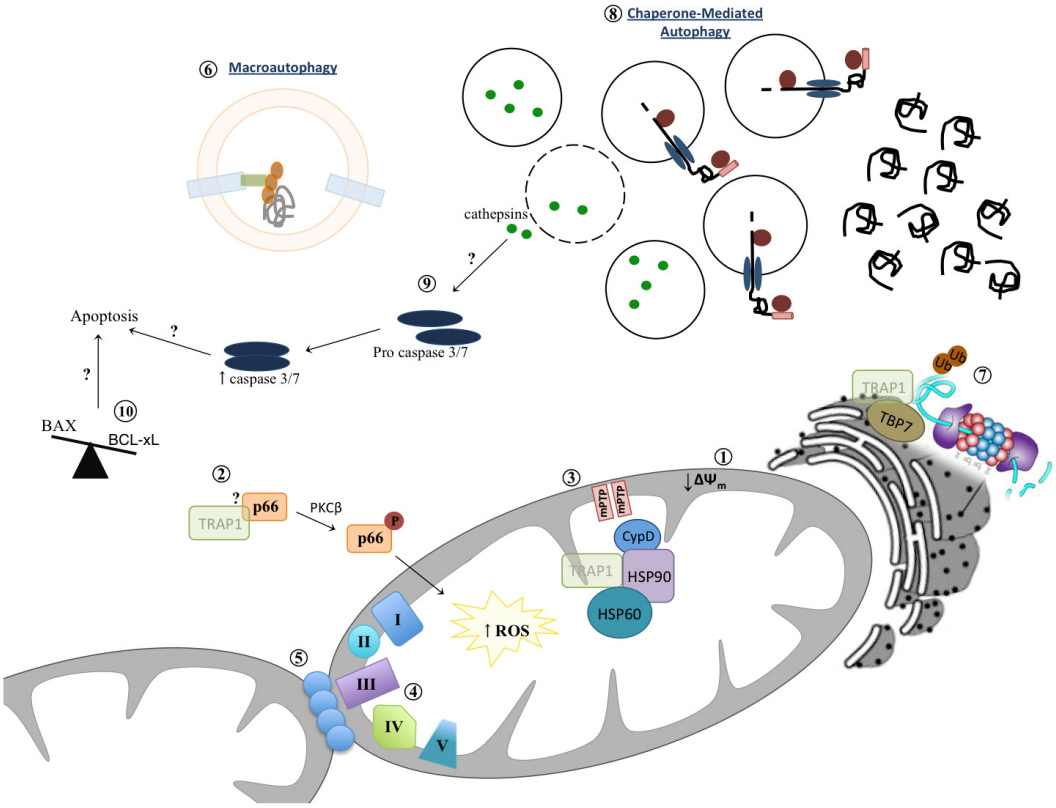

Figure 9.1 - Effects of TRAP1 disruption in A549 cells. TRAP1 silencing (represented in a lighter color) results in mitochondria depolarization (1), and increased ROS production accompanied by increased p66SHC phosphorylation in its Ser36 residue (2). In addition, TRAP1 modulates the mPTP, with its depletion resulting in a more closed mPTP conformation (3). The observed decreased oxygen consumption together with the remaining alterations in mitochondrial function may indicate inhibition of the ETC and/or the phosphorylative system (4). Besides the functional alterations, TRAP1 depletion results in mitochondrial fragmentation (5) resulting from increased DRP1 expression. Although A549 TRAP1-silenced cells experience an accumulation of damaged, fragmented mitochondria, the macroautophagy pathway (represented in a lighter color) levels are decreased (6), which might be explained by the decreased ubiquitin content (7) in these cells. These findings suggest that although TRAP1-depleted cells accumulate intracellular trash, this is not eliminated through autophagy due to the decreased ubiquitination (7). In fact, TRAP1 silencing results in increased lysosomal and LAMP2A content indicating an increase in the CMA pathway (8), probably in an attempt to compensate for the low macroautophagy levels. Eventually, the accumulation of intracellular damage may culminate in cell death. Accordingly, TRAP1 silencing results in increased caspase 3/7-like activity (9) while shifting the BAX/BCL-xL balance towards apoptosis (10). Considering that the increase in caspase 3/7 activity was not accompanied by alterations in any of the analyzed initiator caspases activities, we hypothesize that other mechanisms might be involved in this activation,

namely by the release of lysosomal cathepsins through LMP (illustrated by dashed circle). Abbreviations: BAX - BCL-2 associated X protein; BCL-xL - B-cell lymphoma extra large protein; CMA – chaperone mediated autophagy; CypD – cyclophilin D; DRP1- dynein-related protein 1; ETC – electron transport chain; HSP – heat shock protein; LAMP2A - lysosome-associated membrane protein type 2A; mPTP – mitochondrial permeability transition pore; ROS – reactive oxygen species; TBP7 - Tat-binding protein 7; TRAP1 – tumor necrosis factor receptor associated protein 1.

increased stress resulting from TRAP-1 silencing, although the next exact mechanism of how that occurs is still unknown.

In addition to the observed decrease in $\Delta\Psi_m$ and increased ROS production, our data showed that TRAP1 loss in A549 cells also resulted in decreased oxygen consumption. Together, these results suggest an inhibition of the ETC or upstream metabolite transporters, or even inhibition of the phosphorylative system, although the mitochondrial depolarization associated with TRAP1 silencing suggests that the former two are more likely. In support to this hypothesis, previous works demonstrated that TRAP1 interacts with complex IV of the ETC [503] increasing its activity and thus improving mitochondrial function [444].

Besides maintaining mitochondrial function, TRAP1 was also described to play a role in mitochondrial dynamics [514, 515]. TRAP1 loss in A549 resulted in mitochondrial fragmentation accompanied by an increase in DRP1 expression. Although our results are in accordance with the work of Takamura and collaborators showing that TRAP1 controls mitochondrial fusion/fission balance mainly through the expression of fission proteins, such as DRP1, the authors observed mitochondria elongation [515] rather than fragmentation as we, and Butler and colleagues [514], reported. As discussed in Chapter 8, MRC-5 cells did not show any alterations in mitochondrial function or dynamics upon TRAP1 silencing indicating that in these cells TRAP1 does not play such an important role in mitochondrial maintenance as in A549 cells. Notwithstanding, TRAP1 depletion in MRC-5 cells resulted in decreased levels of autophagy-related proteins, although in a lesser extent than in A549 cells. LC3 is the mammalian homolog of Atg8 in yeast [342]. The 30KDa LC3 protein first undergoes post-translational modifications that culminate with its conversion in the 18KDa cytosolic form LC3-I, which is conjugated to PE through a conjugation process similar to the one occurring to ubiquitin to form the 16KDa LC3-II [518]. LC3 lipidation constitutes an essential step in the autophagy process as LC3-II is recruited to the autophagosomal membranes. Thus, LC3-II is considered a marker for

autophagy and the amount of LC3-II is closely correlated with the number of autophagosomes [332]. Therefore, comparison of the amount of LC3-II has been considered the most accurate method to detect alterations in the autophagic flux [519]. Our results showed a lower LC3-II content in both A549 and MRC-5 cells upon TRAP1 silencing suggesting that cells lacking TRAP1 accumulate less autophagic vesicles containing LC3-II. However, the amount of LC3-II at this specific time point does not implicate a decreased autophagic flux to which the measurement of the amount of p62 may bring more information [519]. The measurement of the p62 levels constitutes another method to evaluate the autophagic flux. Here, we showed that this protein was decreased in both A549 and MRC-5 cells after TRAP1 silencing.

If one analyzes these results independently, the observed overall decrease in the expression of proteins from the autophagic machinery and decreased p62 levels seem to indicate that the cellular quality control systems are working properly and that there is no accumulation of intracellular garbage. However, our results, in particular for A549 cells, showed that TRAP1-depleted cells had less overall ubiquitin content. Therefore, we hypothesize that although there might be an increased damage in these cells, probably due to increased oxidative stress and mitochondrial dysfunction, protein aggregates and defective organelles are not being targeted to autophagy which consequently leads to a reduction in autophagy levels. In support to this hypothesis, we observed increased lysosome content and elevated LAMP2A levels suggesting an increased CMA pathway, which is often activated as a compensatory mechanism upon macroautophagy impairment. Unlike macroautophagy, CMA constitutes a mechanism through which damaged proteins expressing a KFERQ motif are targeted to degradation and thus it is not dependent on protein ubiquitination [367]. Consequently, increased CMA may indicate increased protein damage one which is not solved by the macroautophagy machinery due to decreased protein ubiquitination.

Intriguingly, MRC-5 cells, which also showed decreased p62 expression, did not reveal alterations regarding ubiquitin levels. In MRC-5 cells, TRAP1 depletion seems to have a milder effect on cellular homeostasis suggesting these cells are not as “dependent” on TRAP1 for the maintenance of mitochondrial function and autophagy as A549 cells. Although further studies have to be preformed in order to ascertain the significance of these results, results regarding MRC-5 cells seem to indicate a higher autophagic flux

suggesting that, unlike in A549 cells, TRAP1 does not play a predominant role in homeostasis maintenance in MRC-5 cells.

In addition to decreased autophagy levels, TRAP1-depleted cells showed lower growth rates than the controls. Interestingly, when both cell lines were treated with rapamycin, a mTOR inhibitor used to induce autophagy [539], TRAP1-silenced cells presented higher proliferation rates, whereas inhibition of autophagy with 3-MA had the opposite result. Moreover, A549 control cells showed growth inhibition for both treatments, while MRC-5 cells controls were not widely affected by either rapamycin or 3-MA. Together these findings suggest that TRAP1 role in the maintenance of autophagy levels allows tumor cell homeostasis and thus contributes to tumor growth.

Finally, TRAP1 depletion results in apparent activation of caspase-3 and shifts the BAX/BCL-xL ratio in favor of the apoptotic signal in A549 but not in MRC-5 cells. In conclusion, based on the obtained results, we propose that TRAP1 promotes tumorigenesis by not only maintaining mitochondrial function and integrity, but also allowing the maintenance of constant autophagy levels which are thought to be beneficial for cell growth. Therefore, TRAP1 depletion results in mitochondrial damage, decreased autophagy levels and consequent accumulation of misfolded proteins and damaged organelles, to which cells respond by increasing CMA levels. However, CMA capability is limited and thus when the increased damage is higher than cell buffering ability, there is activation of the apoptotic pathway.

Our work indicates a highly complex and variable role for TRAP1 in neoplastic development, depending on tissue/cell type and reliance on TRAP1. Also important appears to be the localization of TRAP1. Finally, we can hypothesize that the predominant metabolism of the cancer cell itself may also impact how TRAP1 regulates mitochondrial metabolism.

TRAP1-directed therapies may need to have in account several heterogeneity factors which can pre-dispose cells to multiple phenotypes after TRAP1 silencing/inhibition. This can not only compromise the efficacy of anti-cancer therapy directed to that target but also increase damage to healthy cells.

Chapter 10

Future Perspectives

This dissertation has contributed with new insights on the role of TRAP1 in mitochondrial homeostasis providing information regarding its mechanisms of action in two cell lines, one of them with tumoral origin. This study brought new clues for future investigations on this chaperone function as well as its role as an anti-cancer target. Despite this, further work is still required in order to better clarify and complement some of our results.

With the purpose of better understanding the role of p66SHC in the increase in oxidative stress of TRAP1-depleted cells, we plan on investigating whether TRAP1 directly interacts with p66SHC. Moreover, *SHC1* silencing in these cells followed by evaluation of ROS content, specially in TRAP1-silenced cells, will bring valuable information on the relevance of p66SHC function in oxidative stress generation. Therefore, we would expect to observe lower ROS content in double-silenced cells if the massive ROS production was indeed a result of p66SHC activation by TRAP1. In addition, this will allow us to discriminate if ROS increase is responsible for the modulation of mitochondrial morphology and autophagy.

To further explore TRAP1 role in mPTP modulation, we will first verify whether if in A549 cells, similarly to what has been described to other models, TRAP1 interacts with CypD. If so, and considering that TRAP1 function in mPTP has

been attributed to this interaction, it would be interesting to follow CypD expression and content in longer time points, than the ones used in this study after TRAP1 depletion. As described in Chapter 7, higher *PPIF* expression, although not translated in an increment of CypD protein levels was observed. The evaluation of CypD content in a wider time frame can give us valuable information to contrast with previous works [304, 474] and to confirm the hypothesis that TRAP1 modulation of mPTP is due to alterations of CypD content. Alternatively, to evaluate mPTP sensitivity, we will subject the cells to a *calcium-challenging event*, i.e. increasing cytoplasmic calcium concentration by a low ionomycin concentration, in order to promote mitochondrial-calcium accumulation and consequently trigger mPTP. In this assay we will follow mPTP opening in a real-time manner by microplate reader or by confocal microscopy. If TRAP1-depleted cells show a higher sensibility to mPTP opening after this stimulus, we will conclude that, although mPTP is in a more closed conformation under basal conditions, the threshold for its opening is decreased.

Regarding oxygen consumption, further assays need to be performed in order to address the hypothesis of ETC inhibition. First, oxygen consumption levels will be evaluated in intact cells and in the presence of oligomycin (Complex V, i.e. ATP synthase, inhibitor) and FCCP (uncoupler). The different consumption rates will allow discriminating between effects at the ETC level or at the phosphorylative system. Additionally, the assay will be performed with permeabilized cells which although not being a physiologic situation are close to the isolated mitochondrial fractions technique, allowing the incubation with different mitochondrial substrates/inhibitor to pin-point the specific point of TRAP1-deppletion effect. Alternatively, if TRAP1-depleted cells have impaired mitochondria and rely more in glycolysis, growing such cells in galactose-only medium containing pyruvate/glutamine would result in massive cell death or at least arrest of cell cycle. Evaluation of adenine nucleotide levels by HPLC will also indicate the energetic status of these cells and would give a better idea if the impaired mitochondria and possible metabolic shift are still able to provide enough energy for normal cellular physiology.

Since literature is not coherent regarding TRAP1 effects on respiratory complexes it would be interesting to evaluate isolated enzymatic activities for the different ETC enzymes. Moreover, evaluation of the multimeric ETC complexes by blue-native electrophoresis in addition to the same evaluation after immunoprecipitation of TRAP1 will allow proof of concept of TRAP1 interaction and inhibition of ETC enzymes. However, a previous report also stated that differential TRAP1 effects on oxygen consumption are dependent on the expression of c-src [504]. Therefore, it would be interesting to evaluate the content of this protein as well as it activation by Tyr-416 phosphorylation in A549 cells since this information is lacking in the literature.

Lysosomal membrane permeabilization (LMP) results in cathepsin release from the lysosomal lumen to the cytosol [533]. In order to test the hypothesis of cathepsin-dependent caspase 3 activation in TRAP1-depleted cells, we will first evaluate whether in these cells LMP is verified. Accordingly, LMP will be measured through immunofluorescence using acridine orange, which emits red fluorescence when present in lysosomes and loses fluorescence after LMP [540]. The advantage of using this probe instead of lysotracker green is that the latter continues to stain de-acidified lysosomes, while the former allows a better analysis of LMP extent. In addition and to complement this study, we will also use antibodies against cathepsin B and D, and lysosomal membrane proteins, such as LAMP-1, and evaluate the distribution of the proteases in the cell by immunofluorescence. In this case we expect to observe a diffuse cathepsin B or D staining throughout the entire cell suggestive of LMP. Alternatively, proteases activity will be monitored in cytosolic extracts using cathepsin specific substrates.

Although we observed increased caspase 3-like activity for both cell lines and a shift in the BAX/BCL-xL balance in favor of apoptosis in A549 cells, further analysis would allow us to evaluate whether these cells are undergoing apoptotic cell death. An approach to this goal will be achieved by using the dual staining propidium iodide and bromodeoxyuridine to monitor cell death and cell division

[541]. This will allow us to understand if caspase 3 activation culminates with cell death or if TRAP1 depletion just arrests cell cycle.

In Chapter 8, we showed that TRAP1 seems to preferentially locate in extramitochondrial sites in MRC-5 cells. In order to confirm this statement we will proceed to subcellular fractioning namely nuclei, cytoplasm, and mitochondria and evaluate TRAP1 content in each of these extracts. We expect to observe low levels of TRAP1 in the mitochondrial fraction corroborating our initial hypothesis of differential TRAP1 effects due to subcellular localization. If we verify this, it would be interesting to express bioengineered TRAP1 with and without the mitochondrial-targeting sequence in A549 TRAP1-depleted cells. We hypothesize that only TRAP1 present in mitochondria will be able to prevent the traits associated with the chaperone silencing thus demonstrating the importance of TRAP1 compartmentalization in tumor development.

Bibliography

1. Garrison, F.H., *The history of cancer*. Bull N Y Acad Med, 1926. **2**(4): p. 179-85.

2. Hajdu, S.I., *A note from history: landmarks in history of cancer, part 3*. Cancer, 2012. **118**(4): p. 1155-68.

3. Dobson, J., *John Hunter's views on cancer*. Ann R Coll Surg Engl, 1959. **25**: p. 176-81.

4. Robinson, D.H. and A.H. Toledo, *Historical development of modern anesthesia*. J Invest Surg, 2012. **25**(3): p. 141-9.

5. Reese, D.M., *Fundamentals--Rudolf Virchow and modern medicine*. West J Med, 1998. **169**(2): p. 105-8.

6. Brady, L.W., et al., *Innovations in brachytherapy in gynecologic oncology*. Cancer, 1995. **76**(10 Suppl): p. 2143-51.

7. DeVita, V.T., Jr. and E. Chu, *A history of cancer chemotherapy*. Cancer research, 2008. **68**(21): p. 8643-53.

8. Frei, E., 3rd, et al., *A comparative study of two regimens of combination chemotherapy in acute leukemia*. Blood, 1958. **13**(12): p. 1126-48.

9. Huff, J., *Long-term chemical carcinogenesis bioassays predict human cancer hazards. Issues, controversies, and uncertainties*. Ann N Y Acad Sci, 1999. **895**: p. 56-79.

10. Hempelmann, L.H., *Risk of thyroid neoplasms after irradiation in childhood. Studies of populations exposed to radiation in childhood show a dose response over a wide dose range*. Science, 1968. **160**(3824): p. 159-63.

11. Schottenfeld, D. and J.L. Beebe-Dimmer, *Advances in cancer epidemiology: understanding causal mechanisms and the evidence for implementing interventions*. Annu Rev Public Health, 2005. **26**: p. 37-60.

12. Watson, J.D. and F.H. Crick, *Molecular structure of nucleic acids; a structure for deoxyribose nucleic acid*. Nature, 1953. **171**(4356): p. 737-8.

13. Lodish, H., et al., *Proto-Oncogenes and Tumor-Suppressor Genes*, in *Molecular Cell Biology*, H. Lodish, Editor. 2000, W. H. Freeman: New York.

14. Hajdu, S.I., *A note from history: landmarks in history of cancer, part 1*. Cancer, 2011. **117**(5): p. 1097-102.

15. Gallucci, B.B., *Selected concepts of cancer as a disease: from the Greeks to 1900*. Oncol Nurs Forum, 1985. **12**(4): p. 67-71.

16. Javier, R.T. and J.S. Butel, *The history of tumor virology*. Cancer research, 2008. **68**(19): p. 7693-706.

17. Hajdu, S.I., *A note from history: landmarks in history of cancer, part 4*. Cancer, 2012. **118**(20): p. 4914-28.

18. Hajdu, S.I., *A note from history: landmarks in history of cancer, part 2*. Cancer, 2011. **117**(12): p. 2811-20.

19. Rous, P., *A Sarcoma of the Fowl Transmissible by an Agent Separable from the Tumor Cells*. J Exp Med, 1911. **13**(4): p. 397-411.

20. Kew, M.C., *Hepatitis viruses (other than hepatitis B and C viruses) as causes of hepatocellular carcinoma: an update*. J Viral Hepat, 2013. **20**(3): p. 149-57.

21. Joseph, A.W. and G. D'Souza, *Epidemiology of human papillomavirus-related head and neck cancer*. Otolaryngol Clin North Am, 2012. **45**(4): p. 739-64.

22. Warthin, A., *Heredity with reference to carcinoma: As shown by the study of the cases examined in the pathological laboratory of the university of michigan, 1895-1913*. Archives of Internal Medicine, 1913. **XII**(5): p. 546-555.

23. Boyd, J.A. and J.C. Barrett, *Genetic and cellular basis of multistep carcinogenesis*. Pharmacol Ther, 1990. **46**(3): p. 469-86.

24. Futscher, B.W., *Epigenetic changes during cell transformation*. Adv Exp Med Biol, 2013. **754**: p. 179-94.

25. Jones, P.A. and S.B. Baylin, *The fundamental role of epigenetic events in cancer*. Nat Rev Genet, 2002. **3**(6): p. 415-28.

26. Vogelstein, B. and K.W. Kinzler, *Cancer genes and the pathways they control*. Nat Med, 2004. **10**(8): p. 789-99.

27. Osborne, C., P. Wilson, and D. Tripathy, *Oncogenes and tumor suppressor genes in breast cancer: potential diagnostic and therapeutic applications*. Oncologist, 2004. **9**(4): p. 361-77.

28. Bishop, J.M., *The discovery of proto-oncogenes*. The FASEB journal : official publication of the Federation of American Societies for Experimental Biology, 1996. **10**(2): p. 362-4.

29. Huebner, R.J. and G.J. Todaro, *Oncogenes of RNA tumor viruses as determinants of cancer*. Proc Natl Acad Sci U S A, 1969. **64**(3): p. 1087-94.

30. Dehm, S.M. and K. Bonham, *SRC gene expression in human cancer: the role of transcriptional activation*. Biochem Cell Biol, 2004. **82**(2): p. 263-74.

31. Dominguez-Sola, D., et al., *Non-transcriptional control of DNA replication by c-Myc*. Nature, 2007. **448**(7152): p. 445-51.

32. Shortt, J. and R.W. Johnstone, *Oncogenes in cell survival and cell death*. Cold Spring Harb Perspect Biol, 2012. **4**(12).

33. Barrett, J.C., M. Oshimura, and M. Koi, *Role of oncogenes and tumor suppressor genes in a multistep model of carcinogenesis*. Symp Fundam Cancer Res, 1986. **39**: p. 45-56.

34. Oliveira, A.M., J.S. Ross, and J.A. Fletcher, *Tumor suppressor genes in breast cancer: the gatekeepers and the caretakers*. Am J Clin Pathol, 2005. **124 Suppl**: p. S16-28.

35. Levitt, N.C. and I.D. Hickson, *Caretaker tumour suppressor genes that defend genome integrity*. Trends Mol Med, 2002. **8**(4): p. 179-86.

36. Weston, A. and C. Harris, *Gene-Environment Interactions and Interindividual Variation*, in *Holland-Frei Cancer Medicine*, D. Kufe, et al., Editors. 2003, BC Decker: Hamilton, Ontario.

37. Murphree, A.L. and W.F. Benedict, *Retinoblastoma: clues to human oncogenesis*. Science, 1984. **223**(4640): p. 1028-33.

38. Cooper, G., *Tumor Suppressor Genes*, in *The Cell: A Molecular Approach*. 2000, Sinauer Associates: Sunderland, Massachusetts.

39. Wiman, K.G., *The retinoblastoma gene: role in cell cycle control and cell differentiation*. The FASEB journal : official publication of the Federation of American Societies for Experimental Biology, 1993. **7**(10): p. 841-5.

40. Stiewe, T., *The p53 family in differentiation and tumorigenesis*. Nature reviews. Cancer, 2007. **7**(3): p. 165-8.

41. Weinberg, R.A., *The Biology of Cancer*. 2013: Taylor & Francis Group.

42. Walsh, P.C., *Heterogeneity of genetic alterations in prostate cancer: evidence of the complex nature of the disease*. J Urol, 2002. **168**(4 Pt 1): p. 1635-6.

43. Brinton, L.A., et al., *Etiologic heterogeneity in endometrial cancer: evidence from a Gynecologic Oncology Group trial*. Gynecol Oncol, 2013. **129**(2): p. 277-84.

44. Hanahan, D. and R.A. Weinberg, *The hallmarks of cancer*. Cell, 2000. **100**(1): p. 57-70.

45. Hanahan, D. and R.A. Weinberg, *Hallmarks of cancer: the next generation*. Cell, 2011. **144**(5): p. 646-74.

46. Whiteside, T.L., *The tumor microenvironment and its role in promoting tumor growth*. Oncogene, 2008. **27**(45): p. 5904-12.

47. Theodorescu, D., *Cancer cryotherapy: evolution and biology*. Rev Urol, 2004. **6 Suppl 4**: p. S9-S19.

48. Moore, E.J. and M.L. Hinni, *Critical review: transoral laser microsurgery and robotic-assisted surgery for oropharynx cancer including human papillomavirus-related cancer*. Int J Radiat Oncol Biol Phys, 2013. **85**(5): p. 1163-7.

49. Porres, D., D. Pfister, and A. Heidenreich, *Minimally invasive treatment for localized prostate cancer*. Minerva Urol Nefrol, 2012. **64**(4): p. 245-53.

50. Strijker, M., et al., *Robot-assisted pancreatic surgery: a systematic review of the literature*. HPB (Oxford), 2013. **15**(1): p. 1-10.

51. Tait, D.M. and A.E. Nahum, *Conformal therapy*. Eur J Cancer, 1990. **26**(6): p. 750-3.

52. Onishi, H. and T. Araki, *Stereotactic body radiation therapy for stage I non-small-cell lung cancer: a historical overview of clinical studies*. Jpn J Clin Oncol, 2013. **43**(4): p. 345-50.

53. Ahmad, S.S., et al., *Advances in radiotherapy*. BMJ, 2012. **345**: p. e7765.

54. Firer, M.A. and G. Gellerman, *Targeted drug delivery for cancer therapy: the other side of antibodies*. J Hematol Oncol, 2012. **5**: p. 70.

55. Kumar, P., A. Gulbake, and S.K. Jain, *Liposomes a vesicular nanocarrier: potential advancements in cancer chemotherapy*. Crit Rev Ther Drug Carrier Syst, 2012. **29**(5): p. 355-419.

56. Sinha, R., et al., *Nanotechnology in cancer therapeutics: bioconjugated nanoparticles for drug delivery*. Mol Cancer Ther, 2006. **5**(8): p. 1909-17.

57. Wang, M.D., et al., *Nanotechnology for targeted cancer therapy*. Expert Rev Anticancer Ther, 2007. **7**(6): p. 833-7.

58. Stockwell, S., *Classics in oncology. George Thomas Beatson, M.D. (1848-1933)*. CA Cancer J Clin, 1983. **33**(2): p. 105-21.

59. Machtens, S., et al., *The history of endocrine therapy of benign and malignant diseases of the prostate*. World J Urol, 2000. **18**(3): p. 222-6.

60. Arya, M., et al., *Hormone therapy: a revolution in understanding prostate cancer*. Lancet Oncol, 2008. **9**(11): p. 1112.

61. Cakmak, H. and M.P. Rosen, *Ovarian stimulation in cancer patients*. Fertil Steril, 2013. **99**(6): p. 1476-84.

62. Waldmann, T.A., *Immunotherapy: past, present and future*. Nat Med, 2003. **9**(3): p. 269-77.

63. Awada, A. and P.G. Aftimos, *Targeted therapies of solid cancers: new options, new challenges*. Curr Opin Oncol, 2013. **25**(3): p. 296-304.

64. Li, J., et al., *A review on various targeted anticancer therapies*. Target Oncol, 2012. **7**(1): p. 69-85.

65. Soerjomataram, I., et al., *Global burden of cancer in 2008: a systematic analysis of disability-adjusted life-years in 12 world regions*. Lancet, 2012. **380**(9856): p. 1840-50.

66. Jemal, A., et al., *Global cancer statistics*. CA Cancer J Clin, 2011. **61**(2): p. 69-90.

67. Bray, F., et al., *Global cancer transitions according to the Human Development Index (2008-2030): a population-based study*. Lancet Oncol, 2012. **13**(8): p. 790-801.

68. Ferlay, J., et al., *Estimates of worldwide burden of cancer in 2008: GLOBOCAN 2008*. Int J Cancer, 2010. **127**(12): p. 2893-917.

69. Ezzati, M., et al., *Role of smoking in global and regional cancer epidemiology: current patterns and data needs*. Int J Cancer, 2005. **116**(6): p. 963-71.

70. Ferlay, J., et al., *GLOBOCAN 2008 v2.0, Cancer Incidence and Mortality Worldwide*. 2010, International Agency for Research on Cancer: Lyon, France.

71. de Martel, C., et al., *Global burden of cancers attributable to infections in 2008: a review and synthetic analysis*. Lancet Oncol, 2012. **13**(6): p. 607-15.

72. Mackay, J., M.P. Eriksen, and O. Shafey, *The tobacco atlas*. 2nd ed. 2006, Atlanta, Georgia: American Cancer Society.

73. Youlden, D.R., S.M. Cramb, and P.D. Baade, *The International Epidemiology of Lung Cancer: geographical distribution and secular trends*. J Thorac Oncol, 2008. **3**(8): p. 819-31.

74. Pfeifer, G.P., et al., *Tobacco smoke carcinogens, DNA damage and p53 mutations in smoking-associated cancers*. Oncogene, 2002. **21**(48): p. 7435-51.

75. Cogliano, V.J., et al., *Preventable exposures associated with human cancers*. J Natl Cancer Inst, 2011. **103**(24): p. 1827-39.

76. Cote, M.L., et al., *Increased risk of lung cancer in individuals with a family history of the disease: a pooled analysis from the International Lung Cancer Consortium*. Eur J Cancer, 2012. **48**(13): p. 1957-68.

77. Jadus, M.R., et al., *Lung cancer: a classic example of tumor escape and progression while providing opportunities for immunological intervention*. Clin Dev Immunol, 2012. **2012**: p. 160724.

78. Weinberg, F. and N.S. Chandel, *Mitochondrial metabolism and cancer*. Ann N Y Acad Sci, 2009. **1177**: p. 66-73.

79. Mates, J.M., et al., *Glutamine homeostasis and mitochondrial dynamics*. Int J Biochem Cell Biol, 2009. **41**(10): p. 2051-61.

80. Cairns, R.A., I.S. Harris, and T.W. Mak, *Regulation of cancer cell metabolism*. Nature reviews. Cancer, 2011. **11**(2): p. 85-95.

81. Warburg, O., *On the origin of cancer cells*. Science, 1956. **123**(3191): p. 309-14.

82. Lopez-Lazaro, M., *The warburg effect: why and how do cancer cells activate glycolysis in the presence of oxygen?* Anticancer Agents Med Chem, 2008. **8**(3): p. 305-12.

83. Frezza, C. and E. Gottlieb, *Mitochondria in cancer: not just innocent bystanders*. Semin Cancer Biol, 2009. **19**(1): p. 4-11.

84. Vander Heiden, M.G., L.C. Cantley, and C.B. Thompson, *Understanding the Warburg effect: the metabolic requirements of cell proliferation*. Science, 2009. **324**(5930): p. 1029-33.

85. Varum, S., et al., *Energy metabolism in human pluripotent stem cells and their differentiated counterparts*. PLoS One, 2011. **6**(6): p. e20914.

86. Ganapathy, V., M. Thangaraju, and P.D. Prasad, *Nutrient transporters in cancer: relevance to Warburg hypothesis and beyond*. Pharmacol Ther, 2009. **121**(1): p. 29-40.

87. Mathupala, S.P., Y.H. Ko, and P.L. Pedersen, *Hexokinase-2 bound to mitochondria: cancer's stygian link to the "Warburg Effect" and a pivotal target for effective therapy*. Semin Cancer Biol, 2009. **19**(1): p. 17-24.

88. Christofk, H.R., et al., *The M2 splice isoform of pyruvate kinase is important for cancer metabolism and tumour growth*. Nature, 2008. **452**(7184): p. 230-3.

89. Fantin, V.R., J. St-Pierre, and P. Leder, *Attenuation of LDH-A expression uncovers a link between glycolysis, mitochondrial physiology, and tumor maintenance*. Cancer Cell, 2006. **9**(6): p. 425-34.

90. Mazurek, S., et al., *Pyruvate kinase type M2 and its role in tumor growth and spreading*. Seminars in cancer biology, 2005. **15**(4): p. 300-8.

91. Robey, I.F., et al., *Bicarbonate increases tumor pH and inhibits spontaneous metastases*. Cancer research, 2009. **69**(6): p. 2260-8.

92. Stern, R., et al., *Lactate stimulates fibroblast expression of hyaluronan and CD44: the Warburg effect revisited*. Exp Cell Res, 2002. **276**(1): p. 24-31.

93. Rofstad, E.K., et al., *Acidic extracellular pH promotes experimental metastasis of human melanoma cells in athymic nude mice*. Cancer research, 2006. **66**(13): p. 6699-707.

94. Ramos-Montoya, A., et al., *Pentose phosphate cycle oxidative and nonoxidative balance: A new vulnerable target for overcoming drug resistance in cancer*. Int J Cancer, 2006. **119**(12): p. 2733-41.

95. Levine, A.J. and A.M. Puzio-Kuter, *The control of the metabolic switch in cancers by oncogenes and tumor suppressor genes*. Science, 2010. **330**(6009): p. 1340-4.

96. Wang, Z., et al., *Exon-centric regulation of pyruvate kinase M alternative splicing via mutually exclusive exons*. J Mol Cell Biol, 2012.

97. Hitosugi, T., et al., *Tyrosine phosphorylation inhibits PKM2 to promote the Warburg effect and tumor growth*. Sci Signal, 2009. **2**(97): p. ra73.

98. Rossignol, R., et al., *Energy substrate modulates mitochondrial structure and oxidative capacity in cancer cells*. Cancer research, 2004. **64**(3): p. 985-93.

99. DeBerardinis, R.J., et al., *The biology of cancer: metabolic reprogramming fuels cell growth and proliferation*. Cell Metab, 2008. **7**(1): p. 11-20.

100. Weinberg, F., et al., *Mitochondrial metabolism and ROS generation are essential for Kras-mediated tumorigenicity*. Proc Natl Acad Sci U S A, 2010. **107**(19): p. 8788-93.

101. Chiavarina, B., et al., *HIF1-alpha functions as a tumor promoter in cancer associated fibroblasts, and as a tumor suppressor in breast cancer cells: Autophagy drives compartment-specific oncogenesis*. Cell Cycle, 2010. **9**(17): p. 3534-51.

102. Denko, N.C., *Hypoxia, HIF1 and glucose metabolism in the solid tumour*. Nature reviews. Cancer, 2008. **8**(9): p. 705-13.

103. Mills, C.N., S.S. Joshi, and R.M. Niles, *Expression and function of hypoxia inducible factor-1 alpha in human melanoma under non-hypoxic conditions*. Mol Cancer, 2009. **8**: p. 104.

104. Gao, P., et al., *c-Myc suppression of miR-23a/b enhances mitochondrial glutaminase expression and glutamine metabolism*. Nature, 2009. **458**(7239): p. 762-5.

105. Shackelford, D.B. and R.J. Shaw, *The LKB1-AMPK pathway: metabolism and growth control in tumour suppression*. Nature reviews. Cancer, 2009. **9**(8): p. 563-75.

106. Bonuccelli, G., et al., *Ketones and lactate "fuel" tumor growth and metastasis: Evidence that epithelial cancer cells use oxidative mitochondrial metabolism*. Cell Cycle, 2010. **9**(17): p. 3506-14.

107. Bonuccelli, G., et al., *The reverse Warburg effect: glycolysis inhibitors prevent the tumor promoting effects of caveolin-1 deficient cancer associated fibroblasts*. Cell Cycle, 2010. **9**(10): p. 1960-71.

108. Pavlides, S., et al., *The reverse Warburg effect: aerobic glycolysis in cancer associated fibroblasts and the tumor stroma*. Cell Cycle, 2009. **8**(23): p. 3984-4001.

109. Gottlieb, E. and I.P. Tomlinson, *Mitochondrial tumour suppressors: a genetic and biochemical update*. Nature reviews. Cancer, 2005. **5**(11): p. 857-66.

110. King, A., M.A. Selak, and E. Gottlieb, *Succinate dehydrogenase and fumarate hydratase: linking mitochondrial dysfunction and cancer*. Oncogene, 2006. **25**(34): p. 4675-82.

111. Alam, N.A., S. Olpin, and I.M. Leigh, *Fumarate hydratase mutations and predisposition to cutaneous leiomyomas, uterine leiomyomas and renal cancer*. Br J Dermatol, 2005. **153**(1): p. 11-7.

112. Hensen, E.F. and J.P. Bayley, *Recent advances in the genetics of SDH-related paraganglioma and pheochromocytoma*. Fam Cancer, 2010. **10**(2): p. 355-63.

113. Altenberg, B. and K.O. Greulich, *Genes of glycolysis are ubiquitously overexpressed in 24 cancer classes*. Genomics, 2004. **84**(6): p. 1014-20.

114. Zhang, E., et al., *Newly developed strategies for multifunctional mitochondria-targeted agents in cancer therapy*. Drug discovery today, 2010.

115. Dell'Antone, P., *Targets of 3-bromopyruvate, a new, energy depleting, anticancer agent*. Medicinal chemistry, 2009. **5**(6): p. 491-6.

116. Gleiss, B., et al., *Fas-triggered phosphatidylserine exposure is modulated by intracellular ATP*. FEBS letters, 2002. **519**(1-3): p. 153-8.

117. Lynch, R.M., K.E. Fogarty, and F.S. Fay, *Modulation of hexokinase association with mitochondria analyzed with quantitative three-dimensional confocal microscopy*. J Cell Biol, 1991. **112**(3): p. 385-95.

118. Maschek, G., et al., *2-deoxy-D-glucose increases the efficacy of adriamycin and paclitaxel in human osteosarcoma and non-small cell lung cancers in vivo*. Cancer research, 2004. **64**(1): p. 31-4.

119. Egler, V., et al., *Histone deacetylase inhibition and blockade of the glycolytic pathway synergistically induce glioblastoma cell death*. Clin Cancer Res, 2008. **14**(10): p. 3132-40.

120. Xu, R.H., et al., *Synergistic effect of targeting mTOR by rapamycin and depleting ATP by inhibition of glycolysis in lymphoma and leukemia cells*. Leukemia, 2005. **19**(12): p. 2153-8.

121. Mathupala, S.P., Y.H. Ko, and P.L. Pedersen, *Hexokinase II: cancer's double-edged sword acting as both facilitator and gatekeeper of malignancy when bound to mitochondria*. Oncogene, 2006. **25**(34): p. 4777-86.

122. Floridi, A., et al., *Lonidamine, a selective inhibitor of aerobic glycolysis of murine tumor cells*. J Natl Cancer Inst, 1981. **66**(3): p. 497-9.

123. Fulda, S., L. Galluzzi, and G. Kroemer, *Targeting mitochondria for cancer therapy*. Nature reviews. Drug discovery, 2010. **9**(6): p. 447-64.

124. Pratesi, G., M. De Cesare, and F. Zunino, *Efficacy of lonidamine combined with different DNA-damaging agents in the treatment of the MX-1 tumor xenograft*. Cancer chemotherapy and pharmacology, 1996. **38**(2): p. 123-8.

125. Price, G.S., et al., *Pharmacokinetics and toxicity of oral and intravenous lonidamine in dogs*. Cancer Chemother Pharmacol, 1996. **38**(2): p. 129-35.

126. Di Cosimo, S., et al., *Lonidamine: efficacy and safety in clinical trials for the treatment of solid tumors*. Drugs Today (Barc), 2003. **39**(3): p. 157-74.

127. Mansi, J.L., et al., *A phase II clinical and pharmacokinetic study of Lonidamine in patients with advanced breast cancer*. Br J Cancer, 1991. **64**(3): p. 593-7.

128. Michelakis, E.D., L. Webster, and J.R. Mackey, *Dichloroacetate (DCA) as a potential metabolic-targeting therapy for cancer*. British journal of cancer, 2008. **99**(7): p. 989-94.

129. Xiao, L., et al., *Dichloroacetate (DCA) enhances tumor cell death in combination with oncolytic adenovirus armed with MDA-7/IL-24*. Molecular and cellular biochemistry, 2010. **340**(1-2): p. 31-40.

130. Harrison, M.R., et al., *A phase II study of 2-methoxyestradiol (2ME2) NanoCrystal(R) dispersion (NCD) in patients with taxane-refractory, metastatic castrate-resistant prostate cancer (CRPC)*. Invest New Drugs, 2011. **29**(6): p. 1465-74.

131. Kashtan, H., et al., *Photodynamic therapy of cancer of the esophagus using systemic aminolevulinic acid and a non laser light source: a phase I/II study*. Gastrointest Endosc, 1999. **49**(6): p. 760-4.

132. Rudin, C.M., et al., *Phase II study of single-agent navitoclax (ABT-263) and biomarker correlates in patients with relapsed small cell lung cancer*. Clin Cancer Res, 2012. **18**(11): p. 3163-9.

133. Mason, K.D., et al., *In vivo efficacy of the Bcl-2 antagonist ABT-737 against aggressive Myc-driven lymphomas*. Proc Natl Acad Sci U S A, 2008. **105**(46): p. 17961-6.

134. Wolvetang, E.J., et al., *Mitochondrial respiratory chain inhibitors induce apoptosis*. FEBS letters, 1994. **339**(1-2): p. 40-4.

135. Powell, B.L., et al., *Arsenic trioxide improves event-free and overall survival for adults with acute promyelocytic leukemia: North American Leukemia Intergroup Study C9710*. Blood, 2010. **116**(19): p. 3751-7.

136. Wu, K., et al., *Berberine inhibits the proliferation of colon cancer cells by inactivating Wnt/beta-catenin signaling*. Int J Oncol, 2012. **41**(1): p. 292-8.

137. Palmeira, C.M. and K.B. Wallace, *Benzoquinone inhibits the voltage-dependent induction of the mitochondrial permeability transition caused by redox-cycling naphthoquinones*. Toxicology and applied pharmacology, 1997. **143**(2): p. 338-47.

138. Holschneider, C.H., et al., *Bullatacin--in vivo and in vitro experience in an ovarian cancer model*. Cancer chemotherapy and pharmacology, 1994. **34**(2): p. 166-70.

139. Chang, G.C., et al., *Comparative effectiveness of bevacizumab plus cisplatin-based chemotherapy versus pemetrexed plus cisplatin treatment in East Asian non-squamous non-small cell lung cancer patients applying real-life outcomes*. Asia Pac J Clin Oncol, 2011. **7 Suppl 2**: p. 34-40.

140. Carroll, R.E., et al., *Phase IIa clinical trial of curcumin for the prevention of colorectal neoplasia*. Cancer Prev Res (Phila), 2011. **4**(3): p. 354-64.

141. Lifson, J.D., et al., *Evaluation of the safety, immunogenicity, and protective efficacy of whole inactivated simian immunodeficiency virus (SIV) vaccines with conformationally and functionally intact envelope glycoproteins*. AIDS Res Hum Retroviruses, 2004. **20**(7): p. 772-87.

142. Oliveira, P.J. and K.B. Wallace, *Depletion of adenine nucleotide translocator protein in heart mitochondria from doxorubicin-treated rats--relevance for mitochondrial dysfunction*. Toxicology, 2006. **220**(2-3): p. 160-8.

143. Yang, G., et al., *Green tea consumption and colorectal cancer risk: a report from the Shanghai Men's Health Study*. Carcinogenesis, 2011. **32**(11): p. 1684-8.

144. Zheng, J., et al., *Green tea and black tea consumption and prostate cancer risk: an exploratory meta-analysis of observational studies*. Nutr Cancer, 2011. **63**(5): p. 663-72.

145. Fantin, V.R., et al., *A novel mitochondriotoxic small molecule that selectively inhibits tumor cell growth*. Cancer Cell, 2002. **2**(1): p. 29-42.

146. Shoukrun, R., et al., *The 18-kDa translocator protein, formerly known as the peripheral-type benzodiazepine receptor, confers proapoptotic and antineoplastic effects in a human colorectal cancer cell line*. Pharmacogenet Genomics, 2008. **18**(11): p. 977-88.

147. Van Poznak, C., et al., *Oral gossypol in the treatment of patients with refractory metastatic breast cancer: a phase I/II clinical trial*. Breast Cancer Res Treat, 2001. **66**(3): p. 239-48.

148. Simonin, K., et al., *Mcl-1 is an important determinant of the apoptotic response to the BH3-mimetic molecule HA14-1 in cisplatin-resistant ovarian carcinoma cells*. Mol Cancer Ther, 2009. **8**(11): p. 3162-70.

149. Tetef, M., et al., *Mitomycin C and menadione for the treatment of advanced gastrointestinal cancers: a phase II trial*. J Cancer Res Clin Oncol, 1995. **121**(2): p. 103-6.

150. Goodwin, P.J., et al., *Insulin-lowering effects of metformin in women with early breast cancer*. Clin Breast Cancer, 2008. **8**(6): p. 501-5.

151. Britten, C.D., et al., *A phase I and pharmacokinetic study of the mitochondrial-specific rhodacyanine dye analog MKT 077.* Clin Cancer Res, 2000. **6**(1): p. 42-9.

152. Mehta, M.P., et al., *Motexafin gadolinium combined with prompt whole brain radiotherapy prolongs time to neurologic progression in non-small-cell lung cancer patients with brain metastases: results of a phase III trial.* Int J Radiat Oncol Biol Phys, 2009. **73**(4): p. 1069-76.

153. Parikh, S.A., et al., *Phase II study of obatoclax mesylate (GX15-070), a small-molecule BCL-2 family antagonist, for patients with myelofibrosis.* Clin Lymphoma Myeloma Leuk, 2010. **10**(4): p. 285-9.

154. Chen, G., et al., *Preferential killing of cancer cells with mitochondrial dysfunction by natural compounds.* Mitochondrion, 2010. **10**(6): p. 614-25.

155. Wu, C.H., et al., *In vitro and in vivo study of phloretin-induced apoptosis in human liver cancer cells involving inhibition of type II glucose transporter.* Int J Cancer, 2009. **124**(9): p. 2210-9.

156. Wyatt, S.K., et al., *Preclinical molecular imaging of the translocator protein (TSPO) in a metastases model based on breast cancer xenografts propagated in the murine brain.* Current molecular medicine, 2012. **12**(4): p. 458-66.

157. Patel, K.R., et al., *Clinical trials of resveratrol.* Ann N Y Acad Sci, 2011. **1215**: p. 161-9.

158. Lampidis, T.J., et al., *Selective toxicity of rhodamine 123 in carcinoma cells in vitro.* Cancer research, 1983. **43**(2): p. 716-20.

159. Decaudin, D., et al., *Peripheral benzodiazepine receptor ligands reverse apoptosis resistance of cancer cells in vitro and in vivo.* Cancer research, 2002. **62**(5): p. 1388-93.

160. Gonzalez-Coloma, A., et al., *Selective action of acetogenin mitochondrial complex I inhibitors.* Z Naturforsch C, 2002. **57**(11-12): p. 1028-34.

161. Chen, Y., et al., *Mitochondrial electron-transport-chain inhibitors of complexes I and II induce autophagic cell death mediated by reactive oxygen species.* J Cell Sci, 2007. **120**(Pt 23): p. 4155-66.

162. Barreto, M.C., et al., *Inhibition of mouse liver respiration by Chelidonium majus isoquinoline alkaloids.* Toxicology letters, 2003. **146**(1): p. 37-47.

163. Byun, H.O., et al., *Mitochondrial dysfunction by complex II inhibition delays overall cell cycle progression via reactive oxygen species production.* J Cell Biochem, 2008. **104**(5): p. 1747-59.

164. Skildum, A., K. Dornfeld, and K. Wallace, *Mitochondrial amplification selectively increases doxorubicin sensitivity in breast cancer cells with acquired antiestrogen resistance.* Breast Cancer Res Treat, 2010.

165. Fang, J., H. Nakamura, and A.K. Iyer, *Tumor-targeted induction of oxystress for cancer therapy.* Journal of drug targeting, 2007. **15**(7-8): p. 475-86.

166. Neuzil, J., et al., *Mitocans as anti-cancer agents targeting mitochondria: lessons from studies with vitamin E analogues, inhibitors of complex II.* Journal of bioenergetics and biomembranes, 2007. **39**(1): p. 65-72.

167. Bey, E.A., et al., *An NQO1- and PARP-1-mediated cell death pathway induced in non-small-cell lung cancer cells by beta-lapachone*. Proceedings of the National Academy of Sciences of the United States of America, 2007. **104**(28): p. 11832-7.

168. Stockwin, L.H., et al., *Sodium dichloroacetate selectively targets cells with defects in the mitochondrial ETC*. Int J Cancer, 2010. **127**(11): p. 2510-9.

169. Heshe, D., et al., *Dichloroacetate metabolically targeted therapy defeats cytotoxicity of standard anticancer drugs*. Cancer Chemother Pharmacol, 2010.

170. Cao, X., et al., *Glucose uptake inhibitor sensitizes cancer cells to daunorubicin and overcomes drug resistance in hypoxia*. Cancer chemotherapy and pharmacology, 2007. **59**(4): p. 495-505.

171. Finkel, T., *Signal transduction by reactive oxygen species*. J Cell Biol, 2011. **194**(1): p. 7-15.

172. Rigoulet, M., E.D. Yoboue, and A. Devin, *Mitochondrial ROS generation and its regulation: mechanisms involved in H(2)O(2) signaling*. Antioxid Redox Signal, 2010. **14**(3): p. 459-68.

173. Le Bras, M., et al., *Reactive oxygen species and the mitochondrial signaling pathway of cell death*. Histol Histopathol, 2005. **20**(1): p. 205-19.

174. Starkov, A.A., *The role of mitochondria in reactive oxygen species metabolism and signaling*. Ann N Y Acad Sci, 2008. **1147**: p. 37-52.

175. Handy, D.E. and J. Loscalzo, *Redox Regulation of Mitochondrial Function*. Antioxid Redox Signal, 2012.

176. Circu, M.L. and T.Y. Aw, *Reactive oxygen species, cellular redox systems, and apoptosis*. Free Radic Biol Med, 2010. **48**(6): p. 749-62.

177. Grek, C.L. and K.D. Tew, *Redox metabolism and malignancy*. Curr Opin Pharmacol, 2010. **10**(4): p. 362-8.

178. Kryston, T.B., et al., *Role of oxidative stress and DNA damage in human carcinogenesis*. Mutat Res, 2011. **711**(1-2): p. 193-201.

179. Poyton, R.O., K.A. Ball, and P.R. Castello, *Mitochondrial generation of free radicals and hypoxic signaling*. Trends in endocrinology and metabolism: TEM, 2009. **20**(7): p. 332-40.

180. Bell, E.L., T. Klimova, and N.S. Chandel, *Targeting the mitochondria for cancer therapy: regulation of hypoxia-inducible factor by mitochondria*. Antioxidants & redox signaling, 2008. **10**(3): p. 635-40.

181. Verschoor, M.L., L.A. Wilson, and G. Singh, *Mechanisms associated with mitochondrial-generated reactive oxygen species in cancer*. Canadian journal of physiology and pharmacology, 2010. **88**(3): p. 204-19.

182. Veeramani, S., et al., *Mitochondrial redox signaling by p66Shc is involved in regulating androgenic growth stimulation of human prostate cancer cells*. Oncogene, 2008. **27**(37): p. 5057-68.

183. Giorgio, M., et al., *Electron transfer between cytochrome c and p66Shc generates reactive oxygen species that trigger mitochondrial apoptosis*. Cell, 2005. **122**(2): p. 221-33.

184. Pani, G., O.R. Koch, and T. Galeotti, *The p53-p66shc-Manganese Superoxide Dismutase (MnSOD) network: a mitochondrial intrigue to generate reactive oxygen species*. Int J Biochem Cell Biol, 2009. **41**(5): p. 1002-5.

185. Trinei, M., et al., *A p53-p66Shc signalling pathway controls intracellular redox status, levels of oxidation-damaged DNA and oxidative stress-induced apoptosis*. Oncogene, 2002. **21**(24): p. 3872-8.

186. Huang, Y., et al., *Transcriptional inhibition of manganese superoxide dismutase (SOD2) gene expression by DNA methylation of the 5' CpG island*. Free Radic Biol Med, 1997. **23**(2): p. 314-20.

187. Behrend, L., G. Henderson, and R.M. Zwacka, *Reactive oxygen species in oncogenic transformation*. Biochem Soc Trans, 2003. **31**(Pt 6): p. 1441-4.

188. Oberley, L.W. and T.D. Oberley, *Role of antioxidant enzymes in cell immortalization and transformation*. Mol Cell Biochem, 1988. **84**(2): p. 147-53.

189. Jung, K., et al., *Antioxidant enzymes in malignant prostate cell lines and in primary cultured prostatic cells*. Free Radic Biol Med, 1997. **23**(1): p. 127-33.

190. Preuss, M., et al., *Role of antioxidant enzyme expression in the selective cytotoxic response of glioma cells to gamma-linolenic acid supplementation*. Free Radic Biol Med, 2000. **28**(7): p. 1143-56.

191. Slane, B.G., et al., *Mutation of succinate dehydrogenase subunit C results in increased O2.-, oxidative stress, and genomic instability*. Cancer research, 2006. **66**(15): p. 7615-20.

192. Ahmad, I.M., et al., *Mitochondrial O2*- and H2O2 mediate glucose deprivation-induced stress in human cancer cells*. J Biol Chem, 2005. **280**(6): p. 4254-63.

193. Vandy, F.C., G. Sisk, and R. Berguer, *Synchronous carotid body and thoracic paraganglioma associated with a germline SDHC mutation*. J Vasc Surg, 2011. **53**(3): p. 805-7.

194. Pani, G., T. Galeotti, and P. Chiarugi, *Metastasis: cancer cell's escape from oxidative stress*. Cancer Metastasis Rev, 2010. **29**(2): p. 351-78.

195. Xia, C., et al., *Reactive oxygen species regulate angiogenesis and tumor growth through vascular endothelial growth factor*. Cancer research, 2007. **67**(22): p. 10823-30.

196. Chou, W.C., et al., *Role of NADPH oxidase in arsenic-induced reactive oxygen species formation and cytotoxicity in myeloid leukemia cells*. Proc Natl Acad Sci U S A, 2004. **101**(13): p. 4578-83.

197. Jin, Z., et al., *Deficient tumor necrosis factor-related apoptosis-inducing ligand (TRAIL) death receptor transport to the cell surface in human colon cancer cells selected for resistance to TRAIL-induced apoptosis*. The Journal of biological chemistry, 2004. **279**(34): p. 35829-39.

198. Lin, T.S., et al., *Effects of motexafin gadolinium in a phase II trial in refractory chronic lymphocytic leukemia*. Leuk Lymphoma, 2009. **50**(12): p. 1977-82.

199. Yu, W., B.G. Sanders, and K. Kline, *RRR-alpha-tocopheryl succinate-induced apoptosis of human breast cancer cells involves Bax translocation to mitochondria*. Cancer research, 2003. **63**(10): p. 2483-91.

200. Fariss, M.W., et al., *The selective antiproliferative effects of alpha-tocopheryl hemisuccinate and cholesteryl hemisuccinate on murine leukemia cells result from the action of the intact compounds*. Cancer research, 1994. **54**(13): p. 3346-51.

201. Weber, T., et al., *Vitamin E succinate is a potent novel antineoplastic agent with high selectivity and cooperativity with tumor necrosis factor-related apoptosis-inducing ligand (Apo2 ligand) in vivo*. Clin Cancer Res, 2002. **8**(3): p. 863-9.

202. Pelicano, H., et al., *Inhibition of mitochondrial respiration: a novel strategy to enhance drug-induced apoptosis in human leukemia cells by a reactive oxygen species-mediated mechanism*. The Journal of biological chemistry, 2003. **278**(39): p. 37832-9.

203. Grad, J.M., et al., *Ascorbic acid enhances arsenic trioxide-induced cytotoxicity in multiple myeloma cells*. Blood, 2001. **98**(3): p. 805-13.

204. Miller, W.H., Jr., et al., *Mechanisms of action of arsenic trioxide*. Cancer research, 2002. **62**(14): p. 3893-903.

205. Dai, J., et al., *Malignant cells can be sensitized to undergo growth inhibition and apoptosis by arsenic trioxide through modulation of the glutathione redox system*. Blood, 1999. **93**(1): p. 268-77.

206. Mathews, V., et al., *Single-agent arsenic trioxide in the treatment of newly diagnosed acute promyelocytic leukemia: long-term follow-up data*. J Clin Oncol, 2010. **28**(24): p. 3866-71.

207. Xiao, D., et al., *Phenethyl isothiocyanate-induced apoptosis in PC-3 human prostate cancer cells is mediated by reactive oxygen species-dependent disruption of the mitochondrial membrane potential*. Carcinogenesis, 2006. **27**(11): p. 2223-34.

208. Pelicano, H., D. Carney, and P. Huang, *ROS stress in cancer cells and therapeutic implications*. Drug Resist Updat, 2004. **7**(2): p. 97-110.

209. Huang, P., et al., *Superoxide dismutase as a target for the selective killing of cancer cells*. Nature, 2000. **407**(6802): p. 390-5.

210. Ogretmen, B. and Y.A. Hannun, *Biologically active sphingolipids in cancer pathogenesis and treatment*. Nature reviews. Cancer, 2004. **4**(8): p. 604-16.

211. Matei, D., et al., *Activity of 2 methoxyestradiol (Panzem NCD) in advanced, platinum-resistant ovarian cancer and primary peritoneal carcinomatosis: a Hoosier Oncology Group trial*. Gynecol Oncol, 2009. **115**(1): p. 90-6.

212. Wallace, K.B. and A.A. Starkov, *Mitochondrial targets of drug toxicity*. Annu Rev Pharmacol Toxicol, 2000. **40**: p. 353-88.

213. Chen, B., et al., *The HSP90 family of genes in the human genome: insights into their divergence and evolution*. Genomics, 2005. **86**(6): p. 627-37.

214. Chen, V., et al., *Bezielle Selectively Targets Mitochondria of Cancer Cells to Inhibit Glycolysis and OXPHOS*. PLoS One, 2012. **7**(2): p. e30300.

215. Li, N., et al., *Mitochondrial complex I inhibitor rotenone induces apoptosis through enhancing mitochondrial reactive oxygen species production*. The Journal of biological chemistry, 2003. **278**(10): p. 8516-25.

216. Maldonado, E.N., et al., *Free tubulin modulates mitochondrial membrane potential in cancer cells*. Cancer research, 2010. **70**(24): p. 10192-201.

217. Short, B., *The wrong suspect?* The Journal of Cell Biology, 2011. **192**(5): p. 707.

218. Royo, I., et al., *In vitro antitumor SAR of threo/cis/threo/cis/erythro bis-THF acetogenins: correlations with their inhibition of mitochondrial Complex I*. Oncol Res, 2003. **13**(12): p. 521-8.

219. Gomez-Lazaro, M., et al., *Reactive oxygen species and p38 mitogen-activated protein kinase activate Bax to induce mitochondrial cytochrome c release and apoptosis in response to malonate*. Mol Pharmacol, 2007. **71**(3): p. 736-43.

220. Li, Y., et al., *Resveratrol-induced cell inhibition of growth and apoptosis in MCF7 human breast cancer cells are associated with modulation of phosphorylated Akt and caspase-9*. Applied biochemistry and biotechnology, 2006. **135**(3): p. 181-92.

221. Gledhill, J.R. and J.E. Walker, *Inhibition sites in F1-ATPase from bovine heart mitochondria*. The Biochemical journal, 2005. **386**(Pt 3): p. 591-8.

222. Tinhofer, I., et al., *Resveratrol, a tumor-suppressive compound from grapes, induces apoptosis via a novel mitochondrial pathway controlled by Bcl-2*. The FASEB journal : official publication of the Federation of American Societies for Experimental Biology, 2001. **15**(9): p. 1613-5.

223. de la Lastra, C.A. and I. Villegas, *Resveratrol as an antioxidant and pro-oxidant agent: mechanisms and clinical implications*. Biochem Soc Trans, 2007. **35**(Pt 5): p. 1156-60.

224. Bishayee, A., *Cancer prevention and treatment with resveratrol: from rodent studies to clinical trials*. Cancer Prev Res (Phila), 2009. **2**(5): p. 409-18.

225. Li, W., Q. Ma, and E. Wu, *Perspectives on the Role of Photodynamic Therapy in the Treatment of Pancreatic Cancer*. International Journal of Photoenergy, 2012. **2012**.

226. Morgan, J. and A.R. Oseroff, *Mitochondria-based photodynamic anti-cancer therapy*. Advanced drug delivery reviews, 2001. **49**(1-2): p. 71-86.

227. Castano, A.P., T.N. Demidova, and M.R. Hamblin, *Mechanisms in photodynamic therapy: part one--photosensitizers, photochemistry and cellular localization*. Photodiagnosis and photodynamic therapy, 2004. **1**(4): p. 279-293.

228. Hilf, R., *Mitochondria are targets of photodynamic therapy*. Journal of bioenergetics and biomembranes, 2007. **39**(1): p. 85-9.

229. Firuzi, O., et al., *Antioxidant therapy: current status and future prospects*. Current medicinal chemistry, 2011. **18**(25): p. 3871-88.

230. Sanjuan-Pla, A., et al., *A targeted antioxidant reveals the importance of mitochondrial reactive oxygen species in the hypoxic signaling of HIF-1alpha*. FEBS Lett, 2005. **579**(12): p. 2669-74.

231. Rao, V.A., et al., *The antioxidant transcription factor Nrf2 negatively regulates autophagy and growth arrest induced by the anticancer redox agent mitoquinone*. J Biol Chem, 2010. **285**(45): p. 34447-59.

232. Anderson, S., et al., *Sequence and organization of the human mitochondrial genome*. Nature, 1981. **290**(5806): p. 457-65.

233. Modica-Napolitano, J.S., M. Kulawiec, and K.K. Singh, *Mitochondria and human cancer*. Current molecular medicine, 2007. **7**(1): p. 121-31.

234. Penta, J.S., et al., *Mitochondrial DNA in human malignancy*. Mutation research, 2001. **488**(2): p. 119-33.

235. Copeland, W.C., et al., *Mitochondrial DNA alterations in cancer*. Cancer Invest, 2002. **20**(4): p. 557-69.

236. Lu, X., et al., *Differentiation of HT-29 human colonic adenocarcinoma cells correlates with increased expression of mitochondrial RNA: effects of trehalose on cell growth and maturation*. Cancer research, 1992. **52**(13): p. 3718-25.

237. Modica-Napolitano, J.S. and K.K. Singh, *Mitochondrial dysfunction in cancer*. Mitochondrion, 2004. **4**(5-6): p. 755-62.

238. Polyak, K., et al., *Somatic mutations of the mitochondrial genome in human colorectal tumours*. Nature genetics, 1998. **20**(3): p. 291-3.

239. Savre-Train, I., M.A. Piatyszek, and J.W. Shay, *Transcription of deleted mitochondrial DNA in human colon adenocarcinoma cells*. Human molecular genetics, 1992. **1**(3): p. 203-4.

240. Welter, C., et al., *Alteration of mitochondrial DNA in human oncocytomas*. Genes, chromosomes & cancer, 1989. **1**(1): p. 79-82.

241. Selvanayagam, P. and S. Rajaraman, *Detection of mitochondrial genome depletion by a novel cDNA in renal cell carcinoma*. Laboratory investigation; a journal of technical methods and pathology, 1996. **74**(3): p. 592-9.

242. Sharawat, S.K., et al., *Mitochondrial D-loop variations in paediatric acute myeloid leukaemia: a potential prognostic marker*. Br J Haematol, 2010. **149**(3): p. 391-8.

243. Brandon, M., P. Baldi, and D.C. Wallace, *Mitochondrial mutations in cancer*. Oncogene, 2006. **25**(34): p. 4647-62.

244. Vithayathil, S.A., Y. Ma, and B.A. Kaipparettu, *Transmitochondrial cybrids: tools for functional studies of mutant mitochondria*. Methods Mol Biol, 2012. **837**: p. 219-30.

245. Kulawiec, M., K.M. Owens, and K.K. Singh, *mtDNA G10398A variant in African-American women with breast cancer provides resistance to apoptosis and promotes metastasis in mice*. J Hum Genet, 2009. **54**(11): p. 647-54.

246. Ebner, S., et al., *Mitochondrial haplogroups, control region polymorphisms and malignant melanoma: a study in middle European Caucasians*. PLoS One, 2011. **6**(12): p. e27192.

247. Lam, E.T., et al., *Mitochondrial DNA sequence variation and risk of pancreatic cancer*. Cancer research, 2011.

248. Hsu, C.W., et al., *Mitochondrial DNA content as a potential marker to predict response to anthracycline in breast cancer patients*. Breast J, 2010. **16**(3): p. 264-70.

249. Tseng, L.M., et al., *Mitochondrial DNA mutations and mitochondrial DNA depletion in breast cancer*. Genes, chromosomes & cancer, 2006. **45**(7): p. 629-38.

250. Shen, J., et al., *Mitochondrial copy number and risk of breast cancer: a pilot study*. Mitochondrion, 2009. **10**(1): p. 62-8.

251. Bai, R.K., et al., *Mitochondrial DNA content varies with pathological characteristics of breast cancer*. J Oncol, 2011. **2011**: p. 496189.

252. Liang, B.C. and L. Hays, *Mitochondrial DNA copy number changes in human gliomas*. Cancer Lett, 1996. **105**(2): p. 167-73.

253. Xing, J., et al., *Mitochondrial DNA content: its genetic heritability and association with renal cell carcinoma*. J Natl Cancer Inst, 2008. **100**(15): p. 1104-12.

254. Chatterjee, A., E. Mambo, and D. Sidransky, *Mitochondrial DNA mutations in human cancer*. Oncogene, 2006. **25**(34): p. 4663-74.

255. Wang, Y., et al., *Association of decreased mitochondrial DNA content with ovarian cancer progression*. Br J Cancer, 2006. **95**(8): p. 1087-91.

256. Wang, Y., et al., *The increase of mitochondrial DNA content in endometrial adenocarcinoma cells: a quantitative study using laser-captured microdissected tissues*. Gynecol Oncol, 2005. **98**(1): p. 104-10.

257. Park, J.S., et al., *A heteroplasmic, not homoplasmic, mitochondrial DNA mutation promotes tumorigenesis via alteration in reactive oxygen species generation and apoptosis*. Human molecular genetics, 2009. **18**(9): p. 1578-89.

258. Dani, M.A., et al., *Less DeltamtDNA4977 than normal in various types of tumors suggests that cancer cells are essentially free of this mutation*. Genet Mol Res, 2004. **3**(3): p. 395-409.

259. Eshaghian, A., et al., *Mitochondrial DNA deletions serve as biomarkers of aging in the skin, but are typically absent in nonmelanoma skin cancers*. J Invest Dermatol, 2006. **126**(2): p. 336-44.

260. Mitchell, P., *Chemiosmotic coupling in oxidative and photosynthetic phosphorylation. 1966*. Biochimica et biophysica acta, 2011. **1807**(12): p. 1507-38.

261. Itoh, H., et al., *Mechanically driven ATP synthesis by F1-ATPase*. Nature, 2004. **427**(6973): p. 465-8.

262. Summerhayes, I.C., et al., *Unusual retention of rhodamine 123 by mitochondria in muscle and carcinoma cells*. Proc Natl Acad Sci U S A, 1982. **79**(17): p. 5292-6.

263. Bonnet, S., et al., *A mitochondria-K+ channel axis is suppressed in cancer and its normalization promotes apoptosis and inhibits cancer growth*. Cancer Cell, 2007. **11**(1): p. 37-51.

264. Ayyasamy, V., et al., *Cellular model of Warburg effect identifies tumor promoting function of UCP2 in breast cancer and its suppression by genipin*. PLoS One, 2011. **6**(9): p. e24792.

265. Brand, M.D. and T.C. Esteves, *Physiological functions of the mitochondrial uncoupling proteins UCP2 and UCP3*. Cell Metab, 2005. **2**(2): p. 85-93.

266. Modica-Napolitano, J.S. and J.R. Aprille, *Delocalized lipophilic cations selectively target the mitochondria of carcinoma cells*. Advanced drug delivery reviews, 2001. **49**(1-2): p. 63-70.

267. Bernal, S.D., et al., *Anticarcinoma activity in vivo of rhodamine 123, a mitochondrial-specific dye*. Science, 1983. **222**(4620): p. 169-72.

268. Summerhayes, I.C., et al., *Unusual retention of rhodamine 123 by mitochondria in muscle and carcinoma cells*. Proceedings of the National Academy of Sciences of the United States of America, 1982. **79**(17): p. 5292-6.

269. Bernal, S.D., et al., *Rhodamine-123 selectively reduces clonal growth of carcinoma cells in vitro*. Science, 1982. **218**(4577): p. 1117-9.

270. Modica-Napolitano, J.S., et al., *Selective damage to carcinoma mitochondria by the rhodacyanine MKT-077*. Cancer research, 1996. **56**(3): p. 544-50.

271. Koya, K., et al., *MKT-077, a novel rhodacyanine dye in clinical trials, exhibits anticarcinoma activity in preclinical studies based on selective mitochondrial accumulation*. Cancer research, 1996. **56**(3): p. 538-43.

272. Weisberg, E.L., et al., *In vivo administration of MKT-077 causes partial yet reversible impairment of mitochondrial function*. Cancer research, 1996. **56**(3): p. 551-5.

273. Tatsuta, N., et al., *Pharmacokinetic analysis and antitumor efficacy of MKT-077, a novel antitumor agent*. Cancer Chemother Pharmacol, 1999. **43**(4): p. 295-301.

274. Propper, D.J., et al., *Phase I trial of the selective mitochondrial toxin MKT077 in chemo-resistant solid tumours*. Ann Oncol, 1999. **10**(8): p. 923-7.

275. Fantin, V.R. and P. Leder, *F16, a mitochondriotoxic compound, triggers apoptosis or necrosis depending on the genetic background of the target carcinoma cell*. Cancer research, 2004. **64**(1): p. 329-36.

276. Weiss, M.J., et al., *Dequalinium, a topical antimicrobial agent, displays anticarcinoma activity based on selective mitochondrial accumulation*. Proceedings of the National Academy of Sciences of the United States of America, 1987. **84**(15): p. 5444-8.

277. D'Souza, G.G., et al., *DQAsome-mediated delivery of plasmid DNA toward mitochondria in living cells*. Journal of controlled release : official journal of the Controlled Release Society, 2003. **92**(1-2): p. 189-97.

278. Serafim, T.L., et al., *Different concentrations of berberine result in distinct cellular localization patterns and cell cycle effects in a melanoma cell line*. Cancer chemotherapy and pharmacology, 2008. **61**(6): p. 1007-18.

279. Pereira, G.C., et al., *Mitochondrially targeted effects of berberine [Natural Yellow 18, 5,6-dihydro-9,10-dimethoxybenzo(g)-1,3-benzodioxolo(5,6-a) quinolizinium] on K1735-M2 mouse melanoma cells: comparison with direct effects on isolated mitochondrial fractions*. The Journal of pharmacology and experimental therapeutics, 2007. **323**(2): p. 636-49.

280. Kerr, J.F., A.H. Wyllie, and A.R. Currie, *Apoptosis: a basic biological phenomenon with wide-ranging implications in tissue kinetics*. British journal of cancer, 1972. **26**(4): p. 239-57.

281. Elmore, S., *Apoptosis: a review of programmed cell death*. Toxicol Pathol, 2007. **35**(4): p. 495-516.

282. Adams, J.M. and S. Cory, *The Bcl-2 apoptotic switch in cancer development and therapy*. Oncogene, 2007. **26**(9): p. 1324-37.

283. Satou, T., *[Warm drug solution injected into tumor vessel may enhance antitumor effect]*. Gan To Kagaku Ryoho, 1990. **17**(8 Pt 2): p. 1763-7.

284. Wang, C. and R.J. Youle, *The role of mitochondria in apoptosis**. Annu Rev Genet, 2009. **43**: p. 95-118.

285. Dawn, M., *The Balance between Life and Death: Defining a Role for Apoptosis in Aging*. Journal of Clinical & Experimental Pathology, 2012.

286. Kim, H.E., et al., *Formation of apoptosome is initiated by cytochrome c-induced dATP hydrolysis and subsequent nucleotide exchange on Apaf-1*. Proc Natl Acad Sci U S A, 2005. **102**(49): p. 17545-50.

287. Toyama, Y., et al., *Apoptotic force and tissue dynamics during Drosophila embryogenesis*. Science, 2008. **321**(5896): p. 1683-6.

288. Kroemer, G., L. Galluzzi, and C. Brenner, *Mitochondrial membrane permeabilization in cell death*. Physiol Rev, 2007. **87**(1): p. 99-163.

289. Tait, S.W. and D.R. Green, *Mitochondria and cell death: outer membrane permeabilization and beyond*. Nat Rev Mol Cell Biol, 2011. **11**(9): p. 621-32.

290. Bernardi, P., *The mitochondrial permeability transition pore: a mystery solved?* Front Physiol, 2013. **4**: p. 95.

291. Halestrap, A.P., *What is the mitochondrial permeability transition pore?* J Mol Cell Cardiol, 2009. **46**(6): p. 821-31.

292. Varanyuwatana, P. and A.P. Halestrap, *The roles of phosphate and the phosphate carrier in the mitochondrial permeability transition pore*. Mitochondrion, 2012. **12**(1): p. 120-5.

293. Giorgio, V., et al., *Dimers of mitochondrial ATP synthase form the permeability transition pore*. Proc Natl Acad Sci U S A, 2013. **110**(15): p. 5887-92.

294. Kokoszka, J.E., et al., *The ADP/ATP translocator is not essential for the mitochondrial permeability transition pore*. Nature, 2004. **427**(6973): p. 461-5.

295. Baines, C.P., et al., *Loss of cyclophilin D reveals a critical role for mitochondrial permeability transition in cell death*. Nature, 2005. **434**(7033): p. 658-62.

296. Sharaf El Dein, O., et al., *Role of the permeability transition pore complex in lethal inter-organelle crosstalk*. Front Biosci, 2009. **14**: p. 3465-82.

297. Galluzzi, L., et al., *Mitochondrial liaisons of p53*. Antioxid Redox Signal, 2010. **15**(6): p. 1691-714.

298. Sebastian, S., et al., *p53 as the main traffic controller of the cell signaling network*. Frontiers in bioscience : a journal and virtual library. **15**: p. 1172-90.

299. Vousden, K.H., *Functions of p53 in metabolism and invasion*. Biochemical Society transactions, 2009. **37**(Pt 3): p. 511-7.

300. Azoulay-Zohar, H., et al., *In self-defence: hexokinase promotes voltage-dependent anion channel closure and prevents mitochondria-mediated apoptotic cell death*. Biochem J, 2004. **377**(Pt 2): p. 347-55.

301. Brenner, C. and S. Grimm, *The permeability transition pore complex in cancer cell death*. Oncogene, 2006. **25**(34): p. 4744-56.

302. Ghosh, J.C., et al., *Heat shock protein 60 regulation of the mitochondrial permeability transition pore in tumor cells*. Cancer research, 2010. **70**(22): p. 8988-93.

303. Landriscina, M., et al., *Heat shock proteins, cell survival and drug resistance: the mitochondrial chaperone TRAP1, a potential novel target for ovarian cancer therapy*. Gynecol Oncol, 2009. **117**(2): p. 177-82.

304. Kang, B.H., et al., *Regulation of tumor cell mitochondrial homeostasis by an organelle-specific Hsp90 chaperone network*. Cell, 2007. **131**(2): p. 257-70.

305. Casellas, P., S. Galiegue, and A.S. Basile, *Peripheral benzodiazepine receptors and mitochondrial function*. Neurochemistry international, 2002. **40**(6): p. 475-86.

306. Veenman, L., Y. Shandalov, and M. Gavish, *VDAC activation by the 18 kDa translocator protein (TSPO), implications for apoptosis*. Journal of bioenergetics and biomembranes, 2008. **40**(3): p. 199-205.

307. Batarseh, A. and V. Papadopoulos, *Regulation of translocator protein 18 kDa (TSPO) expression in health and disease states*. Mol Cell Endocrinol, 2010. **327**(1-2): p. 1-12.

308. Maaser, K., et al., *Specific ligands of the peripheral benzodiazepine receptor induce apoptosis and cell cycle arrest in human colorectal cancer cells*. British journal of cancer, 2001. **85**(11): p. 1771-80.

309. Wang, J.L., et al., *Structure-based discovery of an organic compound that binds Bcl-2 protein and induces apoptosis of tumor cells*. Proc Natl Acad Sci U S A, 2000. **97**(13): p. 7124-9.

310. van Delft, M.F., et al., *The BH3 mimetic ABT-737 targets selective Bcl-2 proteins and efficiently induces apoptosis via Bak/Bax if Mcl-1 is neutralized*. Cancer Cell, 2006. **10**(5): p. 389-99.

311. Ghiotto, F., et al., *Apoptosis of B-cell chronic lymphocytic leukemia cells induced by a novel BH3 peptidomimetic*. Cancer Biol Ther, 2009. **8**(3): p. 263-71.

312. Leber, B., et al., *Drugs targeting Bcl-2 family members as an emerging strategy in cancer*. Expert reviews in molecular medicine, 2010. **12**: p. e28.

313. O'Brien, S.M., et al., *Phase I study of obatoclax mesylate (GX15-070), a small molecule pan-Bcl-2 family antagonist, in patients with advanced chronic lymphocytic leukemia*. Blood, 2009. **113**(2): p. 299-305.

314. Paik, P.K., et al., *A phase I study of obatoclax mesylate, a Bcl-2 antagonist, plus topotecan in solid tumor malignancies*. Cancer Chemother Pharmacol, 2010. **66**(6): p. 1079-85.

315. Schimmer, A.D., et al., *A phase I study of the pan bcl-2 family inhibitor obatoclax mesylate in patients with advanced hematologic malignancies*. Clin Cancer Res, 2008. **14**(24): p. 8295-301.

316. Yeow, W.S., et al., *Gossypol, a phytochemical with BH3-mimetic property, sensitizes cultured thoracic cancer cells to Apo2 ligand/tumor necrosis factor-related apoptosis-inducing ligand*. The Journal of thoracic and cardiovascular surgery, 2006. **132**(6): p. 1356-62.

317. Yamasaki, T., et al., *Imaging of peripheral-type benzodiazepine receptor in tumor: in vitro binding and in vivo biodistribution of N-benzyl-N-[(11)C]methyl-2-(7-methyl-8-oxo-2-phenyl-7,8-dihydro-9H-purin-9-yl)ace tamide*. Nuclear medicine and biology, 2009. **36**(7): p. 801-9.

318. Shehzad, A., F. Wahid, and Y.S. Lee, *Curcumin in cancer chemoprevention: molecular targets, pharmacokinetics, bioavailability, and clinical trials*. Arch Pharm (Weinheim), 2010. **343**(9): p. 489-99.

319. Serafim, T.L., et al., *Sanguinarine cytotoxicity on mouse melanoma K1735-M2 cells--nuclear vs. mitochondrial effects*. Biochemical pharmacology, 2008. **76**(11): p. 1459-75.

320. Hussain, A.R., et al., *Sanguinarine-dependent induction of apoptosis in primary effusion lymphoma cells*. Cancer research, 2007. **67**(8): p. 3888-97.

321. Kaminskyy, V., O. Kulachkovskyy, and R. Stoika, *A decisive role of mitochondria in defining rate and intensity of apoptosis induction by different alkaloids*. Toxicology letters, 2008. **177**(3): p. 168-81.

322. Choi, W.Y., et al., *Sanguinarine, a benzophenanthridine alkaloid, induces apoptosis in MDA-MB-231 human breast carcinoma cells through a reactive oxygen species-mediated mitochondrial pathway*. Chemotherapy, 2008. **54**(4): p. 279-87.

323. Choi, W.Y., et al., *Sanguinarine sensitizes human gastric adenocarcinoma AGS cells to TRAIL-mediated apoptosis via down-regulation of AKT and activation of caspase-3*. Anticancer research, 2009. **29**(11): p. 4457-65.

324. Pereira, C.V., N.G. Machado, and P.J. Oliveira, *Mechanisms of berberine (natural yellow 18)-induced mitochondrial dysfunction: interaction with the adenine nucleotide translocator*. Toxicological sciences : an official journal of the Society of Toxicology, 2008. **105**(2): p. 408-17.

325. Mikes, V. and V. Dadak, *Berberine derivatives as cationic fluorescent probes for the investigation of the energized state of mitochondria*. Biochimica et biophysica acta, 1983. **723**(2): p. 231-9.

326. Jantova, S., L. Cipak, and S. Letasiova, *Berberine induces apoptosis through a mitochondrial/caspase pathway in human promonocytic U937 cells*. Toxicology in vitro : an international journal published in association with BIBRA, 2007. **21**(1): p. 25-31.

327. Hwang, J.M., et al., *Berberine induces apoptosis through a mitochondria/caspases pathway in human hepatoma cells*. Archives of toxicology, 2006. **80**(2): p. 62-73.

328. Lin, J.P., et al., *Berberine induces cell cycle arrest and apoptosis in human gastric carcinoma SNU-5 cell line*. World journal of gastroenterology : WJG, 2006. **12**(1): p. 21-8.

329. Mantena, S.K., S.D. Sharma, and S.K. Katiyar, *Berberine inhibits growth, induces G1 arrest and apoptosis in human epidermoid carcinoma A431 cells by regulating Cdki-Cdk-cyclin cascade, disruption of mitochondrial membrane potential and cleavage of caspase 3 and PARP*. Carcinogenesis, 2006. **27**(10): p. 2018-27.

330. Galluzzi, L., et al., *Life, death and burial: multifaceted impact of autophagy*. Biochem Soc Trans, 2008. **36**(Pt 5): p. 786-90.

331. Mizushima, N., et al., *Autophagy fights disease through cellular self-digestion*. Nature, 2008. **451**(7182): p. 1069-75.

332. Levine, B. and G. Kroemer, *Autophagy in the pathogenesis of disease*. Cell, 2008. **132**(1): p. 27-42.

333. Ogier-Denis, E. and P. Codogno, *Autophagy: a barrier or an adaptive response to cancer*. Biochimica et biophysica acta, 2003. **1603**(2): p. 113-28.

334. Gozuacik, D. and A. Kimchi, *Autophagy as a cell death and tumor suppressor mechanism*. Oncogene, 2004. **23**(16): p. 2891-906.

335. Choi, A.M., S.W. Ryter, and B. Levine, *Autophagy in human health and disease*. N Engl J Med, 2013. **368**(7): p. 651-62.

336. Levine, B. and D.J. Klionsky, *Development by self-digestion: molecular mechanisms and biological functions of autophagy*. Dev Cell, 2004. **6**(4): p. 463-77.

337. Hailey, D.W., et al., *Mitochondria supply membranes for autophagosome biogenesis during starvation*. Cell, 2010. **141**(4): p. 656-67.

338. Ravikumar, B., et al., *Plasma membrane contributes to the formation of pre-autophagosomal structures*. Nat Cell Biol, 2010. **12**(8): p. 747-57.

339. Tooze, S.A. and T. Yoshimori, *The origin of the autophagosomal membrane*. Nat Cell Biol, 2010. **12**(9): p. 831-5.

340. Klionsky, D.J., et al., *A unified nomenclature for yeast autophagy-related genes*. Dev Cell, 2003. **5**(4): p. 539-45.

341. Mizushima, N., T. Yoshimori, and Y. Ohsumi, *The role of Atg proteins in autophagosome formation*. Annu Rev Cell Dev Biol, 2011. **27**: p. 107-32.

342. Mizushima, N. and M. Komatsu, *Autophagy: renovation of cells and tissues*. Cell, 2011. **147**(4): p. 728-41.

343. Sinha, S. and B. Levine, *The autophagy effector Beclin 1: a novel BH3-only protein*. Oncogene, 2008. **27 Suppl 1**: p. S137-48.

344. Walczak, M. and S. Martens, *Dissecting the role of the Atg12-Atg5-Atg16 complex during autophagosome formation*. Autophagy, 2013. **9**(3): p. 424-5.

345. Tanida, I., T. Ueno, and E. Kominami, *LC3 conjugation system in mammalian autophagy*. Int J Biochem Cell Biol, 2004. **36**(12): p. 2503-18.

346. Lee, J., S. Giordano, and J. Zhang, *Autophagy, mitochondria and oxidative stress: cross-talk and redox signalling*. Biochem J, 2012. **441**(2): p. 523-40.

347. Repnik, U., et al., *Lysosomes and lysosomal cathepsins in cell death*. Biochimica et biophysica acta, 2012. **1824**(1): p. 22-33.

348. Eskelinen, E.L. and P. Saftig, *Autophagy: a lysosomal degradation pathway with a central role in health and disease*. Biochimica et biophysica acta, 2009. **1793**(4): p. 664-73.

349. Johansen, T. and T. Lamark, *Selective autophagy mediated by autophagic adapter proteins*. Autophagy, 2011. **7**(3): p. 279-96.

350. Lamark, T., et al., *NBR1 and p62 as cargo receptors for selective autophagy of ubiquitinated targets*. Cell Cycle, 2009. **8**(13): p. 1986-90.

351. Kubli, D.A. and A.B. Gustafsson, *Mitochondria and mitophagy: the yin and yang of cell death control*. Circ Res, 2012. **111**(9): p. 1208-21.

352. Scherz-Shouval, R., et al., *Reactive oxygen species are essential for autophagy and specifically regulate the activity of Atg4*. EMBO J, 2007. **26**(7): p. 1749-60.

353. Okatsu, K., et al., *p62/SQSTM1 cooperates with Parkin for perinuclear clustering of depolarized mitochondria*. Genes Cells, 2010. **15**(8): p. 887-900.

354. Geisler, S., et al., *PINK1/Parkin-mediated mitophagy is dependent on VDAC1 and p62/SQSTM1*. Nat Cell Biol, 2010. **12**(2): p. 119-31.

355. Narendra, D., et al., *p62/SQSTM1 is required for Parkin-induced mitochondrial clustering but not mitophagy; VDAC1 is dispensable for both*. Autophagy, 2010. **6**(8): p. 1090-106.

356. Strappazzon, F., et al., *Mitochondrial BCL-2 inhibits AMBRA1-induced autophagy*. EMBO J, 2011. **30**(7): p. 1195-208.

357. Van Humbeeck, C., et al., *Parkin interacts with Ambra1 to induce mitophagy*. J Neurosci, 2011. **31**(28): p. 10249-61.

358. Kondo-Okamoto, N., et al., *Autophagy-related protein 32 acts as autophagic degron and directly initiates mitophagy*. J Biol Chem, 2012. **287**(13): p. 10631-8.

359. Hanna, R.A., et al., *Microtubule-associated protein 1 light chain 3 (LC3) interacts with Bnip3 protein to selectively remove endoplasmic reticulum and mitochondria via autophagy*. J Biol Chem, 2012. **287**(23): p. 19094-104.

360. Novak, I., et al., *Nix is a selective autophagy receptor for mitochondrial clearance*. EMBO Rep, 2010. **11**(1): p. 45-51.

361. Jin, S.M., et al., *Mitochondrial membrane potential regulates PINK1 import and proteolytic destabilization by PARL*. J Cell Biol, 2010. **191**(5): p. 933-42.

362. Narendra, D.P., et al., *PINK1 is selectively stabilized on impaired mitochondria to activate Parkin*. PLoS Biol, 2010. **8**(1): p. e1000298.

363. Matsuda, N., et al., *PINK1 stabilized by mitochondrial depolarization recruits Parkin to damaged mitochondria and activates latent Parkin for mitophagy*. J Cell Biol, 2010. **189**(2): p. 211-21.

364. Fischer, F., A. Hamann, and H.D. Osiewacz, *Mitochondrial quality control: an integrated network of pathways*. Trends Biochem Sci, 2012. **37**(7): p. 284-92.

365. Whitworth, A.J. and L.J. Pallanck, *The PINK1/Parkin pathway: a mitochondrial quality control system?* Journal of bioenergetics and biomembranes, 2009. **41**(6): p. 499-503.

366. Bereiter-Hahn, J. and M. Jendrach, *Mitochondrial dynamics*. Int Rev Cell Mol Biol, 2010. **284**: p. 1-65.

367. Dice, J.F., *Peptide sequences that target cytosolic proteins for lysosomal proteolysis*. Trends Biochem Sci, 1990. **15**(8): p. 305-9.

368. Cuervo, A.M., *Chaperone-mediated autophagy: selectivity pays off*. Trends in endocrinology and metabolism: TEM, 2010. **21**(3): p. 142-50.

369. Lv, L., et al., *Acetylation targets the M2 isoform of pyruvate kinase for degradation through chaperone-mediated autophagy and promotes tumor growth*. Mol Cell, 2011. **42**(6): p. 719-30.

370. Kaushik, S. and A.M. Cuervo, *Chaperone-mediated autophagy: a unique way to enter the lysosome world*. Trends Cell Biol, 2012. **22**(8): p. 407-17.

371. Salvador, N., et al., *Import of a cytosolic protein into lysosomes by chaperone-mediated autophagy depends on its folding state*. J Biol Chem, 2000. **275**(35): p. 27447-56.

372. Kaushik, S., et al., *Chaperone-mediated autophagy at a glance*. J Cell Sci, 2011. **124**(Pt 4): p. 495-9.

373. Bandyopadhyay, U., et al., *The chaperone-mediated autophagy receptor organizes in dynamic protein complexes at the lysosomal membrane*. Mol Cell Biol, 2008. **28**(18): p. 5747-63.

374. Agarraberes, F.A., S.R. Terlecky, and J.F. Dice, *An intralysosomal hsp70 is required for a selective pathway of lysosomal protein degradation*. J Cell Biol, 1997. **137**(4): p. 825-34.

375. Cuervo, A.M., J.F. Dice, and E. Knecht, *A population of rat liver lysosomes responsible for the selective uptake and degradation of cytosolic proteins*. J Biol Chem, 1997. **272**(9): p. 5606-15.

376. Liang, X.H., et al., *Induction of autophagy and inhibition of tumorigenesis by beclin 1*. Nature, 1999. **402**(6762): p. 672-6.

377. Qu, X., et al., *Promotion of tumorigenesis by heterozygous disruption of the beclin 1 autophagy gene*. J Clin Invest, 2003. **112**(12): p. 1809-20.

378. Mizushima, N., *Autophagy: process and function*. Genes Dev, 2007. **21**(22): p. 2861-73.

379. Pattingre, S., et al., *Bcl-2 antiapoptotic proteins inhibit Beclin 1-dependent autophagy*. Cell, 2005. **122**(6): p. 927-39.

380. Koneri, K., et al., *Beclin 1 gene inhibits tumor growth in colon cancer cell lines*. Anticancer research, 2007. **27**(3B): p. 1453-7.

381. Yousefi, S., et al., *Calpain-mediated cleavage of Atg5 switches autophagy to apoptosis*. Nat Cell Biol, 2006. **8**(10): p. 1124-32.

382. Feng, Z., et al., *The coordinate regulation of the p53 and mTOR pathways in cells*. Proc Natl Acad Sci U S A, 2005. **102**(23): p. 8204-9.

383. Mathew, R., et al., *Autophagy suppresses tumorigenesis through elimination of p62*. Cell, 2009. **137**(6): p. 1062-75.

384. Carloni, S., et al., *Inhibition of rapamycin-induced autophagy causes necrotic cell death associated with Bax/Bad mitochondrial translocation*. Neuroscience, 2012. **203**: p. 160-9.

385. Degenhardt, K., et al., *Autophagy promotes tumor cell survival and restricts necrosis, inflammation, and tumorigenesis*. Cancer Cell, 2006. **10**(1): p. 51-64.

386. WANG, W.-y., et al., *Effect of autophagy-related gene Beclin 1 on growth of xenografts of human lung adenocarcinoma A549 cells in nude mice*. Tumor, 2011. **31**(12): p. 1061-1066.

387. Apel, A., et al., *Autophagy-A double-edged sword in oncology*. Int J Cancer, 2009. **125**(5): p. 991-5.

388. Kon, M., et al., *Chaperone-mediated autophagy is required for tumor growth*. Sci Transl Med, 2011. **3**(109): p. 109ra117.

389. Bellot, G., et al., *Hypoxia-induced autophagy is mediated through hypoxia-inducible factor induction of BNIP3 and BNIP3L via their BH3 domains*. Mol Cell Biol, 2009. **29**(10): p. 2570-81.

390. White, E. and R.S. DiPaola, *The double-edged sword of autophagy modulation in cancer*. Clin Cancer Res, 2009. **15**(17): p. 5308-16.

391. Kimmelman, A.C., *The dynamic nature of autophagy in cancer*. Genes Dev, 2011. **25**(19): p. 1999-2010.

392. Martinez-Outschoorn, U.E., et al., *Oxidative stress in cancer associated fibroblasts drives tumor-stroma co-evolution: A new paradigm for understanding tumor metabolism, the field effect and genomic instability in cancer cells*. Cell Cycle, 2010. **9**(16): p. 3256-76.

393. Martinez-Outschoorn, U.E., et al., *Autophagy in cancer associated fibroblasts promotes tumor cell survival: Role of hypoxia, HIF1 induction and NFkappaB activation in the tumor stromal microenvironment*. Cell Cycle, 2010. **9**(17): p. 3515-33.

394. Lisanti, M.P., et al., *Understanding the "lethal" drivers of tumor-stroma co-evolution: emerging role(s) for hypoxia, oxidative stress and autophagy/mitophagy in the tumor micro-environment*. Cancer Biol Ther, 2010. **10**(6): p. 537-42.

395. Maycotte, P. and A. Thorburn, *Autophagy and cancer therapy*. Cancer Biol Ther, 2011. **11**(2): p. 127-37.

396. Ballou, L.M. and R.Z. Lin, *Rapamycin and mTOR kinase inhibitors*. J Chem Biol, 2008. **1**(1-4): p. 27-36.

397. Yuan, R., et al., *Targeting tumorigenesis: development and use of mTOR inhibitors in cancer therapy*. J Hematol Oncol, 2009. **2**: p. 45.

398. Yang, Z.J., et al., *Autophagy modulation for cancer therapy*. Cancer Biol Ther, 2011. **11**(2): p. 169-76.

399. Shi, W.Y., et al., *Therapeutic metformin/AMPK activation blocked lymphoma cell growth via inhibition of mTOR pathway and induction of autophagy*. Cell Death Dis, 2012. **3**: p. e275.

400. Ben Sahra, I., et al., *Targeting cancer cell metabolism: the combination of metformin and 2-deoxyglucose induces p53-dependent apoptosis in prostate cancer cells*. Cancer research, 2010. **70**(6): p. 2465-75.

401. Can, G., H.A. Ekiz, and Y. Baran, *Imatinib induces autophagy through BECLIN-1 and ATG5 genes in chronic myeloid leukemia cells*. Hematology, 2011. **16**(2): p. 95-9.

402. Cloonan, S.M. and D.C. Williams, *The antidepressants maprotiline and fluoxetine induce Type II autophagic cell death in drug-resistant Burkitt's lymphoma*. Int J Cancer, 2011. **128**(7): p. 1712-23.

403. Gewirtz, D.A., *Autophagy, senescence and tumor dormancy in cancer therapy*. Autophagy, 2009. **5**(8): p. 1232-4.

404. Rapisarda, A. and G. Melillo, *Role of the hypoxic tumor microenvironment in the resistance to anti-angiogenic therapies*. Drug Resist Updat, 2009. **12**(3): p. 74-80.

405. Yang, Z.J., et al., *The role of autophagy in cancer: therapeutic implications*. Mol Cancer Ther, 2011. **10**(9): p. 1533-41.

406. Yamamoto, A., et al., *Bafilomycin A1 prevents maturation of autophagic vacuoles by inhibiting fusion between autophagosomes and lysosomes in rat hepatoma cell line, H-4-II-E cells*. Cell Struct Funct, 1998. **23**(1): p. 33-42.

407. Hoyvik, H., et al., *Inhibition of autophagic-lysosomal delivery and autophagic lactolysis by asparagine*. J Cell Biol, 1991. **113**(6): p. 1305-12.

408. Young, J.C., et al., *Pathways of chaperone-mediated protein folding in the cytosol*. Nat Rev Mol Cell Biol, 2004. **5**(10): p. 781-91.

409. Chen, B., et al., *Cellular strategies of protein quality control*. Cold Spring Harb Perspect Biol, 2011. **3**(8): p. a004374.

410. Soo, E.T., et al., *Heat shock proteins as novel therapeutic targets in cancer*. In Vivo, 2008. **22**(3): p. 311-5.

411. Parcellier, A., et al., *Heat shock proteins, cellular chaperones that modulate mitochondrial cell death pathways*. Biochem Biophys Res Commun, 2003. **304**(3): p. 505-12.

412. Ciocca, D.R. and S.K. Calderwood, *Heat shock proteins in cancer: diagnostic, prognostic, predictive, and treatment implications*. Cell Stress Chaperones, 2005. **10**(2): p. 86-103.

413. Chen, B., D. Zhong, and A. Monteiro, *Comparative genomics and evolution of the HSP90 family of genes across all kingdoms of organisms*. BMC Genomics, 2006. **7**: p. 156.

414. Mjahed, H., et al., *Heat shock proteins in hematopoietic malignancies*. Exp Cell Res, 2012. **318**(15): p. 1946-58.

415. Fan, A.C., M.K. Bhangoo, and J.C. Young, *Hsp90 functions in the targeting and outer membrane translocation steps of Tom70-mediated mitochondrial import*. J Biol Chem, 2006. **281**(44): p. 33313-24.

416. Donnelly, A. and B.S. Blagg, *Novobiocin and additional inhibitors of the Hsp90 C-terminal nucleotide-binding pocket*. Current medicinal chemistry, 2008. **15**(26): p. 2702-17.

417. Prodromou, C., et al., *The ATPase cycle of Hsp90 drives a molecular 'clamp' via transient dimerization of the N-terminal domains*. EMBO J, 2000. **19**(16): p. 4383-92.

418. Panaretou, B., et al., *ATP binding and hydrolysis are essential to the function of the Hsp90 molecular chaperone in vivo*. EMBO J, 1998. **17**(16): p. 4829-36.

419. Weikl, T., et al., *C-terminal regions of Hsp90 are important for trapping the nucleotide during the ATPase cycle*. J Mol Biol, 2000. **303**(4): p. 583-92.

420. Schneider, C., et al., *Pharmacologic shifting of a balance between protein refolding and degradation mediated by Hsp90*. Proc Natl Acad Sci U S A, 1996. **93**(25): p. 14536-41.

421. Neckers, L. and K. Neckers, *Heat-shock protein 90 inhibitors as novel cancer chemotherapeutic agents*. Expert Opin Emerg Drugs, 2002. **7**(2): p. 277-88.

422. An, W.G., T.W. Schulte, and L.M. Neckers, *The heat shock protein 90 antagonist geldanamycin alters chaperone association with p210bcr-abl and v-src proteins before their degradation by the proteasome*. Cell Growth Differ, 2000. **11**(7): p. 355-60.

423. Jensen, M.R., et al., *NVP-AUY922: a small molecule HSP90 inhibitor with potent antitumor activity in preclinical breast cancer models*. Breast Cancer Res, 2008. **10**(2): p. R33.

424. Eccles, S.A., et al., *NVP-AUY922: a novel heat shock protein 90 inhibitor active against xenograft tumor growth, angiogenesis, and metastasis*. Cancer research, 2008. **68**(8): p. 2850-60.

425. Brough, P.A., et al., *4,5-diarylisoxazole Hsp90 chaperone inhibitors: potential therapeutic agents for the treatment of cancer*. J Med Chem, 2008. **51**(2): p. 196-218.

426. Song, D., et al., *Antitumor activity and molecular effects of the novel heat shock protein 90 inhibitor, IPI-504, in pancreatic cancer*. Mol Cancer Ther, 2008. **7**(10): p. 3275-84.

427. Neckers, L., *Heat shock protein 90: the cancer chaperone*. J Biosci, 2007. **32**(3): p. 517-30.

428. Martinus, R.D., et al., *Role of chaperones in the biogenesis and maintenance of the mitochondrion*. The FASEB journal : official publication of the Federation of American Societies for Experimental Biology, 1995. **9**(5): p. 371-8.

429. Song, H.Y., et al., *Identification of a protein with homology to hsp90 that binds the type 1 tumor necrosis factor receptor*. J Biol Chem, 1995. **270**(8): p. 3574-81.

430. Chen, C.F., et al., *A new member of the hsp90 family of molecular chaperones interacts with the retinoblastoma protein during mitosis and after heat shock*. Mol Cell Biol, 1996. **16**(9): p. 4691-9.

431. Felts, S.J., et al., *The hsp90-related protein TRAP1 is a mitochondrial protein with distinct functional properties*. J Biol Chem, 2000. **275**(5): p. 3305-12.

432. Cechetto, J.D. and R.S. Gupta, *Immunoelectron microscopy provides evidence that tumor necrosis factor receptor-associated protein 1 (TRAP-1) is a mitochondrial protein which also localizes at specific extramitochondrial sites*. Exp Cell Res, 2000. **260**(1): p. 30-9.

433. Leav, I., et al., *Cytoprotective mitochondrial chaperone TRAP-1 as a novel molecular target in localized and metastatic prostate cancer*. Am J Pathol, 2010. **176**(1): p. 393-401.

434. Kang, B.H., et al., *Combinatorial drug design targeting multiple cancer signaling networks controlled by mitochondrial Hsp90*. J Clin Invest, 2009. **119**(3): p. 454-64.

435. Zuehlke, A. and J.L. Johnson, *Hsp90 and co-chaperones twist the functions of diverse client proteins*. Biopolymers, 2010. **93**(3): p. 211-7.

436. Leskovar, A., et al., *The ATPase cycle of the mitochondrial Hsp90 analog Trap1*. J Biol Chem, 2008. **283**(17): p. 11677-88.

437. Pridgeon, J.W., et al., *PINK1 protects against oxidative stress by phosphorylating mitochondrial chaperone TRAP1*. PLoS Biol, 2007. **5**(7): p. e172.

438. Masuda, Y., et al., *Involvement of tumor necrosis factor receptor-associated protein 1 (TRAP1) in apoptosis induced by beta-hydroxyisovalerylshikonin*. J Biol Chem, 2004. **279**(41): p. 42503-15.

439. Hua, G., Q. Zhang, and Z. Fan, *Heat shock protein 75 (TRAP1) antagonizes reactive oxygen species generation and protects cells from granzyme M-mediated apoptosis*. J Biol Chem, 2007. **282**(28): p. 20553-60.

440. Im, C.N., et al., *Iron chelation study in a normal human hepatocyte cell line suggests that tumor necrosis factor receptor-associated protein 1 (TRAP1) regulates production of reactive oxygen species*. J Cell Biochem, 2007. **100**(2): p. 474-86.

441. Coller, H.A., et al., *Expression analysis with oligonucleotide microarrays reveals that MYC regulates genes involved in growth, cell cycle, signaling, and adhesion*. Proc Natl Acad Sci U S A, 2000. **97**(7): p. 3260-5.

442. Montesano Gesualdi, N., et al., *Tumor necrosis factor-associated protein 1 (TRAP-1) protects cells from oxidative stress and apoptosis*. Stress, 2007. **10**(4): p. 342-50.

443. Voloboueva, L.A., et al., *Overexpression of mitochondrial Hsp70/Hsp75 protects astrocytes against ischemic injury in vitro*. J Cereb Blood Flow Metab, 2008. **28**(5): p. 1009-16.

444. Xu, L., et al., *Overexpression of mitochondrial Hsp70/Hsp75 in rat brain protects mitochondria, reduces oxidative stress, and protects from focal ischemia*. J Cereb Blood Flow Metab, 2009. **29**(2): p. 365-74.

445. Kubota, K., et al., *Tumor necrosis factor receptor-associated protein 1 regulates cell adhesion and synaptic morphology via modulation of N-cadherin expression*. J Neurochem, 2009. **110**(2): p. 496-508.

446. Liu, D., et al., *Tumor necrosis factor receptor-associated protein 1(TRAP1) regulates genes involved in cell cycle and metastases*. Cancer Lett, 2010. **296**(2): p. 194-205.

447. Costantino, E., et al., *TRAP1, a novel mitochondrial chaperone responsible for multi-drug resistance and protection from apoptotis in human colorectal carcinoma cells*. Cancer Lett, 2009. **279**(1): p. 39-46.

448. Siegelin, M.D., et al., *Global targeting of subcellular heat shock protein-90 networks for therapy of glioblastoma*. Mol Cancer Ther, 2010. **9**(6): p. 1638-46.

449. He, L. and J.J. Lemasters, *Regulated and unregulated mitochondrial permeability transition pores: a new paradigm of pore structure and function?* FEBS letters, 2002. **512**(1-3): p. 1-7.

450. Landriscina, M., et al., *Mitochondrial chaperone Trap1 and the calcium binding protein Sorcin interact and protect cells against apoptosis induced by antiblastic agents*. Cancer research, 2010. **70**(16): p. 6577-86.

451. Takemoto, K., et al., *Mitochondrial TRAP1 regulates the unfolded protein response in the endoplasmic reticulum*. Neurochemistry international, 2011. **58**(8): p. 880-7.

452. Amoroso, M.R., et al., *TRAP1 and the proteasome regulatory particle TBP7/Rpt3 interact in the endoplasmic reticulum and control cellular ubiquitination of specific mitochondrial proteins*. Cell Death Differ, 2012. **19**(4): p. 592-604.

453. Plescia, J., et al., *Rational design of shepherdin, a novel anticancer agent*. Cancer Cell, 2005. **7**(5): p. 457-68.

454. Siegelin, M.D., *Inhibition of the mitochondrial Hsp90 chaperone network: a novel, efficient treatment strategy for cancer?* Cancer Lett, 2013. **333**(2): p. 133-46.

455. Yi, F. and L. Regan, *A novel class of small molecule inhibitors of Hsp90*. ACS Chem Biol, 2008. **3**(10): p. 645-54.

456. Siegelin, M.D., et al., *Exploiting the mitochondrial unfolded protein response for cancer therapy in mice and human cells*. J Clin Invest, 2011. **121**(4): p. 1349-60.

457. Chae, Y.C., et al., *Control of tumor bioenergetics and survival stress signaling by mitochondrial HSP90s*. Cancer Cell, 2012. **22**(3): p. 331-44.

458. Kamal, A., et al., *A high-affinity conformation of Hsp90 confers tumour selectivity on Hsp90 inhibitors*. Nature, 2003. **425**(6956): p. 407-10.

459. Giard, D.J., et al., *In vitro cultivation of human tumors: establishment of cell lines derived from a series of solid tumors*. J Natl Cancer Inst, 1973. **51**(5): p. 1417-23.

460. Jacobs, J.P., C.M. Jones, and J.P. Baille, *Characteristics of a human diploid cell designated MRC-5*. Nature, 1970. **227**(5254): p. 168-70.

461. Chiu, Y.L. and T.M. Rana, *siRNA function in RNAi: a chemical modification analysis*. RNA, 2003. **9**(9): p. 1034-48.

462. Skehan, P., et al., *New colorimetric cytotoxicity assay for anticancer-drug screening*. J Natl Cancer Inst, 1990. **82**(13): p. 1107-12.

463. Gallagher, S.R., *One-dimensional SDS gel electrophoresis of proteins*. Curr Protoc Mol Biol, 2006. **Chapter 10**: p. Unit 10 2A.

464. Wang, Y., et al., *A novel strategy to engineer DNA polymerases for enhanced processivity and improved performance in vitro*. Nucleic Acids Res, 2004. **32**(3): p. 1197-207.

465. Pfaffl, M.W., *A new mathematical model for relative quantification in real-time RT-PCR*. Nucleic Acids Res, 2001. **29**(9): p. e45.

466. Grist, S.M., L. Chrostowski, and K.C. Cheung, *Optical oxygen sensors for applications in microfluidic cell culture*. Sensors (Basel), 2010. **10**(10): p. 9286-316.

467. Arain, S., et al., *Characterization of microtiterplates with integrated optical sensors for oxygen and pH, and their applications to enzyme activity screening, respirometry, and toxicological assays*. Sensors and Actuators B: Chemical, 2006. **113**(2): p. 639-648.

468. Perry, S.W., et al., *Mitochondrial membrane potential probes and the proton gradient: a practical usage guide*. Biotechniques, 2011. **50**(2): p. 98-115.

469. Pendergrass, W., N. Wolf, and M. Poot, *Efficacy of MitoTracker Green and CMXrosamine to measure changes in mitochondrial membrane potentials in living cells and tissues*. Cytometry A, 2004. **61**(2): p. 162-9.

470. Pereira, C.V., et al., *The contribution of oxidative stress to drug-induced organ toxicity and its detection in vitro and in vivo*. Expert Opin Drug Metab Toxicol, 2012. **8**(2): p. 219-37.

471. Martin, C., et al., *tert-Butyl hydroperoxide-induced lipid signaling in hepatocytes: involvement of glutathione and free radicals*. Biochem Pharmacol, 2001. **62**(6): p. 705-12.

472. Petronilli, V., et al., *Imaging the mitochondrial permeability transition pore in intact cells*. Biofactors, 1998. **8**(3-4): p. 263-72.

473. Halestrap, A.P. and A.M. Davidson, *Inhibition of Ca2(+)-induced large-amplitude swelling of liver and heart mitochondria by cyclosporin is probably caused by the inhibitor binding to mitochondrial-matrix peptidyl-prolyl cis-trans isomerase and preventing it interacting with the adenine nucleotide translocase*. Biochem J, 1990. **268**(1): p. 153-60.

474. Xiang, F., et al., *Mitochondrial chaperone tumour necrosis factor receptor-associated protein 1 protects cardiomyocytes from hypoxic injury by regulating mitochondrial permeability transition pore opening*. FEBS J, 2010. **277**(8): p. 1929-38.

475. Fang, W., et al., *Transcriptional patterns, biomarkers and pathways characterizing nasopharyngeal carcinoma of Southern China*. J Transl Med, 2008. **6**: p. 32.

476. Nieminen, A.L., et al., *Contribution of the mitochondrial permeability transition to lethal injury after exposure of hepatocytes to t-butylhydroperoxide*. Biochem J, 1995. **307 (Pt 1)**: p. 99-106.

477. Jones, R.A., A. Smail, and M.R. Wilson, *Detecting mitochondrial permeability transition by confocal imaging of intact cells pinocytically loaded with calcein*. Eur J Biochem, 2002. **269**(16): p. 3990-7.

478. Maddalena, F., et al., *Resistance to paclitxel in breast carcinoma cells requires a quality control of mitochondrial antiapoptotic proteins by TRAP1*. Mol Oncol, 2013.

479. Minotti, G., et al., *Anthracyclines: molecular advances and pharmacologic developments in antitumor activity and cardiotoxicity*. Pharmacol Rev, 2004. **56**(2): p. 185-229.

480. Petronilli, V., et al., *Transient and long-lasting openings of the mitochondrial permeability transition pore can be monitored directly in intact cells by changes in mitochondrial calcein fluorescence*. Biophys J, 1999. **76**(2): p. 725-34.

481. Bonora, M., et al., *Role of the c subunit of the FO ATP synthase in mitochondrial permeability transition*. Cell Cycle, 2013. **12**(4): p. 674-83.

482. Murphy, M.P., *How mitochondria produce reactive oxygen species*. Biochem J, 2009. **417**(1): p. 1-13.

483. Grandemange, S., S. Herzig, and J.C. Martinou, *Mitochondrial dynamics and cancer*. Semin Cancer Biol, 2009. **19**(1): p. 50-6.

484. Youle, R.J. and M. Karbowski, *Mitochondrial fission in apoptosis*. Nat Rev Mol Cell Biol, 2005. **6**(8): p. 657-63.

485. Twig, G., et al., *Fission and selective fusion govern mitochondrial segregation and elimination by autophagy*. EMBO J, 2008. **27**(2): p. 433-46.

486. Komatsu, M. and Y. Ichimura, *Physiological significance of selective degradation of p62 by autophagy*. FEBS letters, 2010. **584**(7): p. 1374-8.

487. Fleming, A., et al., *Chemical modulators of autophagy as biological probes and potential therapeutics*. Nat Chem Biol, 2011. **7**(1): p. 9-17.

488. Kondo, Y., et al., *The role of autophagy in cancer development and response to therapy*. Nature reviews. Cancer, 2005. **5**(9): p. 726-34.

489. Kurokawa, M. and S. Kornbluth, *Caspases and kinases in a death grip*. Cell, 2009. **138**(5): p. 838-54.

490. Bojes, H.K., et al., *Bcl-2 and Bcl-xL in peroxide-resistant A549 and U87MG cells*. Toxicological sciences : an official journal of the Society of Toxicology, 1998. **42**(2): p. 109-16.

491. Wu, F., et al., *Studies of phosphoproteomic changes induced by nucleophosmin-anaplastic lymphoma kinase (ALK) highlight deregulation of tumor necrosis factor (TNF)/Fas/TNF-related apoptosis-induced ligand signaling pathway in ALK-positive anaplastic large cell lymphoma*. Mol Cell Proteomics, 2010. **9**(7): p. 1616-32.

492. Barbosa, I.A., et al., *Mitochondrial remodeling in cancer metabolism and survival: potential for new therapies*. Biochimica et biophysica acta, 2012. **1826**(1): p. 238-54.

493. Migliaccio, E., et al., *The p66shc adaptor protein controls oxidative stress response and life span in mammals*. Nature, 1999. **402**(6759): p. 309-13.

494. Orsini, F., et al., *The life span determinant p66Shc localizes to mitochondria where it associates with mitochondrial heat shock protein 70 and regulates trans-membrane potential*. J Biol Chem, 2004. **279**(24): p. 25689-95.

495. Pinton, P., et al., *Protein kinase C beta and prolyl isomerase 1 regulate mitochondrial effects of the life-span determinant p66Shc*. Science, 2007. **315**(5812): p. 659-63.

496. Pacini, S., et al., *p66SHC promotes apoptosis and antagonizes mitogenic signaling in T cells*. Mol Cell Biol, 2004. **24**(4): p. 1747-57.

497. Galimov, E.R., *The Role of p66shc in Oxidative Stress and Apoptosis*. Acta Naturae, 2010. **2**(4): p. 44-51.

498. Koch, O.R., et al., *Role of the life span determinant P66(shcA) in ethanol-induced liver damage*. Laboratory investigation; a journal of technical methods and pathology, 2008. **88**(7): p. 750-60.

499. Camici, G.G., et al., *Genetic deletion of p66(Shc) adaptor protein prevents hyperglycemia-induced endothelial dysfunction and oxidative stress*. Proc Natl Acad Sci U S A, 2007. **104**(12): p. 5217-22.

500. Green, D.R. and G. Kroemer, *The pathophysiology of mitochondrial cell death*. Science, 2004. **305**(5684): p. 626-9.

501. Nakagawa, T., et al., *Cyclophilin D-dependent mitochondrial permeability transition regulates some necrotic but not apoptotic cell death*. Nature, 2005. **434**(7033): p. 652-8.

502. Forte, M., et al., *Cyclophilin D inactivation protects axons in experimental autoimmune encephalomyelitis, an animal model of multiple sclerosis*. Proc Natl Acad Sci U S A, 2007. **104**(18): p. 7558-63.

503. Sciacovelli, M., et al., *The mitochondrial chaperone TRAP1 promotes neoplastic growth by inhibiting succinate dehydrogenase*. Cell Metab, 2013. **17**(6): p. 988-99.

504. Yoshida, S., et al., *Molecular chaperone TRAP1 regulates a metabolic switch between mitochondrial respiration and aerobic glycolysis*. Proc Natl Acad Sci U S A, 2013. **110**(17): p. E1604-12.

505. Goetz, M.P., et al., *The Hsp90 chaperone complex as a novel target for cancer therapy*. Ann Oncol, 2003. **14**(8): p. 1169-76.

506. Xiong, L., et al., *Heat shock protein 90 is involved in regulation of hypoxia-driven proliferation of embryonic neural stem/progenitor cells*. Cell Stress Chaperones, 2009. **14**(2): p. 183-92.

507. Bagatell, R. and L. Whitesell, *Altered Hsp90 function in cancer: a unique therapeutic opportunity*. Mol Cancer Ther, 2004. **3**(8): p. 1021-30.

508. Richard, D.E., E. Berra, and J. Pouyssegur, *Nonhypoxic pathway mediates the induction of hypoxia-inducible factor 1alpha in vascular smooth muscle cells*. J Biol Chem, 2000. **275**(35): p. 26765-71.

509. Jung, S.N., et al., *Reactive oxygen species stabilize hypoxia-inducible factor-1 alpha protein and stimulate transcriptional activity via AMP-activated protein kinase in DU145 human prostate cancer cells*. Carcinogenesis, 2008. **29**(4): p. 713-21.

510. Yuneva, M.O., et al., *The metabolic profile of tumors depends on both the responsible genetic lesion and tissue type*. Cell Metab, 2012. **15**(2): p. 157-70.

511. Suski, J.M., et al., *Relation between mitochondrial membrane potential and ROS formation*. Methods Mol Biol, 2012. **810**: p. 183-205.

512. Skulachev, V.P., *Uncoupling: new approaches to an old problem of bioenergetics*. Biochimica et biophysica acta, 1998. **1363**(2): p. 100-24.

513. Youle, R.J. and A.M. van der Bliek, *Mitochondrial fission, fusion, and stress*. Science, 2012. **337**(6098): p. 1062-5.

514. Butler, E.K., et al., *The mitochondrial chaperone protein TRAP1 mitigates alpha-Synuclein toxicity*. PLoS Genet, 2012. **8**(2): p. e1002488.

515. Takamura, H., et al., *TRAP1 controls mitochondrial fusion/fission balance through Drp1 and Mff expression*. PLoS One, 2012. **7**(12): p. e51912.

516. Chang, C.R. and C. Blackstone, *Dynamic regulation of mitochondrial fission through modification of the dynamin-related protein Drp1*. Ann N Y Acad Sci, 2010. **1201**: p. 34-9.

517. Rodriguez-Enriquez, S., L. He, and J.J. Lemasters, *Role of mitochondrial permeability transition pores in mitochondrial autophagy*. Int J Biochem Cell Biol, 2004. **36**(12): p. 2463-72.

518. Tanida, I., T. Ueno, and E. Kominami, *LC3 and Autophagy*. Methods Mol Biol, 2008. **445**: p. 77-88.

519. Mizushima, N. and T. Yoshimori, *How to interpret LC3 immunoblotting*. Autophagy, 2007. **3**(6): p. 542-5.

520. Bjorkoy, G., et al., *p62/SQSTM1 forms protein aggregates degraded by autophagy and has a protective effect on huntingtin-induced cell death*. J Cell Biol, 2005. **171**(4): p. 603-14.

521. Kuusisto, E., T. Suuronen, and A. Salminen, *Ubiquitin-binding protein p62 expression is induced during apoptosis and proteasomal inhibition in neuronal cells*. Biochem Biophys Res Commun, 2001. **280**(1): p. 223-8.

522. Chien, W.L., et al., *Impairment of oxidative stress-induced heme oxygenase-1 expression by the defect of Parkinson-related gene of PINK1*. J Neurochem, 2011. **117**(4): p. 643-53.

523. Costa, A.C., S.H. Loh, and L.M. Martins, *Drosophila Trap1 protects against mitochondrial dysfunction in a PINK1/parkin model of Parkinson's disease*. Cell Death Dis, 2013. **4**: p. e467.

524. Zhang, L., et al., *TRAP1 rescues PINK1 loss-of-function phenotypes*. Human molecular genetics, 2013. **22**(14): p. 2829-41.

525. Elmore, S.P., et al., *The mitochondrial permeability transition initiates autophagy in rat hepatocytes*. The FASEB journal : official publication of the Federation of American Societies for Experimental Biology, 2001. **15**(12): p. 2286-7.

526. Carreira, R.S., et al., *Cyclophilin D is required for mitochondrial removal by autophagy in cardiac cells*. Autophagy, 2010. **6**(4): p. 462-72.

527. Kaushik, S., et al., *Constitutive activation of chaperone-mediated autophagy in cells with impaired macroautophagy*. Mol Biol Cell, 2008. **19**(5): p. 2179-92.

528. Wang, Y., et al., *Loss of macroautophagy promotes or prevents fibroblast apoptosis depending on the death stimulus*. J Biol Chem, 2008. **283**(8): p. 4766-77.

529. Suen, D.F., K.L. Norris, and R.J. Youle, *Mitochondrial dynamics and apoptosis*. Genes Dev, 2008. **22**(12): p. 1577-90.

530. Montessuit, S., et al., *Membrane remodeling induced by the dynamin-related protein Drp1 stimulates Bax oligomerization*. Cell, 2010. **142**(6): p. 889-901.

531. Ishisaka, R., et al., *Participation of a cathepsin L-type protease in the activation of caspase-3*. Cell Struct Funct, 1999. **24**(6): p. 465-70.

532. Hishita, T., et al., *Caspase-3 activation by lysosomal enzymes in cytochrome c-independent apoptosis in myelodysplastic syndrome-derived cell line P39*. Cancer research, 2001. **61**(7): p. 2878-84.

533. Johansson, A.C., et al., *Regulation of apoptosis-associated lysosomal membrane permeabilization*. Apoptosis, 2010. **15**(5): p. 527-40.

534. Bidere, N., et al., *Cathepsin D triggers Bax activation, resulting in selective apoptosis-inducing factor (AIF) relocation in T lymphocytes entering the early commitment phase to apoptosis*. J Biol Chem, 2003. **278**(33): p. 31401-11.

535. Boya, P., et al., *Lysosomal membrane permeabilization induces cell death in a mitochondrion-dependent fashion*. J Exp Med, 2003. **197**(10): p. 1323-34.

536. Altieri, D.C., et al., *TRAP-1, the mitochondrial Hsp90*. Biochimica et biophysica acta, 2012. **1823**(3): p. 767-73.

537. McSharry, B.P., et al., *Human telomerase reverse transcriptase-immortalized MRC-5 and HCA2 human fibroblasts are fully permissive for human cytomegalovirus*. J Gen Virol, 2001. **82**(Pt 4): p. 855-63.

538. Ryter, S.W., S.M. Cloonan, and A.M. Choi, *Autophagy: A critical regulator of cellular metabolism and homeostasis*. Mol Cells, 2013. **36**(1): p. 7-16.

539. Nyfeler, B., et al., *Quantitative visualization of autophagy induction by mTOR inhibitors*. Methods Mol Biol, 2012. **821**: p. 239-50.

540. Boya, P. and G. Kroemer, *Lysosomal membrane permeabilization in cell death*. Oncogene, 2008. **27**(50): p. 6434-51.

541. Lowe, S.W., et al., *p53-dependent apoptosis modulates the cytotoxicity of anticancer agents*. Cell, 1993. **74**(6): p. 957-67.

Appendix

Copy Right License Agreements

ELSEVIER LICENSE
TERMS AND CONDITIONS

Sep 12, 2013

This is a License Agreement between Ines Barbosa ("You") and Elsevier ("Elsevier") provided by Copyright Clearance Center ("CCC"). The license consists of your order details, the terms and conditions provided by Elsevier, and the payment terms and conditions.

All payments must be made in full to CCC. For payment instructions, please see information listed at the bottom of this form.

Supplier	Elsevier Limited The Boulevard,Langford Lane Kidlington,Oxford,OX5 1GB,UK
Registered Company Number	1982084
Customer name	Ines Barbosa
Customer address	Rua Fonte do bispo Edificio Uniao 8G Coimbra, Coimbra 3030-243
License number	3226570952886
License date	Sep 12, 2013
Licensed content publisher	Elsevier
Licensed content publication	Cell
Licensed content title	Hallmarks of Cancer: The Next Generation
Licensed content author	Douglas Hanahan,Robert A. Weinberg
Licensed content date	4 March 2011
Licensed content volume number	144
Licensed content issue number	5
Number of pages	29
Start Page	646
End Page	674
Type of Use	reuse in a thesis/dissertation
Portion	figures/tables/illustrations
Number of figures/tables/illustrations	1
Format	both print and electronic
Are you the author of this	No

Elsevier article?	
Will you be translating?	No
Order reference number	
Title of your thesis/dissertation	TRAP1 in the regulation of mitochondrial homeostasis and cellular quality control
Expected completion date	Sep 2013
Estimated size (number of pages)	200
Elsevier VAT number	GB 494 6272 12
Permissions price	0.00 EUR
VAT/Local Sales Tax	0.0 USD / 0.0 GBP
Total	0.00 EUR
Terms and Conditions	

INTRODUCTION

1. The publisher for this copyrighted material is Elsevier. By clicking "accept" in connection with completing this licensing transaction, you agree that the following terms and conditions apply to this transaction (along with the Billing and Payment terms and conditions established by Copyright Clearance Center, Inc. ("CCC"), at the time that you opened your Rightslink account and that are available at any time at http://myaccount.copyright.com).

GENERAL TERMS

2. Elsevier hereby grants you permission to reproduce the aforementioned material subject to the terms and conditions indicated.

3. Acknowledgement: If any part of the material to be used (for example, figures) has appeared in our publication with credit or acknowledgement to another source, permission must also be sought from that source. If such permission is not obtained then that material may not be included in your publication/copies. Suitable acknowledgement to the source must be made, either as a footnote or in a reference list at the end of your publication, as follows:

"Reprinted from Publication title, Vol /edition number, Author(s), Title of article / title of chapter, Pages No., Copyright (Year), with permission from Elsevier [OR APPLICABLE SOCIETY COPYRIGHT OWNER]." Also Lancet special credit - "Reprinted from The Lancet, Vol. number, Author(s), Title of article, Pages No., Copyright (Year), with permission from Elsevier."

4. Reproduction of this material is confined to the purpose and/or media for which permission is hereby given.

5. Altering/Modifying Material: Not Permitted. However figures and illustrations may be

altered/adapted minimally to serve your work. Any other abbreviations, additions, deletions and/or any other alterations shall be made only with prior written authorization of Elsevier Ltd. (Please contact Elsevier at permissions@elsevier.com)

6. If the permission fee for the requested use of our material is waived in this instance, please be advised that your future requests for Elsevier materials may attract a fee.

7. Reservation of Rights: Publisher reserves all rights not specifically granted in the combination of (i) the license details provided by you and accepted in the course of this licensing transaction, (ii) these terms and conditions and (iii) CCC's Billing and Payment terms and conditions.

8. License Contingent Upon Payment: While you may exercise the rights licensed immediately upon issuance of the license at the end of the licensing process for the transaction, provided that you have disclosed complete and accurate details of your proposed use, no license is finally effective unless and until full payment is received from you (either by publisher or by CCC) as provided in CCC's Billing and Payment terms and conditions. If full payment is not received on a timely basis, then any license preliminarily granted shall be deemed automatically revoked and shall be void as if never granted. Further, in the event that you breach any of these terms and conditions or any of CCC's Billing and Payment terms and conditions, the license is automatically revoked and shall be void as if never granted. Use of materials as described in a revoked license, as well as any use of the materials beyond the scope of an unrevoked license, may constitute copyright infringement and publisher reserves the right to take any and all action to protect its copyright in the materials.

9. Warranties: Publisher makes no representations or warranties with respect to the licensed material.

10. Indemnity: You hereby indemnify and agree to hold harmless publisher and CCC, and their respective officers, directors, employees and agents, from and against any and all claims arising out of your use of the licensed material other than as specifically authorized pursuant to this license.

11. No Transfer of License: This license is personal to you and may not be sublicensed, assigned, or transferred by you to any other person without publisher's written permission.

12. No Amendment Except in Writing: This license may not be amended except in a writing signed by both parties (or, in the case of publisher, by CCC on publisher's behalf).

13. Objection to Contrary Terms: Publisher hereby objects to any terms contained in any purchase order, acknowledgment, check endorsement or other writing prepared by you, which terms are inconsistent with these terms and conditions or CCC's Billing and Payment terms and conditions. These terms and conditions, together with CCC's Billing and Payment terms and conditions (which are incorporated herein), comprise the entire agreement between you and publisher (and CCC) concerning this licensing transaction. In the event of any conflict between your obligations established by these terms and conditions and those established by CCC's Billing and Payment terms and conditions, these terms and conditions

shall control.

14. Revocation: Elsevier or Copyright Clearance Center may deny the permissions described in this License at their sole discretion, for any reason or no reason, with a full refund payable to you. Notice of such denial will be made using the contact information provided by you. Failure to receive such notice will not alter or invalidate the denial. In no event will Elsevier or Copyright Clearance Center be responsible or liable for any costs, expenses or damage incurred by you as a result of a denial of your permission request, other than a refund of the amount(s) paid by you to Elsevier and/or Copyright Clearance Center for denied permissions.

LIMITED LICENSE

The following terms and conditions apply only to specific license types:

15. **Translation**: This permission is granted for non-exclusive world **English** rights only unless your license was granted for translation rights. If you licensed translation rights you may only translate this content into the languages you requested. A professional translator must perform all translations and reproduce the content word for word preserving the integrity of the article. If this license is to re-use 1 or 2 figures then permission is granted for non-exclusive world rights in all languages.

16. **Website**: The following terms and conditions apply to electronic reserve and author websites:
Electronic reserve: If licensed material is to be posted to website, the web site is to be password-protected and made available only to bona fide students registered on a relevant course if:
This license was made in connection with a course,
This permission is granted for 1 year only. You may obtain a license for future website posting,
All content posted to the web site must maintain the copyright information line on the bottom of each image,
A hyper-text must be included to the Homepage of the journal from which you are licensing at http://www.sciencedirect.com/science/journal/xxxxx or the Elsevier homepage for books at http://www.elsevier.com , and
Central Storage: This license does not include permission for a scanned version of the material to be stored in a central repository such as that provided by Heron/XanEdu.

17. **Author website** for journals with the following additional clauses:

All content posted to the web site must maintain the copyright information line on the bottom of each image, and the permission granted is limited to the personal version of your paper. You are not allowed to download and post the published electronic version of your article (whether PDF or HTML, proof or final version), nor may you scan the printed edition to create an electronic version. A hyper-text must be included to the Homepage of the journal from which you are licensing at http://www.sciencedirect.com/science/journal/xxxxx . As part of our normal production process, you will receive an e-mail notice when your article appears on Elsevier's online service ScienceDirect (www.sciencedirect.com). That e-

mail will include the article's Digital Object Identifier (DOI). This number provides the electronic link to the published article and should be included in the posting of your personal version. We ask that you wait until you receive this e-mail and have the DOI to do any posting.

Central Storage: This license does not include permission for a scanned version of the material to be stored in a central repository such as that provided by Heron/XanEdu.

18. **Author website** for books with the following additional clauses:
Authors are permitted to place a brief summary of their work online only.
A hyper-text must be included to the Elsevier homepage at http://www.elsevier.com . All content posted to the web site must maintain the copyright information line on the bottom of each image. You are not allowed to download and post the published electronic version of your chapter, nor may you scan the printed edition to create an electronic version.

Central Storage: This license does not include permission for a scanned version of the material to be stored in a central repository such as that provided by Heron/XanEdu.

19. **Website** (regular and for author): A hyper-text must be included to the Homepage of the journal from which you are licensing at
http://www.sciencedirect.com/science/journal/xxxxx. or for books to the Elsevier homepage at http://www.elsevier.com

20. **Thesis/Dissertation**: If your license is for use in a thesis/dissertation your thesis may be submitted to your institution in either print or electronic form. Should your thesis be published commercially, please reapply for permission. These requirements include permission for the Library and Archives of Canada to supply single copies, on demand, of the complete thesis and include permission for UMI to supply single copies, on demand, of the complete thesis. Should your thesis be published commercially, please reapply for permission.

21. **Other Conditions**:

v1.6

If you would like to pay for this license now, please remit this license along with your payment made payable to "COPYRIGHT CLEARANCE CENTER" otherwise you will be invoiced within 48 hours of the license date. Payment should be in the form of a check or money order referencing your account number and this invoice number RLNK501111394.
Once you receive your invoice for this order, you may pay your invoice by credit card. Please follow instructions provided at that time.

Make Payment To:
Copyright Clearance Center
Dept 001
P.O. Box 843006
Boston, MA 02284-3006